DOCTOR OF PHILOSOPHY

Characterisation of novel genome regulation functions of the cancer-associated proteins Translin and Trax

Alzahrani, Othman

Award date:
2018

Awarding institution:
Bangor University

Characterisation of novel genome regulation functions of the cancer-associated proteins Translin and Trax

A thesis is submitted for the degree of Doctror of Philosophy
at Bangor University By

Othman Rashed Ahmed Alzahrani

North West Cancer Research Fund Institute

School of Biological Science

University of Bangor

United Kingdom

December, 2017

Declaration and Consent

Details of the Work

I hereby agree to deposit the following item in the digital repository maintained by Bangor University and/or in any other repository authorized for use by Bangor University.

Author Name: .....

Title: .....

Supervisor/Department: .....

Funding body (if any): .....

Qualification/Degree obtained: .....

This item is a product of my own research endeavours and is covered by the agreement below in which the item is referred to as "the Work". It is identical in content to that deposited in the Library, subject to point 4 below.

Non-exclusive Rights

Rights granted to the digital repository through this agreement are entirely non-exclusive. I am free to publish the Work in its present version or future versions elsewhere.

I agree that Bangor University may electronically store, copy or translate the Work to any approved medium or format for the purpose of future preservation and accessibility. Bangor University is not under any obligation to reproduce or display the Work in the same formats or resolutions in which it was originally deposited.

Bangor University Digital Repository

I understand that work deposited in the digital repository will be accessible to a wide variety of people and institutions, including automated agents and search engines via the World Wide Web.

I understand that once the Work is deposited, the item and its metadata may be incorporated into public access catalogues or services, national databases of electronic theses and dissertations such as the British Library's EThOS or any service provided by the National Library of Wales.

Statement 1:

This work has not previously been accepted in substance for any degree and is not being concurrently submitted in candidature for any degree unless as agreed by the University for approved dual awards.

Signed …….. (candidate)

Date ……..

Statement 2:

This thesis is the result of my own investigations, except where otherwise stated. Where correction services have been used, the extent and nature of the correction is clearly marked in a footnote(s).

All other sources are acknowledged by footnotes and/or a bibliography.

Signed ……. (candidate)

Date …….

Statement 3:

I hereby give consent for my thesis, if accepted, to be available for photocopying, for inter-library loan and for electronic repositories, and for the title and summary to be made available to outside organisations.

Signed ……. (candidate)

Date …….

NB: Candidates on whose behalf a bar on access has been approved by the Academic Registry should use the following version of Statement 3:

Statement 3 (bar):

I hereby give consent for my thesis, if accepted, to be available for photocopying, for inter-library loans and for electronic repositories after expiry of a bar on access.

Signed …… (candidate)

Date ……

Statement 4:

Choose **one** of the following options

a)	I agree to deposit an electronic copy of my thesis (the Work) in the Bangor University (BU) Institutional Digital Repository, the British Library ETHOS system, and/or in any other repository authorized for use by Bangor University and where necessary have gained the required permissions for the use of third party material.	
b)	I agree to deposit an electronic copy of my thesis (the Work) in the Bangor University (BU) Institutional Digital Repository, the British Library ETHOS system, and/or in any other repository authorized for use by Bangor University when the approved **bar on access** has been lifted.	
c)	I agree to submit my thesis (the Work) electronically via Bangor University's e-submission system, however I **opt-out** of the electronic deposit to the Bangor University (BU) Institutional Digital Repository, the British Library ETHOS system, and/or in any other repository authorized for use by Bangor University, due to lack of permissions for use of third party material.	

Options B should only be used if a bar on access has been approved by the University.

In addition to the above I also agree to the following:

1. That I am the author or have the authority of the author(s) to make this agreement and do hereby give Bangor University the right to make available the Work in the way described above.

2. That the electronic copy of the Work deposited in the digital repository and covered by this agreement, is identical in content to the paper copy of the Work deposited in the Bangor University Library, subject to point 4 below.

3. That I have exercised reasonable care to ensure that the Work is original and, to the best of my knowledge, does not breach any laws – including those relating to defamation, libel and copyright.

4. That I have, in instances where the intellectual property of other authors or copyright holders is included in the Work, and where appropriate, gained explicit permission for the inclusion of that material in the Work, and in the electronic form of the Work as accessed through the open access digital repository, *or* that I have identified and removed that material for which adequate and appropriate permission has not been obtained and which will be inaccessible via the digital repository.

5. That Bangor University does not hold any obligation to take legal action on behalf of the Depositor, or other rights holders, in the event of a breach of intellectual property rights, or any other right, in the material deposited.

6. That I will indemnify and keep indemnified Bangor University and the National Library of Wales from and against any loss, liability, claim or damage, including without limitation any related legal fees and court costs (on a full indemnity bases), related to any breach by myself of any term of this agreement.

Signature: …… Date : ……

Abstract

Translin and TRAX are a highly conserved pair of proteins that have a close functional relationship with one another. Originally, these nucleic acid binding proteins were implicated in chromosomal translocation in human leukaemia cells, but subsequently, they have been shown to function in a wide range of biological processes, including RNA interference passenger strand removal, tRNA precursor processing, and neuronal mRNA transport and, more recently, in the degradation of microRNA in oncogenesis. This led to the proposal that they could be druggable targets for a large number of cancers. Moreover, it has previously been proposed that they function at telomeres, although no direct evidence has been provided to support this. Previous analysis on *Schizosaccharomyces pombe* orthologues of Translin and TRAX, Tsn1 and Tfx1, have shown no notable functional role (*Saccharomyces cerevisiae* has no *tsn1/tfx1* orthologue). Given the link to RNAi regulation in higher eukaryotic organisms, a series of double mutants of *tsn1* and *tfx1* and RNAi regulatory genes, *ago1* and *dcr1*, were generated to investigate whether Tsn1 and Tfx1 have a redundant role with the RNAi regulators. Different approaches were used to demonstrate that loss of Tfx1, but not Tsn1, can partially suppress the chromosomal instability caused by loss of Ago1, without restoring centromere heterochromatin formation. We extend this to reveal that deletion of four sub-telomeric *tlh* genes also suppress the need for Ago1, as does the mutation of *taz1*—a factor that is required for telomere length control, although the mechanisms appear to be different. Extended analysis of Tfx1-and Tsn1-defective cells identify differential roles for these proteins in regulating the levels of distinct transcripts associated with the telomeres and sub-telomeres. These findings not only reveal two novel regulators of telomere dynamics, but also propose that modulating the transcriptional status at sub-telomeres partially suppresses the chromosome segregation defects conferred by loss of Ago1. This reveals a counterbalance between centromeres and telomeres in maintaining chromosome stability. Further analysis of Tsn1 and Tfx1 function led to the revelation of a novel and fundamentally important role for Tsn1 in the DNA damage recovery response in the absence of Dcr1, a function that may be linked to its original proposed role in generating chromosomal translocation. Our data not only separates the functions of Tsn1 and Tfx1 in *S. pombe*, but also reveals important functional roles for these paralogues in chromosome stability maintenance.

Acknowledgements

This study was funded by Tabuk University in Saudi Arabia. Our research group would like to thank Prof Chris Norbury and Dr. Julia Cooper for providing the *tlhΔ4* and *Otrt1Δ* strains, respectively. Special thanks go to my family. Special mention also goes to my parents, whose love and guidance have been with me throughout the years. Words cannot express how grateful I am to my loving and supportive wife, Shuruq, and my two brilliant kids, Larin and Jassar, for encouraging me through all the years of my doctoral research. Most importantly, I thank my supervisor and our group leader, Dr. Ramsay McFarlane, for his great and continuous support and guidance, which helped me throughout the project research and during the writing of this thesis. I am also hugely appreciative to Dr. Natalia Gomez-Escobar for all her frequent help and advice on most of the laboratory techniques we used in this research. Finally, I thank all the former and current members of the D7 Lab for being helpful and supportive. Thank you, all.

List of Abbreviations

3': Three prime end of DNA

5': Five prime end of DNA

ALT: alternative lengthening of telomeres

ARIA: TERRA antisense transcript C-rich telomeric RNA repeats

ARRET: Sub-telomeric long non-coding RNA

αARRET: Sub-telomeric transcripts complementary to ARRET

ATM: Ataxia telangiectasia mutated

BDNF: Brain-derived neurotrophic factor

BIR: break-induced replication

bp: base pair

cDNA: Complementary DNA

CDGS: Chromatin-dependent gene silencing

CDKs: cyclin-dependent kinases

CLRC: cryptic loci regulator complex

CML: chronic myelogenous leukaemia

CpG: -cytosine-phosphate-guanine-

CPT: camptothecin

C3PO: component 3 promoter of RISC

DAPI: 4',6-diamidino-2-phenylindole

DDK: Cdc7-Dbf4 kinases

DDR: DNA damage responses

dH_2O: Distilled water

dHJ: double Holliday junction

D-loop: Displacement loop

DMSO: Dimethyl sulphoxide

DNA: Deoxyribonucleic acid

DNA-PK: DNA-dependent protein kinase

DNMT: DNA methyltransferasaes

dNTP: deoxyribonucleotide triphosphate

DRIP: DNA:RNA immunoprecipitation

dsDNA: double-stranded DNA

dsRNA: double-stranded RNA

DSBs: double strand breaks

DSBR: double strand break repair

g: Gram

GADD: growth arrest and DNA damage

EDTA: ethylenediamine tetraacetic acid

FL: follicular lymphoma

HAT: histone acetyltransferase

HP1: heterochromatin protein 1

HDAC: histone deacetylase

HJ: Holliday junction

HR: homologous recombination

HU: hydroxyurea

IR: ionizing radiation

kb: kilobase

kDa: kilo Dalton

L: Litre

LB: Luria-Bertani media

LiAC: lithium acetate

MCM: mini-chromosome maintenance

MEFs : mice embryotic fibroblasts

MMC: mitomycin C

MMS: methyl methane sulfonate

MRN: MRE11-RAD50-NBS1 complex

mg: Milligram

miRNA: micro-RNAs

µg: Microgram

µl: Microliter

ml: Milliliter

mM: Millimolar

mRNA: messenger RNA

ml: Milliliter

mM: Millimolar

mRNA: messenger RNA

NB: nitrogen base

NBL: nitrogen base liquid

NE: nuclear envelope

NHEJ: non-homologous end joining

ng: Nanogram

NLS: nuclear localization signal

ORF: open reading frame

PCNA: proliferating cell nuclear antigen

PCR: polymerase chain reaction

pmol: picomole

PEG: polyethylene glycol

RC: replicative complex

rDNA: ribosomal DNA

RDRP: RNA-dependent RNA polymerase

PTGS: post-transcriptional gene silencing

piRNA: PIWI-interacting RNAs

RFB: replication fork barriers

RFC: replication factor C clamp loader

rDNA: ribosomal DNA

RISC: RNA-induced silencing complex

RITSC: RNAi-induced transcriptional silencing complex

RLC: RISC loading complex

RNA Ribonucleic acid

RNAi: RNA interference

RT-PCR: Reverse transcriptase PCR

q-RT-PCR: Quantitative real-time PCR

RNA Pol: RNA polymerase

RPA: replication protein A

SDS: Sodium Dodecyl Sulfate

SDSA: synthesis-dependent strand annealing

siRNA: small interference RNA

ssDNA: single-stranded DNA

TB-RBP: testis–brain RNA-binding protein

TGS*:* transcriptional gene silencing

TERRA: telomeric repeat-containing RNA

TFs: transcription factors

TK: tyrosine kinase

TRAX: Translin-associated factor X

tRNA: transfer RNA

TBZ: thiabendazole

UTR: untranslated region

UV: ultra-violet

V(D)J: variable (V), diversity (D) and joining (J) coding segments

YE: yeast extract

YEA: yeast extract agar

YEL: yeast extract liquid

Table of contents

List of Figures

Chapter 1

Chapter 3

Chapter 4

Chapter 5

Chapter 6

Chapter 7

Appendecies

List of Tables

Chapter 2

Chapter 1: Introduction

1. Introduction

1.1 Genomic instability

Genomic instability plays a crucial role in cancer development (Choi & Lee, 2013; McGranahan et al., 2012; Fragkos & Naim, 2017; Tubbs & Nussenzweig, 2017). Therefore, the maintenance of genome stability is vital to the proper functioning of cells (Yao & Dai, 2014; Felipe-Abrio et al., 2015; Faggioli et al., 2011; Aguilera & García-Muse, 2013). The stability of the genome is threatened by a range of genetic modifications such as point mutations, chromosomal rearrangements, deletions and alterations in chromosome number, which may result in the gain or loss of complete chromosomes (Ferguson et al., 2015; McGranahan et al., 2012; Aguilera & Gomez-Gonzalez, 2008). In addition to alterations in the DNA sequence, epigenetic aberration can also lead to genomic instability by altering the chromatin assembly, including histone modifications and DNA methylation (Choi & Lee, 2013; Katto & Mahlknecht, 2011). These changes in the structure and number of chromosomes, epigenetic alterations and gene mutations are hallmarks of most tumour cells, and they all play a crucial role in cancer initiation and progression (Aronica et al., 2016; Katto & Mahlknecht, 2011; Gordon et al., 2012; Lord & Ashworth, 2012; McGranahan et al., 2012; Weberpals et al., 2011). In addition to DNA lesions, chromosomal instability is also caused by defects in some important natural processes, such as DNA replication, chromosome segregation, telomere maintenance and DNA damage repair (Choi & Lee, 2013; Fragkos & Naim, 2017; Bartkova et al., 2005; Harrison & Foroni, 2002; Felipe-Abrio et al., 2015; Anderson, 2001).

The human genome is frequently put at risk by a range of challenges by both exogenous and endogenous stresses (Choi & Lee, 2013; Fragkos & Naim, 2017; Tubbs & Nussenzweig, 2017). These genotoxic stresses require efficient cellular responses in order to preserve genomic stability because they can cause numerous problems or lesions in the DNA, including single- or double-strand DNA breaks (So et al., 2017; Choi & Lee, 2013). In order to respond to and correct these lesions, eukaryotic cells have developed a collection of DNA damage responses (DDR), including checkpoint activation, DNA repair and the activation of programmed cell death (apoptotic pathways) in the case of irreparable DNA damage (Choi & Lee, 2013; Yang et al., 2016; Talens et al., 2017).

Therefore, the lack of any of these defence mechanisms may result in genetic instability, which leads to cancer development evolution and ageing-related diseases (Figure 1.1) (Ferguson et al., 2015; Yang et al., 2016; So et al., 2017; Ohle et al., 2016; Lombard et al., 2005).

Importantly, if DNA fails to replicate correctly, genetic recombination can take place, which may lead to chromosomal translocations and various other significant structural modifications if they are mediated through a wrong partner. These modifications can result in altered cell behaviour, leading to the possible development of diseases such as cancer. Thus, all mechanisms that occur during cell proliferation need to be perfectly coordinated to avoid generating genomic instability, including chromosomal rearrangements (Lord & Ashworth, 2012; Labib & Hodgson, 2007).

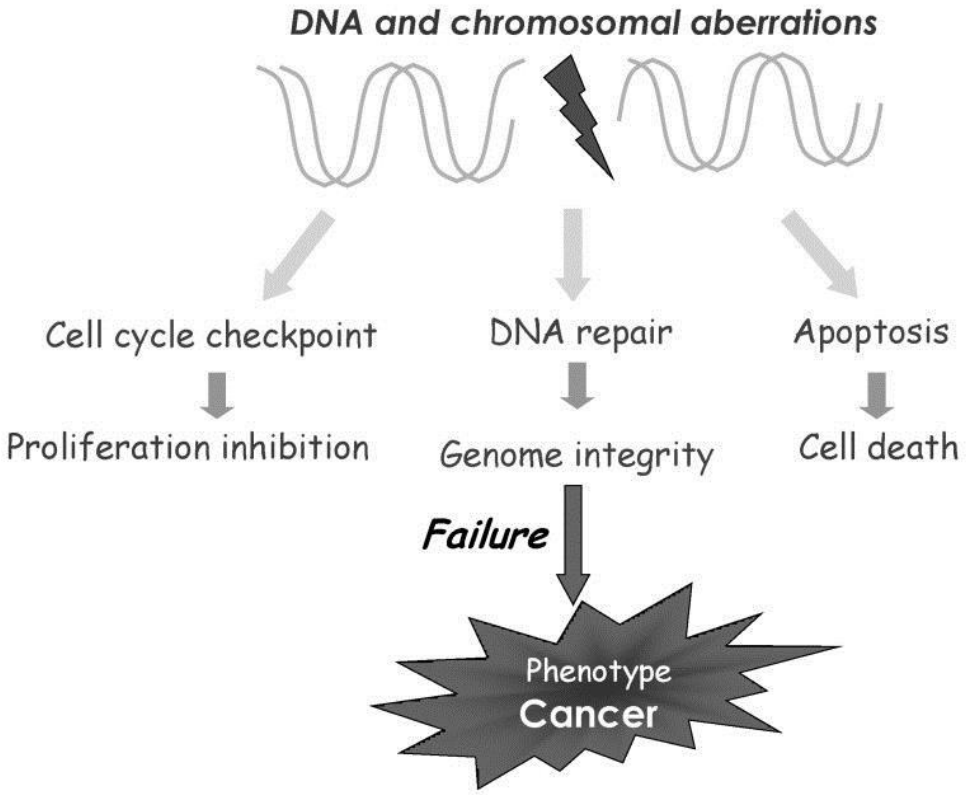

Figure 1.1 Cancer route in genome instability
Failure to respond to DNA damage leads to instability in the genome, which could induce cancer. Checkpoints arrest proliferation in response to allow the cell to repair damaged sites of chromosome correctly and in time, which is done by various DNA repair mechanisms. However, if any defects exist in these defence mechanisms, the damaged cells undergo apoptosis to maintain genomic integrity (adapted from Choi & Lee, 2013).

1.2 Chromosomal translocations

Chromosomal rearrangements are alterations in the structure of the original chromosome, which results in new arrangements of the chromosome through deletions, inversions and translocations (Figure1.2.A) (Harewood & Fraser, 2014). Chromosomal translocation is a major type of chromosomal rearrangements and contributes to genome instability (Nambiar & Raghavan, 2011). Translocation plays a significant role in cancer initiation and progression, particularly in lymphoma and leukaemia although the precise mechanisms of translocation generation are not well understood (Zheng, 2013; Nambiar & Raghavan, 2011). A chromosome translocation is an abnormality in a chromosome in which a chromosome breaks and is subsequently attached, either in whole or in part, to another chromosome. In other words, translocations occur due to abnormal recombination events between non-homologous chromosomes (Figure1.2.A) (Roukos & Misteli, 2014; Tucker, 2010).

There are two main classes of translocations: reciprocal and non-reciprocal. Reciprocal translocations, which are the most typical form of translocation, can be described as the swapping of segments of material between a pair of non-homologous chromosomes, whereas non-reciprocal translocations occur when only a single segment of a chromosome is translocated to a non-homologous chromosome (i.e., one-way translocations) (Zhang et al., 2010; Ferguson & Alt, 2001). Chromosome translocations are either balanced (i.e., reciprocal), in which chromosome sequences are translocated between the non-homologous chromosomes without the gain or loss of genetic material, or they are unbalanced, in which an unequal number of chromosome sequences is exchanged between the different chromosomes, resulting in the gain or loss of genetic material (Harewood & Fraser, 2014; Chang et al., 2013).

Depending on the location of chromosome breakpoints, the translocation of chromosomes can result in the production of fusion genes or interrupt and inactivate the tumour suppressor genes (Roukos & Misteli, 2014; Nambiar & Raghavan, 2011; Hasty & Montagna, 2014). Moreover, translocations can also result in the activation of proto-oncogenes, which are a set of genes that alters the phenotype of cells from normal to cancerous when activated or mutated, all of which could give rise to a tumour (Figure1.2.B) (Zheng, 2013; Aquino et al., 2013; Nambiar & Raghavan, 2011; Gates & Fink, 2008; Roukos & Misteli, 2014).

Modifications in the key genes involved in DNA damage checkpoints or in the repair of double-strand DNA breaks (DSBs) also cause translocation (Lengauer et al., 1998). DSBs are considered critical translocation-initiating events, and they can be induced through exogenous agents, such as ionising radiation (IR), or endogenous factors, such as stalled replication forks (So et al., 2017; Hogenbirk et al., 2016). In response to these errors or breaks, DNA repair mechanisms, including homologous recombination (HR) (see Section 1.6.2) are initiated by cells to rescue genomic stability by repairing these lesions. However, failures in repairing these lesions can lead to chromosomal rearrangement (Roukos & Misteli, 2014; So et al., 2017; Ferguson & Alt, 2001; Gelot et al., 2015). Therefore, defective chromosome replication can result in chromosomal translocations, the main causes of which are thought to be recombination at stalled replication forks (Labib & Hodgson, 2007).

A typical example of a chromosomal abnormality is the Philadelphia chromosome, which induces protein fusion and causes chromosomal translocation between chromosomes 9 and 22 at the *BCR* and *ABL1* genes, creating a novel chimeric *ABL/BCR* fusion gene, which results in the abnormal tyrosine kinase (TK) activity of ABL1 protein. The t(9;22) is associated with chronic myelogenous leukaemia (CML) (Meaburn et al., 2007; Nambiar & Raghavan, 2011; Zheng, 2013; Tabarestani & Movafagh, 2016). Another well-understood example is the translocation between chromosomes 14 and 18 t(14;18), which leads to the over production of BCL2, the anti-apoptotic protein. This over production results in a survival benefit for the cells and a potential gain in additional mutations and alterations that induce follicular lymphoma (FL) (Nambiar et al., 2008; Nambiar & Raghavan, 2011; Raghavan & Lieber, 2006; Bakhshi et al., 1985).

Translin is a DNA binding protein that was first found to bind to breakpoint junctions of chromosomal translocations in various cases of lymphoid neoplasms in humans (see Section 1.11) (Aoki et al., 1995; Kasai et al., 1997). This discovery led to proposals that Translin is involved in mediating chromosomal rearrangement breakpoints (Gajecka et al., 2006). However, the mechanistic importance of Translin binding to breakpoint junctions in cancer has not yet been elucidated.

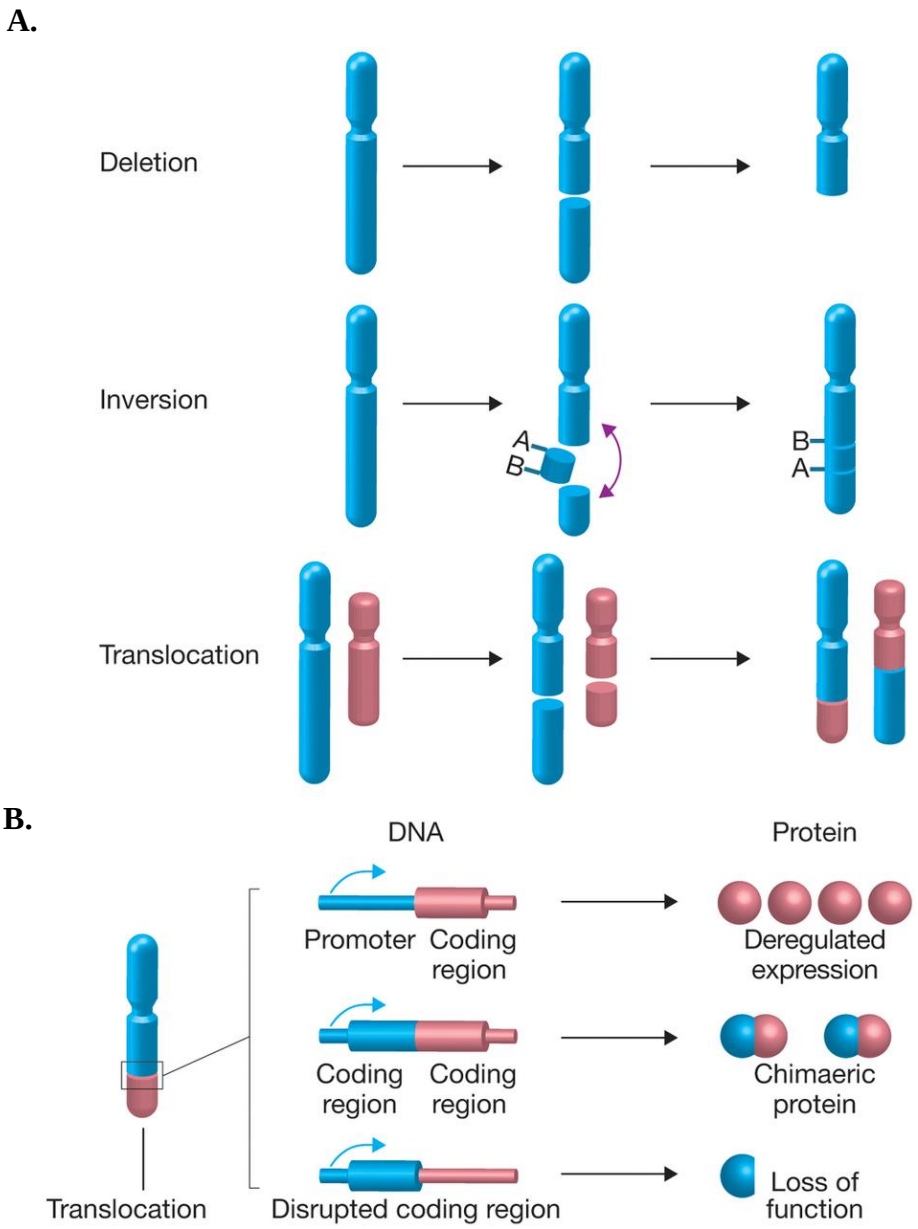

Figure 1.2 Examples of chromosome rearrangement and consequences

A. There are several types of chromosomal rearrangements, including deletion, inversion, and translocation. Deletion is known as the breakage of a chromosome, which leads to the removal of a segment of DNA. Inversion occurs when a segment of chromosome is disassociated from it, inverted 180 degrees and then re-introduced into the same location as the chromosome without the loss of DNA. Chromosomal translocations occur when two segments of DNA are swapped from non-homologous chromosomes.

B. A translocation may lead to the generation of oncogenes by producing a chimeric fusion protein, via the interruption and inactivation of a tumour suppressor gene or by the fusion of a tumour-promoting gene with a solid transcriptional promoter (adapted from Roukos & Misteli, 2014).

1.3 DNA replication

The cell cycle is composed of four distinct phases: G1, S, G2 and M. DNA replication is included in this process, which operates in the S phase when the parental DNA is copied before each cell division. Therefore, the faithful replication of DNA is crucial to ensure the correct transformation of genetic information to cell generations, which is essential in maintaining genomic stability (Gelot et al., 2015; Gadaleta & Noguchi, 2017; Kang et al., 2017; Stillman, 2008; Lujan et al., 2016; Mladenov & Iliakis, 2011; Petermann et al., 2010). In eukaryotes, the replication of the genome starts at multiple origins (particular genomic start sites enriched in AT content) on the chromosome (Kang et al., 2017; Parker et al., 2017; Duzdevich et al., 2015; Fragkos & Naim, 2017). The formation and activation of various complexes at replication origins are necessary for replicating DNA (Aves, 2009). In the early G1 phase, these origins are recognised and bound by a complex called origin recognition complex (ORC). When ORC is bound at these origins, it then serves as a platform for the loading of another group of proteins called pre-replicative complex (pre-RC), which occurs in the late G1 phase (Kang et al., 2017, Duzdevich et al., 2015). The pre-RC contains the conserved core replicative helicase, the mini-chromosome maintenance (MCM) protein complex. In addition to its activity in unwinding the double-stranded DNA at the origin (see later), MCM inhibits DNA from replicating more than once per cell cycle, and at least two copies of the MCM proteins are required to load at the replication origin to form a bidirectional replication fork (Remus & Diffley, 2009; Evrin et al., 2009; Duzdevich et al., 2015; Burgers & Kunkel, 2017). The activation of the MCM proteins is dependent on protein kinase activity, including Cdc7-Dbf4 kinases (DDK) and S-phase cyclin-depedent kinases (CDK), which guides the DNA replication initiation and progression (Leman & Noguchi, 2013; Evrin et al., 2009; Kang et al., 2017; Chang & Stirling, 2017; Burgers & Kunkel, 2017; Lei, 2005).

1.4 Replication fork progression

The replication fork is the point at which the DNA duplex (dsDNA) is unwound into two DNA single strands (ssDNA). In this process, the DNA helicase enzyme uses the energy of ATP hydrolysis to break the inter-strand hydrogen bounds, creating a Y-shape (Figure 1.3).

The stability of the unpaired ssDNA is preserved by a heterotrimeric complex that is called the replication protein A (RPA) (Stillman, 2008; Branzei & Foiani, 2007).

The two ssDNA strands, known as the leading and lagging strands, are the templates that are used by the replicative polymerases for base pairing in the synthesis of the new daughter strands. The leading strand is oriented in the same direction as the replication fork (3' to 5' direction), while the lagging strand is oriented away from the replication fork (5' to 3' direction); thus, the two strands are replicated in different processes. Because DNA replication proceeds in the 5' to 3' direction, the leading strand is replicated continuously, in which the primase enzyme adds a short RNA primer (10 nucleotides) to the 3' end of the strand. This short piece of RNA acts as the initial point of polymerase ε (epsilon) in the synthesis of the daughter strand (Figure 1.3). Because DNA polymerases can only synthesise DNA in one direction (5' to 3'), loops are formed on the lagging strand templates. The lagging strands are therefore replicated discontinuously (i.e., in a fragmented manner) in which multiple short RNA primers are added at different regions alongside the strand. Then pieces of DNA called Okazaki fragments (100–200 bases) are fused by polymerase δ (delta) between these RNA primers in the lagging strand (Figure 1.3). When both strands are made, all the RNA primers are removed from both strands by an exonuclease enzyme and then substituted by proper nucleotides. Next, the newly made strands are proofread in order to correct any mistakes and mispairings that may occur during this process. Finally, the Okazaki fragments are joined together by the DNA ligase enzyme to form two continuous double strands (Leman & Noguchi, 2013; Pellegrini & Costa, 2016; Berti & Vindigni, 2016; Stillman, 2008; Lujan et al., 2016; Burgers & Kunkel, 2017; Clark & Pazdernik, 2012; Chilkova et al., 2007).

. In addition to the indicated core factors, many other key protein complexes, such as the fork protection complex (FPC), the replication factor C clamp loader (RFC) and the proliferating cell nuclear antigen (PCNA) are involved in both the initiation and the replication fork progression to assemble an extensive conglomerate that is termed the replisome. Checkpoint proteins are also required, and they associate with the replisome, which functions as a surveillance mechanism in DNA replication and genome stability (Leman & Noguchi, 2013).

Replication fork monitoring and regulation are essential for the cell to preserve genomic stability such that interfering with the replisome could result in replication fork arrest (Kang et al., 2017; Lin & Pasero, 2012). Arrested forks are extremely recombinogenic. When they are subjected to the induction of unscheduled HR, chromosomal translocation could result, leading to cancer (So et al., 2017; Gelot et al., 2015; Gadaleta & Noguchi, 2017; Pryce et al., 2009; Duch et al., 2013; Castel et al., 2014; Brambati et al., 2015).

The DNA replication fork is affected by DNA lesions that originate from various endogenous and exogenous sources (Berti & Vindigni, 2016; Jones & Petermann, 2012). In addition to DNA lesions, replication fork progression is blocked through natural impediments that function as replication fork barriers (RFB) (Gadaleta & Noguchi, 2017), which inhibit or stall the progression of DNA forks, leading to fork collapse, which promotes HR and drives genome instability if it is not controlled accurately (Gadaleta & Noguchi, 2017; Pryce et al., 2009; Lin & Pasero, 2012). An example of an element of natural impediment that could stall the DNA replication fork and induce genomic instability is the conflict between replication and transcription machinery, which may result in the replication stress that is associated with breakpoints and chromosomal instability (Brambati et al., 2015; Koyama et al., 2017; Chang & Stirling, 2017; Ren et al., 2015; Fragkos & Naim, 2017; Garcia-Muse & Aguilera, 2016; Gaillard & Aguilera, 2016; Aguilera & Gaillard, 2014).

Stalled DNA replication forks could also occur in response to drugs, such as the ribonucleotide reductase inhibitor hydroxyurea (HU), which blocks DNA synthesis by inhibiting dNTP synthesis **(**deoxyribonucleotide triphosphate**)** but permits the replicative helicase to carry out the process by unwinding the parental DNA duplex. This response may result in the collapse of the replication forks and consequently the formation of DSBs (Labib & Hodgson, 2007; Petermann et al., 2010; Aguilera & García-Muse, 2013).

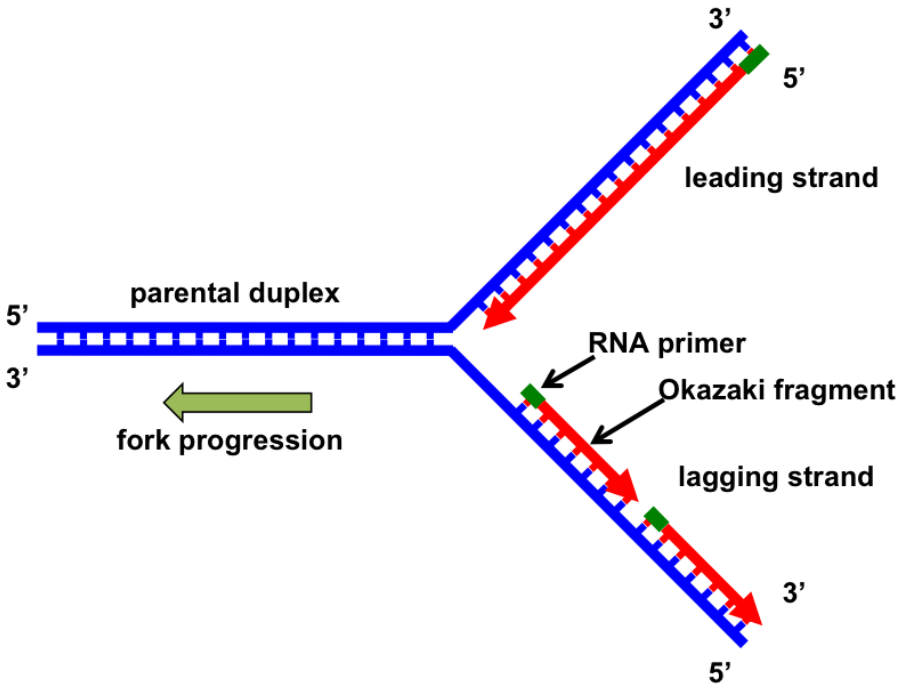

Figure 1.3 Basic Schematic demonstration of a replication fork
Replication of DNA proceeds in the 5' to 3' direction, resulting in the continuous replication of the leading strand and discontinuous replication in short sections of the lagging strand. The initiation of leading strand synthesis as well as each Okazaki fragment on the lagging strand require the presence of short RNA primers (green) (adapted from Leman & Noguchi, 2013).

1.5 Replication fork barriers and recombination

In the S phase, the same DNA template is used by both the replication and the transcription machineries (Bermejo et al., 2012; Brambati et al., 2015; Duch et al., 2013; Lin & Pasero, 2012). Therefore, interference between the two processes is unavoidable. A collision between the two activities may lead to stalling the replication fork, which may collapse if the issue is not resolved (Felipe-Abrio et al., 2015; Koyama et al., 2017; Ren et al., 2015; Fragkos & Naim, 2017; Lin & Pasero, 2012; Gadaleta & Noguchi, 2017; Aguilera & García-Muse, 2013). The collapse of the replication fork may lead to the formation of DSBs (Gadaleta & Noguchi, 2017). The collapsed replication fork needs to be repaired by HR, which may result in chromosomal rearrangements, including translocations (Felipe-Abrio et al., 2015; Castel et al., 2014; Lin & Pasero, 2012).

Because the directional polarity of the synthesis of both DNA and RNA is the same, a head-to-head collision between replication and transcription occurs on the lagging strand template, whereas a co-directional collision (head-to-tail) between the two occurs on the leading strand template (Bermejo et al., 2012; Brambati et al., 2015; Oestergaard & Lisby, 2017). Although both collisions affect the stability of the replication fork, head-on (head-to-head) collisions are thought to be more damaging (Bermejo et al., 2012; Brambati et al., 2015; Chang & Stirling, 2017; Lin & Pasero, 2012). For example, recombination rates are higher due to head-on collisions than in co-directional collisions (Oestergaard & Lisby, 2017).

Transcription–replication conflicts have been examined extensively in a wide range of organisms, including bacteria and yeast. Several strategies and mechanisms have been identified as regulating the coordination between the two machineries and limiting the induction of recombinogenic lesions (Ren et al., 2015; Brambati et al., 2015; Bermejo et al., 2012; Felipe-Abrio et al., 2015; Gadaleta & Noguchi, 2017). In bacteria, essential and highly transcribed RNA polymerase II genes are found on the leading strand template. Therefore, the transcription–replication co-orientation of the bacterial genome provides a feature that assists in avoiding head-on collisions between the two machineries, which leads to maintaining genomic stability (Brambati et al., 2015; Srivatsan et al., 2010; Bermejo et al., 2012; Felipe-Abrio et al., 2015).

Nonetheless, bacteria develop various mechanisms to prevent and resolve the collisions between the two machineries. These mechanisms include the removal of proteins and/or R-loops (DNA-RNA hybrids caused by the nascent transcript) by the accessory DNA helicases of the replisome. In addition, transcription regulators are involved in this process by rescuing stalled or backtracked RNA polymerases (Brambati et al., 2015).

In eukaryotes, collisions between transcription and replication can be observed at distinct genomic loci: for example, tRNA genes and rDNA locus (Mirkin & Mirkin, 2007). Many tRNA genes have been identified in eukaryotic genomes, including 186 tRNA genes in *Schizosaccharomyces pombe*. In addition to their contribution to the translation process, the *S. pombe* tRNA genes function as chromatin barriers in the centromeres (see Section 1.8) (Gadaleta & Noguchi, 2017). It has been noted that the sites of tRNA genes (tDNA) display greater levels of genomic instability when DNA replication is inhibited, which may suggest that this instability is somehow linked to DNA replication. This effect was later confirmed by the finding that *S. pombe* tRNA genes inserted within *ade6*$^{+}$ affected and slowed the progression of replication forks, and tRNA genes have been demonstrated to provide strong RFB activity (Pryce et al., 2009; Labib & Hodgson, 2007). Therefore, it is suggested that head-on (head-to-head) collisions between RNA polymerase III, which mediates the transcription of tRNA genes and the replication machinery (i.e., replisome) results in the DNA replication fork instability (Bermejo et al., 2012; Mirkin & Mirkin, 2007; Pryce et al., 2009; Lin & Pasero, 2012). Importantly, the DNA replication-associated fragile sites in *Saccharomyces cerevisiae* have been found to be enriched for tRNA genes, which implicates these genes in the formation of recombinogenic lesions (Admire et al., 2006; Pryce et al., 2009).

In eukaryotes, similar to bacteria, DNA helicases are necessary in replication to avoid obstacles that disturb the completion of the replication fork. For example, in *S. cerevisiae*, DNA helicase Rrm3 is required to resolve collisions between transcription and replication (Felipe-Abrio et al., 2015). However, unresolved collisions between replication and transcription may result in an accumulation of RNA polymerases that mediate transcription, which cause the fork to collapse, resulting in subsequent DNA damage and genomic instability (Ren et al., 2015; Castel et al., 2014).

In the fission yeast *S. pombe*, the RNA interference (RNAi) pathway is required in the pericentromeric heterochromatin to release the stalled RNA polymerase II (pol II), which is due to transcription–replication encounters during S phase. The failure to remove pol II is associated with stalled replication forks, which consequently induces genome stability (Castel et al., 2014; Ren et al., 2015; Zaratiegui et al., 2011).

Outside the pericentromeric regions, a mechanism in *S. pombe* has been recently identified as resolving replication–transcription collisions, in which the RNAi component Dcr1, independent of the canonical RNAi pathway, induces the termination of transcription at sites of replication stress and DNA damage (i.e., sites of collision), which leads to preserving genome integrity (Ren et al., 2015; Castel et al., 2014). Dicer is an enzyme that possesses endonuclease activity, which cleaves double-stranded RNA (dsRNA) molecules into 20–25 nucleotide (nt)-long siRNA duplexes and then proceeds through the other components of the RNAi machinery to mediate gene silencing (see Section 1.10). Additionally, Dicer has been identified as a haploinsufficient tumour suppressor gene, and mutations of this gene are associated with cancer (see Section 1.14) (Kumar et al., 2009; Swahari et al., 2016). The specific role of *S. pombe* Dcr1 promotes the termination of transcription by releasing RNA polymerase II from the 3' end of the highly transcribed RNA pol II genes and, unexpectedly, from the antisense transcription of rDNA and tDNA (tRNA genes), which are mainly transcribed by RNA polymerase I and RNA polymerase III, respectively, leading to promotion of fork progression (Castel et al., 2014). However, in the absence of Dcr1, HR is necessary to resolve the collision between RNA pol II and the replisome, and restart the replication fork, which may lead to chromosomal instability and rearrangements, including translocations, contributing to tumorigenesis (Figure 1.4) (Castel et al., 2014; Brambati et al., 2015). In addition, Castel et al. (2014) found that the loss of Dcr1 results in the accumulation of RNA:DNA hybrids (R loops) at the rDNA locus, which is likely due to collision between replication and transcription (Castel et al., 2014).

RNA:DNA hybrids are formed when nascent RNA transcripts are re-annealed to their template DNA strand, forming an R-loop. R loops were thought to occur naturally during replication and transcription (Fragkos & Naim, 2017; Aguilera & Garcia-Muse, 2012; Felipe-Abrio et al., 2015; Oestergaard & Lisby, 2017; Wahba et al., 2013; Mirkin & Mirkin, 2007; Ohle et al., 2016; Santos-Pereira & Aguilera, 2015).

However, several studies on prokaryotes and eukaryotes have demonstrated that the accumulation of RNA:DNA hybrids are a major internal source of DNA damage, which can influence the functioning of cells and threaten genomic stability (Brambati et al., 2015; Aguilera & Garcia-Muse, 2012; Felipe-Abrio et al., 2015; Bermejo et al., 2012; Lin & Pasero, 2012; Ohle et al., 2016; Santos-Pereira & Aguilera, 2015). The RNA:DNA hybrid is a central element that blocks progression of the replication fork and transcription elongation, which leads to replicative stress and the formation of DSBs (Bermejo et al., 2012; Castel et al., 2014; Lin & Pasero, 2012; Ohle et al., 2016). Moreover, the hybrids that accumulated at the sites of transcription–replication collision are highly recombinogenic, which results in recruiting HR factors, including Rad52, indicating that the misregulation of R-loops can potentially promote the initiation and progression of cancer (Castel et al., 2014; Wahba et al., 2013; Lin & Pasero, 2012; Brambati et al., 2015). Thus, *S. pombe* Dcr1 plays a novel role in removing RNA:DNA hybrids, which also resolved transcription–replication collision. This new functional role of Dicer may be ascribed to its previously identified function as a tumour suppressor (Kumar et al., 2009; Swahari et al., 2016). Interestingly, many factors in the pathways that mediate the resolution of transcription–replication collision are tumour suppressors, including RAD52 (Ren et al., 2015).

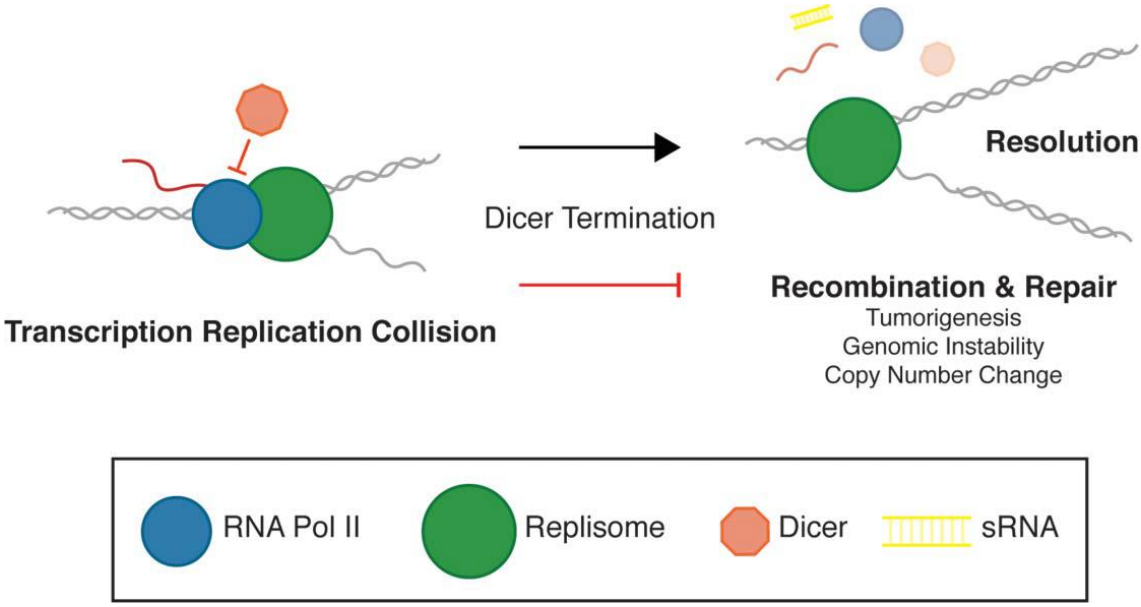

Figure 1.4 *S. pombe* strategy that resolves the replication–transcription collisions to preserve genomic integrity

The RNA pol II mediates transcription (blue) –replisome (replication machinery) (green) collisions lead to replication fork progression stalling and the accumulation of pol II at the template. At sites of collisions, Dcr1 (orange) functions to terminate transcription by releasing RNA pol II, leading to the completion of replication and the inhibition of the small RNA (sRNA) (yellow) generated by Dcr1 in loading into Ago1. However, in the absence of Dcr1, HR is required to resolve the collision and restart the replication fork, which may lead to chromosomal instability and copy number change, thus inducing cancer (adapted from Ren et al., 2015).

In order to avoid the formation of unscheduled RNA:DNA hybrids, eukaryotic cells have developed various mechanisms to degrade these hybrids, such as RNaseH proteins, which are a class of enzymes that destroy the RNA moiety of RNA:DNA hybrids, leading to the suppression of replication stress and the maintenance of genomic integrity (Fragkos & Naim, 2017; Wahba et al., 2013; Brambati et al., 2015; Ohle et al., 2016). Alternatively, these hybrids are degraded by RNA-DNA helicases, such as Sen1 in *S. cerevisiae*, by unwinding RNA-DNA hybrids or by minimising their formation (Santos-Pereira & Aguilera, 2015).

Remarkably, a recent finding in *S. pombe* challenged the current proposal that the presence of RNA-DNA hybrids only induces DNA damage genomic instability. The findings indicated an unexpected positive role of these hybrids during the DNA repair process, which is essential to maintain genome integrity. It has been found that RNA:DNA hybrids are required in moderate amounts (not too much and not too little) in order to allow the proficient completion of the DSB repair facilitated by HR (see Section 1.6.2). Ohle et al. (2016) found that RNA:DNA hybrids regulated the end resection process, particularly in the recruitment of RPA complex to the resected DNA strand. This observation indicated that these hybrids need to be both produced and removed, a process that is mainly dependent on RNase H1 (Rnh1) and RNase H2 (Rnh2.1) (Figure 1.5) (Ohle et al., 2016; Plosky, 2016). This surprising observation should be confirmed in further intensive studies on *S. pombe* and beyond to identify any other factors that contribute to the formation of RNA:DNA hybrids at breaks and to explore other roles played by these hybrids to preserve genome stability. Although many factors and mechanisms that inhibit RNA:DNA hybrid formation are well recognised, very little is known about the mechanisms that induce the formation of these structures (Wahba et al., 2013; Lin & Pasero, 2012).

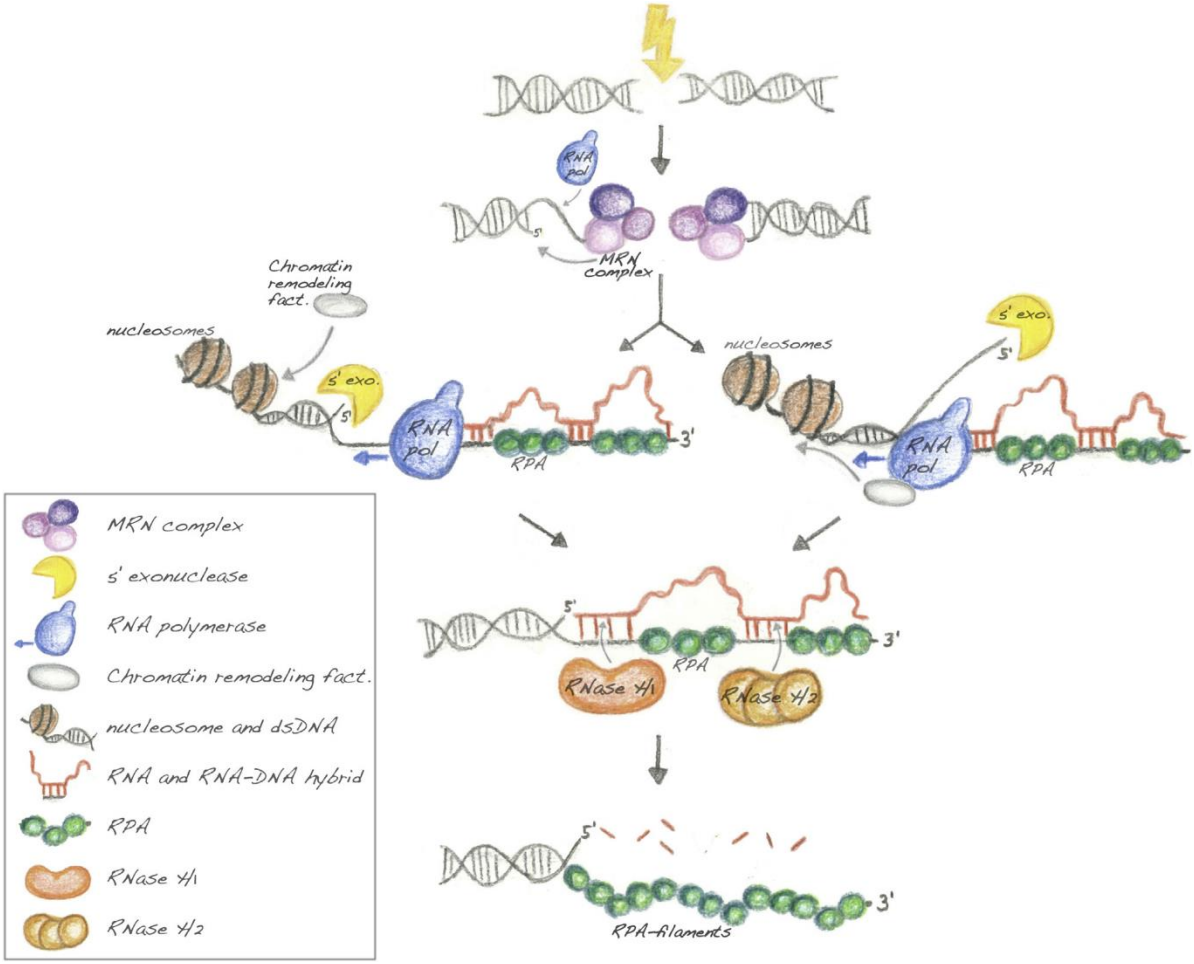

Figure 1.5 A Suggested model for the role of RNA-DNA hybrids in the repair of DSBs mediated by HR

Once DSB is formed, the MRN complex is recruited to the broken DNA ends, and it interacts with other factors including exonuclease Exo1 to mediate (5'→3') resection at the DSB ends, resulting in the creation of single-stranded DNA (ssDNA) overhangs with 3' OH ends. RNA Pol II is recruited to the ssDNA overhangs and initiates transcription. The nascent RNA transcripts are reannealed to their template DNA strand (ssDNA), forming RNA:DNA hybrids, which in turn may control the end resection process by terminating RNA Pol II transcription, and recruiting the ssDNA-binding RPA complex to the resected DNA strand. Subsequently, these RNA-DNA intermediates are degraded by RNase H enzymes (RNase H1 and RNase H2) to obtain the complete loading of RPA on ssDNA overhangs and to allow the efficient completion of the process of DSB repair (see Section 1.6.2) (adapted from Ohle et al., 2016).

1.6 DNA double-strand breaks repair pathways

The genome is continuously assaulted by various endogenous and exogenous sources, which can generate tens of thousands of DNA lesions, thus inducing DNA damage and genomic instability (Takagi, 2017; Brugmans et al., 2007; Tian et al., 2015; Davis & Chen, 2013). Therefore, to maintain genomic integrity, it is crucial for the cells to repair the DNA lesion rapidly and precisely to avoid the further mutations and genomic rearrangements that ultimately result in cancer (Uckelmann & Sixma, 2017; Tian et al., 2015; Davis & Chen, 2013; Mladenov & Iliakis, 2011). This damage includes DSBs, which are considered the most hazardous DNA lesion, in which both strands of DNA are broken, potentially leading to chromosome rearrangements (Schwartz et al., 2005; Chang et al., 2017; Davis & Chen, 2013; Mladenov & Iliakis, 2011; Ohle et al., 2016). DSBs can be generated by numerous external elements, including IR such as gamma rays and X-rays. However, programmed DSBs also occur naturally during certain recombination processes, such as meiosis and immune cell development (Brugmans et al., 2007; Takagi, 2017; Tian et al., 2015; Lieber, 2010). Additionally, during the normal S phase, DNA replication forks can be stalled when the DNA template is affected by damage, which results in the generation of non-programmed DSBs to restart the replication fork (Brugmans et al., 2007; Gadaleta & Noguchi, 2017; Lieber, 2010; Davis & Chen, 2013). To repair chromosomal DSBs, eukaryotic cells have evolved highly efficient specialised DNA repair pathways that are conserved from human to yeast, including homologous recombination (HR) and non-homologous DNA end joining (NHEJ) (Brugmans et al., 2007; Lieber, 2010; Davis & Chen, 2013; Zaboikin et al., 2017; Zhao et al., 2017; Ohle et al., 2016). Whether HR or NHEJ is the pathway required to repair breaks is controlled partly by the cell cycle, and the incorrect choice of the repair pathway may lead to cancer. For example, in the S and G2 phases, the HR pathway precedes the DNA lesion because a homologous template (a sister chromatid) is available to be used as a repair template although NHEJ pathway can also be initiated during S/G2 when a homology donor is not available near a DSB. However, NHEJ repair is predominant outside S/G2, by which the broken ends of DNA are directly re-joined without the need for template repair (i.e., a homology donor) (Brugmans et al., 2007; Takagi, 2017; Tian et al., 2015; Lieber, 2010; Davis & Chen, 2013; Zaboikin et al., 2017; Zhao et al., 2017).

1.6.1 The non-homologous DNA end joining repair pathway

NHEJ is a direct and simple mechanism in which DNA integrity is restored by joining the two DNA ends without requiring a homologous template (Mladenov & Iliakis, 2011; Peng & Lin, 2011). However, it is known as an error-prone repair system because it may be associated with small-scale mutations and chromosomal rearrangement. This repair pathway potentially mediates the re-ligation of any broken DNA ends. Unlike HR, its activation is not limited to a specific cell cycle phase (Davis & Chen, 2013; Daley et al., 2005; Zaboikin et al., 2017; Ohle et al., 2016; Peng & Lin, 2011). Numerous proteins are used in the NHEJ repair pathway to recognise, resect, polymerise and ligate the two broken DNA ends. However, in this process, faults can potentially result in translocations and telomere fusion (Chang et al., 2017; Espejel et al., 2002). These factors include the Ku heterodimer (Ku70-Ku80 subunit), DNA-dependent protein kinase catalytic subunit (DNA-PKcs), Artemis, X-ray repair cross-complementing protein 4 (XRCC4), DNA ligase IV (LigIV), and XRCC4-like factor (XLF) (Boboila et al., 2012).

In higher eukaryotes, the Ku70–Ku80 heterodimer initiates the process by recognising and binding to the free ends of the DSB DNA. The Ku heterodimer then acts as platform for the binding of the core factors of the NHEJ machinery to the target damage site, including DNA-PKcs. When DNA-PKcs is recruited to the broken DNA ends, an active Ku70/Ku80/DNA-PKcs complex is formed, which leads to the phosphorylation and recruiting of the endonuclease Artemis. The repair continues by cleaving any overhangs at the DNA ends, which make it compatible with the re-ligation process (Davis & Chen, 2013; Mladenov & Iliakis, 2011; Boboila et al., 2012; Grabarz et al., 2012; Li & Xu, 2016; Khalil et al., 2012).
It has been proposed that in many organisms the MRN complex (MRE11-RAD50-NBS1), which also mediates the HR pathway (see later), as well as DNA polymerases and other nucleases, may be required to process the ends before ligation (Boboila et al., 2012; Manolis et al., 2001). In the final step, XRCC4-DNA LigaseIV complex is recruited to ligate the DNA ends, which results in the restoration of the integrity of the DNA.

XLF interacts directly with XRCC4/ LigaseIV complex, but its precise function in NHEJ pathway repair is still unknown. However, it may be involved in stimulating the ligation activity of the XRCC4/ LigaseIV complex (Figure 1.6) (Grabarz et al., 2012; Davis & Chen, 2013; Mladenov & Iliakis, 2011; Boboila et al., 2012; Khalil et al., 2012).

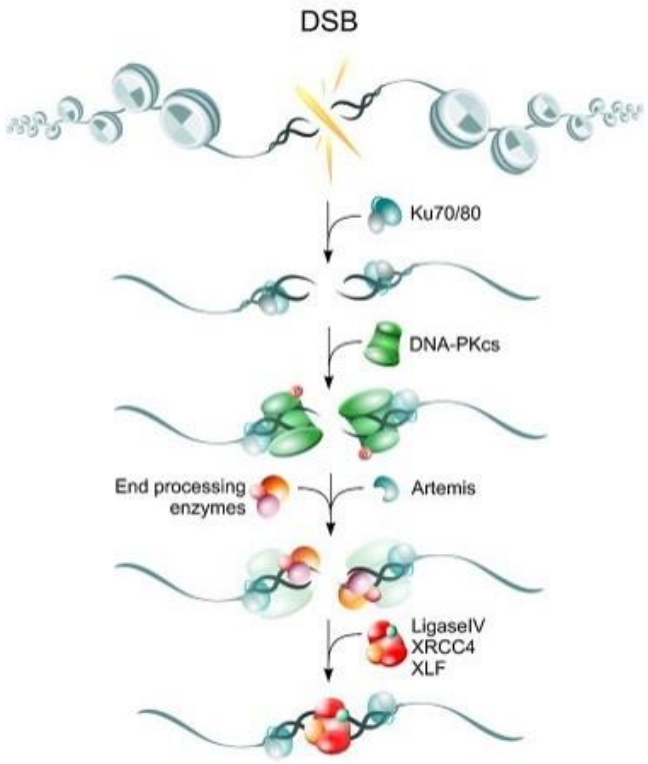

Figure 1.6 Summary of the main stages of the NHEJ repair pathway
Broken DNA ends are recognised and bound by the Ku70/80 complex, which then recruits the DNA-PKcs that stimulate the end processing by phosphorylating Artemis nuclease. Artemis processes the DNA ends to be appropriate for the ligation step. Finally, LigIV/XRCC4/XLF complex acts to re-join the broken DNA ends (adapted from Mladenov & Iliakis, 2011).

1.6.2 The homologous recombination repair pathway

HR is described as a high-fidelity repair pathway that requires a homologous template (e.g., a sister chromatid) for repairing DSBs. This mechanism has been recognised as generally error free (Zhao et al., 2017; Essani at al. et al., 2015; Khalil et al., 2012; Zhao et al., 2017). HR is crucial in maintaining genomic integrity and diversity by accurately repairing DSBs that are generated by exogenous factors, as well as repairing impaired DNA replication forks. In addition, it participates in telomere maintenance by repairing incomplete telomeres, such as in the absence of telomerase. Furthermore, HR is required during meiosis for chromosomal pairing and exchanging, which enables genetic diversity and reductional segregation (Symington & Gautier, 2011; Kasparek & Humphrey, 2011; McFarlane et al., 2011; Krejci et al., 2012; Biessmann & Mason, 1997; Li & Heyer, 2008).

DSBs can be repaired by a number of HR repair pathways, including double-strand break repair (DSBR), synthesis-dependent strand annealing (SDSA), and break-induced replication (BIR) (Sakofsky et al., 2012). All the three pathways are initiated by the formation of a DSB that is detected by the conserved Mre11, Rad50 and Nbs1 (MRN complex) (Li & Heyer, 2008; Khalil et al., 2012), which may lead to the requirement of the checkpoint kinase Ataxia telangiectasia mutated (ATM). ATM then phosphorylates and activates different elements of DNA repair, including all members of the MRN complex. It also activates the full DNA damage response in the cell (Ohle et al., 2016; Peng & Lin, 2011; Khalil et al., 2012; Talens et al., 2017). In addition, the MRN complex interacts with exonuclease Exo1 or the Dna2-Sgs1/BLM complex to mediate (5'→3') resection at the DSB ends, which leads to the creation of single-stranded DNA (ssDNA) overhangs with 3ˈ OH ends (Ohle et al., 2016; Suwaki et al., 2011; Zhao et al., 2017). The formed ssDNA tails are bound by the DNA replication protein A (RPA), which prevents the formation of a secondary structure that could interfere with RAD51 at the ssDNA tails (Heyer et al., 2010; Khalil et al., 2012; Suwaki et al., 2011). Rad52/BRCA2 function to aid in replacing the RPA complex by the pivotal HR protein RAD51, which forms a nucleoprotein filament on the ssDNA (Ohle et al., 2016; Zhao et al., 2017; Talens et al., 2017).

The RAD51 recombinase filament searches for and invades a homologous intact duplex DNA, where it forms a displacement loop (D-loop) (So et al., 2017; Grabarz et al., 2012; Li & Heyer, 2008; Suwaki et al., 2011). The 3' end of the invading strand, within the D-loop, is extended by DNA polymerases. Once the invading strand is extended, there are three main proposed pathways HR mechanism (Figure 1.7).

In the DSBR pathway, the extended invading strand can be annealed with the other end of the DSB, and this annealing results in the formation of a double Holliday junction (dHJ) (Lord & Ashworth, 2016; Li & Heyer, 2008; Essani et al., 2015; Zhao et al., 2017). On one hand, the resolution of dHJ can be processed either by the detachment of the two sets of strands, which generates a non-crossover product, or by its endonucleolytic cleavage facilitated by resolvases, which results in a crossover event (Figure 1.7). On the other hand, the Holliday junction can be dissolved by a pathway that involves BLM-promoted branch migration and TOPOIIIα, resulting in non-crossover event (Khalil et al., 2012; Essani et al., 2015; Li & Heyer, 2008; Suwaki et al., 2011; Zhao et al., 2017). In the SDSA pathway, the D-loop can be unwound and the extended invading strand re-anneals with the second end of the DSB, and DNA synthesis completes repair by using the re-annealed strand as a template. Unlike DSBR pathway, only non-crossover event can be generated in the SDSA pathway, which decreases the possibility of generating chromosomal rearrangements (Figure 1.7) (Heyer et al., 2010; Sugiyama et al., 2006). However, in some cases, if there are collapsed replication forks or in lengthening of telomeres (in the absence of telomerase), for example, a broken DNA may have only one repairable end. This leads to the activation of the break-induced replication (BIR) pathway in order to rescue chromosomal integrity (Mehta & Haber, 2014; MalkovaIra, 2013; Sakofsky et al., 2012). In this pathway, the formed D-loop can become a replication fork that can copy DNA sequence distal to the site of the donor molecule up to the end of the chromosome. For complete DNA replication, BIR needs the synthesis of both leading and lagging strands (Figure 1.7) (Llorente et al., 2008; Sakofsky & Malkova, 2017; Heyer et al., 2010; Malkova & Ira, 2013).

BIR is thought to be responsible for mediating alternative lengthening of telomeres (ALT), a mechanism that is utilised by telomerase-compromised tumour cells to preserve their telomere length (Sakofsky et al., 2012; Roumelioti et al., 2016). In addition, a very recent finding has shown that DSBs that occur at sub-telomeric regions are repaired by BIR (Batte et al., 2017). Moreover, in *S. cerevisiae*, it has also been proposed that the accumulation of R-loops at DNA damage sites such as rDNA induces repair by BIR (Amon & Koshland, 2016).

Although BIR is crucial for restarting the stalled replication forks and preserving telomeres, it can, however, induce chromosomal instability by causing an extensive loss of heterozygosity (LOH) (for example, when the DSB end invades a homologue rather than a sister chromatid molecule). In addition, BIR can generate complex genomic rearrangements, including non-reciprocal translocations (for example, when the invasion of the broken DNA end is initiated at a non-allelic chromosomal position) (Llorente et al., 2008; MalkovaIra, 2013; McEachern & Haber, 2006; Hastings et al., 2009; Sakofsky et al., 2012; Sakofsky & Malkova, 2017).

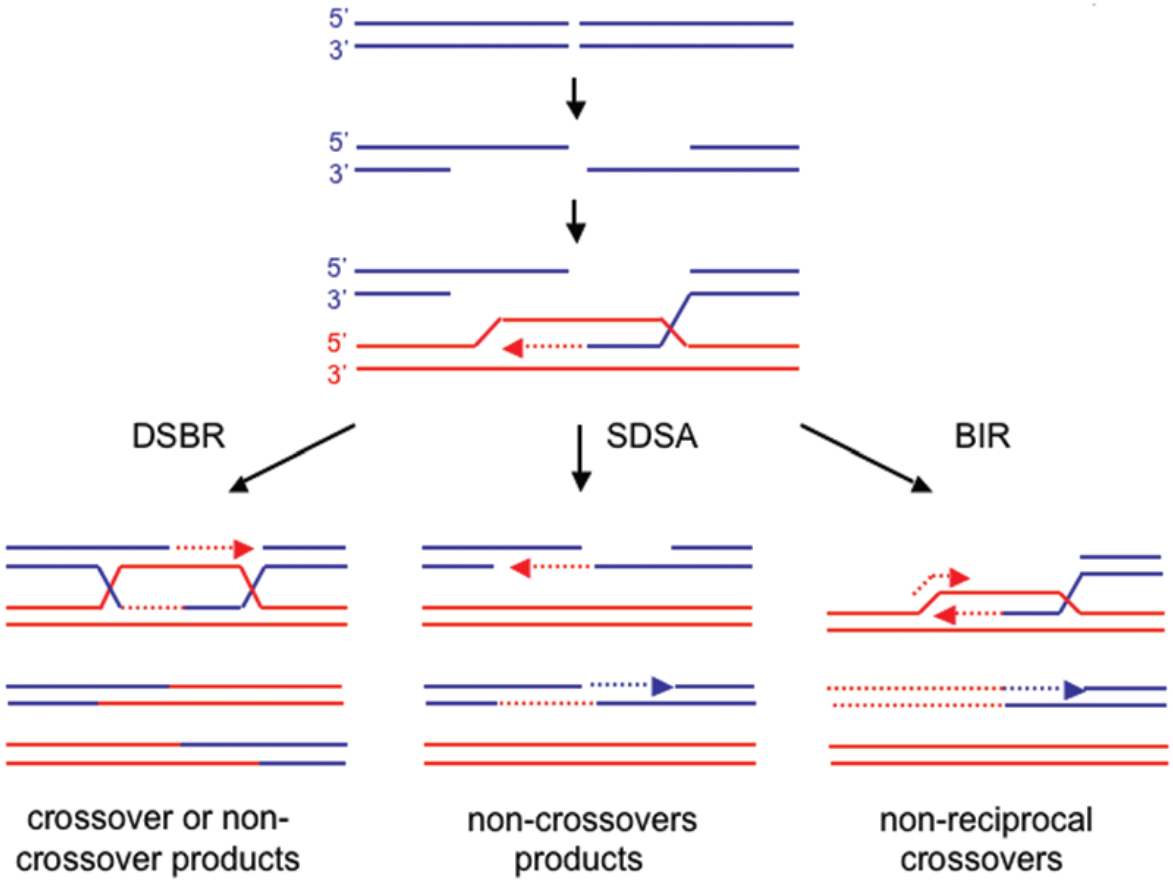

Figure 1.7 Schematic models of the DSB repair by HR pathways
After recognition of the DSB, all three pathways initiated by 5'→3' resection at the broken ends. Once the homologous sequence is found, one ssDNA 3' end invades the homologous template which results in the formation of D-loop. After priming DNA synthesis, the extended invading strand can be annealed with the other end of the DSB, which results in the formation of a double Holliday junction (DSBR pathway). The resolution of HJ may be processed by a resolvase, such as GEN1, SLX1/4 Mus81-Eme1, which can lead to a non-crossover or a crossover recombination product. However, the dissolution of HJ is processed by a mechanism involving BLM/ TOPOIIIα complex, leading to non-crossover product. Alternatively, the extended invading strand may be unwound and re-anneals with the other end of the DSB, and DNA synthesis completes the repair (SDSA pathway), resulting in non-crossover products. In the BIR pathway, strand invasion can result in the creation of a complete (unidirectional) replication fork that can copy all DNA information distal to the site of homology until the end of the chromosome. Repair by BIR can lead to non-reciprocal crossovers. Arrowheads show 3' ends and dashed lines represent newly synthesised DNA (adapted from Llorente et al., 2008).

1.7 Chromatin: a basic overview

Chromatin is a highly organized nucleoprotein complex in which DNA is packaged and compacted (Shen et al., 2017; Nikolov & Taddei, 2016; Tadeo et al., 2013). This structure is fundamental for protecting genetic information as well as for controlling almost every aspect of genome dynamics (Li & Zhang, 2012; Sadaie et al., 2004). The basic component of chromatin is the nucleosome, which consists of an octamer comprising two molecules of each of the four core histones (H3, H4, H2A, H2B), surrounded by approximately 147 DNA base pairs (Li & Zhang, 2012; Ordog et al., 2012; Hammond et al., 2017; Koyama et al., 2017; Westhorpe & Straight, 2014). The nucleosomes are connected together by linker DNA (20-80 bp) that is bound by another histone, Histone 1 (H1), which results in the formation of the highly structured chromatin within the nucleus (Koyama et al., 2017; Li & Zhang, 2012). Each histone has a flexible N-terminal tail, which is modified by a variety of enzymes, resulting in changes in chromatin structure, and consequently, DNA accessibility (Maeshima et al., 2014; Luger et al., 2012; Bauer & Martin, 2017; Hammond et al., 2017). Histone tails are subject to a number of post-translational modifications, including methylation and acetylation (Bauer & Martin, 2017; Hammond et al., 2017). Histone acetylation is mediated by histone acetyltransferases enzymes (HAT). These enzymes modify the chromatin structure by acetylating lysine residues in N-terminal histone tails, which results in changing the positive charge of the lysine to neutral. Because the neutral charge reduces the contact between the histone tails and the DNA, there is a disassociation of the DNA around the histones, and increased accessibility of the DNA by the transcription factors (TF) and other DNA binding proteins. In the reverse reaction, histone deacetylation occurs when histone deacetylases enzymes (HDAC) remove acetyl groups (Ac) from lysines, which results in the re-association of the DNA around the histones, causing gene repression. DNA can also undergo modification to regulate chromatin structure. DNA methylation at cytosine residues in gene promoters is mostly associated with gene silencing. DNA methylation is mediated by DNA methyltransferasaes enzymes (DNMT) in which a methyl group (CH_3) is added to the 5' position of cytosine bases at the CpG islands (i.e., genomic regions of DNA mostly located in a promoter gene enriched in GC content) altering it to 5-methylcytosine. This process results in the association of DNA with histones, inhibiting the TF from binding to DNA and consequently shutting down gene expression (Figure 1.8) (Hegarty et al., 2016; Labbé et al., 2016; Ballestar, 2011).

In addition to histone modifications, ATP-dependent chromatin remodelling complexes regulate the chromatin structure by restructuring nucleosomes (histone–DNA contacts). Several proteins are involved in this process by acting mainly in large complexes; for example, the conserved SWI/SNF complex. In this mechanism, the energy of ATP hydrolysis is used by these chromatin remodellers to change the assembly, compaction and positioning of nucleosomes, allowing the DNA to be more accessible to DNA binding factors, including TFs (Manning & Yusufzai, 2017; Zhang et al., 2015; Tang et al., 2010; Lusser & Kadonaga, 2003).

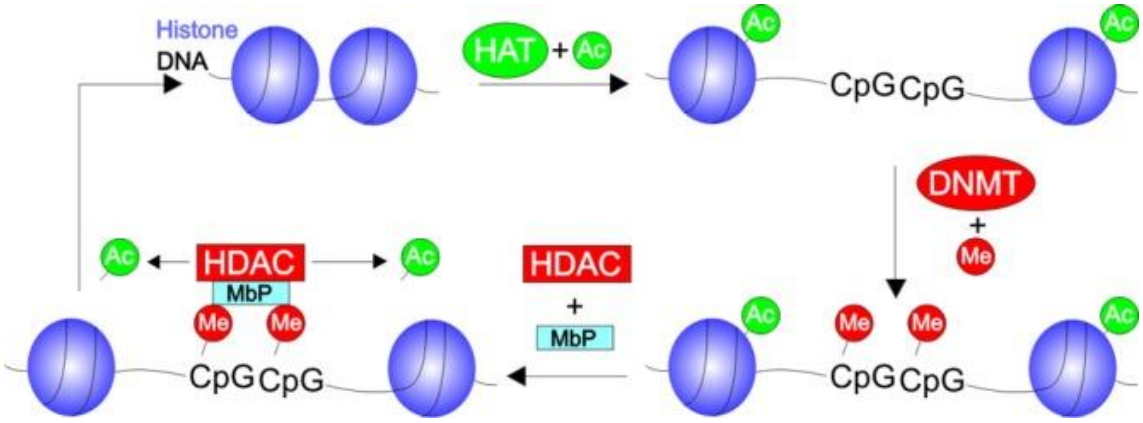

Figure 1.8 Schematic demonstration of epigenetic modification of gene expression
Epigenetic modification is regulated by a group of enzymes that modify chromatin structure, which affects gene expression. For instance, acetyl groups (AC) are added to histone H3 tails by histone acetylransferases enzymes (HAT), which leads to the loss of DNA around the histone, thus enhancing the transcription machinery. In the opposite effect, these ACs are removed by histone deacetylase enzymes (HDAC), which results in blocking gene expression. DNA methylation is the only epigenetic modification that directly targets the DNA. In this mechanism, DNA methyltransferases enzymes (DNMTs) methylate CpG islands. These methylated cytosines play a fundamental role in inhibiting transcription factors (TF) from binding, thus repressing gene expression. In addition, these methylated islands are involved in recruiting transcriptional repressor complexes that maintain transcriptional repression by deacetylation. Ac = Acetyl group; CpG = cytosine-phosphoric acid-guanine motif; DNMT = DNA methyltranferase; HAT = histone acetyltransferase(s); HDAC = histone deacetylase(s); Mbp = myelin basic protein (adapted from Hegarty et al., 2016).

Epigenetic modifications play a fundamental role in the assembly of chromatin structures, and thus, influence gene expression or silencing, which are reliant on the state of chromatin (Alper et al., 2012; Tadeo et al., 2013). Such epigenetic processes play a crucial role in regulating gene activation and silencing transcription at the chromatin level by directing how DNA and histones are compacted into the chromatin complex. For instance, DNA sequences that are loosely connected with histones have a more 'open' chromatin structure and are generally transcriptionally active; this is generally referred to as 'euchromatic'. In contrast, DNA sequences that are strongly associated with histones in a highly folded chromatin structure are transcriptionally inactive, and are associated with specific markers; these regions are generally referred to as 'heterochromatin' (Figure 1.9) (Gan et al., 2007; Woolcock & Buhler, 2013; Creamer & Partridge, 2011; Nikolov & Taddei, 2016). Thus, gene expression is influenced by the state of chromatin. Genes located within heterochromatic loci, including centromeres and telomeres, are transcriptionally silent. However, most genes found in euchromatin regions are transcriptionally active (Goto & Nakayama, 2012; Li & Zhang, 2012; Creamer & Partridge, 2011).

The best studies post-translational modifications that promote epigenetic regulation occur at histone H3 tails, important regulatory residues being H3 lysine 4 (H3K4) and H3 lysine 9 (H3K9) (Creamer & Partridge, 2011; Goto & Nakayama, 2012). Euchromatic formation is characterised by methylation of H3 lysine 4 (H3K4me) and acetylation of H3 lysine 9 (H3K9ac) (Yang & Ernst, 2017; Creamer & Partridge, 2011). However, methylation of H3 lysine 9 (H3K9me) is the core event in the establishment of heterochromatin (Alper et al., 2012; Creamer & Partridge, 2011; Audergon et al., 2015; Wang et al., 2016a; Buhler & Gasser, 2009; Tadeo et al., 2013), and this site is bound by the conserved Heterochromatin Protein 1 (HP1) (Figure 1.9) (Goto & Nakayama, 2012; Kusevic et al., 2017; Stunnenberg et al., 2015, Audergon et al., 2015; Tadeo et al., 2013).

Heterochromatin formation and maintenance are critical for controlling many genomic functions, including gene expression, and optimal centromere and telomere functions (Li & Zhang, 2012; Lejeune et al 2010; Cusanelli & Chartrand, 2015; Tadeo et al., 2013; Zocco et al., 2016). Heterochromatin assembly has conserved features in higher and lower eukaryotes, including humans and yeast (Zocco et al., 2016; Goto & Nakayama, 2012). The mechanisms of heterochromatin assembly were best characterized in the fission yeast *S. pombe* (Tadeo et al., 2013; Moazed, 2009).

Several loci in the *S. pombe* genome are heterochromatic, including centromeres, sub-telomeres, and the mating type locus (Figure 1.10) (Alper et al., 2012; Creamer & Partridge, 2011; Wang et al., 2016a; Tadeo et al., 2013). In *S. pombe*, heterochromatin loci are characterised by methylation of H3 lysine 9, which then functioned as the binding site for heterochromatin proteins, including Swi6 (the HP1 orthologue).

The RNA interference (RNAi) machinery is also required for the formation of heterochromatin, particularly at centromeres (see Section 1.10) (Greenwood & Cooper, 2012; Li & Zhang, 2012; Kanoh et al., 2005; Tadeo et al., 2013). Defects in the RNAi machinery significantly influence heterochromatin structures at centromeres (Sadeghi et al., 2015; Buhler & Gasser, 2009; Volpe et al., 2003; Volpe et al., 2002; Tadeo et al., 2013; Kanoh et al., 2005; Chan & Wong, 2012) but have only a weak effect on heterochromatin (Swi6 localisation) at telomeres (Kanoh et al., 2005; Tadeo et al., 2013). This indicates that factors or mechanisms other than RNAi contribute to the establishment of heterochromatin at the end of chromosomes (Kanoh et al., 2005). Additional studies revealed that the telomere-associated protein Taz1 (an orthologue of mammalian telomere repeat factors) is involved in heterochromatin formation at telomeres by inducing methylation of H3 lysine 9 by the histone methyltransferase Clr4, which results in the creation of a binding site for Swi6 (Buhler & Gasser, 2009; Kanoh et al., 2005). Additionally, mutation of *taz1*, a gene encoding a telomere length regulator, and any RNAi genes, such as *dcr1*, results in the loss of Swi6 localisation to the telomere, indicating that RNAi and Taz1 work in redundant pathways to establish heterochromatin (Swi6 localisation) at the telomere (Kanoh et al., 2005; Tadeo et al., 2013).

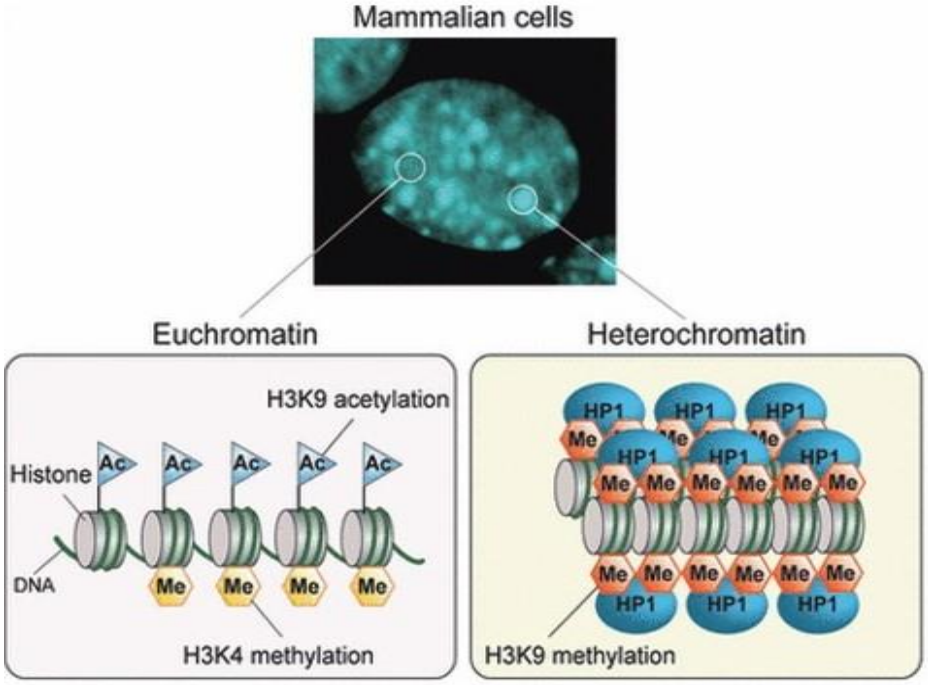

Figure 1.9 Chromatin modifications that lead to the formation of euchromatin or heterochromatin

Euchromatin formation is achieved by H3K9 acetylation and H3K4 methylation. In contrast, H3K9 methylation occurs in heterochromatin, which is an extremely compacted chromatin structure that appears to be located in the densely stained nuclear regions, as shown in mouse cells stained with DAPI (adapted from Goto & Nakayama, 2012).

1.8 Centromeres

During the eukaryotic cell cycle, proper chromosome segregation is crucial for transferring genetic material accurately to daughter cells (Mutazono et al., 2017; Brouwers et al., 2017). Failure in this process is associated with a wide range of genetic diseases such as cancer (Santaguida & Amon, 2015). Each chromosome of the eukaryotic genome has distinct regions that are essential for ensuring accurate segregation of chromosomes, including centromeres (Steiner & Henikoff, 2015; Westhorpe & Straight, 2014; Chan & Wong, 2012; Tadeo et al., 2013). A centromere is a chromosomal locus that provides a site where a multi-subunit structure, the kinetochore, is assembled, and which then serves as an attachment point for spindle microtubules. Thus, centromeres are essential for accurate segregation of chromosomes during mitosis and meiosis (Moreno-Moreno et al., 2017; Thakur et al., 2015; Buhler & Gasser, 2009; Westhorpe & Straight, 2014). Failure in maintaining centromere structure or function can cause mis-segregation via loss or gain of chromosomes, an outcome that is implicated in cancer (Volpe et al., 2002; Lee et al., 2013; Ekwall et al., 1999; Carmichael et al., 2004; Santaguida & Amon, 2015). Centromeres, which are in highly repetitive DNA regions, are heterochromatic and undergo H3K9 methylation (Buhler & Gasser, 2009; Schoeftner & Blasco, 2009; Zeng et al., 2010; Stimpson & Sullivan, 2010; Zocco et al., 2016; Wang et al., 2016a; Chan & Wong, 2012; Tadeo et al., 2013). Heterochromatin establishment at centromeres is vital for kinetochore function, and therefore, it is essential for the accurate segregation of chromosomes (Mutazono et al., 2017; Buhler & Gasser, 2009; Schoeftner & Blasco, 2009; Zeng et al., 2010; Stimpson & Sullivan, 2010; Schmidt & Cech, 2015). The RNAi machinery is required for mediating transcriptionally silenced heterochromatin formation at centromere regions in many organisms, including *S. pombe,* and thus, mutation of the central players of the RNAi pathway influences the functions of heterochromatin at the centromere. (Buhler & Gasser, 2009; Volpe et al., 2002; Chan & Wong, 2012; Tadeo et al., 2013). In *S. pombe,* centromeres range in size from 35–110 kb. They contain three different regions, including the central core (*cnt*) where the assembly of the kinetochore occurs. The *cnt* region consists of unique non-canonical nucleosomes that contain CENP-A (Cnp1) instead of H3. The *cnt* region is surrounded by two inverted innermost repeats (*imr*) containing transfer RNA (tRNA genes) that function as heterochromatin barriers (boundary elements) between the Cnp1 (*cnt*) and the Swi6 heterochromatic loci (Figure 1.11).

The *imr* regoins are additionally flanked by outer repeat regions (*otr*), which consists of two types of repeat sequences, *dg* and *dh*, which play a key role in the establishment of centromeric heterochromatin. In these repetitive sequences, Swi6 binds to H3K9me to initiate heterochromatin formation, and then the pericentromeric regions undergo silencing (Figure 1.11) (Takahashi et al., 2000; Creamer & Partridge, 2011; Buhler & Gasser, 2009; Shiroiwa et al., 2011; Thakur et al., 2015; Goto & Nakayama, 2012). Therefore, reporter genes, such as *ura4*$^{+}$, inserted into any of the centromere heterochromatic regions, will be affected by the heterochromatic status of transcription (Allshire et al., 1994; Buhler & Gasser, 2009). Additionally, mutation of any gene coding central RNAi components, including *ago1* and *dcr1*, influences centromeric transcripts from these repetitive sequences (*otr*), which results in the loss of centromeric H3K9 methylation and Swi6 localization, an outcome that causes mis-segregation of chromosomes (Buhler & Gasser, 2009; Volpe et al., 2002; Holoch & Moazed, 2015; Creamer & Partridge, 2011; Chan & Wong, 2012).

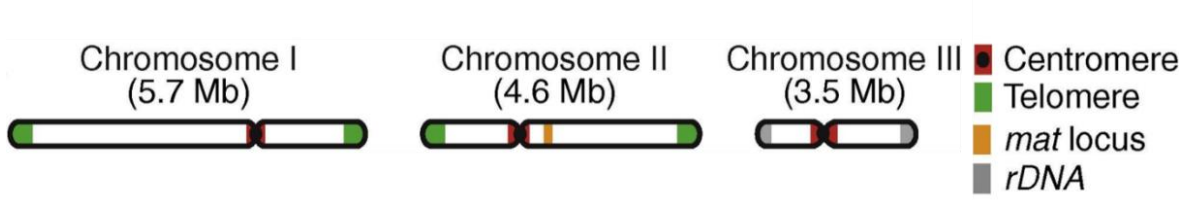

Figure 1.10 A map of the *S. pombe* chromosomes
There are only three chromosomes (three centromeres) in the *S. pombe* genome. They consist of 3.5, 4.6, and 5.7 Mb with different regions of heterochromatin, including centromeres, telomeres, the mating type (*mat*) and rDNA (adapted from Mizuguchi et al., 2015).

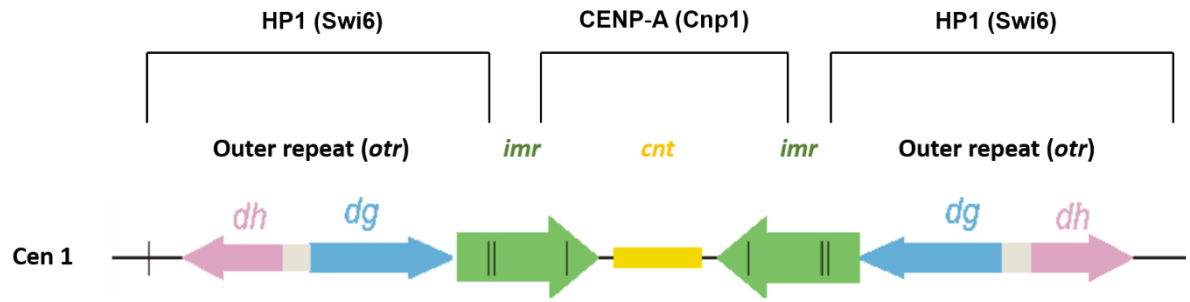

Figure 1.11 Schematic demonstration of *S. pombe* Centromere 1
The centromeric regions consist of two distinguishable regions, *cnt* (yellow) and *imr* (green). These regions are surrounded by the *otr* (light blue / purple) region, which consists of two repetitive sequences, *dh* (purple) and *dg* (light blue). The vertical lines within the *imr* regions represent the boundary elements (tRNA genes).

1.9 Telomeres

The ends of linear eukaryotic chromosomes are highly repetitive in nature, and covered with unique nucleoprotein-like structures termed telomeres (Chatterjee, 2017; Zocco et al., 2016; Wang et al., 2016a; Kupiec, 2014; Lorenzi et al., 2015). Telomere maintenance is regulated by a specialized reverse transcriptase enzyme termed telomerase, which is required for DNA extension at the ends of chromosomes (Hsu & Lue, 2017; Buhler & Gasser, 2009; Ohno et al., 2016). Telomeres protect the ends of chromosomes from degradation and from being recognised as DSBs (Maestroni et al., 2017; Vancevska et al., 2017; Schoeftner & Blasco, 2009; Buhler & Gasser, 2009; Lorenzi et al., 2015). In addition, telomeres are required for the attachment of chromosomes to the nuclear envelope (NE), which assists in localising and organising the chromosomes inside the nucleus (Chikashige et al., 2009; Kupiec, 2014; Li et al., 2017). Telomeres are associated with specific protein complexes, termed shelterins, that facilitate telomere functions, including telomere length regulation, in order to avoid dysfunction of the ends of chromosomes. (Maestroni et al., 2017; Vancevska et al., 2017). Thus, telomeres are critical for many aspects of genome dynamics, and failure in maintaining telomere and telomerase functions, and components are associated with many genetic diseases, including cancer (Chatterjee, 2017; Sarek et al., 2015). Because of their heterochromatin state, telomeres were initially thought to be transcriptionally inactive (Buhler & Gasser, 2009; Schoeftner & Blasco, 2009; Novo & Londoño-Vallejo, 2013; Lorenzi et al., 2015). However, it was later revealed that telomeres are transcribed into large non-coding G-rich telomeric repeat-containing RNA (TERRA) molecules, which are transcribed by RNA polymerase II (RNA Pol II) from the subtelomere towards the telomere (Feretza et al., 2017; Azzalin & Lingner, 2015; Cusanelli & Chartrand, 2015; Rippe & Luke, 2015; Maicher et al., 2014; Wang et al., 2015). TERRA was first identified in humans (Schoeftner & Blasco, 2008; Azzalin et al., 2007), and has been implicated in numerous aspects of telomere-associated functions, including DNA damage response, telomere length control, telomerase activity regulation, and telomeric heterochromatin formation (Azzalin & Lingner, 2015; Cusanelli & Chartrand, 2015; Maicher et al., 2014; Rippe & Luke, 2015; Wang et al., 2015). The regulation of TERRA expression is crucial for maintaining genome integrity and stability (Cusanelli & Chartrand, 2015).

In addition to TERRA, *S. pombe* generates distinct transcripts associated with telomeres and sub-telomeres, including TERRA antisense transcript C-rich telomeric RNA repeats termed ARIA, as well as ARRET and αARRET, which are transcribed from the subtelomeric heterochromatic region and which lack telomeric sequences (Figure 1.12) (Bah et al., 2012; Greenwood & Cooper, 2012; Azzalin & Lingner, 2015; Lorenzi et al., 2015). In *S. pombe*, TERRA was recently shown to be required for telomerase association and telomere elongation (Moravec et al., 2016). Although RNAi is required for heterochromatin establishment at sub-telomeric regions of *S. pombe* that are enriched in the heterochromatin modifications H3K9me and Swi6, mutation of the RNAi genes *ago1* or *dcr1* does not affect these telomeric and sub-telomeric transcript levels (Greenwood & Cooper, 2012) to the same degree observed in centromeric heterochromatin. Further investigation revealed that *S. pombe* transcripts are regulated by the core components of shelterin, i.e. the double-strand telomere-binding proteins Taz1 and Rap1, as mutation of any one of these proteins results in elevation of all telomeric and subtelomeric transcripts (Greenwood & Cooper, 2012). Furthermore, Taz1 is also required for suppressing the sub-telomeric RecQ-like *tlh* genes (orthologous to the human *BLM* gene) (Hansen et al., 2006), which are normally silent, with unknown function, although they have been implicated in the metabolism of telomeres during crises initiated by the loss of telomerase (Mandell et al., 2005). Similar to the regulation of telomeric transcripts, *tlh* expression is not highly influenced by mutation of RNAi components, including *ago1* and *dcr1* (Hansen et al., 2006). In addition to its role in repressing transcription at telomeres and subtelomeres, the telomere-associated protein Taz1 is involved in a wide range of functions at the ends of chromosomes, including telomere length maintenance, DNA damage response, and regulation of telomerase recruitment (Pan et al., 2015; Harland et al., 2014).

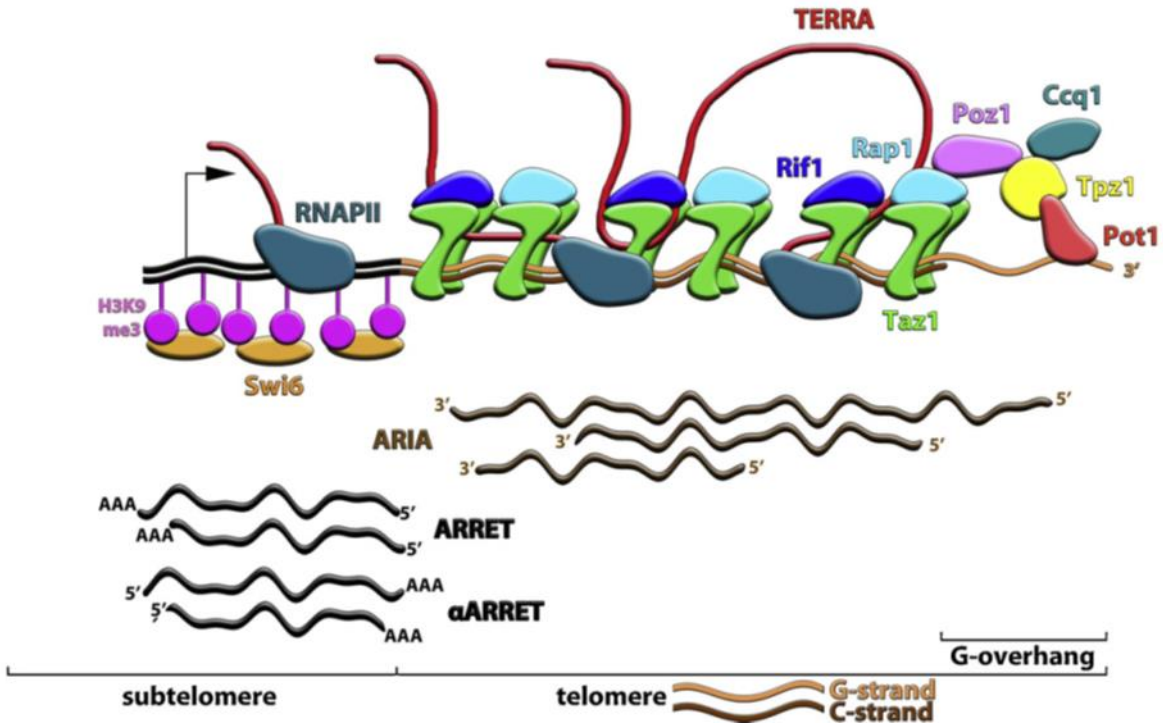

Figure 1.12 Biogenesis of RNA species produced at chromosome ends in fission yeast
S. pombe telomeric repeats are associated with a multiprotein complex that consists of shelterin components, including Taz1, Rap1, Rif1, Poz1, Tpz1, Pot1, and Ccq1, that binds to and protects telomeres. Although the chromosome ends of *S. pombe* are enriched in heterochromatin factors such as H3K9me3 and Swi6, *S. pombe* produces TERRA that is mainly transcribed by RNA Pol II, promoted from subtelomere regions (black arrow) towards the ends of the chromosome (telomeres), which remaining connected to the telomeres, perhaps via Taz1. In addition to TERRA, the chromosome ends of *S. pombe* generate other distinct molecules, including ARIA, ARRET, and αARRET (adapted from Bah et al., 2012).

1.10 RNA interference

RNAi regulates gene expression in a wide variety of eukaryotic organisms at the transcriptional and/or post-transcriptional level (Kalantari et al., 2016; Chan & Wong, 2012; Li & Zhang, 2012; Holoch & Moazed, 2015; Kanoh et al., 2005). The process uses small, non-coding RNA molecules, approximately 20–30 nucleotides long, to regulate the activity of genes by controlling whether they are translated or their transcripts are degraded/ not translated (Holoch & Moazed, 2015; Castel & Martienssen, 2013; Meng & Lu, 2017; Bayne et al., 2010). These short RNAs regulate gene expression via two pathways. The first is post-transcriptional gene silencing (PTGS), which silences target mRNAs within the cytoplasm to stop them being translated. The second mechanism is chromatin-dependent gene silencing (CDGS), which represses specific genes at the level of transcription by promoting the generation of heterochromatin (Creamer & Partridge, 2011; Moazed, 2009; Castel & Martienssen, 2013). Several types of short regulatory RNAs have been recognised: first, short interfering RNAs (siRNAs), which induce transcriptional degradation; second, microRNAs (miRNAs), which induce translational repression; and third, PIWI-interacting RNAs (piRNAs), which are implicated in transposon transcription in the germlines of animals (Castel & Martienssen, 2013; Holoch & Moazed, 2015; Moazed, 2009). The main mediators, siRNAs and miRNAs, are involved in both PTGS and CDGS. However, piRNAs are implicated in the inhibition of 'parasitic' DNAs. These small non-coding RNA molecules play a crucial role as a guide in the RNAi pathway (Pushpavalli et al., 2012; Moazed, 2009).

The process of RNAi (PTGS) is initiated with long double-stranded RNA (dsRNA) molecules, which are generated via a number of ways, including antisense transcription and long-hairpin RNAs. This induces an enzyme called Dicer, which possesses endonuclease activity, to cleave the dsRNA molecules into 20–25 nucleotide (nt)-long siRNA duplexes. Next, the duplex siRNA is integrated into a complex called RNA-induced silencing complex (RISC). RISC, which includes effector proteins such as Argonaute, possesses endoribonuclease activity and is an essential factor for RNAi processes. Once the process of loading the duplex siRNA into the Argonaute protein (RISC) is completed, one strand, acting as the 'guide', remains bound to RISC while the other strand, the 'passenger', is discarded. Then, the guide strand directs the RISC complex, including Argonaute, to cleave and silence the target mRNA.

This occurs via precise binding through sequence-specific base-pairing between siRNA and mRNA, as the siRNA has perfect complementarity with its target mRNA, resulting in transcriptional degradation (Castel & Martienssen, 2013; Moazed, 2009; Kalantari et al., 2016; Swarts et al., 2014; Volpe & Martienssen, 2011; Kawamata & Tomari, 2010; Malone & Hannon, 2009). A complex of two proteins Translin/ Trax (see Section 1.11), known as component 3 promoter of RISC (C3PO), has been shown to act as an endoribonuclease in the cleavage of the passenger strand of the siRNA, following the loading of duplex siRNA onto the Argonaute protein (RISC). This has been observed in both *Drosophila melanogaster* and human cells (see Section 1.13) (Ye et al., 2011; Tian et al., 2011; Liu et al., 2009; Kalantari et al., 2016).

In addition, RNAi processes can specifically affect individual genes by regulating epigenetic modifications of chromatin leading to transcription repression and/or heterochromatin formation. This includes acting on histones and DNA methyltransferases, termed transcriptional gene silencing (TGS) (Holoch & Moazed, 2015; Castel & Martienssen, 2013). RNAi pathways that mediate heterochromatin formation are best characterised in *S. pombe* (Caste & Martienssen, 2013; Holoch & Moazed, 2015; Alper et al., 2012; Reyes-Turcu & Grewal, 2012; Pushpavalli et al., 2012). In this organism, nuclear siRNA RNA mediates heterochromatin formation by targeting nascent centromeric RNA molecules that are generated by RNA polymerase II (Holoch & Moazed, 2015; Castel & Martienssen, 2013). *S. pombe* has single-copy genes from the RNAi pathway, including Argonaute (*ago1*), Dicer (*dcr1*), and RNA-dependent RNA polymerase (*rdp1*), and mutation of any of these genes influences the functions of heterochromatin at the centromere via loss of H3K9 methylation and Swi6 (HP1) localization (Buhler & Gasser, 2009; Volpe et al., 2002; Holoch & Moazed, 2015; Creamer & Partridge, 2011; Chan & Wong, 2012). In *S. pombe*, the process of RNAi (CDGS) begins with the action of RNA polymerase II (RNA Pol II), which transcribes the pericentromeric DNA repeat into dsRNA, with the assistance of an RNA-dependent RNA polymerase complex (RDRC). Then, these dsRNAs are processed by the ribonuclease Dicer into siRNAs, which then bind to the Argonaute siRNA chaperone complex (ARC). Next, they are loaded onto the RNA-induced transcriptional silencing (RITS) complex, which contains Ago1, Chp1, and Tas3. Subsequently, the RITS complex binds to nascent RNA transcripts from DNA repeats (centromere) through the Chp1 chromodomain protein, resulting in the recruitment of the Clr4-Rik1-Cul4 (CLRC) complex to the centromeric repeats. The CLRC complex contains Clr4 (histone methyltransferase), which methylates H3 on lysine 9.

The modified histone (H3K9me) forms a binding site for the Swi6 protein, which is required for heterochromatin assembly and spreading. Finally, the RDRC complex (Rdp1) is recruited by Chp1 to create more dsRNAs, which are then cleaved by Dcr1 for further methylation. (Figure 1.13) (Tadeo et al., 2013; Castel & Martienssen, 2013; Creamer & Partridge, 2011; Holoch& Moazed, 2015; Creamer& Partridge, 2011; Kalantari et al., 2016; Zocco et al., 2016).

In addition to the main heterochromatin loci in *S. pombe*, RNAi (RITS) is also required for the formation of heterochromatin at other genomic sites, such as transposon long terminal repeats (Woolcock et al., 2011). Additionally, RNAi contributes to silencing two meiotic genes, *mei4* and *ssm4*. In this mechanism, RITS is recruited by the Mmi1 RNA surveillance machinery to degrade these specific meiotic mRNAs (Hiriart et al., 2012; Tashiro et al., 2013; Egan et al., 2014).

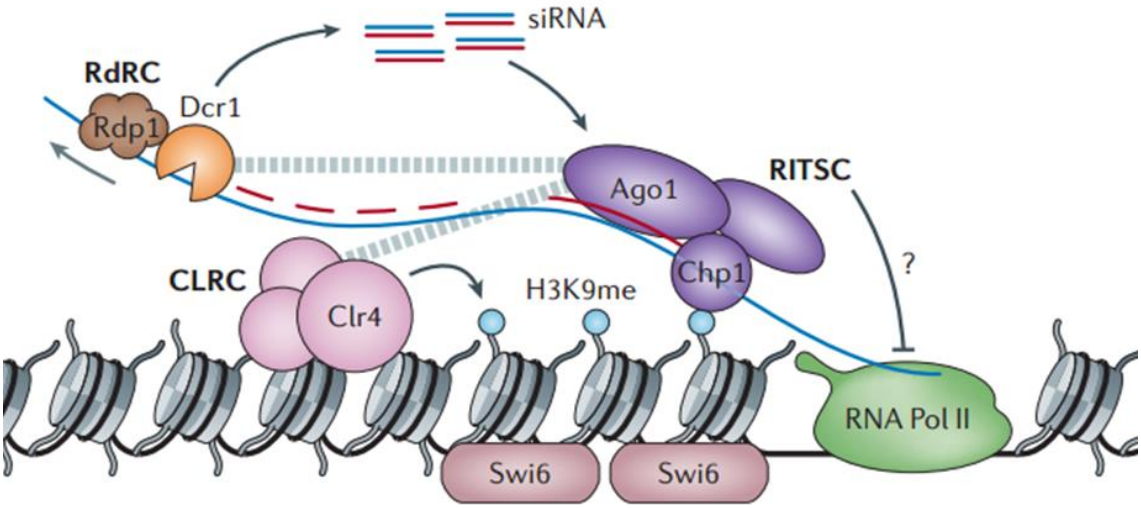

Figure 1.13 A model for RNAi in heterochromatin assembly in *S. pombe*
The RITS complex, which contains siRNA, Ago1, and Chp1, targets nascent transcripts (long blue line) via siRNA base pairing, resulting in the inhibition of RNA Pol II transcription by an unidentified mechanism (shown by the question mark). The interaction between Chp1 and H3 on lysine 9 leads to the recruitment of Clr4 to methylate histone H3 at lysine 9 at target loci, which then serves as a binding site for Swi6. The resultant double-stranded RNA (dsRNA), which consists of siRNA and the nascent strand, is used by the RDRC complex (Rdp1) to generate more dsRNAs, which are then cleaved by Dcr1 into siRNA. The cycles of RNA and H3K9me are strongly connected through the RITS complex to facilitate effective heterochromatin assembly (adapted from Castel & Martienssen, 2013).

1.11 Translin and TRAX

Analysis of the breakpoint junctions of chromosomal translocations common in lymphoid malignancies in humans has identified a novel DNA binding protein, Translin, which binds to the single-stranded consensus nucleotide sequences motifs 5'-ATGCAG-3' and GCCC(A/T)(G/C)(G/C)(A/T). These translocation breakpoint junctions include 1p32, 3q27, 5q31, 8q24, 9q34, 9q34.3, 10q24, 11p13,14q11, 14q32, 14q32.1, 17q22, 18q21, 19p13, and 22q11 (Aoki et al., 1995; Kasai et al., 1997; Kasai et al., 1994). Translin is also implicated in a type of sarcoma (liposarcoma) as Translin consensus binding sequences have been identified at the breakpoints of reciprocal translocations between fused in sarcoma (FUS) on the short arm of chromosome 16 and CHOP on the long arm of chromosome 12 (Kanoe et al., 1999; Hosaka et al., 2000). DNA binding sites of Translin were also identified in other kinds of cancer-associated chromosomal translocation breakpoints, hot spots of human male meiotic recombination and various other chromosomal rearrangement breakpoints in humans (Chalk et al., 1997; Abeysinghe et al., 2003; Wei et al., 2003; Visser et al., 2005; Gajecka et al., 2006a; Gajecka et al., 2006b). The existence of Translin-binding sites at chromosomal translocation breakpoints led to the proposal that Translin is implicated in the initiation and regulation of recombination (Jaendling & Mcfarlane, 2010; Parizotto et al., 2013), but a direct mechanistic role in this process has not yet been demonstrated. However, this proposal was later challenged by the finding that Translin-null mutants, in some eukaryotic organisms including mice, *Drosophila* and *S. pombe*, show no apparent errors and defects in mechanisms involving recombination such as meiotic recombination and DNA damage recovery, or NHEJ (Chennathukuzhi et al., 2003; Yang et al., 2004; Claussen et al., 2006; Jaendling et al., 2008; Jaendling & Mcfarlane, 2010).

Translin (whose name was derived from the word ‘translocation’) is a 26 KDa human protein comprising 228 amino acids (Lluis et al., 2010; Jaendling & Mcfarlane, 2010). The Translin gene in mice was discovered independently as the gene that encodes the testis–brain RNA-binding protein (TB-RBP) (Wu et al., 1997), which has also been implicated in mRNA regulation in neurons and spermatogenesis (Li et al., 2008; Moazed, 2009; Jaendling & McFarlane, 2010).

In support of the involvement of Translin in the neuronal mRNA processing, several studies on mice and fruit flies that are deficient in Translin showed multiple neurological and behavioural abnormalities (Chennathukuzhi et al., 2003; Stein et al., 2006; Suseendranathan et al., 2007; Jaendling et al., 2008).

Using Translin as 'bait' in a yeast two-hybrid system identified a second protein, called Translin-associated factor X, or TRAX (a 33 KDa) protein, whose amino acid sequence is paralogous to Translin (Aoki et al., 1997), indicating a close relationship between Translin and TRAX. Subsequently, it has been shown that TRAX stability depends on the stability and presence of Translin, highlighting the close functional association between the two pairing proteins. This feature is observed in different organisms, including mice, *Drosophila* and *S. pombe*. Consistently, all eukaryotic organisms that have a Translin orthologue also have a TRAX orthologue (Chennathukuzhi et al., 2003; Yang et al., 2004; Claussen et al., 2006; Jaendling et al., 2008; Jaendling & Mcfarlane, 2010). Translin regulates TRAX levels post-transcriptionally. This was discovered by deleting the gene encoding Translin (in mice and *S. pombe)* and then comparing the levels of TRAX mRNA and protein, which resulted in a substantial reduction in TRAX protein levels but no change in its mRNA level (Yang et al., 2004; Jaendling et al., 2008). Although Translin is necessary for the stability of TRAX, the stability of Translin is not dictated by TRAX (Claussen et al., 2006). As found with *S. pombe tsn1* (Translin)-null mutants, *S. pombe tfx1* (TRAX) mutants did not show any measurable defects in recombination in standard genetic background assays (Jaendling et al., 2008). However, it has not yet been examined whether Translin and/or TRAX have a redundant role in recombination and DNA repair processes, which could account for their proposed role in translocation formation (Jaendling & Mcfarlane, 2010). Translin and TRAX are highly conserved in evolution from human to fission yeast, indicating that they likely play a fundamentally important biological role (Laufman et al., 2005; Martienssen et al., 2005; Jaendling & Mcfarlane, 2010). Since their first identification, Translin and TRAX have been implicated in numerous biological functions, including genome stability, DNA damage response, cell growth regulation, RNA interference, the control of mRNA transport and translation, tRNA maturation and more recently in the degradation of microRNA in oncogenesis, which led to the proposal that both proteins could be druggable targets in oncology (Aoki et al., 1995; Wu et al., 1997; Jaendling et al., 2008; Liu et al., 2009; Jaendling & McFarlane, 2010; Tian et al., 2011; Li et al., 2012; Asada et al., 2014; Eliahoo et al., 2014).

Biochemical, crystallographic and electron microscopy studies have shown that the native Translin protein forms an octameric ring structure (Kasai et al., 1997), which is very similar to the structures of the family of helicase enzymes that are linked to DNA repair, recombination and replication processes (VanLoock et al., 2001; Ishida et al., 2002; Jaendling et al., 2008; Fukuda et al., 2008; Jaendling & Mcfarlane, 2010). Translin in this multimeric form binds single-stranded DNA, but not double-stranded DNA, and it has been suggested that this octameric ring structure of Translin is responsible for the recognition of the DNA ends at recombination hotspots in human genome (Kasai et al., 1997; Eliahoo et al., 2014). More recently, crystallographic studies have shown that TRAX and Translin form a 2:6 barrel-like octamer (Ye et al., 2011; Tian et al., 2011; Parizotto et al., 2013; Zhang et al., 2016) that was recently recognised as C3PO (component 3 promoter of the RNA-induced silencing complex [RISC]), which is involved in RNA silencing (see Section 1.13) (Sahu et al., 2014; Liu et al., 2009).

Translin binds to single-stranded DNA (ssDNA) or RNA, and initially it was assumed that its capability to bind to ssDNA is an indication of its involvement in the process of DNA repair. This proposal was later supported by numerous studies (see Section 1.12) (Aoki et al., 1995; Kasai et al., 1997; Gajecka et al., 2006; Tian et al., 2011; Gupta & Kumar, 2012; Eliahoo et al., 2014). Translin and TRAX form a heterodimeric complex that has RNase activity dependent on TRAX, and this heteromeric complex has a greater ability to bind to ssDNA sequences but a reduced ability to bind to ssRNA sequences compared to the Translin octomer on its own, which is able to bind to ssRNA sequences (Liu et al., 2009; Jaendling & Mcfarlane, 2010; Lluis et al., 2010; Parizotto et al., 2013; Fu et al., 2016). Translin has been shown to have RNase activity in *vitro*, but no DNase activity has been identified (Wang et al., 2004).

TRAX does not bind to nucleic acids on its own, and is usually localised in the cytoplasm, whereas Translin is found in both the nuclear and cytoplasmic compartments (Chennathukuzhi et al., 2001; Li et al., 2008; Eliahoo et al., 2014). More recently, TRAX has been shown to bind directly to ssDNA in the form of a heteromeric Translin-TRAX complex (Gupta & Kumar, 2012). An early study showed that mouse TRAX inhibits mouse Translin (TB-RBP) from binding to RNA, and enhances the binding of Translin to specific ssDNA sequences (Chennathukuzhi et al., 2001).

It has been shown that human Translin has a great affinity to bind to single-stranded microsatellite GT repeats (d[GT]$_n$) and G-strand telomeric repeats (d[TTAGGG]$_n$), which indicates a possible functional role in microsatellite repeat or telomere dynamics (Jacob et al., 2004; Laufman et al., 2005; Jaendling et al., 2008; Yu & Hecht, 2008), although no evidence of this was established prior to this current study. In contrast to human Translin, *S. pombe* Tsn1 has been shown to have a stronger affinity for G-rich ssRNA than for G-rich ssDNA, leading to the proposal that its role is more likely to be in the regulation of RNA metabolism rather than DNA metabolism (Laufman et al., 2005; Yu & Hecht, 2008; Jaendling & Mcfarlane, 2010).

Numerous lines of evidence have implicated Translin and TRAX in the regulation of mRNA in both spermatogenesis and neuronal dynamics. For example, mouse Translin was involved in the transport and/or stabilisation of mRNA in the brain and testis cells, in which it binds to precise RNA sequences in the end of 3′-UTRs (untranslated regions) of target mRNAs (Han et al., 1995; Han et al., 1995). Additionally, Translin was shown to bind and stabilise a precise miRNA in germ cells, indicating a possible functional role for Translin in posttranscriptional regulation of gene expression in male germ cells (Yu & Hecht, 2008). Moreover, in mammalian cells, the complex of Translin and TRAX has been shown to mediate the targeting of brain-derived neurotrophic factor (*BDNF*) mRNA to neuronal dendrites, and mutation in the Translin and TRAX binding region within *BDNF* mRNA has been associated with human neurological disorders (Chiaruttini et al., 2009), implying a role for Translin and TRAX in the function and progress of the nervous system (Jaendling & McFarlane, 2010).

In mammalian cells, Translin and TRAX have been shown to be essential for controlling mitotic cell proliferation (Yang et al., 2004; Yang & Hecht, 2004). In support of this, studies aiming to compare basal expression levels of different proteins when the cells are dividing mitotically have determined that there is a relationship between the level of Translin and the rate of cell proliferation. It was found that overexpression of the Translin gene (*TSN*) led to an acceleration in the level of cell proliferation (Ishida et al., 2002).

Moreover, it has also been shown that the expression of *TSN* occurs periodically during the cell cycle: it is initiated in the S phase and during the G2/M phase it reaches its optimum, indicating a potential functional role for Translin in replication of DNA and acceleration of cell division (Ishida et al., 2002). Further analysis using confocal microscopy suggested the involvement of Translin in accelerating the organisation of microtubules and segregation of chromosome during mitosis (Ishida et al., 2002). However, loss of *S. pombe* Tsn1 and Tfx1 resulted in a slight increase in the rate of cell proliferation (Laufman et al., 2005), indicating that both proteins are not essential for the fission yeast (Jaendling & Mcfarlane, 2010). Together, these findings indicate that Translin and TRAX may have fundamentally important biological roles involved in various essential genetic pathways.

1.12 Evidence for the roles of Translin and TRAX in DNA repair

There is sufficient evidence to implicate Translin and TRAX in DNA repair processes. Firstly, in a range of experiments involving HeLa cells treated with etoposide or mitomycin C, Translin was found to localise from the cytoplasm to the nucleus, indicating a signalling mechanism taking place in the damaged cells (Kasai et al., 1997; Jaendling & Mcfarlane, 2010). Additionally, it has been shown that Translin-deficient mice have hematopoietic stem cell recovery problems after exposure to X-rays, which potentially indicates a tissue specific role for Translin in DNA damage recovery (Fukuda et al., 2008; Jaendling & Mcfarlane, 2010). However, similar experiments that aimed at identifying the repairing role of Translin in mice embryotic fibroblasts (MEFs) did not establish any difference between TB-RBP-null fibroblasts and unexposed cells in terms of the number of DNA gaps and breaks, nor in the survival of these cells (Yang et al., 2004). Moreover, *S. pombe tsn1*-null mutants (and *tfx1*-null mutants) previously showed no sensitivity to a wide range of DNA damaging chemicals, including mitomycin C (Jaendling et al., 2008). The fact that Translin lacks a nuclear localisation signal (NLS) has led to the proposal that the nuclear transport of Translin depends on its interaction with other proteins that carry a NLS such as TRAX (Aoki et al., 1997; Aoki et al., 1997; Laufman et al., 2005).

There are several studies showing that Translin and TRAX bind to other proteins that participate in the response to DNA damage. For example, using a yeast-two hybrid system, murine Translin was shown to bind to the apoptosis inhibitor protein GADD34 (a DNA damage-inducible and growth arrest protein) (Hasegawa & Isobe, 1999, Jaendling & Mcfarlane, 2010). GADD34 was implicated in the initiation of translation (Patterson et al., 2006), and this led to the suggestion that the function of Translin in conjunction with GADD34 may be somehow linked to an RNA-processing/binding activity rather than a direct involvement with DNA damage (Jaendling & Mcfarlane, 2010), although it has been assumed that GADD34 may participate in the transport of Translin from the cytoplasm to the nucleus in response to damaged cells (Hasegawa & Isobe, 1999; Hasegawa et al., 2000).

Following exposure to gamma radiation, TRAX was found to interact directly with the DNA-dependent protein kinase (DNA-PK) activator, C1D protein, which participates in DNA repair in both HR and NHEJ pathways (Erdemir et al., 2002; Li et al., 2008). Nonetheless, the direct role of TRAX in DNA damage repair remains largely unidentified. More recently, however, a central functional role for murine TRAX was found in the repair of DNA damage by interacting with ATM-mediated pathway for DSB repair, and stabilising the MRN complex at DSBs (Wang et al., 2016b). These findings also show that the dysfunction of TRAX leads to inactivation of ATM, indicating that TRAX is a key factor involved in DNA damage repair (Wang et al., 2016b). However, a functional role for Translin in this response, if any, has not been demonstrated.

1.13 Translin and TRAX: RNAi interference

In more recent studies, the Translin/TRAX hetero-octamer complex has been shown to have a critical role in the regulation of RNA interference (RNAi) in both *Drosophila* and human cells (Liu et al., 2009; Ye et al., 2011). Specifically, the TRAX subunits in these hetero-octamers have been described as having ribonuclease activity (Tian et al., 2011; Parizotto et al., 2013; Eliahoo et al., 2014), thus, point mutation of the main catalytic residues in TRAX eliminates the RNase activity of the Translin/TRAX complex (Tian et al., 2011; Fu et al., 2016).

RNAi is mediated by small interfering RNAs (siRNAs) with involvement of the RNA-induced silencing complex (RISC) (see Section 1.10). In order to activate the RISC and enhance silencing activity, the passenger strand of the siRNA precursor duplex must be removed to allow the guide strand directing RISC (Ago2) to cleave and silence targeted mRNAs. The precise mechanism of removing the passenger strand has not yet been revealed, however, the Translin/TRAX complex (C3PO), was recently identified as functioning as an endoribonuclease in the cleavage of the passenger strand of siRNA, following loading of duplex siRNA onto the Argonaute protein (Figure 1.14) (Liu et al., 2009; Ye et al., 2011).

C3PO does not function in RNAi in the yeast *S. cerevisiae*, as C3PO orthologues and other regulators of RNAi are deficient in this species (Laufman et al., 2005; Jaendling & Mcfarlane, 2010). Moreover, the role of C3PO in RNAi may be limited to specific animal eukaryotic species. For example, C3PO is not involved in RNAi in the filamentous fungus *Neurospora crassa*. Instead, however, *N. crassa* C3PO has been shown to function as a ribonuclease in the processing of tRNA, specifically in the maturation of pre-tRNAs to tRNAs. Following ribonuclease P (RNase P) processing of pre-tRNAs, C3PO removes sequences at the 5' end of the pre-tRNA (Li et al., 2012). In addition, Li et al. (2012) revealed that C3PO is also implicated in the processing of tRNA in mouse embryonic fibroblast cells (Li et al., 2012).

Surprisingly, very recent observations have suggested that C3PO could have reverse influences on silencing activity that is facilitated by siRNAs and miRNAs. It has been found *in vitro* that C3PO degrades pre-miRNAs, indicating that C3PO functions to reduce miRNA that mediates silencing, which is opposite to the effect it has in enhancing silencing in *Drosophila* (see Section 1.14) (Asada et al., 2014; Fu et al., 2016).

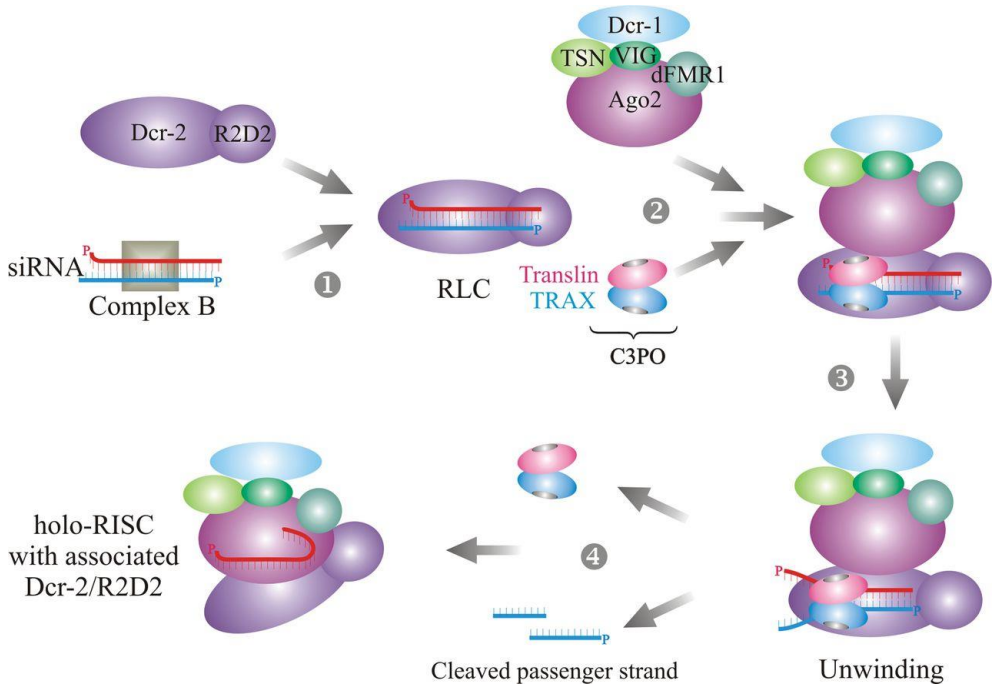

Figure 1.14 Schematic diagram of the role of Translin and TRAX in the *Drosophila* RNAi pathway

The diagram shows the translocation of the small interfering RNA (siRNA) duplex (consisting of the passenger and the guide strands) from complex B to RLC (RISC loading complex), which contains Dcr-2 and R2D2. After this, C3PO (Translin and TRAX) is joined with the RLC complex, along with the RISC complex, which contains a complex of components, including Ago2 and Dcr-1, which result in the generation of the holoRISC by a Drc-2–Ago2 interaction. Next, the endoribonuclease activity of C3PO induces the removal of the passenger strand from the siRNA duplex. Finally, holoRISC complex targets the selected mRNA (adapted from Jaendling & Mcfarlane, 2010).

1.14 The role of Translin and TRAX in oncogenesis

In addition to its roles in other cellular processes, Dicer is most known for its function as a riboendonuclease enzyme in the generation of small RNAs, including siRNA and miRNA. Dicer is a critical regulator for the biogenesis and maturation of most miRNAs. The RNaseIII Dicer processeds precursor miRNA (pre-miRNA) to mature miRNA, which in turn directs Argonaute to mediate translational suppression of selected mRNAs (Asada et al., 2014; Fiorenza & Barco, 2016; Hata & Kashima, 2016; Mei et al., 2016; Svobodova et al., 2016; Song & Rossi, 2017). miRNAs are involved in the modulation and regulation of approximately 30% of human gene expression, and deregulation of these small non-coding RNAs is frequently observed in numerous human cancers. miRNAs inhibit various tumour-suppressive and oncogenic mRNAs, which has led to the proposal that these small RNAs function as both oncogenes or tumour suppressor genes (Zhang et al., 2007; Kumar et al., 2009; Gurtner et al., 2016; Hata & Kashima, 2016; Voglova et al., 2016). The accumulation of pre-miRNAs and the reduction of mature miRNAs have been identified in human cancer tissue in comparison to normal tissue (Gurtner et al., 2016). In addition, the complete deletion of the miRNA-generating enzyme Dicer is harmful to tumour formation and progression (Kumar et al., 2009; Asada et al., 2016). Dicer deficiency is seen in up to 40% of cancers and is linked to poor patient prognoses. Therefore, Dicer is described as a haploinsufficient tumour suppressor (Kumar et al., 2009; Asada et al., 2014; Foulkes et al., 2014; Asada et al., 2016; Gurtner et al., 2016; Hata & Kashima, 2016).

It is known that Dicer deficiency results in a depletion of miRNA levels and their tumour suppressor activities through impaired miRNA processing activity (Asada et al., 2014; Fu et al., 2016; Hata & Kashima, 2016). However, it has been recently found that the miRNA depletion with Dicer deficiency is not only due to the loss of miRNA-generating activity, but it is in combination with a catalytic function of Translin/TRAX (TSN/TSNAX). Remarkably, the C3PO complex was found to function as an RNase enzyme, in that it degrades pre-miRNAs in *Dicer1* haploinsufficiency. These findings also showed that genetic inhibition of C3PO results in a restoration of both miRNA and tumour suppression (Asada et al., 2014).

Collectively, these remarkable observations indicate that the C3PO complex plays an oncogenic role in *Dicer1* haploinsufficient cancer, and this has led to the proposal that both proteins could be druggable targets for miRNA function restoration in tumours and emerging Dicer deficiencies (Figure 1.15) (Asada et al., 2014; Asada et al., 2016).

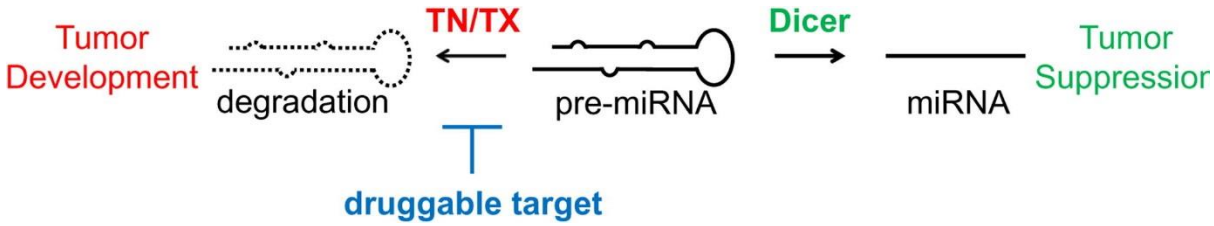

Figure 1.15 Translin/TRAX complex is a potential druggable target in tumours
Translin/TRAX (TSN/TSNAX) complex is a possible therapeutic solution for restoring normal silencing function. A normal level of Dicer processes pre-miRNA to mature miRNA, which maintains tumour suppression. However, with Dicer haploinsufficiency, the ribonuclease complex TSN/TSNAX degrades pre-miRNAs, which leads to tumour development. Significantly, genetic inhibition of TSN/TSNAX would rescue loss of both miRNA and tumour suppression in Dicer deficiency (adapted from Asada et al., 2016).

1.15 *S. pombe* as a model eukaryote

The fission yeast *S. pombe* is a brewing yeast found in Africa. Linder extracted this yeast from millet beer and termed it 'Pombe', meaning 'beer'. It was later developed as an experimental model in the 1950s (Nurse, 2002). The genome of *S. pombe* is approximately 13.8 Mb in size, and carried by three chromosomes consisting of 3.5, 4.6, and 5.7 Mb (Wood et al., 2002; Koyama et al., 2017). Sequencing of the *S. pombe* genome, which contains approximately 5000 genes, was completed in 2002 (Wood et al., 2002). Various genes are conserved between *S. pombe* and humans, but are absent in other model organisms such as the budding yeast *S. cerevisiae* (Wood et al., 2002; Koyama et al., 2017). Importantly, *S. pombe* has recently been utilized as an effective tool for exploring RNAi and cellular epigenetics (Tadeo et al., 2013; Buhler & Gasser, 2009; Koyama et al., 2017). *S. pombe* has single-copy genes from the RNAi pathway, including *ago1*, *dcr1*, and *rdp1* (Martienssen et al., 2005; Holoch & Moazed, 2015). The structure and regulators of *S. pombe* telomeres exhibit a high degree of similarity with those of humans, which makes this organism a perfect model for studying telomere dynamics (Lorenzi et al., 2015; Jain & Cooper, 2010; Koyama et al., 2017). More recently, *S. pombe* has been used as an important model organism for identifying the roles and regulators of TERRA molecules in telomere function, which is an emerging area of interest (Greenwood & Cooper, 2012; Bah et al., 2012). More importantly, the C3PO complex (consisting of Translin and Trax) has been proposed as an anti-cancer drug target (see Section 1.14) (Asada et al., 2014). This complex is found in *S. pombe* but not in *S. cerevisiae*. *S. pombe* is a genetically tractable organism and is genetically manipulated more easily than other organisms, including humans. Thus, this yeast can be used as an experimental model organism for investigating the complex genetic functions.

1.16 Overarching aim of this study

We aimed to investigate whether Tfx1 (Trax) and Tsn1 (Translin) function in genome maintenance pathways.

Chapter 2: Materials and Methods

2. Materials and Methods

2.1 Media and strains used in this study

Media used in this study are listed in Table 2.1. Strains of *S. pombe* and *Escherichia coli* used in this study are listed in Tables 2.2 and 2.3. *De novo* deletion (direct gene mutation) was used in this study to construct all appropriate mutation strains (Bähler et al., 1998), and correct deletions were confirmed by PCR analysis of genomic DNA.

Media and supplements required in this study were purchased from Difco (Becton Dickinson) and Sigma. At a final concentration of 200 mg/L, the appropriate amino acid supplements were added to the minimal media. An antibiotic concentration of 100 µg/mL was utilised in the relative media. Nourseothricin (Warner BioAgents), Ampicillin (Sigma), Geneticin (G418) (Sigma), and Hygromycin (Sigma) were the antibiotics used in this study.

2.2 Plasmid Extraction from *E. coli*

Plasmid extraction from E. coli was carried out using the QIAGEN Miniprep kit. E. coli strains that were stored at -80°C were streaked on Luria-Bertani (LB) agar containing ampicillin and incubated overnight at 37°C. A single colony was inoculated into 5 mL LB liquid media containing ampicillin and incubated overnight at 37°C in an orbital shaker incubator. Cells obtained were centrifuged at 3000 *g* for 5 minutes and then resuspended in 250 µL P1 buffer containing RNase A. This mixture was then transferred to an Eppendorf tube, and 250 µL of P2 lysis buffer was used in the cell lysis step. Invert mixing was performed 4-5 times; after that, 350 µL N3 buffer (neutralising/binding buffer) was added in the same tube. Invert mixing was again performed 4-5 times to homogenise the contents of the tube. The tube was then spun at a speed of 12,000 *g* for 10 min; the pellet was removed, while the supernatant was transferred to a QIAprep tube (QIAGEN), which was again centrifuged at the same speed for 30-60 seconds. The supernatant was removed, and the pellet was washed with 500 µL PB buffer (washing buffer) and then spun at 12,000 *g* for 30-60 seconds. After that, the supernatant was removed, and the pellet was washed with 750 µL PE buffer and spun at 12,000 *g* for 30-60 seconds. Following this, the supernatant was discarded, and the plasmid DNA was eluted from the filter by adding 50 µL of elution buffer (EB).

Table 2.1 Yeast and bacterial media recipes

YEA	**Per 1 litre add:**
Yeast extract	5 g
Glucose	30 g
Agar	14 g
LBA	**Per 1 litre add:**
Tryptone	10 g
Yeast extract	5 g
Sodium chloride	10 g
Agar	14 g
NBA	**Per 1 litre add:**
Nitrogen base	1.7 g
Glucose	10 g
$(NH_4)_2\ SO_4$	5 g
Agar	24 g
Drugs	**Concentrations**
Thiabendazole (TBZ) (Sigma)	(12, 13, 14, 15 ug/ml)
Methyl Methanesulfonate (MMS) (Sigma)	(0.005, 0.0075, 0.01%)
Mitomycin C (Sigma)	(0.15 mM)
Phleomycin (Sigma)	(2.5, 3, 4, 5, 8 ug/ml)
Hydroxyurea (HU) (Sigma)	(8, 10 mM)
Camptothecin (Sigma)	(1, 1.2, 1.4, 1.8 ug/ml)

2.3 *S. pombe* gene deletions using the PCR method

From the *S. pombe* genome, different genes were selected to be knocked out; the method for this was adapted from the Bähler approach (Bähler et al., 1998). In this protocol, pFA6a-natMX6, pFA6a-kanMX6, and pFA6a-hphMX6 were the plasmids used as template DNAs for PCR amplification of the antibiotic-resistant marker. The primers used in the PCR contain 80 bp homologous sequences directly to the upstream and downstream of open reading frame of target genes to be deleted and contained 20 bp homologous sequence to the target antibiotic resistant marker (plasmids). The oligonucleotide sequences used in these experiments are shown in Table 2.4. The Bähler lab genome regulation software was used to design these primers:
http://www.bahlerlab.info/cgi-bin/PPPP/pppp_deletion.pl

The plasmid and primer were diluted 10-fold in 1X TE buffer (1.0 M Tris-HCl maintained at 8.0 pH and EDTA 1.0 M) prior to the PCR. The 50-µL PCR reactions contained: 1 µL high fidelity Phusion polymerase (NEB), 1 µL of DNA template (20 ng of plasmid DNA), 1 µL of 10 x dNTPs, 1 µL of 20 ng/µL each of forward and reverse primers, 10 µL 5x Phusion™ GC buffer, 32.5 µL of sterile distilled water, and 2.5 µL of DMSO. The chosen marker cassettes were amplified using the following program: 98°C for 1 min followed by 30 cycles of 10 s at 98ºC, 30 s at 59ºC, as well as 1 min 50 s at 72ºC, which was then extended to 5 min at 72ºC. The PCR products were then purified using the phenol/chloroform method.

2.4 Phenol/Chloroform Purification of DNA

The DNA was mixed with equal amounts of phenol/chloroform and 0.1 M NaCl (with 1:1 ratio) in an Eppendorf tube. This mixture was then centrifuged at 12,000 *g* for 15 min. The aqueous layer formed on top of the solution was poured off into another Eppendorf containing 100% ethanol. DNA precipitation was achieved by freezing the cells at -80ºC for 1 hour. The precipitated DNA was spun at 12,000 *g* for 30 min at 4ºC; after that, the supernatant was removed, pellet was washed with 70% ethanol by centrifuging at 12,000 *g* for 15 minutes, and the ethanol was completely removed. DNA was resuspended in 40 µL of 1X TE buffer. The DNA cassette was then stored at -20ºC. Transformation of the products into *S. pombe* was carried out using the lithium acetate (LiAC) method.

Table 2.2 *S. pombe* strains utilised in this project

Strain number	Genotype	Source
BP90	*h⁻ ade6-M26 ura4-D18 leu1-32*	McFarlane, Bangor University
BP118	*h⁻ ade6-M216 ura4-D18 leu1-32 taz1::ura4⁺*	McFarlane, Bangor University
BP743	*h⁻ rad3-136*	McFarlane, Bangor University
BP1079	*h⁻ ade6-M26 ura4-D18 leu1-32 tsn1::kanMX6*	McFarlane, Bangor University
BP1080	*h⁻ ade6-M26 ura4-D18 leu1-32 tsn1::kanMX6*	McFarlane, Bangor University
BP1089	*h⁻ ade6-M26 ura4 -D18 leu1-32 tfx1::kanMX6*	McFarlane, Bangor University
BP1090	*h⁻ ade6-M26 ura4 -D18 leu1-32 tfx1::kanMX6*	McFarlane, Bangor University
BP1478	*h⁻ ade6::tRNAGLU (1) his3-D1 ura4–18 lys1–37 leu1–32*	McFarlane, Bangor University
BP1508	*h⁻ ade6::tRNAGLU (2) his3-D1 ura4–18 lys1–37 leu1–32*	McFarlane, Bangor University
BP1534	*h⁻ ade6::tRNAGLU (1) his3-D1 ura4–18 lys1–37 leu1–32* (pSRS5)	McFarlane, Bangor University
BP1535	*h⁻ ade6::tRNAGLU (2) his3-D1 ura4–18 lys1–37 leu1–32* (pSRS5)	McFarlane, Bangor University
BP1685	*h⁻ ade6::tRNAGLU (1) his3-D1 ura4–18 lys1–37 leu1–32 swi1::ura4* (pSRS5)	McFarlane, Bangor University

BP1687	*h⁻ ade6::tRNAGLU (2) his3-D1 ura4–18 lys1–37 leu1–32 swi1::ura4 (pSRS5)*	McFarlane, Bangor University
BP2746	*h⁻ ade6-M26 ura4-D18 leu1-32 dcr1::ura4⁺*	McFarlane, Bangor University
BP2748	*h⁻ ade6-M26 ura4-D18 leu1-32 tsn1:: kanMX6 dcr1::ura4⁺*	McFarlane, Bangor University
BP2749	*h⁻ ade6-M26 ura4-D18 leu1-32 tsn1:: kanMX6 dcr1::ura4⁺*	McFarlane, Bangor University
BP2750	*h⁻ ade6-M26 ura4-D18 leu1-32 tfx1:: kanMX6 dcr1::ura4⁺*	McFarlane, Bangor University
BP2757	*h⁻ ade6-M26 ura4-D18 leu1-32 ago1::ura4⁺*	McFarlane, Bangor University
BP2758	*h⁻ ade6-M26 ura4-D18 leu1-32 ago1::ura4⁺*	McFarlane, Bangor University
BP2759	*h⁻ ade6-M26 ura4-D18 leu1-32 tsn1:: kanMX6 ago1::ura4⁺*	McFarlane, Bangor University
BP2761	*h⁻ ade6-M26 ura4-D18 leu1-32 tfx1::kanMX6 ago1::ura4⁺*	McFarlane, Bangor University
BP2762	*h⁻ ade6-M26 ura4-D18l eu1-32 tfx1::kanMX6 ago1::ura4⁺*	McFarlane, Bangor University
BP3246	*h⁻ade6-M26 ura4-D18 leu1-32 tfx1:: kanMX6 ago1::ura4⁺ tsn1::natMX6*	McFarlane, Bangor University
BP3247	*h⁻ade6-M26 ura4-D18 leu1-32 tfx1:: kanMX6 ago1::ura4⁺ tsn1::natMX6*	McFarlane, Bangor University
BP3248	*h⁻ ade6-M26 ura4-D18 leu1-32 tfx1::kanMX6 tsn1::natMX6*	McFarlane, Bangor University

BP3249	*h⁻ ade6-M26 ura4-D18 leu1-32 tfx1::kanMX6 tsn1::natMX6*	McFarlane, Bangor University
BP3250	*h⁻ ade6-M26 ura4-D18 leu1-32 tsn1:: kanMX6 dcr1::ura4⁺ tfx1::natMX6*	McFarlane, Bangor University
BP3273	*h⁻ ade6-M26 ura4-D18 leu1-32 tlh1::ura4⁺ tlh2::kanMX6 tlh3::kanMX6 tlh4::ura4⁺*	C. Norbury collection
BP3274	*h⁻ ade6-M26 ura4-D18 leu1-32 tlh1::ura4⁺ tlh2::kanMX6 tlh3::kanMX6 tlh4::ura4⁺ ago1::hph*	This study
BP3275	*h⁻ ade6-M26 ura4-D18 leu1-32 tlh1::ura4⁺ tlh2::kanMX6 tlh3::kanMX6 tlh4::ura4⁺ ago1::hph*	This study
BP3278	*h⁻ ade6-M26 ura4-D18 leu1-32 tlh1::ura4⁺ tlh2::kanMX6 tlh3::kanMX6 tlh4::ura4⁺ tfx1::natMX6*	This study
BP3279	*h⁻ ade6-M26 ura4-D18 leu1-32 tlh1::ura4⁺ tlh2::kanMX6 tlh3::kanMX6 tlh4::ura4⁺ tfx1::natMX6*	This study
BP3282	*h⁻ ade6-M26 ura4-D18 leu1-32 tlh1::ura4⁺ tlh2::kanMX6 tlh3::kanMX6 tlh4::ura4⁺ ago1::hph tfx1::natMX6*	This study
BP3283	*h⁻ ade6-M26 ura4-D18 leu1-32 tlh1::ura4⁺ tlh2::kanMX6 tlh3::kanMX6 tlh4::ura4⁺ ago1::hph tfx1::natMX6*	This study
BP3285	*h⁻ ade6-M26 ura4-D18 leu1-32 ago1::ura4⁺ taz1::natMX6*	This study
BP3286	*h⁻ ade6-M26 ura4-D18 leu1-32 ago1::ura4⁺ taz1::natMX6*	This study
BP3287	*h⁻ ade6-M26 ura4-D18 leu1-32 ago1::ura4⁺ taz1::natMX6*	This study
BP3288	*h⁻ ade6-M26 ura4-D18 leu1-32 tsn1::kanMX6 taz1::natMX6*	This study

BP3289	*h⁻ ade6-M26 ura4-D18 leu1-32 tsn1::kanMX6 taz1::natMX6*	This study
BP3291	*h⁻ ade6-M26 ura4 -D18 leu1-32 tfx1::kanMX6 rap1::natMX6*	This study
BP3293	*h⁻ ade6-M26 ura4-D18 leu1-32 tsn1::kanMX6 rap1::natMX6*	This study
BP3294	*h⁻ ade6-M26 ura4-D18 leu1-32 tsn1::kanMX6 rap1::natMX6*	This study
BP3295	*h⁻ ade6-M26 ura4-D18 leu1-32 tsn1::kanMX6 rap1::natMX6*	This study
BP3296	*h⁻ ade6-M26 ura4 -D18 leu1-32 tfx1::kanMX6 rap1::natMX6*	This study
BP3297	*h⁻ ade6-M26 ura4-D18 leu1-32 ago1::ura4⁺ bqt4::natMX6*	This study
BP3298	*h⁻ ade6-M26 ura4-D18 leu1-32 bqt4::natMX6*	This study
BP3301	*h⁻ ade6-M210 ura4-D18 leu1-32 his3-D1 Otrt::his3*	J. P Cooper collection
BP3313	*h⁻ ade6::tRNAGLU (1) his3-D1 ura4–18 lys1–37 leu1–32 dcr1::natMX6*	This study
BP3314	*h⁻ ade6::tRNAGLU (1) his3-D1 ura4–18 lys1–37 leu1–32 dcr1::natMX6 tsn1::kanMX6*	This study
BP3322	*h⁻ ade6::tRNAGLU (1) his3-D1 ura4–18 lys1–37 leu1–32 tsn1::kanMX6* (pSRS5)	This study
BP3324	*h⁻ ade6::tRNAGLU (1) his3-D1 ura4–18 lys1–37 leu1–32 dcr1::natMX6* (pSRS5)	This study

BP3325	*h⁻ ade6::tRNAGLU (1) his3-D1 ura4–18 lys1–37 leu1–32 dcr1::natMX6* (pSRS5)	This study
BP3326	*h⁻ ade6::tRNAGLU (1) his3-D1 ura4–18 lys1–37 leu1–32 dcr1::natMX6 tsn1::kanMX6* (pSRS5)	This study
BP3327	*h⁻ ade6::tRNAGLU (1) his3-D1 ura4–18 lys1–37 leu1–32 dcr1::natMX6 tsn1::kanMX6* (pSRS5)	This study
BP3328	*h⁻ ade6::tRNAGLU (1) his3-D1 ura4–18 lys1–37 leu1–32 tsn1::kanMX6* (pSRS5)	This study
BP3335	*h⁻ ade6::tRNAGLU (1) his3-D1 ura4–18 lys1–37 leu1–32 tsn1::kanMX6*	This study
BP3336	*h⁻ ade6::tRNAGLU (2) his3-D1 ura4–18 lys1–37 leu1–32 tsn1::kanMX6*	This study
BP3343	*h⁻ ade6::tRNAGLU (2) his3-D1 ura4–18 lys1–37 leu1–32 dcr1::kanMX6*	This study
BP3344	*h⁻ ade6::tRNAGLU (2) his3-D1 ura4–18 lys1–37 leu1–32 tsn1::kanMX6* (pSRS5)	This study
BP3345	*h⁻ ade6::tRNAGLU (2) his3-D1 ura4–18 lys1–37 leu1–32 tsn1::kanMX6* (pSRS5)	This study
BP3348	*h⁻ ade6::tRNAGLU (2) his3-D1 ura4–18 lys1–37 leu1–32 dcr1::kanMX6* (pSRS5)	This study
BP3349	*h⁻ ade6::tRNAGLU (2) his3-D1 ura4–18 lys1–37 leu1–32 dcr1::kanMX6* (pSRS5)	This study
BP3362	*h⁻ ade6::tRNAGLU (2) his3-D1 ura4–18 lys1–37 leu1–32 tsn1::kanMX6 dcr1::natMX6*	This study
BP3364	*h⁻ ade6::tRNAGLU (2) his3-D1 ura4–18 lys1–37 leu1–32 tsn1::kanMX6 dcr1::natMX6* (pSRS5)	This study

BP3365	*h⁻ ade6::tRNAGLU (2) his3-D1 ura4–18 lys1–37 leu1–32 tsn1::kanMX6 dcr1::natMX6* (pSRS5)	This study

Table 2.3 *E. coli* strain and plasmid utilised in this project

Bangor strains number	***E.coli* strain and plasmid**	**Source**
BE9	pARC782 (*kanMX6 amp* ^{R})	McFarlane, Bangor University
BE122	DH5α (pSRS5)	McFarlane, Bangor University
BE183	pYL16 (*natMX6 amp* ^{R})	E. Hartsuiker, Bangor University
BE193	pFA6a (*hphMX6 amp* ^{R})	Oliver Fleck, Bangor University

2.5 Transformation of *S. pombe* cells using lithium acetate (LiAC)

2.5.1 Transformation of *S. pombe* strains using a DNA knockout cassette

A single colony of *S. pombe* was grown overnight with shaking at 30ºC in 5 mL YEL containing supplemental adenine (200 mg/L). The next day, 100-200 µL of the culture was inoculated in 100 mL of YEL containing supplemental adenine (200 mg/L) to a density of 1x 10^7 cells/mL and cultured overnight. The cells obtained after culturing were spun at 3,000 *g* for 5 minutes and then washed using sterile dH_2O; they were then centrifuged again at 3,000 *g* for 5 minutes. The cells were resuspended in 1 mL sterile dH_2O and transferred to 1.5 mL Eppendorf tubes; after that, they were washed once with 1 mL 0.1 M LiAc/1X TE. After washing, the cells were resuspended in LiAC/TE to maintain the cellular concentration at 2 x 10^9 cells/mL. Following this, 100 µL of the cell suspension was removed and mixed with 2 µL of 10 mg/mL sheared herring testis DNA (Invitrogen) and 10-20 µg of cassette DNA . Following 10 minutes of incubation at room temperature, 260 µL of 40% PEG/LiAC/TE (maintained at pH 7.3) was introduced. The mixture was mixed gently and incubated for 1 hour in a water bath at 30ºC after which, 43 µL of DMSO was added, and cells were heat shocked for 5 minutes at 42ºC in another water bath. The mixture was then allowed to cool at room temperature for 10 minutes, and then washed with 1 mL sterile dH_2O by centrifuging for 3 minutes. The cells were then resuspended in 0.5 mL sterile dH_2O and plated onto YEA (100 µL of the mixture per plate). The plates were then incubated for 18 hour at 30ºC. Finally, the plates were replicated onto YEA plates (containing selective antibiotic drugs) and incubated at 30ºC for 3-4 days.

2.5.2 Transformation with plasmids

The lithium acetate (LiAC) procedure described in Section 2.5.1 was used for the transformation of *S. pombe* strains with plasmids except that only 1 µg of plasmid DNA was used, and cells were plated onto selective NBA for selection of transformants after which they were incubated for 2-4 days at 30ºC.

2.6 Genomic DNA Extraction

Single colonies were inoculated into mL YEL containing supplemental adenine (200 mg/L) and allowed to grow overnight with shaking at 30ºC until cell saturation occurred. The cells obtained after culturing were spun at 3,000 *g* for 5 minutes and then washed using sterile dH_2O and transferred to 1.5 mL screw cap tubes and a*g*ain centrifuged for 1 minute. Then, 200 µL of lysis buffer (containing 5 mL 10% SDS, 1 mL Triton X-100, 0.5 mL of TE100X, and 5 mL of 1 M NaCl) along with 100 µL chloroform, 100 µL phenol, and acid washed beads weighing 0.3 g were added to the tubes. Cells were disrupted for 30 seconds by a Bead-Beater (FastPrep120, ThermoSavant.) and spun at 12,000 *g* for 15 minutes. The aqueous layer formed on top of the solution was aspirated off into another Eppendorf tube containing 100% ethanol. The mixture was left at -20ºC for 1 hour and then centrifuged at 12,000 *g* for 12 minutes. The pellets formed were washed using 1 mL 70% ethanol and then air-dried. After that, 100 µL 1X TE buffer was used to resuspend the final cell pellet.

2.7 Confirmation of Gene Knockout by PCR Screening

After extracting the genomic DNA for the knock out strain, appropriate primers were designed for the knockout cassettes and target genes; oligonucleotide sequences used in these experiments are shown in Table 2.5. The PCR reaction mixture (for a 25 µL reaction) was as follows: 12.5 µL MyTaq™ Red Mix (BioLine), 0.5 µL of 20 ng/µL forward as well as reverse primers, 1 µL of the extracted genomic DNA (10% dilution), and 10.5 µL of sterile dH_2O. The PCR machine was set at the following program: at 96°C for 1 min followed by 35 cycles of 1 minute at 96°C, 30 seconds at X °C, and 30 seconds at 72°C. An extension was set at 72°C for 5 minutes. The annealing temperature (X) was set, based on the sequence of the primers. Finally, the PCR- amplified products were run on a 1% agarose gel to obtain an estimate of the product sizes.

2.8 Drop Tests for Drug Sensitivity

A single colony of *S. pombe* was inoculated in 5 mL YEL containing supplemental adenine (200 mg/L) and grown overnight with shaking at 30°C. The next day, cells were counted using a light microscope (40X) by adding 10 µL of the cells to the end of the coverslip of a haemocytometer; they were then resuspended with sterile dH_2O to obtain a concentration of 5 x 10^6 cells/mL.

Four serial dilutions of the cell mixture were performed, and 10 µL of each dilution was spotted onto YEA plates containing supplemental adenine (200 mg/L) with the required, appropriate drugs (complete details of drug concentrations are shown in Table 2.1). A set of control plates was made by replacing the drugs with drug solvents (either DMSO or H_2O). The plates were incubated at an appropriate temperature for 3-4 days.

2.9 Storage of *S. pombe* Strains

Single colonies were introduced into 5 mL of YEL containing supplemental adenine (200 mg/L) and allowed to grow with shaking until cell saturation occurred. To achieve a final concentration of 30%, glycerol was added to 700 µL of the cultures and vortexed. The cultures were then stored at -80^{o}C.

2.10 Ultraviolet (UV) irradiation of *S. pombe*

Serial dilutions of *S. pombe* strains were set up as previously described in section 2.8, and 10 µL of each dilution was spotted onto YEA plates containing supplemental adenine (200 mg/L) and allowed to dry. Plates were then exposed to UV irradiation (CL-1000 UV cross linker) using a range of doses including 50, 60, and 70 J/m^2. The plates were then incubated at an appropriate temperature for a period of 3-4 days.

2.11 DAPI staining (Ethanol Fixation) and Microscopy

Single colonies were introduced into 5 mL of YEL containing supplemental adenine (200 mg/L) and allowed to grow with shaking to mid-log phase. Cells obtained were centrifuged at 1159 *g* for 3 minutes at 4°C, and then the supernatant was removed. The formed pellets were then resuspended in 70% ethanol (1 mL) and incubated at room temperature for 10 minutes. The mixture was centrifuged at 3000 *g* for 1 minute, and the supernatant was removed. The pellets were washed using 1 mL of 1X PBS buffer. The last step was repeated three times. Cells were then resuspended in 100 µL of 1X PBS, and the tubes were kept on ice. After that, 1 µL of cells were mixed with 1 µL of DAPI (50 µg/mL) on poly-l-lysine slides (Sigma P8920). The mixtures were then covered with a cover slip (22x22 mm) and sealed using nail polish. The slides were then ready for examination under a fluorescent microscope.

Table 2.4 PCR primers utilised to delete target genes

Primer name	Sequence	Notes
Ago1HphMX6-F	5′-TAT GAT GAG TCC TAA TCT AGG GTT TGG TAT ATA TAA GCT TCC AAC CGC CAA AGC GAA TTG TCT TCA GCC AAC TCG TCC TTT ATG ATT CAG AGT GAG TAG GCG GAT CCC CGG GTT AAT TAA-3′	Forward primer for the Hygromycin cassette for *ago1* replacement
Ago1HphMX6-R	5′-AAA AAC AGA AGC AGA TTT AAT AAG GAA GTA AAA GTT GTG GGC AAT CCA GTA GTC AAT CGT ATA TCT ATT TCA TTA CTT ATT GCA TGC AAT CCA TCA AAC AGA ATT CGA GCT CGT TTA AAC-3′	Reverse primer for the Hygromycin cassette for *ago1* replacement
Tfx1NatMX6-F	5′-TAT AGA CTT ATA CAT TTA TAC CTT CCA CAC GGC TTT GCT GAA TTG AGG ATA TTA TAA AAC TTT AAC CGA ATT TGC CAA ATC GGA TCC CCG GGT TAA TTA A -3′	Forward primer for the Nourseothricin^{R} cassette for *tfx1* replacement
Tfx1NatMX6-R	5′-ATT ATG ATT TTC AAA AGC TGC AAA ACA GAA AAA CTT TTA ATA AAC TAG TAA GGT GTC TGT CGA GAG CTG TCG ATC ATA TAT GAA TTC GAG CTC GTT TAA AC -3′	Reverse primer for the Nourseothricin^{R} cassette for *tfx1* replacement
Taz1NatMX6-F	5'-CTA AGG GAT TAT GAT AAT TTT ATA ATT GTT TAG TGA AAT TCG TAA TTC AAC CT CTT TCA CCA TAC AAT CGA GGG CAG TTG CGG ATC CCC GGG TTA ATTAA-3'	Forward primer for the Nourseothricin^{R} cassette for *taz1* replacement
Taz1NatMX6-R	5'-ATT AAC AAA ACT ATC CGA GTC TTG TCA ATA TTA TTC ATT AAA AAA GCA ATC ATG AAC AAA CTC TAT CCG GAG ACG AAA AAG AAT TCG AGC TCGT TTA AAC-3'	Reverse primer for the Nourseothricin^{R} cassette for *taz1* replacement
Rap1NatMX6-F	5'-CCA GCA TTT CTT GAT TGT AAA GTA AAT TAC TTA TTT TTT AAC TCA TTT TTA CGC GCA AAA AAA GAA TAA AAG TAT GAA CTC GGA TCC CCG GGT TAA TTA A-3'	Forward primer for the Nourseothricin^{R} cassette for *rap1* replacement

Rap1NatMX6-R	5'-TAT GCA TAA AAA GAT TCG TAA TAT TGT ACA AGT TTA GGT CTC TTT AGA GAA ATA GAA TTT GGG CAG AGA TGC TCG GCA ATG AAT TCG AGC TCG TTT AAAC-3'	Reverse primer for the Nourseothricin^{R} cassette for *rap1* replacement
Bqt4NatMX6-F	5′-TAC ATA AAC GTT GTA AGA GAG GAA TTA TAC AAA CGT CGA CGA CGG CGA TTA ATT GTT ACC TTT CCC CTT AAT TGA ATA CCC GGA TCC CCG GGT TAA TTA A-3′	Forward primer for the Nourseothricin^{R} cassette for *bqt4* replacement
Bqt4NatMX6-R	5′-TAC ATC AAC AAA TTA AAG CAC ATA TGT CAC ATT AAA TTC TAA CAT CCA GTA GTT TCA AAA TGG TAA AGG GCC CTA TTA AAG AAT TCG AGC TCG TTT AAA C-3′	Reverse primer for the Nourseothricin^{R} cassette for *bqt4* replacement
Tsn1-Kan-F	5′-TTA TTT GCA TAC TGA AAA CATCAT TCG AAT ATC AAC ACT ACTCAA CAG CAT ACA TTA CAG ATTAAG TCG ACG GAT CCC CGG GTT AAT TAA-3′	Forward primer for the Kanamycin cassette for *tsn1* replacement
Tsn1-Kan-R	5′-ATA TTA AAA AAG CAA TTT TATCGG CTC AAT TTT AGT CAA GCGTAC AGC TGG CAA ATA AAT TGTTAG CAA TGA ATT CGA GCT CGT TTA AAC-3′	Reverse primer for the Kanamycin cassette for *tsn1* replacement
Dcr1NatMX6-F	5′-ACA TAT GCA TGT TTA TTT GAA TAG CTT AGG ATT CAT TAT TTT TTA AGA GAC AAA TTT CTC GTC AAT TGA ATG AAA CCT TCC GCC TTT ATT TTC TTT TTG ACG GAT CCC CGG GTT AAT TAA-3′	Forward primer for the Nourseothricin^{R} cassette for *dcr1* replacement
Dcr1NatMX6-R	5′-AAT ATC ACG AAA GGA TCC GTG CTT TGG AGA CCC AAA TTG AAA GTT TGA AAA GTT ACA AGG GCC GCG GTC ATA AAA AAT GAA ATA CTG TAT ATT TCA AGT CGA ATT CGA GCT CGT TTA AAC-3′	Reverse primer for the Nourseothricin^{R} cassette for *dcr1* replacement
Dcr1-Kan-F	5′-ATA GCT TAG GAT TCA TTA TTT TTT AAG AGA CAA ATT TCT CGT CAA TTG AAT GAA ACC TTC CGC CTT TAT TTT CTT TTT GA C GGA TCC CCG GGT TAA TTA A-3′	Forward primer for the Kanamycin cassette for *dcr1* replacement

Dcr1-Kan-R	5′-GCT TTG GAG ACC CAA ATT GAA AGT TTG AAA AGT TAC AAG GGC CGC GGT CAT AAA AAA TGA AAT ACT GTA TAT TTC AAG TCG AAT CGA GCT CGT TTA AAC-3′	Reverse primer for the Kanamycin cassette for *dcr1* replacement

2.12 RNA Extraction and DNase treatment

Single colonies were inoculated into 5 mL of YEL containing supplemental adenine (200 mg/L) and allowed to grow with shaking to exponential phase (OD_{600} of 0.6–0.8); after that, RNA was extracted using the MasterPure™ Yeast RNA Purification Kit (Epicentre). Following this, 1.5 mL of mid-log cultures was centrifuged at 3000 *g* for 1 minute, and the supernatant was removed. The formed pellets were vortexed, and 300 µL of a mixture, containing 300 µL of extraction reagent for RNA and 1 µL of 50 µg/µL proteinase K, was added to the tubes, vortexed, and incubated at 70°C for 15 minutes (tubes were vortexed and mixed every 5 minutes). Tubes were placed on ice for 3 minutes, and 175 µL of MPC protein precipitation reagent was added to the tubes and vortexed. Mixtures were centrifuged at 10,000 *g* for 10 minutes at 4°C. The supernatant was then transferred to another Eppendorf tube. After this, 500 µL of isopropanol was added to the tubes, inverted, and then centrifuged again at 4°C for 10 minutes at 10,000 *g*. Residual isopropanol was removed, and the pellets were completely resuspended in 200 µL of DNase I solution (containing 20 µL of 10X DNase buffer, 175 µL of deionized water, and 5 µL of RNase-free DNase I) and incubated at room temperature for 15 minutes. After that, 200 µL of 2X T and C Lysis Solution along with 200 µL of MPC protein precipitation reagent was added to the tubes, vortexed, and placed on ice for 3 minutes. Mixtures were then centrifuged at 4°C for 10 minutes at 10,000 *g*. The supernatant was then transferred to another Eppendorf tube; 500 µL of isopropanol was added to the tubes, inverted, and centrifuged again at 4°C for 10 minutes at 10,000 *g*. The residual isopropanol was carefully removed, and pellets were carefully washed twice, using 1 mL of 70% ethanol. Residual ethanol was completely removed, and the RNA was resuspended in 350 µL of TE buffer; after that, 1 µL of RiboGuard™ RNase Inhibitor was added to the RNA. Quality and concentration of the RNA was assessed using a NanoDrop (ND_1000) spectrophotometer.

Finally, the RNA was treated with RNase-free DNase (Promega) by mixing 1 µg of RNA with 1 µL of RNase-Free DNase 10X reaction buffer along with 1 µL RNase-Free DNase, and up to 10 µL nuclease-free water was added to the tube. The tubes were incubated for 30 minutes at 37°C. Then, 1 µL of DNase Stop Solution (Promega) was added to the mixture, which was further incubated at 65°C for 10 minutes. RNA was then stored at -20°C.

2.13 Reverse Transcription PCR

In this stage, 1 µg of RNA was reverse transcribed by mixing 10 µL of primer mix (containing 1 µL of 10 mM dNTP mix, 1 µL of 2 pmol/µL specific primer, and up to 10 µL nuclease-free water). For no-primer control reaction, the same volume of sterile dH_2O replaced the primer. Then, the RNA was denatured in the presence or absence of primers at 90°C for 1 minute. After that, 7 µL of the reverse transcriptase mix was added to the RNA tube after incubation at 55°C for 50 minutes. The RT mix contained 4 µL 5X RT buffer, 1 µL 0.1 M DTT, 1 µL RNaseOUT™, and 1 µL SuperScript™ III RT (Invitrogen, 18080-051). The tube was then incubated at 85°C for 5 minutes before it was placed on ice for 1 minute and spun briefly. Finally, 1 µL of RNase H was added to the tube followed by incubation at 37°C for 20 minutes. cDNA was then stored at -20°C.

For the TERRA and ARRET RT–PCR experiments, 2 µL of the cDNA was used for PCR amplification using MyTaq™ Red Mix (Bioline). PCR with subtelomeric primers at 10 pmol/µL was performed with the following program: 95°C for 3 minutes followed by 35 cycles of 30 seconds at 95°C, 20 seconds at 62°C, and 30 seconds at 72°C. An extension was set at 72°C for 5 minutes. PCR with *act1* primers was conducted using the same cycling condition at an annealing temperature of 58°C for 25 cycles.

For TERRA and ARRET qRT–PCR experiments: cDNA was PCR amplified using the QuantiTect SYBR Green PCR Kit (Qiagen; 204054) on a CFX96 real-time system (Bio-Rad) according to the manufacturer's protocol. The reaction mixture (for a 20 µL reaction) was as follows: 10 µL of SYBR™ Green master mix, 2 µL of 10 pmol/µL forward as well as reverse primers, 4 µL of the diluted cDNA (containing 1.5 µL cDNA and 2.5 µL of nuclease-free water), and 2 µL of sterile dH_2O. Samples (in three replicates) were loaded into 96-well PCR plates (BioRad) and amplified using the following program: 3 minutes at 95°C, followed by 40 cycles of 10 seconds at 95°C, 30 seconds at 60°C, and 10 seconds at 95°C. Oligonucleotide sequences used in these experiments are shown in Table 2.5.

2.14 Determination of Recombination Frequency (Fluctuation test)

The plasmid-by-chromosome recombination assay (Fluctuation test) was conducted using pSRS5 plasmid, which carries a recombination marker *ade6* mutant allele (*ade6-ΔG1483*) which was constructed by deleting a guanine at nucleotide position 1482 within the ORF of the *ade6* gene (Pryce *et al*., 2009).

A single colony of S. *pombe* strains to be tested was inoculated into 5 mL of an appropriate liquid medium (for plasmid retention) and grown overnight with shaking at 30°C. An appropriate dilution of the growing cultures was plated onto an appropriate solid medium (for plasmid retention) and incubated at 30°C until micro-colonies were visible. For one repeat, seven whole micro-colonies were inoculated individually into distinct 5 mL of an appropriate liquid media (for plasmid retention) and allowed to grow with shaking at 30°C until the cultures were saturated. After that, serial dilutions were made, and 100 μL of the lower concentration dilutions (10 to 10^{-2}) were plated onto YE+guanine plates (containing 100 μg/mL guanine final concentration from 20 mg/mL guanine dissolved in 0.35 M NaOH/ddH_2O stock, final plate pH adjusted to 6.5 with 1 M HCl) to measure the adenine prototroph counts (Ade^+ recombinant totals) within the culture (high concentrations of guanine inhibit the growth of non-recombinant ade^- cells). In addition, 100 μL of higher concentration dilutions (10^{-3} to 10^{-5}) were plated onto YEA plates to measure the viable cells counts within the culture. Plates were incubated at 30°C for 3 days; after that, the colonies were counted. This experiment was conducted 3 times, and the mean value of the three independent median values (adenine prototrophs/viable cell) of each strain were utilised for calculating the recombination frequency.

Table 2.5 Sequence of PCR primers used in this study

Primer name	Sequence	Notes
Tfx1 check-F	5′-CAAATAGTCATCTTGATTTGC-3′	Upstream of *tfx1* ORF
Tfx1 check-R	5′-TCTAACATATAGAAAGCAGCG-3′	Downstream of *tfx1* ORF
Tfx1-int-F	5′-ATAAGAGGGAGAAAATTATTC G-3′	Forward primer inside *tfx1*
Tfx1-int-R	5′-CTCCTCGGGAGGAGTTGC -3′	Reverse primer inside *tfx1*
HphMX6-F	5′-CTGTGTAGAAGTACTCGCCG-3′	Forward primer inside Hygromycin cassette
HphMX6-R	5'-AACTTCTCGACAGACGTCGC-3′	Reverse primer inside Hygromycin cassette
Tsn1 check-F	5′-GAT CTA AAC AAC CCA AGC G-3′	Upstream of *tsn1* ORF
Tsn1 check-R	5′-GCATTCATCATAGGACTGCC-3′	Downstream of *tsn1* ORF
Tsn1-int-F	5'-AAACTGACTGCAGAGGTC G-3'	Forward primer inside *tsn1*
Tsn1-int-R	5'-GAACACAGAGATAGTACTGC- 3'	Reverse primer inside *tsn1*
NatMX6-F	5′-CATGGGTACCACTCTTGACG- 3'	Forward primer inside Nourseothricin^{R} cassette
NatMX6-R	5′-CTCAGTGGCAAATCCTAACC- 3'	Revers primer inside Nourseothricin^{R} cassette
Ago check-F	5′-ACTTATGTTGCGTTTGCGTGC - 3'	Upstream of *ago1* ORF
Ago check-R	5′-AGCTATCAACAGTGGATAGAGC-3′	Downstream of *ago1* ORF
Ago1-int F	5′-AGGTACTTGTTAGCTTCATTCG-3′	Forward primer inside *ago1*
Ago1-int R	5′-AGTACCGACATTATTGCGATGC-3′	Reverse primer inside *ago1*

Taz1 check-F	5′-ACAGTTCCTTTCTTTTCGCTT G-3'	Upstream of *taz1* ORF
Taz1 check-R	5′-TGCATACTTCGGACAATTAACG-3′	Downstream of *taz1* ORF
Taz1-int-F	5′-ACAGGCTTGATTGATCTCCT-3′	Forward primer inside *taz1*
Taz1-int-R	5′-ACTCGCTCACGAAGCCTGTT-3′	Reverse primer inside *taz1*
Rap1check-F	5′-GCCTTCTGCTTATTCGCATACT-3′	Upstream *rap1* ORF
Rap1check-R	5′-TGGACCTGCTCCAATTTTATTT-3′	Downstream of *rap1* ORF
Rap1-int-F	5′-AGTCGCAGAAGATGAACGCG-3′	Forward primer inside *rap1*
Rap1-int-R	5′-ACTTATAATGTTGCCGCCAG-3′	Reverse primer inside *rap1*
Bqt4 check-F	5′-ATCCCAACAGAAAAGCGTAAAA-3′	Upstream *bqt4* ORF
Bqt4 check-R	5′-GGTCTCCAATCCCAAATCATAA--3′	Downstream of *bqt4* ORF
Bqt4-int-F	5′-GTACGCGCTTCCCGAAATTA-3′	Forward primer inside *bqt4*
Bqt4-int-R	5′-CCATAGTCCAGCAACACGTT-3′	Reverse primer inside *bqt4*
KanMX6-F	5′-CGGATGTGATGTGAGAACTG-3′	Forward primer inside kan R cassette
KanMX6-R	5′-CAGTTCTCACATCACATCCG-3′	Reverse primer inside kan R cassette
Dcr1 check-F	5′-AGTATTCTGCTCGTGTGATTG-3	Upstream of *dcr1* ORF
Dcr1 check-R	5′-TGATTGAAACTCGAGATGCTTTG-3′	Upstream *dcr1* ORF
Dcr1-int-F	5′-ATTCGACGAATGTCATCATGC-3′	Forward primer inside *dcr1*
Dcr1-int-R	5′-AGACGATATCATCAGTCACACG-3′	Reverse primer inside *dcr1*

oC	5′-GTAACCCCTGTAACCGTAACCC-3′	Telomeric primer used for the first strand cDNA synthesis for TERRAs. See Figure 4.3A
o3	5′-GTGTGGAATTGAGTATGGTGAA-3′	Sub-telomeric primer used for the first strand cDNA synthesis for ARRETs. See Figure 4.3A
o2	5′-GTGTAATACAGTAGTGCAGTG-3′	Forward sub-telomeric PCR primer for amplification of both TERRAs and ARRETs. See Figure 4.3A
o4	5′CGGCTGACGGGTGGGGCCCAATA-3′	Reverse sub-telomeric PCR primer for amplification of both TERRAs and ARRETs. See Figure 4.3A
act1-F	5′-ATGGAAGAAGAAATCGCAG-3′	Forward primer inside *act1*
act1-R	5′-CAAAACAGCTTGAATAGC-3′	Reverse primer inside *act1*

Chapter 3: Results

Tfx1-Tsn1: a role in chromosome stability

3. Tfx1-Tsn1: a role in chromosome stability

3.1 Introduction

In eukaryotic cells, the accurate segregation of chromosomes ensures that genetic material is properly transmitted to daughter cells (Mutazono et al., 2017; Brouwers et al., 2017). During the eukaryotic cell cycle, the failure of this process is associated with a wide range of genetic diseases, including cancer (Santaguida & Amon, 2015; Potapova & Gorbsky, 2017). Centromeres and telomeres are eukaryote chromosomal loci that are crucial for proper chromosomal segregation and maintenance (Steiner & Henikoff, 2015; Jain & Cooper, 2010; Fennell et al., 2015). Centromeres facilitate the link between chromosomes and spindle microtubules (Forsburg & Shen, 2017; Moreno-Moreno et al., 2017; Thakur et al., 2015; Buhler & Gasser, 2009; Westhorpe & Straight, 2014), and telomeres protect the ends of linear chromosomes from degradation and DNA damage response activation (Maestro et al., 2017, Vancevska et al., 2017; Schoeftner & Blasco, 2009; Buhler & Gasser, 2009; Lorenzi et al., 2015). Consequently, proper maintenance of centromere and telomere function is essential for genomic integrity (Harland et al., 2014).

Failure to preserve the structure or function of centromeres can result in mis-segregation via loss or gain of chromosomes, an outcome that is associated with cancer (Volpe et al., 2002; Lee et al., 2013; Ekwall et al., 1999; Carmichael et al., 2004; Santaguida & Amon, 2015). Centromere regions are heterochromatic and are marked by methylation of H3K9, followed by capture of heterochromatin protein 1 (Swi6 in *S. pombe*) (Buhler & Gasser, 2009; Schoeftner & Blasco, 2009; Zeng et al., 2010; Stimpson & Sullivan, 2010; Zocco et al., 2016; Wang et al., 2016a; Chan & Wong, 2012; Tadeo et al., 2013). The formation of heterochromatin at the centromeres is important for the full function of kinetochores, which are necessary for proper segregation of chromosomes (Mutazono et al., 2017; Buhler & Gasser, 2009; Schoeftner & Blasco, 2009; Zeng et al., 2010; Stimpson & Sullivan, 2010; Schmidt & Cech, 2015). The RNAi machinery is required to mediate heterochromatin formation and maintenance at the centromeres in many eukaryotes, including *S. pombe*.

Thus, deletion of key RNAi genes, including *ago1*, impacts centromeric function by reducing H3K9 methylation and Swi6 association and, consequently, chromosomal mis-segragation, causing a high rate of cells with aberrant mitosis and a high sensitivity to the microtubule disrupting agent TBZ (Buhler & Gasser, 2009; Volpe et al., 2002; Chan & Wong, 2012; Tadeo et al., 2013; Holoch & Moazed, 2015; Creamer & Partridge, 2011; Shimada et al., 2016; Volpe et al., 2003; Sadeghi et al., 2015; Lee et al., 2013). Translin-TRAX complex (C3PO) is involved in the RNAi pathway in humans and *D. melanogaster*; it mediates the removal of the passenger strand from the small interfering RNAs involved in RISC complex-mediated silencing (Liu et al., 2009; Ye et al., 2011; Holoch & Moazed, 2015; Tian et al., 2011; Jaendling & McFarlane, 2010). Previous studies on the null mutants of *S. pombe*, *tsn1* and *tfx1*, have shown no measureable phenotypic change (Jaendling et al., 2008; Laufman et al., 2005), indicating that they are not essential for fission yeast (Jaendling & Mcfarlane, 2010). However, more recently, researchers in the McFarlane group found a phenotype associated with *tfx1* mutation, but not *tsn1* mutation, in an *ago1Δ* background. They found that the *ago1Δ tfx1Δ* double mutant is more resistant to TBZ, than the *ago1Δ* single mutant (N. Al-mobadel, PhD thesis, Bangor University; Z. Al-shehri, PhD thesis, Bangor University). In addition, mutation of *tfx1* is found to partially supress mini-chromosome instability caused by an *ago1Δ* mutation (N. Al-mobadel, PhD thesis, Bangor University). Further work has shown that mutation of *tsn1Δ* in the *ago1Δ tfx1Δ* background affects TBZ resistance because the *ago1Δ tfx1Δ tsn1Δ* triple mutant exhibits hypersensitivity to TBZ (N. Al-mobadel, PhD thesis, Bangor University). These findings are the first to implicate Tfx1 and Tsn1 in chromosome stability control.

The chromosome instability of *ago1Δ* cells is thought to be caused by defective centromere heterochromatin which elevates transcription from centromeric regions normally subjected to heterochromatic silencing (Volpe et al., 2003; Holoch & Moazed, 2015). Interestingly, further analysis found that there was no suppression of the elevated centromeric transcription in the *ago1Δ tfx1Δ* double mutant relative to the *ago1* single mutant (they measured activation of the expression of an *ura4* marker gene in the centromeric heterochromatic regions of chromosome 1 for the *ago1Δ* and *ago1Δ tfx1Δ* strains; N. Al-mobadel, PhD thesis, Bangor University).

These findings indicate that the suppression of the chromosomal instability of *ago1Δ* cells by mutation of *tfx1* is not associated with restoring the pericentromeric heterochromatin silencing state, and suggesting a distinct suppression mechanism. These results point to the possibility that the chromosomal instability observed in an *ago1Δ* mutant is potentially centromere-independent. Thus, in order to identify the Tfx1 function, whole genome transcriptional data was examined using tiled microarrays to detect any changes of expression at other genomic loci when comparing the *ago1Δ* and the *ago1Δ tfx1Δ* strains. These analyses determined that the only statistically significant difference of note was the activation of one or more of the normally silent sub-telomeric RecQ-like genes, *tlh1-4* (N. Al-mobadel, PhD thesis, Bangor University; Figure 3.7). *S. pombe* has three chromosomes, and there are only four sub-telomereic *tlh* genes located at the ends of chromosome 1 and chromosome 2, as chromosome 3 contains ribosomal DNA (rDNA) repeats in the sub-telomeric regions (Figure 1.10). The *S. pombe tlh* genes, which are orthologous to the human *BLM* gene (Hansen et al., 2006), are normally transcriptionally inactive, although they have been shown to participate in the metabolism of telomeres during telomere crisis initiated by the loss of telomerase (Mandell et al., 2005). Morever, the upregulation of *tlh* genes was also the only notable difference when comparing the *tfx1Δ* single mutant and wild-type (WT) strains. However, similar activation of *tlh* genes was not observed in *tsn1Δ* relative to the WT strain (N. Al-mobadel, PhD thesis, Bangor University; Figure 3.7).

Given that sub-telomeric *tlh* genes are activated in the *ago1Δ tfx1Δ* double mutant, this led us to hypothesise that the suppression of chromosomal instability of an *ago1Δ* mutant is somehow related to the activation of the *tlh* genes. Therefore, at the onset of this study, the working hypothesis postulated that *tlh* gene activation following mutation of *tfx1*, but not *tsn1*, was required to partially suppress the chromosome instability phenotype of an *ago1Δ* mutant.

3.2 Results

3.2.1 Mutation of *tfx1* suppresses the chromosomal instability phenotype of the *ago1*Δ mutant in a *tsn1*-dependent fashion

We set out to confirm the previous finding that *tfx1Δ* mutation suppresses the chromosome instability defect of *ago1*Δ cells (all appropriate strains containing single mutants of *tsn1Δ* and *tfx1Δ*, and double mutants with *ago1Δ* were constructed by others in the McFarlane group, but they were verified here using PCR prior to use).

3.2.1.1 TBZ sensitivity spot assay

Cells that are defective in chromosome segregation, such as those in the *ago1*Δ mutant, show high sensitivity to TBZ (Sadeghi et al., 2015; Buhler & Gasser, 2009; Volpe et al., 2003; Volpe et al., 2002; Lee et al., 2013). Therefore, appropriate strains were exposed to TBZ. Single mutants of *tfx1*Δ and *tsn1*Δ and the *tfx1*Δ *tsn1*Δ double mutant showed no sensitivity to TBZ relative to the WT strain (Figure 3.1.A), consistent with previous work of Jaendling et al. (2008). Consistent with previous results, the high TBZ sensitivity of the *ago1Δ* mutant was found to be significantly suppressed by the *tfx1*Δ mutation, but not by *tsn1*Δ (Figure 3.1.B). The *ago1*Δ *tfx1*Δ *tsn1*Δ triple mutant was hypersensitive to TBZ in comparison to the *ago1*Δ single mutant (Figure 3.1.B).

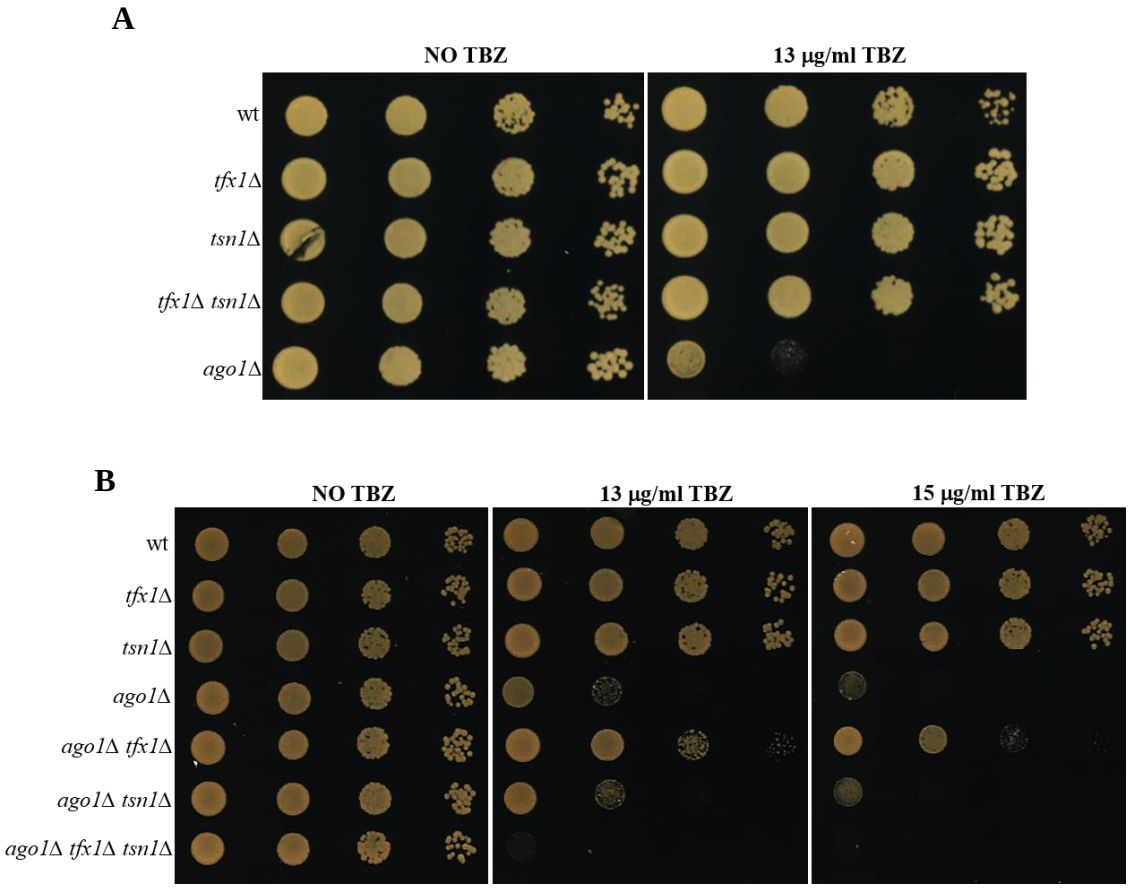

Figure 3.1 Mutation of *tfx1*, but not *tsn1*, suppressed TBZ sensitivity of *ago1Δ*.
Serial dilutions of the indicated *S. pombe* mutants were made and exposed to different concentrations of TBZ. The plates were then incubated at 30°C for 3 days. **A.** A Single mutants of *tfx1*Δ and *tsn1*Δ and the *tfx1*Δ *tsn1*Δ double mutant showed no sensitivity to TBZ in comparison to the isogenic WT strain. The *ago1Δ* strain was utilised as a positive control, which displayed high sensitivity to TBZ. **B.** The *ago1*Δ *tfx1*Δ double mutant has significantly suppressed sensitivity relative to the *ago1*Δ mutant, whereas the *ago1*Δ *tsn1*Δ double mutant exhibited TBZ sensitivity similar to that seen in the *ago1*Δ single mutant. The *ago1*Δ *tfx1*Δ *tsn1*Δ triple mutant is hyper sensitive to TBZ, with a sensitivity greater than the *ago1Δ* single mutant.

3.2.1.2 Colony growth test

The chromosome instability defects of *ago1*Δ cells can be observed when they are streaked to single colonies on yeast extract agar (YEA), as the growth of *ago1*Δ was found to be less than the WT growth (Figure 3.2). However, we noticed that the growth of the *ago1*Δ *tfx1*Δ double mutant, but not the *ago1*Δ *tsn1*Δ double mutant, was much better than the growth of the *ago1*Δ single mutant and more similar to the WT growth (Figure 3.2), which is consistent with the TBZ sensitivity pattern (Figure 3.1). The growth phenotype of the *ago1*Δ *tfx1*Δ *tsn1*Δ triple mutant was similar to that of the *ago1*Δ single mutant (Figure 3.2). These results further support the suggestion that the *tfx1* mutation partially restores genome stability to *ago1Δ* cells, which is apparently dependent on the presence of Tsn1 in a Tfx1-free context.

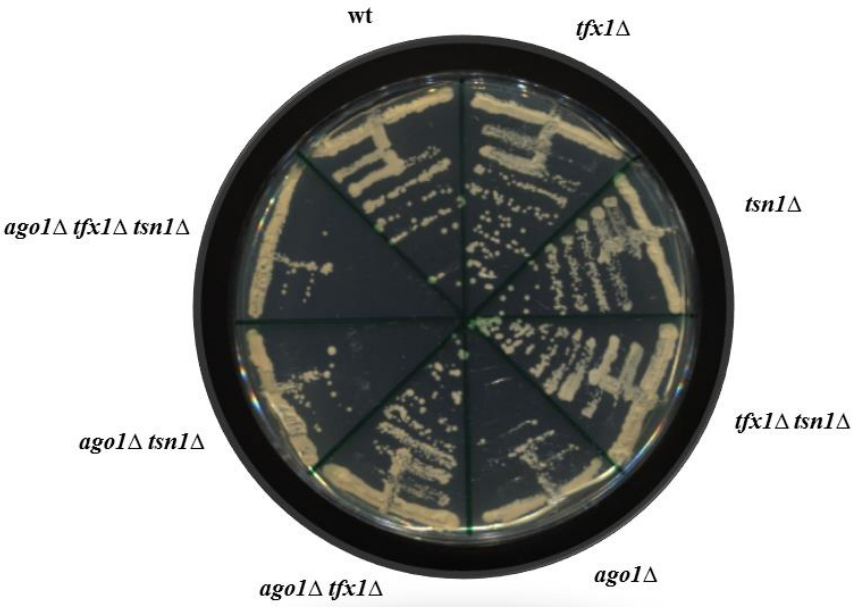

Figure 3.2 Colony forming capacity of *ago1Δ* is enhanced by mutating *tfx1*.
The indicated *S. pombe* strains were streaked on YEA plate and then incubated at 30°C for 3 days. The *tfx1*Δ and *tsn1*Δ single mutants and the *tfx1*Δ *tsn1*Δ double mutant have a growth phenotype similar to the WT. The *ago1*Δ single mutant growth was significantly lower than the WT, whereas the *ago1*Δ *tfx1*Δ double mutant growth was much higher than the *ago1*Δ single mutant and more similar to the WT. Similar growth phenotype defects of an *ago1Δ* single mutant were observed in the *ago1*Δ *tsn1*Δ double mutants and the *ago1*Δ *tfx1*Δ *tsn1*Δ triple mutant.

3.2.1.3 Microscopy analysis of aberrant mitoses

The *ago1*Δ mutant was found to have high rates of cells with aberrant mitoses (Volpe et al., 2003). In the present study, mitotically dividing cells were stained with 4',6-diamidino-2-phenylindole (DAPI) and monitored for the frequency of anaphase defects (Figure 3.3). We found that aberrant mitosis occurred less frequently in the *tfx1Δ* and *tsn1Δ* single mutants, which was statistically indistinguishable from the frequency of the aberrant mitosis seen in the WT (Figure 3.3.B) (examples of WT phenotypes are shown in Figure 3.3.A, left-hand panel). As previously reported, we found that, in the *ago1Δ* mutant, the chromosomes frequently failed to segregate normally at anaphase, which resulted in abnormal mitosis (examples of *ago1Δ* phenotypes are shown in Figure 3.3.A, right-hand panel). Interestingly, we found that the mutation of *tfx1*, but not *tsn1*, strongly reduced the high number of aberrant mitosis events observed in the *ago1Δ* background (Figure 3.3.B), which is consistent with its TBZ sensitivity phenotype (Figure 3.1) and growth phenotype (Figure 3.2). The *ago1*Δ *tfx1*Δ *tsn1*Δ triple mutant had abnormal mitosis that was statistically indistinguishable from the abnormal mitosis levels seen in the *ago1*Δ single mutant (Figure 3.3.B). These results indicate that the loss of Tfx1 partially suppresses the chromosomal segregation defects of Ago1-deficient cells.

A

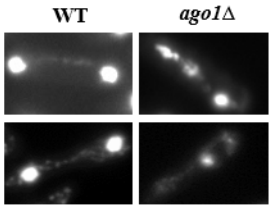

B

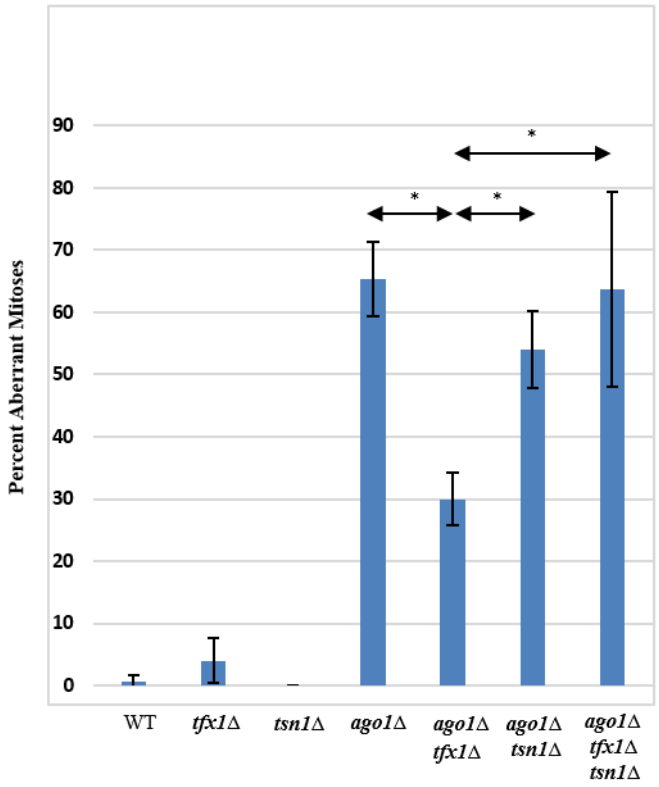

Figure 3.3 Fluorescence microscope analyses of the *S. pombe* strains grown at 30°C and stained with DAPI showing the percentage of aberrant mitosis.

A. Example phenotypes of WT (left) and *ago1*Δ (right) cells in anaphase with DAPI stain using a fluorescence microscope.

B. The plot shows that the *tfx1*Δ and *tsn1*Δ single mutants exhibited no measureable increase in the percentage of aberrant mitosis in comparison to the WT. However, the *ago1*Δ single mutant displayed a high level of abnormal mitosis (approximately 65%). The *ago1*Δ *tfx1*Δ double mutant had significantly reduced numbers of abnormal mitosis events compared to the *ago1*Δ mutant, whereas both the *ago1*Δ *tsn1*Δ double mutant and the *ago1*Δ *tfx1*Δ *tsn1*Δ triple mutant had an aberrant mitosis statistically indistinguishable from that seen in the *ago1*Δ single mutant. * = P value <0.05; Student's t-test; error bars are standard deviation. The percentage of aberrant mitosis was obtained from the average of three independent experiments by observing at least 100 cells per sample in each experiment.

3.2.2 Loss of Tfx1 does not restore centromeric heterochromatin

As indicated, analysis of silencing the marker genes in the centromeric heterochromatic regions showed that activation of expression of a *ura4*$^{+}$ marker gene in the heterochromatic regions in an *ago1Δ* mutant is not suppressed by mutating *tfx1* (N. Al-mobadel, PhD thesis, Bangor University). Based on this finding, we set out to ask whether the marker expression assay that we used was accurate enough to discern precise alterations in *ura4*$^{+}$ expression. To address this, we applied a quantitative method to analyse transcriptional activity in the centromeric regions for appropriate mutants. We conducted microarray analysis using tilted arrays covering the whole *S. pombe* genome to examine the centromeric expression profiles for all three *S. pombe* centromeres (the previous marker expression study only covers *cenI*). The array analysis showed that both the *tsn1Δ* and *tfx1Δ* single mutants exhibit similar levels of silencing of the WT strain. Importantly, while mutation of *ago1* significantly elevates the centromeric heterochromatic transcription relative to the WT strain, the *ago1*Δ *tfx1*Δ double mutant was indistinguishable from the *ago1*Δ single mutant for transcription from both forward and reverse strands and for all regions of all three *S. pombe* centromeres (Figure 3.4, Figure 3.5 and Figure 3.6).

Taken together, these results further confirm that the partial suppression of the *ago1Δ* mutant chromosomal instability by *tfx1Δ* is not due to full or partial re-establishment of the centromeric heterochromatic state; this suggests a centromere-independent suppression mechanism. Microarray analysis was performed by a colleague (Julia Feichtinger; currently based at the Graz University of Technology, Austria).

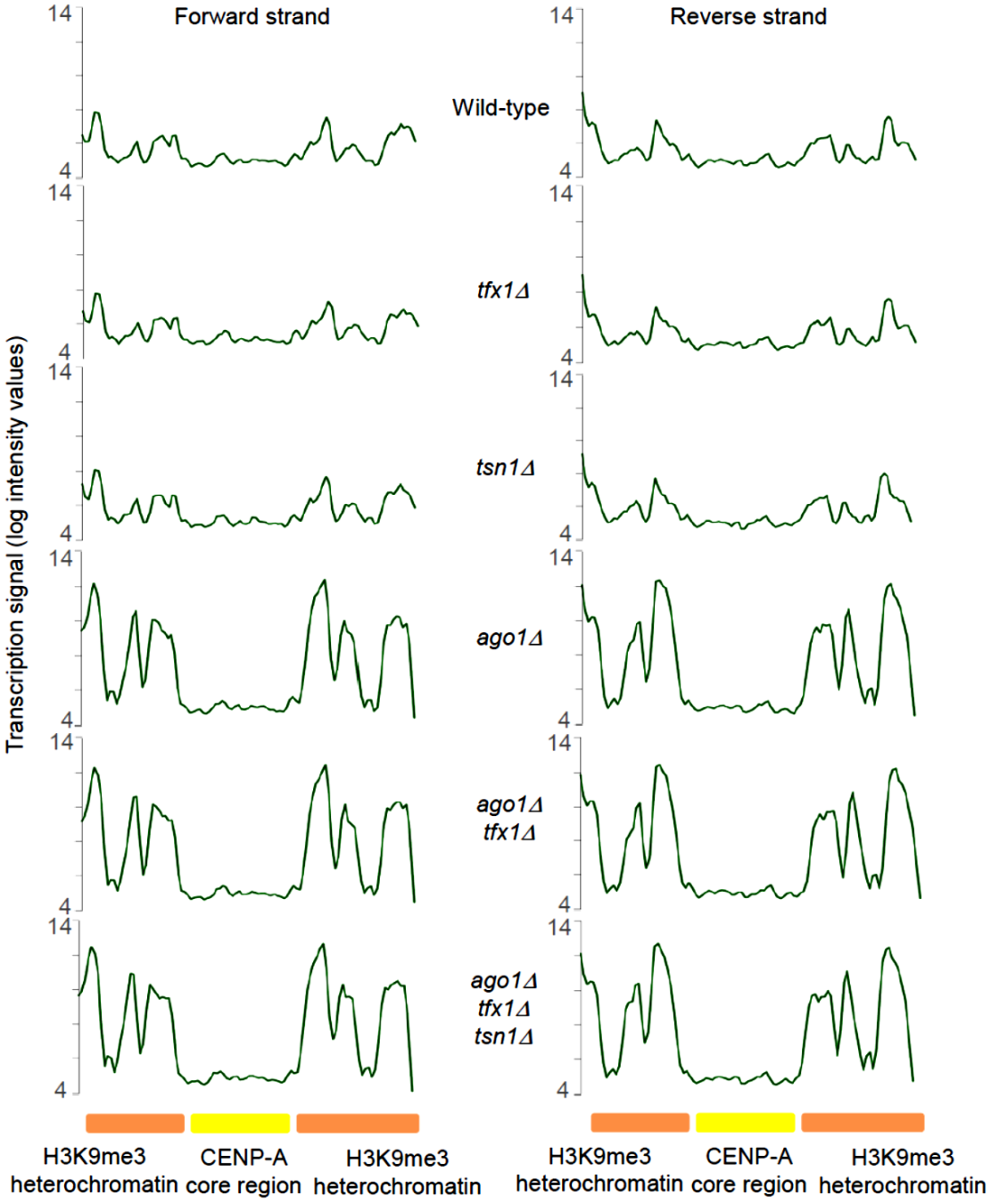

Figure 3.4 The high levels of centromere 1 transcripts in the *ago1Δ* mutant are not altered by mutating *tfx1*.

The transcriptional profiles of the forward (left) and reverse (right) strands from the centromeric regions for *cen1* are shown for the indicated *S. pombe* strains. The plot showed that the *ago1Δ* single mutant had elevated transcription in the centromeric heterochromatic region in comparison to the WT (and *tsn1Δ* and *tfx1Δ* single mutants, which were indistinguishable from the WT). The centromeric transcript levels of the *ago1Δ tfx1Δ* and *ago1Δ tfx1Δ tsn1Δ* mutants were indistinguishable from the *ago1Δ* single mutant from both strands. The centromere core region, which associates with Cnp1 (CENP-A), and heterochromatic region are indicated (the *S. pombe* nucleotide coordinates shown for *cen1* are chromosome 1: 3,754,000–3,790,000).

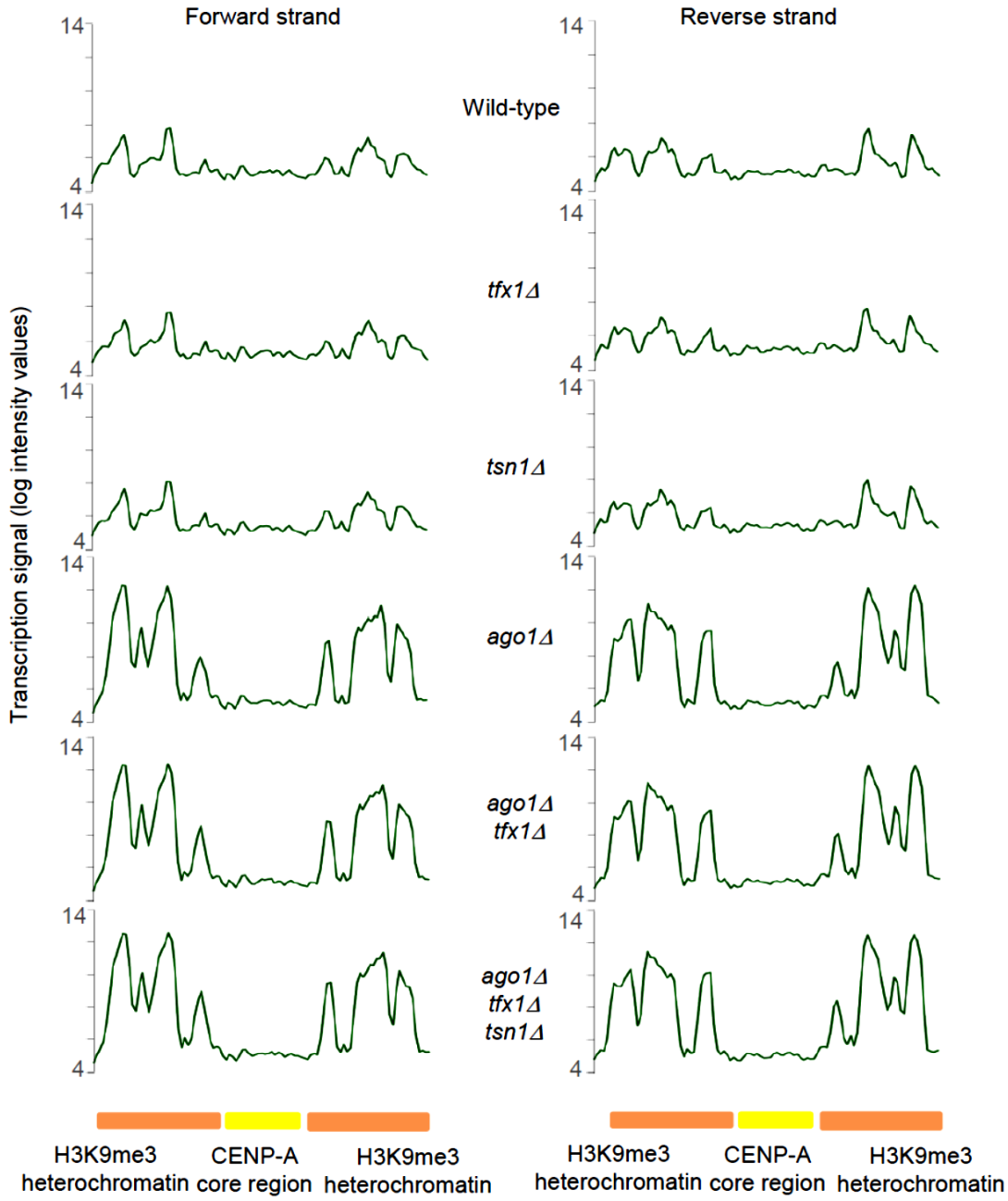

Figure 3.5 The high levels of centromere 2 transcripts in the *ago1Δ* mutant are not altered by mutating *tfx1*.

The transcriptional profiles of the forward (left) and reverse (right) strands from the centromeric regions for *cen2* are shown for the indicated *S. pombe* strains. The plot showed that the *ago1Δ* single mutant had elevated transcription in the centromeric heterochromatic region in comprison to the WT (and *tsn1Δ* and *tfx1Δ* single mutants, which were indistinguishable from the WT). The centromeric transcript levels of the *ago1Δ tfx1Δ* and *ago1Δ tfx1Δ tsn1Δ* mutants were indistinguishable from the *ago1Δ* single mutant from both strands. The centromere core region, which associates with Cnp1 (CENP-A), and heterochromatic region are indicated (the *S. pombe* nucleotide coordinates shown for *cen2* are chromosome 2: 1,600,000 – 1,645,000).

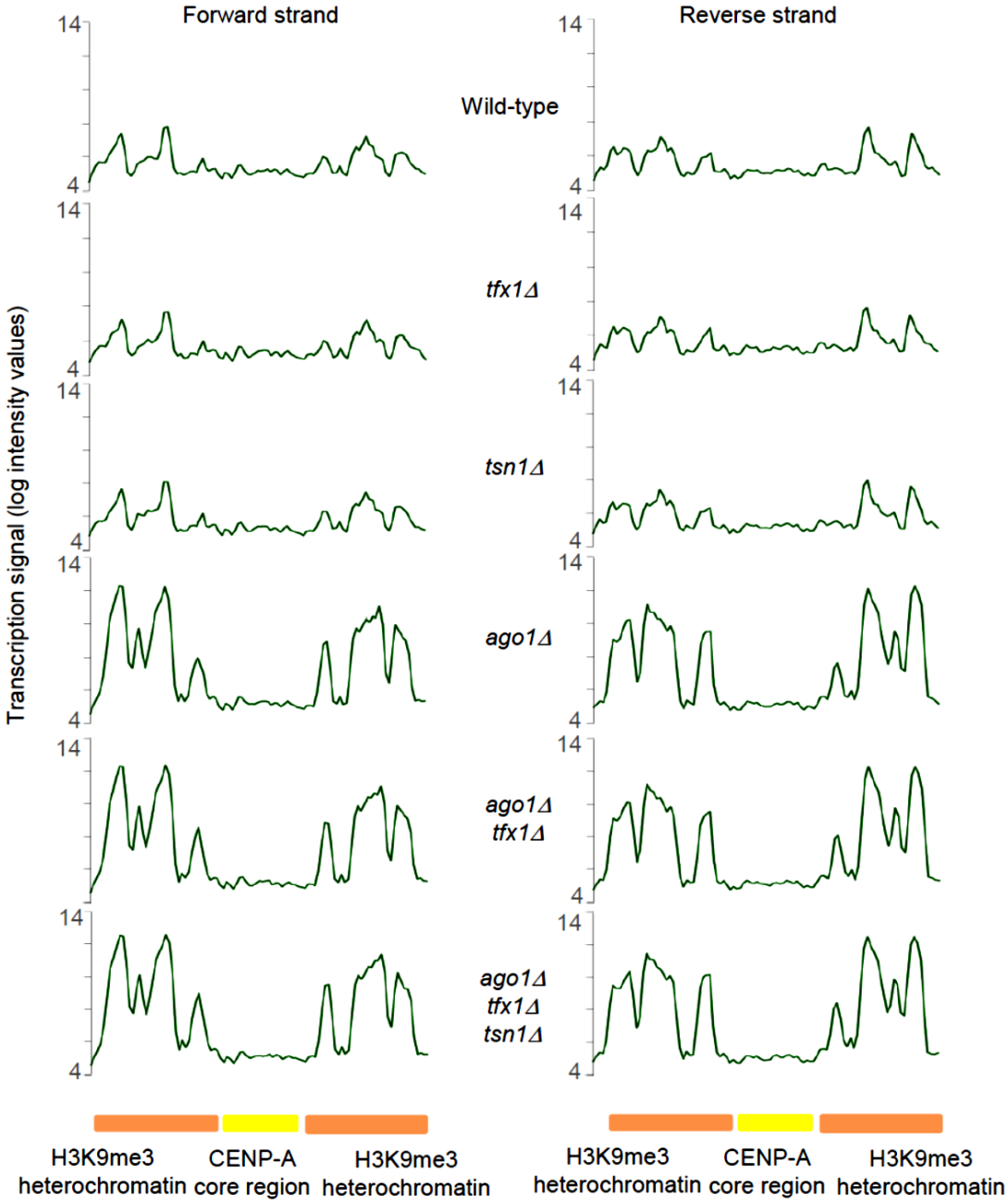

Figure 3.6 The high levels of centromere 3 transcripts in the *ago1Δ* mutant are not altered by mutating *tfx1*.

The transcriptional profile of the forward (left) and reverse (right) strands from the centromeric regions for *cen3* are shown for the indicated *S. pombe* strains. The plot showed that the *ago1Δ* single mutant had elevated transcription in the centromeric heterochromatic region in comparison to the WT (and *tsn1Δ* and *tfx1Δ* single mutants, which were indistinguishable from the WT). The centromeric transcript levels of the *ago1Δ tfx1Δ* and *ago1Δ tfx1Δ tsn1Δ* mutants were indistinguishable from the *ago1Δ* single mutant from both strands. The centromere core region, which associates with Cnp1 (CENP-A), and heterochromatic region are indicated (the *S. pombe* nucleotide coordinates shown for *cen3* are chromosome 3: 1,070,000 – 1,137,000).

3.2.3 Investigation of whether *tlh* gene activation by *tfx1* mutation can suppress the Ago1 requirement

As explained, when comparing the *ago1Δ* and *ago1Δ tfx1Δ* strains, the tiled microarrays revealed no measurable alterations of the transcript levels in the centromeric heterochromatic regions (Figure 3.4, Figure 3.5 and Figure 3.6). These results indicate that the observed rescue of the chromosome instability phenotype of the *ago1Δ* mutant, following mutation of *tfx1*, is not due to the restoration of the heterochromatin function in the centromeres. Extending this led to the finding that the normally silent sub-telomeric *tlh* genes are upregulated in the *ago1Δ tfx1Δ* double mutant (N. Al-mobadel, PhD thesis, Bangor University; an example of the plot profile for the *tlh1* transcript is shown in Figure 3.7). These analyses may suggest that the activation of *tlh* genes drive the *ago1Δ* suppressor phenotype.

In *S. pombe*, sub-telomeres, like centromeres, are heterochromatic and they undergo H3K9 methylation, followed by the association of Swi6 (Buhler & Gasser, 2009; Schoeftner & Blasco, 2009; Shimada et al., 2016; Tadeo et al., 2013; Zeng et al., 2010). Of the four sub-telomeric *tlh* paralogous sequences (*tlh1–tlhl4*), only *tlh1* and *tlh2* have been included in the *S. pombe* genome database (http://www.pombase.org) at this time. The sub-telomeric *tlh* genes are normally silenced and they have no known function. Researchers in the Norbury group (Oxford University) previously constructed a strain carrying a mutation of all four *tlh* genes (referred to as *tlhΔ4*); they found no apparent phenotype when these genes were disrupted (C. Norbury, personal communication). To test the hypothesis that *tlh* genes activation, by *tfx1* mutation, suppresses the requirement for Ago1, appropriate mutant strains, containing a mutation of all *tlh* genes (*tlhΔ4*) (obtained from C. Norbury, Oxford University), were constructed (Figures 3.10 and 3.11) and then exposed to TBZ (Figure 3.12).

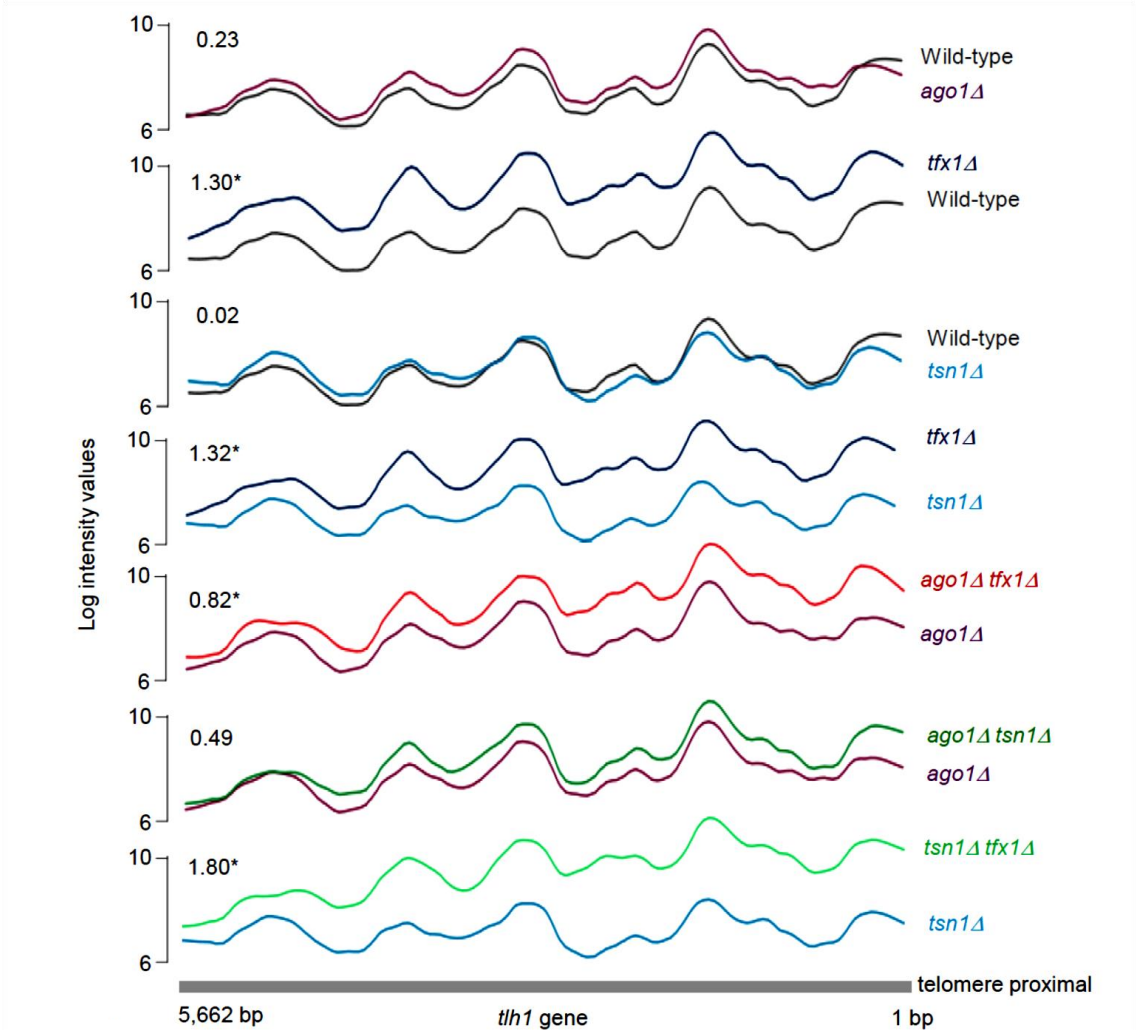

Figure 3.7 The sub-telomeric *tlh1* transcript is elevated in the *ago1Δ tfx1Δ* double mutant. Analysis of tiled whole genome expression data comparing *ago1Δ* with *ago1Δ tfx1Δ* showed that the sub-telomeric *tlh1* gene transcript is activated. The *tlh1* gene is also upregulated in the *tfx1Δ* single mutants. Similar activation of *tlh1* is not seen in the *tsn1Δ* mutant. The plots show the transcriptional activity for the *tlh1* open reading frame. Seven pairwise plots of transcriptional signals are shown for various strains. The log 2-fold change (lg2FC) for each plot is given as a numerical value within the plot (* = P<0.05). Similar results are seen for the other annotated *tlh2* paralog (see Appendix 1).

3.2.3.1 Constructing appropriate mutant strains

De novo deletion (direct gene mutation) was used in the present study to construct all the appropriate mutation strains. No strains were constructed via genetic crossing, as an early study conducted by the McFarlane group observed non-Mendelian patterns of segregation following mating involving the *tsn1Δ* mutation, which suggests an as yet undefined meiotic haplo-insufficiency for Tsn1 (R. McFarlane, communication), or a role in poison-antidote meiotic drive (Nuckolls et al., 2017; Hu et al., 2017; Shropshire et al., 2017). Additionally, another recent study aiming to identify non-essential mutants of *S. pombe* that are defective in mating and related processes, such as sporulation, found that *tsn1*Δ mutants have very high levels of sporulation defects (Dudin et al., 2017). These findings indicate that the phenomenon observed in *tsn1*Δ mutants is a post-meiotic defect, and so we opted to make *de novo* deletion mutants (in duplicate, at least), which also facilitated maintaining all four *tlhΔ* alleles in the background.

To generate the 'double' mutant, *ago1* and *tfx1* were deleted from the parent strain, carrying a mutation of all four *tlh* genes, (*tlh*Δ*4* background, BP3273). To generate the 'triple' mutant, *tfx1* was deleted from the newly constructed 'double' mutant *tlh*Δ*4 ago1Δ* background (BP3274) by replacing it with selectable antibiotic resistant cassettes using polymerase chain reaction (PCR)-based gene targeting methods (Bähler et al., 1998) (see Section 2.3) (note: for ease of reading I refer to *tlhΔ4* as a single mutation; therefore, *tlhΔ4* with a second mutation will be referred to as a 'double' mutant, and so on). Plasmids containing the required antibiotic resistant cassettes were isolated from *E. coli* (see Table 2.3). The hygromycin-resistance gene (*hphMX6*) and the nourseothricin-resistance gene (*natMX6*) were the replacement cassettes used to delete *ago1* and *tfx1*, respectively. The replacement cassettes were amplified using PCR with primers containing 80 bp homologous sequences directly flanking, upstream and downstream, the *ago1* and *tfx1* open reading frames (ORFs); they also contained a 20 bp homologous sequence to the antibiotic-resistant markers on the *hphMX6* and *natMX6* genes of the plasmids (Figure 3.8). The purified PCR product was then chemically transformed into the appropriate *S. pombe* strains (see Section 2.5.1). To confirm the gene deletion, *ago1*Δ and *tfx1Δ* candidates were screened via PCR (Figures 3.10 and 3.11) using three sets of primers, as shown in Figure 3.9.

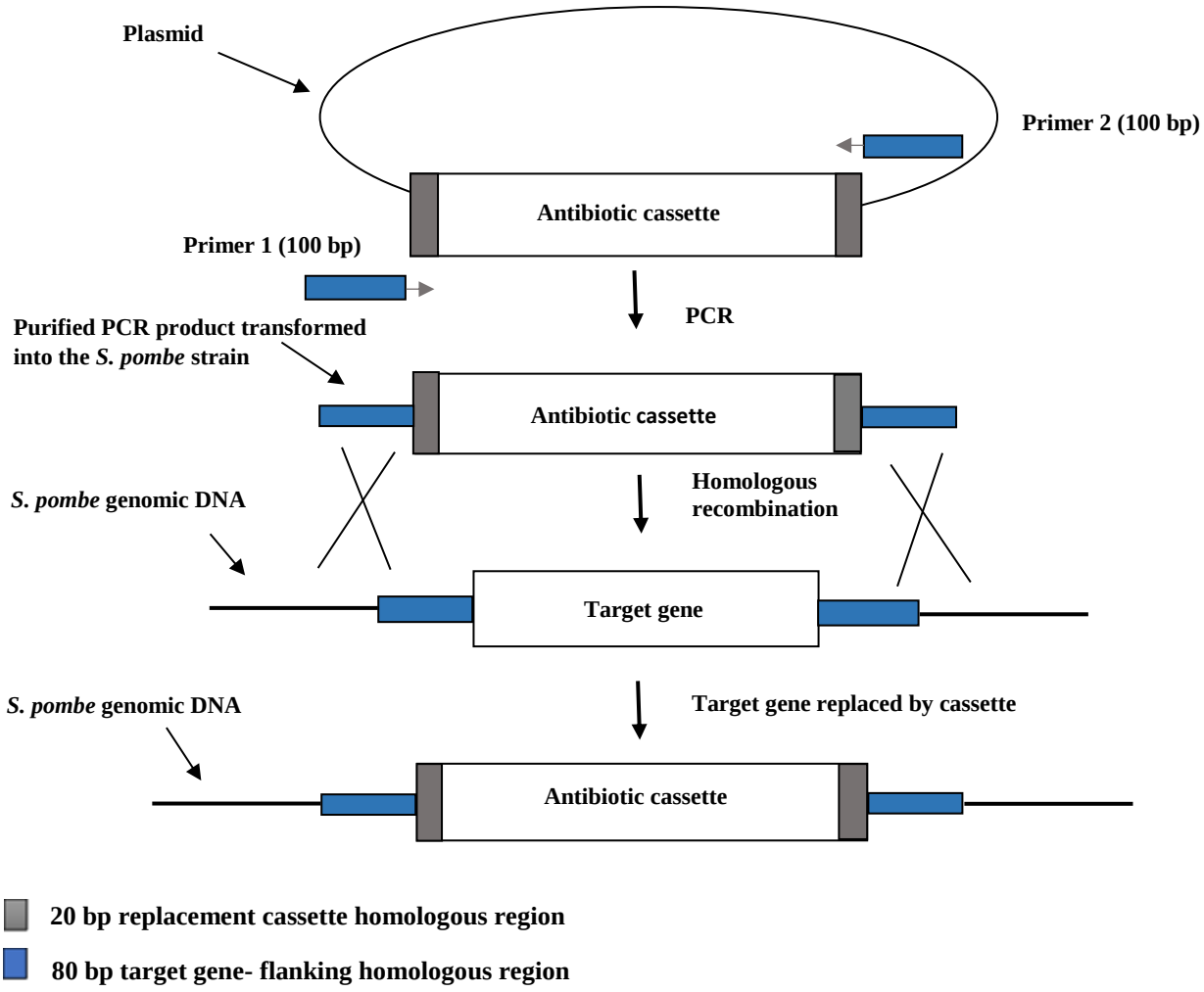

Figure 3.8 Diagram describing the target gene knockout process.
Different plasmids were utilised as templates for amplification of selectable antibiotic resistant cassettes using PCR primers containing a 20 bp (grey box) homologous sequence to the plasmid that contains a target antibiotic resistant marker and 80 bp homologous sequences directly to the upstream and downstream target gene ORF to be deleted (blue box). The purified PCR product was then chemically transformed into the *S. pombe* strain; the target gene was replaced by a replacement cassette.

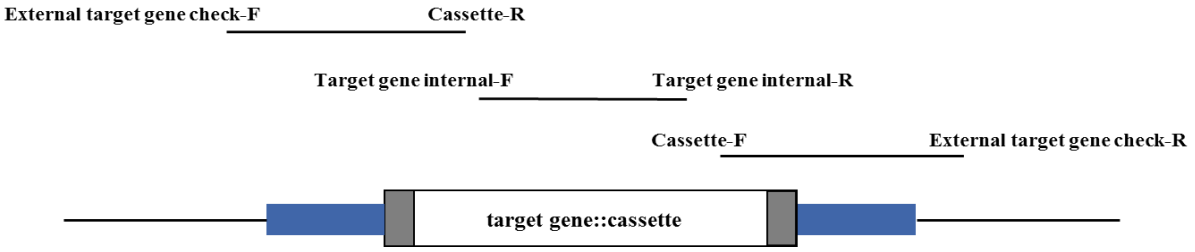

Figure 3.9 Diagram demonstrating the primers position used to confirm the correct deletion of the gene of interest.

All the target genes were deleted by replacement with antibiotic resistant cassettes as described by Bähler et al. (1998) (see Figure 3.8). Three sets of checking primers, which are shown at their approximate location, were used to confirm the deletion of the target genes. These include the Target gene Internal-F/Target gene Internal-R primer set, which should give no PCR products for the successfully deleted gene candidates due to the deletion of the target genes by the cassette replacements. The External target gene check-F/Cassette-R and Cassette-F/External target gene check-R primer sets should give PCR products, at the expected size, for the successfully deleted gene candidates due to the presence of the cassettes.

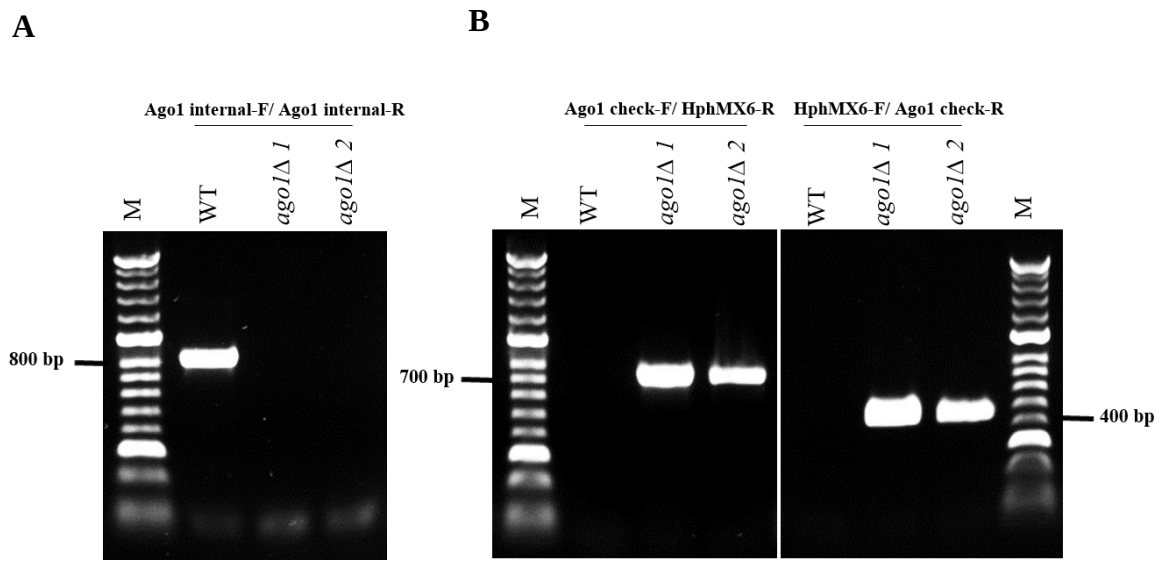

Figure 3.10 PCR screening of successful *ago1Δ* candidates.
A. Agarose gel image displays the PCR products for the WT strain (BP90) and *ago1*Δ 1 and 2 (BP3274 *tlh*Δ*4 ago1*Δ and BP3275 *tlh*Δ*4 ago1*Δ, respectively) using Ago1-int-F and Ago1-int-R primers. The expected PCR product size of the *ago1* gene is 845 bp; clearly, the gel image shows no PCR products in the successful *ago1*Δ candidate strains. **B**. PCR products for the WT and *ago1*Δ candidate strains using Ago1 check-F and HphMX6-R primers. Band sizes of approximately 700 bp were seen in the *ago1*Δ strains, but not in the *ago1*$^{+}$ strains (WT). The HphMX6-F and Ago1check-R primers were utilised to amplify the WT and *ago1*Δ candidate strains. A product size of 497 bp is present in the *ago1*Δ strains, but not in the *ago1*$^{+}$ strains (WT). M = markers.

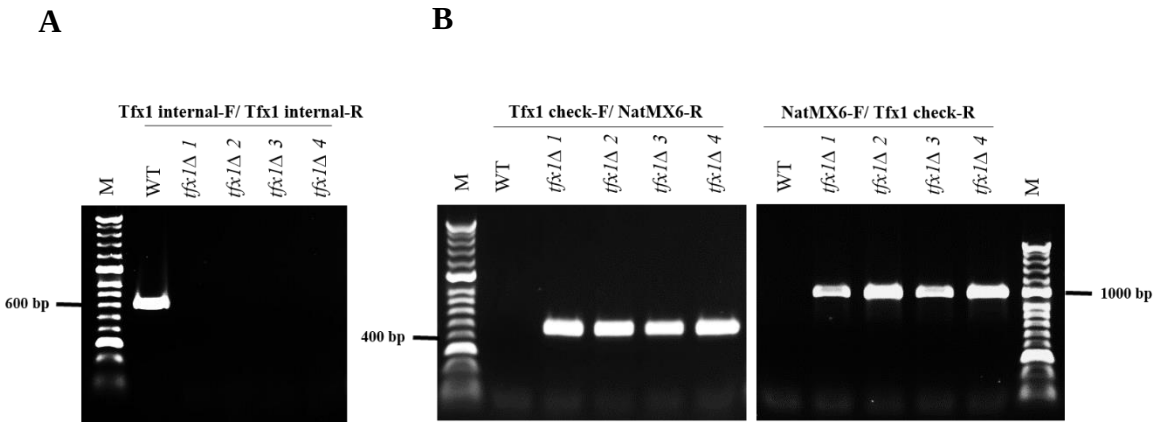

Figure 3.11 PCR screening of successful *tfx1Δ* candidates.
A. Agarose gel image displays the PCR products for the WT strain (BP90) and *tfx1*Δ 1, 2, 3 and 4 (BP3278 *tlh*Δ*4 tfx1*Δ, BP3279 *tlh*Δ*4 tfx1*Δ, BP3282 *tlh*Δ*4 ago1*Δ *tfx1Δ*, BP3283 *tlh*Δ*4 ago1*Δ *tfx1Δ*, respectively) using Tfx1-int-F and Tfx1-int-R primers. The expected PCR product size of the *tfx1* gene is approximately 626 bp; clearly, the gel image shows no PCR products in the successful *tfx1*Δ candidate strains. **B**. The PCR products for the WT and *tfx1*Δ candidate strains using Tfx1 check-F and NatMX6-R primers. Band sizes of approximately 461 bp were seen in the *tfx1*Δ strains, but not in the *tfx1*$^{+}$ strains (WT). NatMX6-F and Tfx1check-R primers were utilised to amplify the WT and *tfx1*Δ candidate strains. A product size of approximately 978 bp is present in the *tfx1*Δ strains, but not in the *tfx1*$^{+}$ strains (WT). M = markers.

3.2.3.2 TBZ sensitivity tests for the *tlhΔ4 ago1Δ* and *tlhΔ4 tfx1Δ* double mutants and the *tlhΔ4 ago1Δ tfx1Δ* triple mutant

In order to test whether *tlh* genes activation by loss of Tfx1 might suppress the chromosome instability of the *ago1Δ* background, the appropriate strains were made and exposed to TBZ. If the hypothesis is correct, the mutation of *tlhΔ4* in the *ago1Δ tfx1Δ* background will affect the TBZ resistance activity of the *ago1Δ tfx1Δ* cells. However, we found that the *tlhΔ4 ago1Δ tfx1Δ* triple mutant exhibited a TBZ suppression phenotype that was similar to the *ago1Δ tfx1Δ* double mutant (Figure 3.12), indicating that activation of *tlh* genes *per se* is not driving the *ago1Δ* suppressor phenotype. Remarkably, we revealed that the mutation of the four *tlh* genes in the *ago1Δ* background also results in significant suppression of the *ago1Δ* TBZ sensitivity, similar to the level seen with the *ago1Δ tfx1Δ* double mutant (Figure 3.12). This indicates that the *tlh* genes are also implicated in *ago1Δ* chromosomal instability suppression, possibly suggesting that disruption of the telomeres or sub-telomere structures, caused by mutations of the *tlh* genes, can suppress the Ago1 requirement.

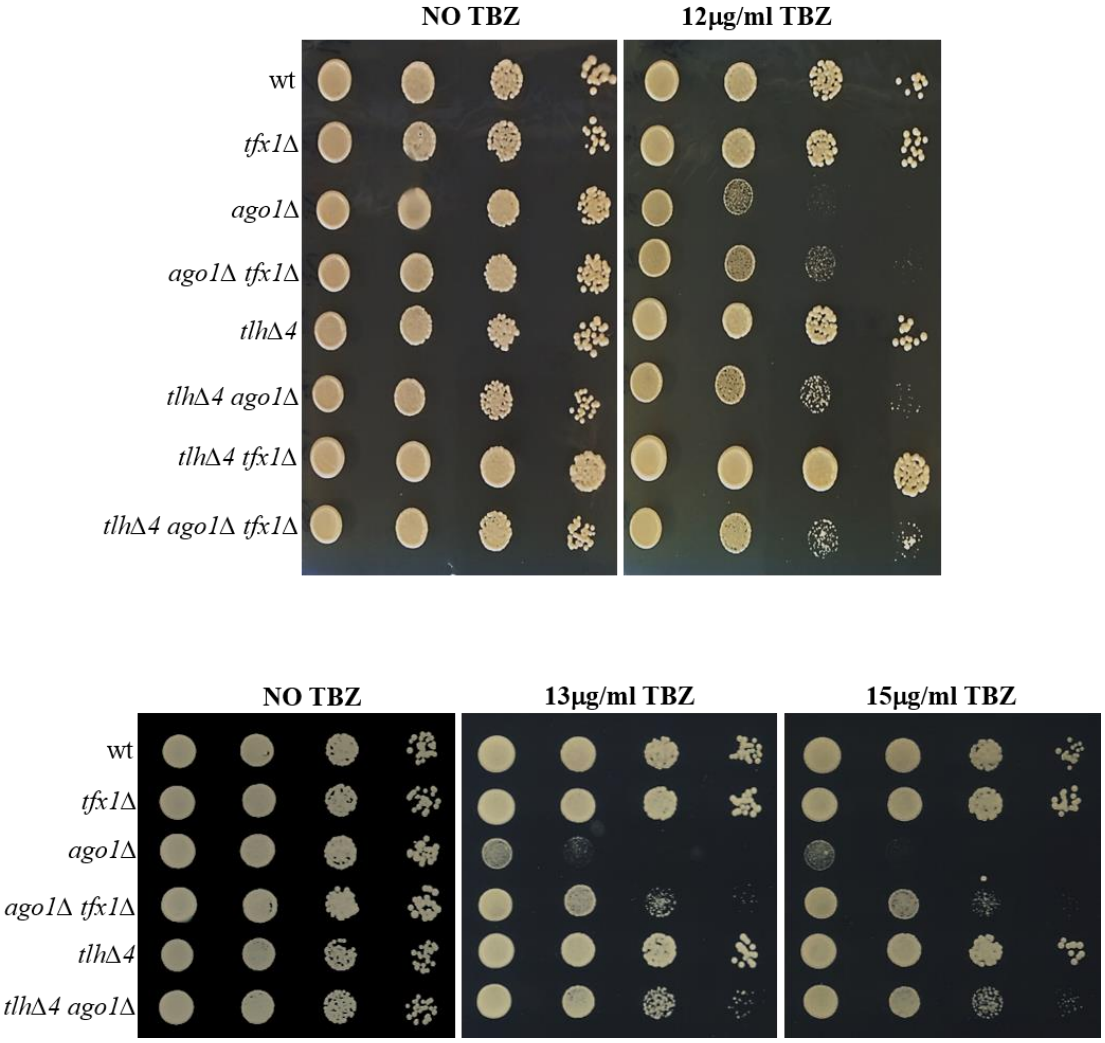

Figure 3.12 Mutation of all *tlh* genes results in suppression of *ago1Δ* TBZ sensitivity to similar levels seen in the *ago1Δ tfx1Δ* double mutant.
Serial dilutions of the indicated *S. pombe* strains were made and exposed to different concentrations of TBZ. The plates were then incubated at 30°C for 3 days. Both the *tlh*Δ4 mutant and the *tlhΔ4 tfx*1Δ 'double' mutant displayed no measureable sensitivity to TBZ relative to the WT. Interestingly, the *tlh*Δ4 *ago1*Δ double mutant suppressed the TBZ sensitivity phenotype of the *ago1*Δ to similar levels seen in the *ago1*Δ *tfx1*Δ background. A suppression phenotype similar to that seen in the *ago*1Δ *tfx1*Δ double mutant was observed in the *tlhΔ4 ago1*Δ *tfx1*Δ 'triple' mutant.

3.2.4 Investigating whether disruption of the telomere structure can suppress the Ago1 requirement

RNAi machinery is required to initiate the heterochromatin state at the sub-telomeres; however, for maintenance, it is only necessary at the centromeres (Lorenzi et al., 2015; Buhler & Gasser; 2009; Kanoh et al., 2005). In addition to RNAi, the telomere-associated protein Taz1, which is an orthologue of mammalian TRF proteins, contributes to heterochromatin formation at telomeres (Buhler & Gasser, 2009; Kanoh et al., 2005). The DNA double-stranded binding protein Taz1 is implicated in a wide range of functions at the end of chromosomes, including telomere length control, DNA damage response and regulation of telomerase recruitment (Pan et al., 2015; Harland et al., 2014; Cooper et al., 1997; Cooper et al., 1998; Miller & Cooper, 2003). To further explore the possibility that compromised telomere structures suppress the need for Ago1, *taz1* was deleted in the *ago1Δ* background and tested for TBZ sensitivity. Additionally, *taz1* and *rap1* (another telomere regulator gene) were deleted in the *tfx1Δ* and *tsn1Δ* backgrounds (we were able to generate *tsn1Δ taz1Δ*, *tsn1Δ rap1Δ* and *tfx1Δ rap1Δ* double mutants), and then exposed to TBZ with the aim of investigating whether loss of Tfx1 or Tsn1 in combination with telomere regulators affected TBZ sensitivity.

3.2.4.1 Constructing appropriate mutant strains

As indicated, all the *S. pombe* strains were generated by replacement with antibiotic resistant cassettes using PCR-based gene targeting methods (Bähler et al., 1998). The *taz1* and *rap1* genes were deleted from the parent strains, which were previously constructed in the McFarlane group, to generate the double mutants of *ago1Δ taz1Δ*, *tsn1Δ taz1Δ*, *tsn1Δ rap1Δ* and *tfx1Δ rap1Δ*. The plasmid pYL16-natMX6, carrying the antibiotic resistant cassette *natMX6*, was isolated from *E. coli* strains (see Table 2.3). The antibiotic resistant *natMX6* was the replacement cassette used to delete both *taz1* and *rap1*, which was amplified using PCR with primers designed with 80 bp homologous sequences directly flanked upstream and downstream from the *taz1* and *rap1* ORFs, and which contained a 20 bp homologous sequence to the plasmid that carries the *natMX6* gene. The purified PCR product was then chemically transformed into the appropriate *S. pombe* strains. To confirm the correct gene deletions, the *taz1*Δ and *rap1Δ* candidates were screened via PCR (Figures 3.13 and 3.14) using three sets of primers, as previously shown in Figure 3.9.

A **B**

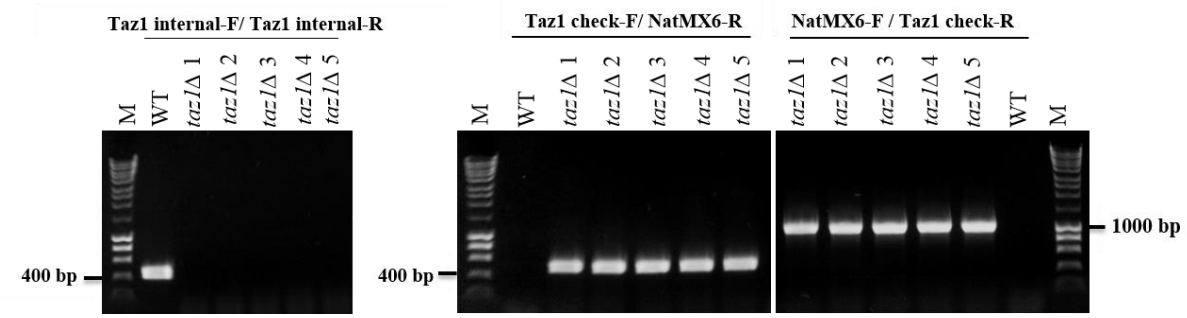

Figure 3.13 PCR screening of successful *taz1*Δ candidates.
A. Agarose gel image displays the PCR products for the WT strain and *taz1*Δ 1, 2, 3, 4 and 5 (BP3285 *ago1*Δ *taz1*Δ, BP3286 *ago1*Δ *taz1*Δ, BP3287 *ago1*Δ *taz1*Δ, BP3288 *tsn1*Δ *taz1*Δ and BP3289 *tsn1*Δ *taz1*Δ, respectively) using Taz1-int-F and Taz1-int-R primers. The expected PCR product size of the *taz1* gene is approximately 470 bp. The gel image shows no PCR products in the successful *taz1*Δ candidate strains. **B**. PCR products for the WT and *taz1*Δ candidate strains using the Taz1 check-F and NatMX6-R primers. Band sizes of approximately 542 bp were seen in the *taz1*Δ strains, but not in the *taz1*$^{+}$ strains (WT). NatMX6-F and Taz1check-R primers were utilised to amplify the WT and *taz1*Δ candidate strains. A product size of approximately 1072 bp is seen in the *taz1*Δ strains, but not in the *taz1*$^{+}$ strains (WT). M = markers.

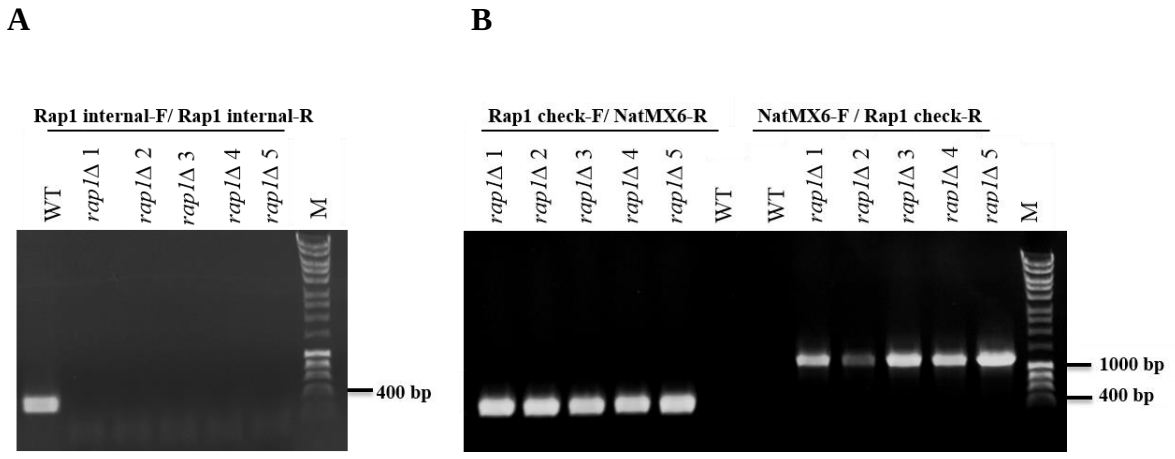

Figure 3.14 PCR screening of successful *rap1*Δ candidates.
A. Agarose gel image displays the PCR products for the WT strain and *rap1*Δ 1, 2, 3, 4 and 5 (BP3293 *tsn1*Δ *rap1*Δ, BP3294 *tsn1*Δ *rap1*Δ, BP3295 *tsn1*Δ *rap1*Δ, BP3291 *tfx1*Δ *rap1*Δ and BP3296 *tfx1*Δ *rap1*Δ, respectively) using Rap1-int-F and Rap1-int-R primers .The expected PCR product sizes of the *rap1* gene is approximately 347 bp. The gel image shows no PCR products in the successful *rap1*Δ candidate strains. **B**. PCR products for the WT and *rap1*Δ candidate strains using Rap1 check-F and NatMX6-R primers. Band sizes of approximately 490 bp were seen in the *rap1*Δ strains, but not in the $rap1^{+}$ strains (WT). NatMX6-F and Rap1 check-R primers were utilised to amplify the WT and *rap1*Δ candidate strains. A product size of approximately 1212 bp is present in *the rap1*Δ strains, but not in the $rap1^{+}$ strains (WT). M = markers.

3.2.4.2 Microtubule destabilizing sensitivity tests for the *ago1Δ taz1Δ*, *tsn1Δ taz1Δ*, *tsn1Δ rap1Δ* and *tfx1Δ rap1Δ* double mutants

As demonstrated, we found that mutation of *tlh* genes in the *ago1Δ* mutant background strongly suppresses TBZ sensitivity similar to the *ago1Δ tfx1Δ* double mutant. Following this discovery, we proposed that disruption of the telomere structure can alleviate the Ago1 defects. In order to test this hypothesis, the telomere regulator *taz1* was deleted in the *ago1Δ* background and exposed to TBZ. Interestingly, the result showed that the *taz1Δ* mutation also significantly suppressed the TBZ sensitivity of the *ago1Δ* cells (Figure 3.15), demonstrating that disruption of telomeric factors can suppress the need for Ago1. Moreover, the *tsn1Δ taz1Δ*, *tsn1Δ rap1Δ* and *tfx1Δ rap1Δ* double mutants were tested for their response to TBZ with the aim of investigating whether the mutation of *tsn1* or *tfx1* with telomere regulator genes alters sensitivity to TBZ. However, the data showed no increase in sensitivity to TBZ in any strains relative to the WT strain (Figure 3.16).

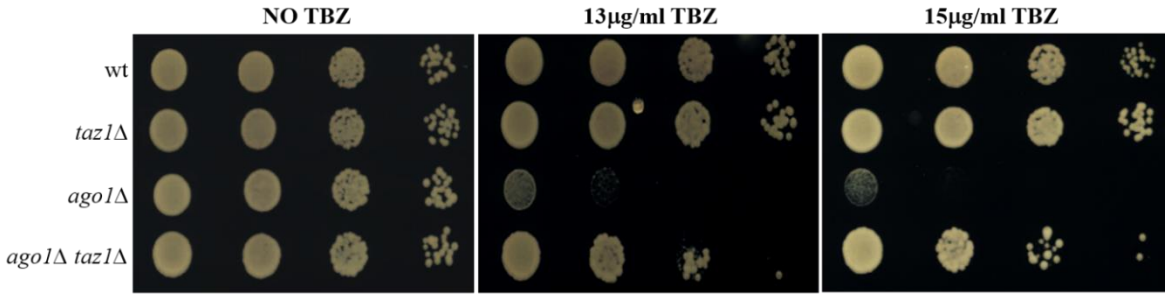

Figure 3.15 Mutation of *taz1* results in a similar suppression of *ago1Δ* TBZ sensitivity.
Serial dilutions of the *S. pombe* strains were made and exposed to different concentrations of TBZ. The plates were then incubated at 30°C for 3 days. The data showed that loss of Taz1 results in significant suppression of *ago1*Δ TBZ sensitivity, as does deletion of *tfx1*and the four *tlh* genes.

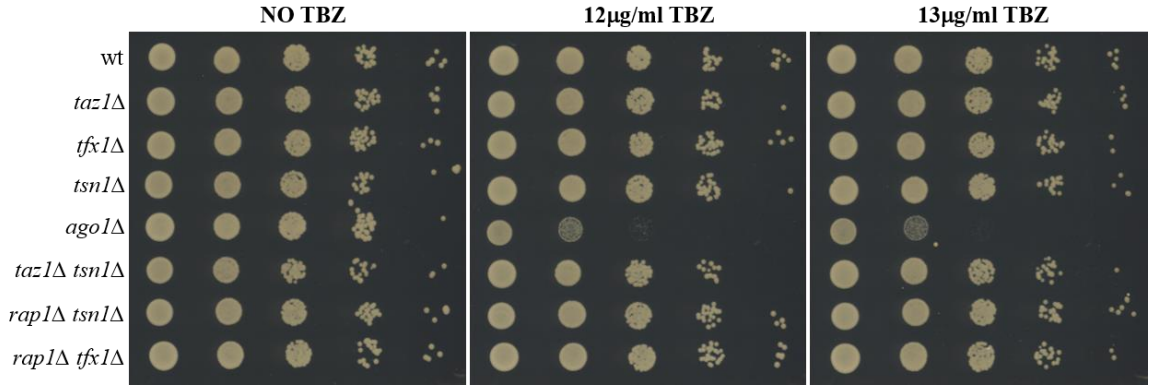

Figure 3.16 TBZ sensitivity spot assay for the *taz1*Δ *tsn1*Δ, *rap1*Δ *tsn1*Δ and *rap1*Δ *tfx1*Δ double mutants.

Serial dilutions of the indicated *S. pombe* strains were made and exposed to different concentrations of TBZ. The plates were then incubated at 30°C for 3 days. No measureable increase in sensitivity to TBZ was observed for the *taz1*Δ *tsn1*Δ, *rap1*Δ *tsn1*Δ and *rap1*Δ *tfx1*Δ double mutants in comparison to the WT strain. The *rap1Δ* single mutant was already shown to exhibit no sensitivity to TBZ relative to WT (Tadeo et al., 2013).

3.3 Discussion

3.3.1 Loss of Tfx1 supresses the chromosome instability of Ago1-defective cells in a Tsn1-dependent fashion

Centromeres are partly heterochromatic, and they are required for mediating the link between chromosomes and spindle microtubules. Thus, centromeres are necessary for the faithful segregation of chromosomes during mitosis and meiosis (Forsburg & Shen, 2017; Moreno-Moreno et al., 2017; Thakur et al., 2015; Buhler & Gasser, 2009; Westhorpe & Straight, 2014; Fennell et al., 2015). In *S. pombe*, the RNAi machinery is needed to establish heterochromatin at centromeres (Shimada et al., 2016; Tadeo et al., 2013; Mutazono et al., 2017). Therefore, mutations in RNAi genes, such as *ago1*, affect centromere function, which results in chromosome mis-segragation. Cells that have a chromosome segregation defect show high sensitivity to a microtubule destabilizing agent, such as TBZ (Sadeghi et al., 2015; Buhler & Gasser, 2009; Volpe et al., 2003; Volpe et al., 2002; Lee et al., 2013). C3PO has been implicated in many aspects of the RNA regulation pathway, including the RNAi pathway in *D. melanogaster* and human cells, in which C3PO assists in the removal of the passenger strand of siRNA-facilitated silencing (Liu et al., 2009; Ye et al., 2011; Holoch & Moazed, 2015; Tian et al., 2011). Previous work on null mutants of *S. pombe tsn1* and *tfx1* genes did not identify any observable change in genome stability (*S. cerevisiae* has no *tsn1/tfx1* orthologous) (Jaendling et al., 2008; Laufman et al., 2005). This indicates that they are not involved in the primary functions of fission yeast, but they could function in redundant or secondary pathways (Jaendling & McFarlane, 2010). Following this finding, the McFarlane group showed that mutation of *S. pombe tfx1*, but not *tsn1*, partially suppresses the chromosomal instability defect of *ago1Δ* cells, a suppression that requires Tsn1 (N. Al-mobadel, PhD thesis, Bangor University). In the present study, multiple routes were used to further confirm this finding. Firstly, the TBZ sensitivity tests were repeated and the data were consistent with the previous findings; the *ago1Δ* mutant TBZ sensitivity was found to be partly suppressed by the *tfx1Δ* mutation, but not by *tsn1Δ*. Consistently, the *ago1*Δ *tfx1*Δ *tsn1*Δ triple mutant was found to be very sensitive to TBZ; in fact, the TBZ sensitivity was greater than that of the *ago1*Δ single mutant (Figure 3.1).

Secondly, all the appropriate strains were grown to single colonies on non-selective YEA plates. We showed that that the growth of the *ago1*Δ *tfx1*Δ double mutant, but not the *ago1*Δ *tsn1*Δ double mutant, was much better than the growth of the *ago1*Δ single mutant and more similar to the growth of the WT strain. However, the growth phenotype of the *ago1*Δ *tfx1*Δ *tsn1*Δ triple mutant was found to be similar to that of the *ago1*Δ single mutant (Figure 3.2). Thirdly, microscope analysis was used to assess endogenous chromosome segregation by monitoring the rate of the anaphase defects of the appropriate strains. We found that the mutation of *tfx1*, but not *tsn1*, significantly reduced the high levels of aberrant mitosis events and chromosomal mis-segragation of the *ago1Δ* mutant. High rates of aberrant mitoses were restored following additional mutation of *tsn1* in the *ago1*Δ *tfx1*Δ cells; the triple mutant had abnormal mitosis statistically indistinguishable from that seen in the *ago1*Δ single mutant (Figure 3.3).

Collectively, three independent analyses have supported the previous findings that the *tfx1Δ* mutation supresses the requirement of Ago1 in maintaining chromosome stability. The results also confirm that the mutation of *tsn1* in the *ago1*Δ *tfx1*Δ background restores and exacerbates Ago1 genomic instability. These results lead us to propose that the loss of Tfx1 may free up Tsn1 to mediate a positive function that suppresses the need for Ago1 in maintaining genomic stability. Moreover, it is important to note that the TBZ sensitivity of the *ago1*Δ *tfx1*Δ *tsn1*Δ triple mutant is higher than the sensitivity observed in the *ago1Δ* single mutant (Figure 3.1), which may indicate the need for a redundant joint function by Tsn1 and Tfx1 to maintain genomic integrity in the absence of Ago1. Additionally, the finding that the mutation of *tsn1*, unlike *tfx1*, cannot suppress the chromosomal instability of the *ago1Δ* mutant suggests no effect for Tsn1 in the absence of Ago1. It also indicates that, in the absence of Tfx1, Tsn1 can make a larger contribution to the genome stability of the *ago1Δ* mutant than can be made by Tfx1 in a Tsn1-free background. It has been shown that, in the absence of Tsn1, levels of Tfx1 are significantly reduced due Translin's ability to mediate stabilisation of the Tfx1 levels (Jaendling et al., 2008). However, the finding that the *ago1*Δ *tfx1*Δ *tsn1*Δ triple mutant is hypersensitive to TBZ, but the *ago1*Δ *tsn1*Δ double mutant is not (it is the same as the *ago1Δ* single mutant) (Figure 3.1), indicates that the very low Tfx1 levels found in the *tsn1*Δ mutant are sufficient to avoid TBZ hypersensitivity. Thus, the low levels of residual Tfx1 found in the *tsn1Δ* mutant have a biological function in maintaining chromosomal stability.

Additionally, the observation that the loss of Tsn1 cannot restore the chromosome stability of *ago1Δ* cells, to the levels seen for *tfx1Δ*, is interesting because it shows that, unlike other organisms, in *S. pombe* Tsn1 and Tfx1 can function with some degree of independence.

Remarkably, we revealed a novel aspect of the chromosome biology, which challenges the current proposal that the chromosome instability of *ago1*Δ cells is caused solely due to a defect in centromere heterochromatin formation (Volpe et al., 2003; Holoch & Moazed, 2015). Using tiled microarrays, we found that the high activation of centromeric transcription caused by loss of Ago1 function is not suppressed by mutating *tfx1*, whilst TBZ sensitivity is suppressed (Figures 3.4, 3.5 and 3.6). These interesting results indicate that loss of Tfx1 partially suppresses the chromosome instability caused by loss of Ago1 without restoring centromere heterochromatin formation, suggesting that an additional scenario is at play.

3.3.2 Telomeric disruption can suppress the requirement for Ago1

The lack of centromeric dysfunction suppression in the *ago1Δ tfx1Δ* double mutant led us to propose that the chromosomal instability of Ago1-deficient cells is, in part, due to the inability to prevent some function(s) that are mediated by Tfx1 at other sites on the genome. This led us to hypothesise that this suppression phenotype could, somehow, be due to activation of the normally silent sub-telomeric *tlh* genes in the *ago1Δ tfx1Δ* background as these genes become activated in the *tfx1Δ* mutant but not in the *tsn1Δ* (Figure 3.7). Therefore, appropriate mutants were made in the *tlhΔ4* strain background, and then tested for TBZ sensitivity with the aim of addressing whether the *tlh* genes were required to suppress the chromosome instability of the *ago1Δ* mutant following loss of Tfx1. However, we found that the mutation of *tlhΔ4* in the *ago1Δ tfx1Δ* background exhibited a TBZ sensitivity suppression phenotype similar to that seen in the *ago1Δ tfx1Δ* double mutant (Figure 3.12). This indicates that activation of *tlh* genes is unlikely to be responsible for driving the *ago1Δ* suppressor phenotype of the *ago1Δ tfx1Δ* double mutant. This suppression may suggest that disruption of the telomere or sub-telomere structure (i.e. mutation of the four *tlh* genes caused structural changes) can suppress the Ago1 requirement for maintaining chromosomal stability.

The findings that Tfx1, but not Tsn1, is necessary for controlling *tlh* transcript levels is further evidence that the function of Tsn1 and Tfx1 can be separated in *S. pombe*. Importantly, Southern blotting analysis was used to assess telomere length in the defects in the *tfx1, tsn1, ago1* and double mutants; the data showed no measurable extensive alteration in the length of the telomeres in any of the strains in comparison to the WT strain although small length changes cannot dismissed. This indicates that the activation of *tlh* genes in a *tfx1Δ* mutant is not due to measurable alterations in the telomere length (Southern blot analysis was conducted by a colleague within our group, see Appendix 2).

3.3.3 Loss of Taz1 also suppresses the Ago1 requirement

We deleted the telomere regulator gene *taz1* in the *ago1Δ* background to test the possibility that disruption of the telomeric structure can suppress the chromosome instability of the *ago1Δ* mutant. We found that the *taz1Δ* mutant also partly suppresses the TBZ sensitivity phenotype of *ago1Δ* (Figure 3.15), indicating that disruption of telomeric factors partially suppresses the requirement for Ago1. More importantly, these findings demonstrate that Tfx1 shares a telomere regulator feature in suppressing TBZ sensitivity of an *ago1Δ* mutant, indicating that Tfx1, and possibly Tsn1, may function in telomeric regulation although not via a gross length regulation mechanism, as for Taz1 (Cooper et al., 1997; see Appendix 2). Consequently, loss of the telomere-associated function of Tfx1 might be responsible for the suppression of the chromosome segregation defects caused by the loss of Ago1.

During the course of this project, work from Jia and co-workers also demonstrated that the *taz1Δ* mutation suppresses the TBZ sensitivity of the *ago1Δ* mutant, and it was demonstrated that this is due to a partial reversal of heterochromatin function at the centromere. Thus, a model was proposed suggesting that loss of Taz1 function in the *ago1Δ* background results in the redistribution of the heterochromatic factors from the subtelomeric regions to the centromere at the heterochromatin regions (Figure 3.17) (Tadeo et al., 2013). Moreover, it has been reported that *tlh* genes are also activated in the *taz1Δ* mutant (Hansen et al., 2006). However, the suppression of the chromosomal instability of the *ago1Δ* background, by loss of Tfx1, is not accompanied by a restoration of centromeric heterochromatin function in our strains as measured by centromeric transcripts.

This demonstrates that redistribution of heterochromatin factors is unlikely to be responsible for the chromosomal stability observed in the *ago1Δ tfx1Δ* cells. However, it is important to note that we only measured centromeric heterochromatin based on the transcription profiles (Figures 3.4, 3.5 and 3.6). Therefore, further analysis is needed to confirm these observations and to exclude an effect of Tfx1 directly on the centromeric heterochromatin. For example, measuring the heterochromatin marks levels at the centromeric heterochromatin regions, including H3K9-me and Swi6, as well as RNA Pol II occupancy.

Collectively, these findings may indicate that when centromere heterochromatin is defective (i.e. in an *ago1Δ* mutant), chromosomes can still segregate relatively efficiently when some features of normal chromosome biology, which are facilitated by Tfx1, are disrupted. This implicates Tfx1 in restricting segregation in cells which is counter balanced by Ago1, which we hypothesis is a mechanism linked to telomeres. Importantly, these observations also indicate a poorly understood association between centromeres and telomeres in preserving chromosome stability.

3.3.4 *tsn1Δ* or *tfx1Δ* mutants with telomere regulators are not sensitive to TBZ

We set out to investigating whether the mutation of *tfx1* or *tsn1* with telomere regulators *taz1* or *rap1* is affected by TBZ and causes any defect in chromosome stability. However, the analysis showed no alteration of sensitivity to TBZ in any strains relative to the WT strain (Figure 3.16). This suggests that Tsn1 and Tfx1 have no measurable functions in genome stability when disrupted with the shelterin components Taz1 or Rap1.

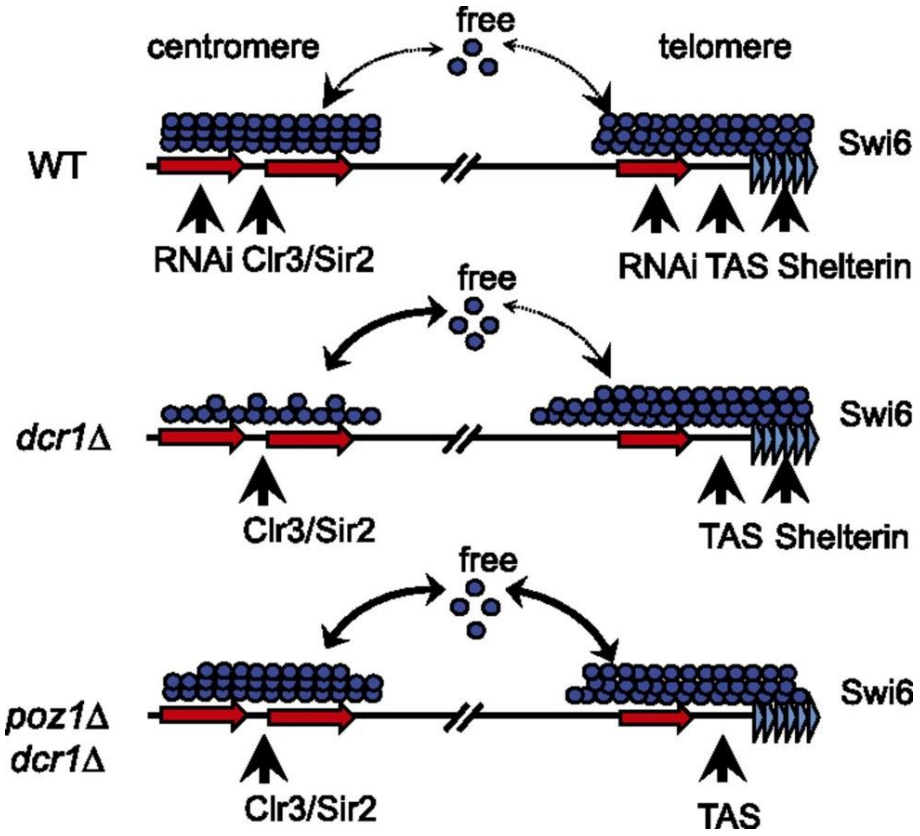

Figure 3.17 A model for restoring centromeric heterochromatin function.
The model suggests that the loss of RNAi and shelterin components results in a redistribution of heterochromatin silencing factors, such as Swi6, from the sub-telomeric regions to the centromeric heterochromatin regions (Tadeo et al., 2013).

3.4 Conclusion

1- Mutation of *tfx1* suppresses the chromosome instability of the *ago1Δ* mutant in a Tsn1-dependent fashion.
2- Low levels of Tfx1 in a *tsn1Δ* background have a biological function in regulating chromosomal stability.
3- Tsn1 and Tfx1 functions can be separated in *S. pombe.*
4- Activation of *tlh* genes *per se* does not appear to be required for driving the *ago1Δ* suppressor phenotype.
5- The chromosomal instability of the *ago1Δ* mutant is not only due to the centromeric heterochromatin dysfunction; it might also be linked to telomere dynamics.
6- Disruption of the telomeric structure can suppress the requirement for Ago1 in maintaining chromosomal stability.
7- Tfx1 and Tsn1 might play a role in regulating telomere dynamics.

Chapter 4: Results

Analysis of novel telomere-associated functions of Tfx1 and Tsn1

4. Analysis of novel telomere-associated functions of Tfx1 and Tsn1

4.1 Introduction

Telomeres are necessary to protect the ends of chromosomes from degradation and from being recognised as DSBs (Buhler & Gasser, 2009; Schoeftner & Blasco, 2009; Lorenzi et al., 2015; Maestroni et al., 2017; Vancevska et al., 2017). In addition, telomeres are required for connecting the chromosomes to the nuclear envelope (NE), which contributes to the chromosomal positioning within the nucleus (Chikashige et al., 2009; Novo & Londoño-Vallejo, 2013; Kupiec, 2014; Li et al., 2017). Thus, telomeres are critical for the stability of chromosomes, and they are associated with shelterin components, including TRF proteins (Taz1 in *S. pombe*), which regulate telomere dynamics (Maestroni et al., 2017; Vancevska et al., 2017). Failure in preserving telomere function(s) is associated with various genetic diseases, including cancer (Hockemeyer & Collins, 2015; Huang et al., 2017; Sarek et al., 2015). Telomeres are normally subjected to heterochromatic silencing, although noncoding telomeric repeat containing RNA (TERRA) is transcribed by RNA Pol II from the sub-telomere toward the ends of chromosome (Maicher et al., 2014; Azzalin & Lingner, 2015; Cusanelli & Chartrand, 2015; Fennell et al., 2015; Rippe & Luke, 2015; Wang et al., 2015; Feretzaki & Lingner, 2017).

TERRAs are implicated in a wide range of telomere functions, including DNA damage response, telomere length control, telomerase activity regulation and telomeric heterochromatin formation (Maicher et al., 2014; Azzalin & Lingner, 2015; Cusanelli & Chartrand, 2015; Rippe & Luke, 2015; Wang et al., 2015). The regulation of TERRA transcripts is important for preserving genome stability (Cusanelli & Chartrand, 2015). However, little is known about regulators of these telomeric RNAs. The Translin-TRAX complex possesses RNase activity and has the ability to bind to and process nucleic acids (Wang et al., 2004; Eliahoo et al., 2010; Jaendling & McFarlane, 2010; Jaendling & McFarlane, 2010; Li et al., 2012; Parizotto et al., 2013). Translin and TRAX are implicated in the regulation of RNA, and they have been previously proposed to function on telomeric sequences based on DNA sequence binding preferences (Jacob et al., 2004; Laufman et al., 2005; Jaendling & McFarlane, 2010), although no direct evidence of this was provided prior to the current study (see below).

In the present study, it was found that Tfx1 has an apparent telomere regulator feature in suppressing TBZ sensitivity of the *ago1Δ* mutant, indicating that Tfx1, and possibly Tsn1, may function in telomeric regulation (see Chapter 3). The work in this chapter aims to determine the telomere-associated function of Tfx1, and if any, of Tsn1, by addressing the two following possibilities:

1- The partial suppression of chromosomal segregation defects of the *ago1Δ* mutant is due to de-tethering of telomeres from the NE, implying a functional role for Tfx1, and possibly Tsn1, in controlling telomere tethering to the NE.

2- Dysregulation of transcription in the sub-telomeric regions may be responsible for the partial rescue of the chromosomal instability of the *ago1*Δ mutant, inferring a role for Tfx1, and possibly Tsn1, in controlling telomere-associated transcripts.

4.2 Results

4.2.1 Genetic investigation of whether de-tethering of telomeres from the nuclear envelope is responsible for the *ago1Δ* suppression phenotype

Centromeres and telomeres are regions of eukaryotic genomes essential for the correct segregation and maintenance of chromosomes (Steiner & Henikoff, 2015; Harland et al., 2014). In *S. pombe*, the RNAi machinery is required for the full function of centromeres; thus, mutation of *ago1* results in centromere dysfunction, and consequently, chromosomal mis-segregation; this causes a high sensitivity to TBZ and current dogma postulates that it is solely the loss of centromeric function that is responsible for the TBZ sensitivity of the *ago1Δ* mutant (Volpe et al., 2003; Buhler & Gasser, 2009; Lee et al., 2013; Tadeo et al., 2013; Lorenzi et al., 2015; Sadeghi et al., 2015). In the current study, the data suggested that compromised telomere structures partially suppress the *ago1*Δ mutant chromosomal segregation defects, a phenomenon that has been recently also revealed for *taz1*Δ mutant which are defective in telomere length regulation (Tadeo et al., 2013; Figure 3.15); concerning this phenomenon, Jia and co-workers proposed that compromising telomeric heterochromatin results in the redistribution of the silencing factors from the sub-telomeric regions to the centromeric heterochromatic regions to compensate for the defective state cause by loss of Ago1 (Tadeo et al., 2013). Importantly, in the *ago1Δ tfx1Δ* background, the rescue of Ago1 loss comes without restoring centromeric heterochromatin formation, as measured by centromeric transcripts, which differs from the *ago1Δ taz1Δ* mutant (Figures 3.4, 3.5 and 3.6); this indicates that a distinct telomere-dependent suppression mechanism is in play. Extending this led us to speculate that the chromosomal mis-segregation of cells defective in Ago1 is partly caused by the fact defective centromeres cannot counter a structural feature of chromosomes mediated by the tethering of telomeres to the NE. An *S. pombe* mutant defective in the tethering of the telomeres to the NE is *bqt4Δ* (Chikashige et al., 2009). Therefore, this model can be readily tested by deleting *bqt4* in *ago1Δ* cells and exposing the *ago1Δ bqt4Δ* strain to TBZ; if the hypothesis is correct, then de-tethering of telomeres from the NE should partly suppress the *ago1Δ* TBZ sensitivity. These experiments may indicate whether loss of Tfx1 causes de-tethering of telomeres from the NE.

4.2.1.1 Construction of the *bqt4Δ* mutant strains

The *bqt4Δ* strains were generated by replacement of the *bqt4* ORF with the antibiotic resistant cassette *natMX6* using PCR-based gene targeting methods (Bähler et al., 1998). The *bqt4* gene was deleted from both the WT and *ago1Δ* backgrounds to generate the single mutant *bqt4Δ* and double mutant *ago1Δ bqt4Δ*, respectively. The *natMX6* cassette was amplified using PCR with primers containing 80 bp homologous sequences immediately flanked upstream and downstream from the *bqt4* ORF; they also had a 20 bp homologous sequence to the *natMX6* gene (Figure 3.8). The purified PCR product was then chemically transformed into the appropriate *S. pombe* strains (see Section 2.5.1). To confirm the correct gene deletion, *bqt4Δ* candidates were screened via PCR (Figure 4.1) using three sets of primers, as previously shown in Figure 3.9.

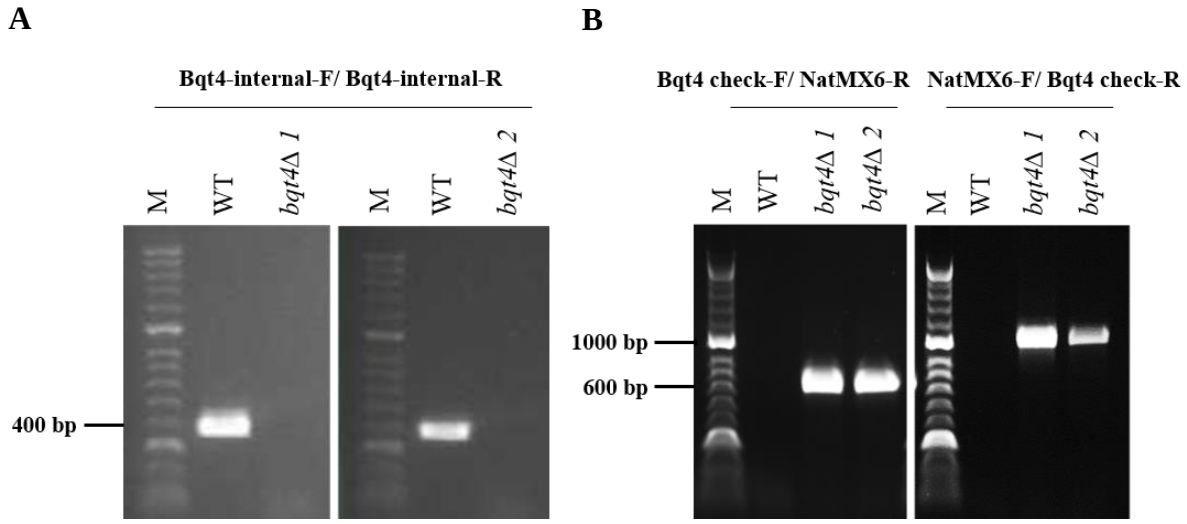

Figure 4.1 PCR screening of successful *bqt4Δ* candidates.
A. Agarose gel image displays the PCR products for the WT strain and *bqt4*Δ 1 and 2 (BP3298 *bqt4Δ* and BP3297 *ago1Δ bqt4Δ*, respectively) using the Bqt4-int-F and Bqt4-int-R primers. The expected PCR product sizes of the *bqt4* gene was approximately 410 bp. The gel image shows no PCR products in the successful *bqt4*Δ candidate strains. **B.** PCR products for the WT and *bqt4*Δ candidates strains using the Bqt4 check-F and NatMX6-R primers. Band sizes of approximately 641 bp were seen in the *bqt4*Δ strains, but not in the *bqt4*$^{+}$ strains (WT). NatMX6-F and Bqt4 check-R primers were utilised to amplify the WT and *bqt4*Δ candidate strains. A product size of approximately 989 bp was observed in the *bqt4*Δ strains, but not in the *bqt4*$^{+}$ strains (WT). M = markers.

4.2.1.2 TBZ sensitivity tests for *ago1Δ bqt4Δ* double mutant

To test whether de-tethering of telomeres from the NE caused the suppression of the chromosomal mis-segregation of the *ago1Δ* mutant, the constructed strains where exposed to TBZ. The mutation of *bqt4* in the *ago1Δ* background would supress the TBZ sensitivity of *ago1Δ* if the hypothesis were correct. However, we found that the double mutant of *bqt4*Δ *ago1*Δ developed sensitivity to TBZ that was greater than that of the *ago1*Δ single mutant, although the single mutant of *bqt4*Δ showed no sensitivity to TBZ relative to the WT (Figure 4.2). These results indicate that the suppression of chromosomal segregation defects of the *ago1Δ* mutant was not due to disconnection of telomeres from the NE, although *bqt4Δ* mutants may have additional defects that mask a suppression phenotype. While the increase of sensitivity seen in *ago1Δ bqt4Δ* is interesting, it does not explain the findings observed in the *ago1Δ tfx1Δ* strain.

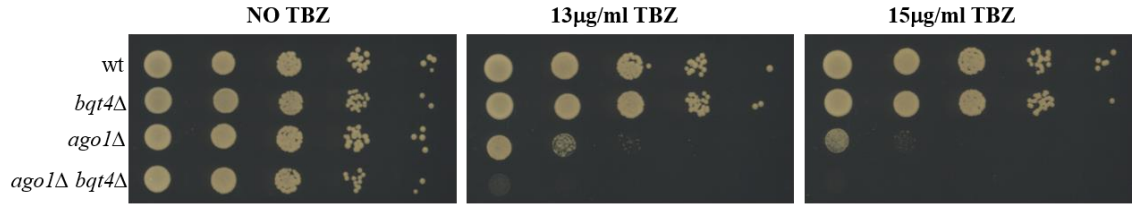

Figure 4.2 TBZ sensitivity of the *ago1Δ* mutant is not suppressed by *bqt4Δ* mutation.
Serial dilutions of the indicated *S. pombe* mutants were made and exposed to different concentrations of TBZ. The plates were then incubated at 30°C for 3 days. Single mutants of *bqt4*Δ showed no sensitivity to TBZ compared with the WT. However, unexpectedly, the *bqt4*Δ *ago1*Δ double mutant exhibited hypersensitivity to TBZ that was higher than that of the *ago1*Δ single mutant.

4.2.2 Investigation of whether Tfx1 and Tsn1 control telomere-associated transcripts

Human and *S. pombe* telomeres are actively transcribed into TERRA molecules (Bah et al., 2012; Greenwood & Cooper, 2012; Maicher et al., 2014; Azzalin & Lingner, 2015; Cusanelli & Chartrand, 2015; Rippe & Luke, 2015; Wang et al., 2015; Feretzaki & Lingner, 2017). In addition to TERRA, *S. pombe* produce distinct transcripts associated with the telomeres and sub-telomeres, including ARIAs, ARRETs and α-ARRETs (Figure 1.12) (Bah et al., 2012; Greenwood & Cooper, 2012; Azzalin & Lingner, 2015; Lorenzi et al., 2015; Moravec et al., 2016). The regulation of these telomeric transcripts in *S. pombe* depends on the telomere-binding proteins Taz1 and Rap1; thus, mutation of either of these two proteins causes a significant elevation of all telomeric and sub-telomeric transcripts (Greenwood & Cooper, 2012). Notably, comparable to the loss of Tfx1, mutation of *taz1* resulted in activation of the sub-telomeric *tlh* transcript levels (Hansen et al., 2006). Given this finding, it was hypothesised that the mutation of *tfx1* may activate *tlh* transcript levels because Tfx1 controls the telomere and/or sub-telomeric transcriptome. It should be noted that the tiled arrays used to assess the transcriptome of the *tfx1Δ* mutant did not have coverage of the telomeres, so telomere transcripts have not previously been measured in the *tfx1Δ* mutant.

To assess this hypothesis, ARRET (immediate sub-telomeric regions; Figure 4.3A) and TERRA (telomeric regions; Figure 4.3A) transcript levels were analysed in a range of *S. pombe* mutant strains using previously developed RT-PCR/qRT-PCR assays (Greenwood & Cooper, 2012; Lorenzi et al., 2015). RT-PCR products of ARIA and α-ARRET specific transcripts were not discernable from those generated by first-strand cDNA primed using endogenous priming so they could not be measured. However, endogenous priming was eliminated in the analyses of both TERRAs and ARRETs (i.e. the absence of first-strand primers generated no PCR products; Figures 4.3 and 4.4).

Interestingly, as was found for the sub-telomeric *tlh* transcripts (Figure 3.7), the loss of Tfx1, but not Tsn1, results in elevated sub-telomere associated ARRET. This elevation depends on Tsn1, as an additional mutation of *tsn1* in the *tfx1Δ* background results in a reduction of the levels of ARRET to the WT level (Figures 4.3 and 4.5). These results indicated that in the absence of Tfx1, Tsn1 is needed to preserve elevated ARRET levels. Remarkably, we found that the loss of Tsn1, but not Tfx1, strongly elevated telomere associated transcripts, TERRA, and in reciprocal fashion, this was Tfx1 dependent, as the high levels of TERRAs were restored to those seen in the WT following the additional loss of Tfx1 in the *tsn1Δ* background (Figures 4.4 and 4.6).

These findings indicated that in the absence of Tsn1, Tfx1 is necessary to stabilise the TERRA levels. Taken together, these results demonstrated that Tfx1 is required to suppress ARRET transcripts in a Tsn1-dependent fashion, and in a reciprocal control mechanism, Tsn1 is required to suppress TERRA transcripts in a Tfx1-dependent fashion. Remarkably, these observations revealed important novel telomere regulatory factors, and they indicated a functional distinction of Tfx1 and Tsn1 in the telomere regions.

In *ago1Δ* backgrounds, as observed for the *tlh* transcript (Figure 3.7), mutation of *tfx1*, but not *tsn1*, resulted in an elevation of the ARRET transcript levels. This elevated level of ARRET transcripts was slightly reduced following the additional mutation of *tsn1* in the *ago1Δ tfx1Δ* background (Figure 4.3), suggesting that this elevation is Tsn1 dependent. Importantly, these results point to the possibility that the transcription defects in the sub-telomeric regions may be responsible for the observed suppression of chromosomal segregation defects of Ago1-defective cells (see Discussion). Analysis of TERRAs in *ago1Δ* backgrounds showed no measurable increase in the telomere transcript levels in the *ago1Δ* single mutant and *ago1Δ tfx1Δ* double mutant (Figure 4.4). The elevation of TERRA in the *tsn1Δ* was, however, not as pronounced in the *ago1Δ tsn1Δ* double mutant. Remarkably, the TERRA levels were as highly elevated in the *ago1Δ tfx1*Δ *tsn1*Δ triple mutant, as seen in the *taz1Δ* mutant (Figure 4.4). This increased accumulation of TERRAs in the triple mutant correlated with hyper-levels of chromosome instability, as measured with the TBZ growth assay (Figure 3.1), possibly pointing to a functional link. Following this discovery, we hypothesised that the observed phenomenon in the triple mutant may be linked to DNA damage response at the telomeres (see Section 4.2.3).

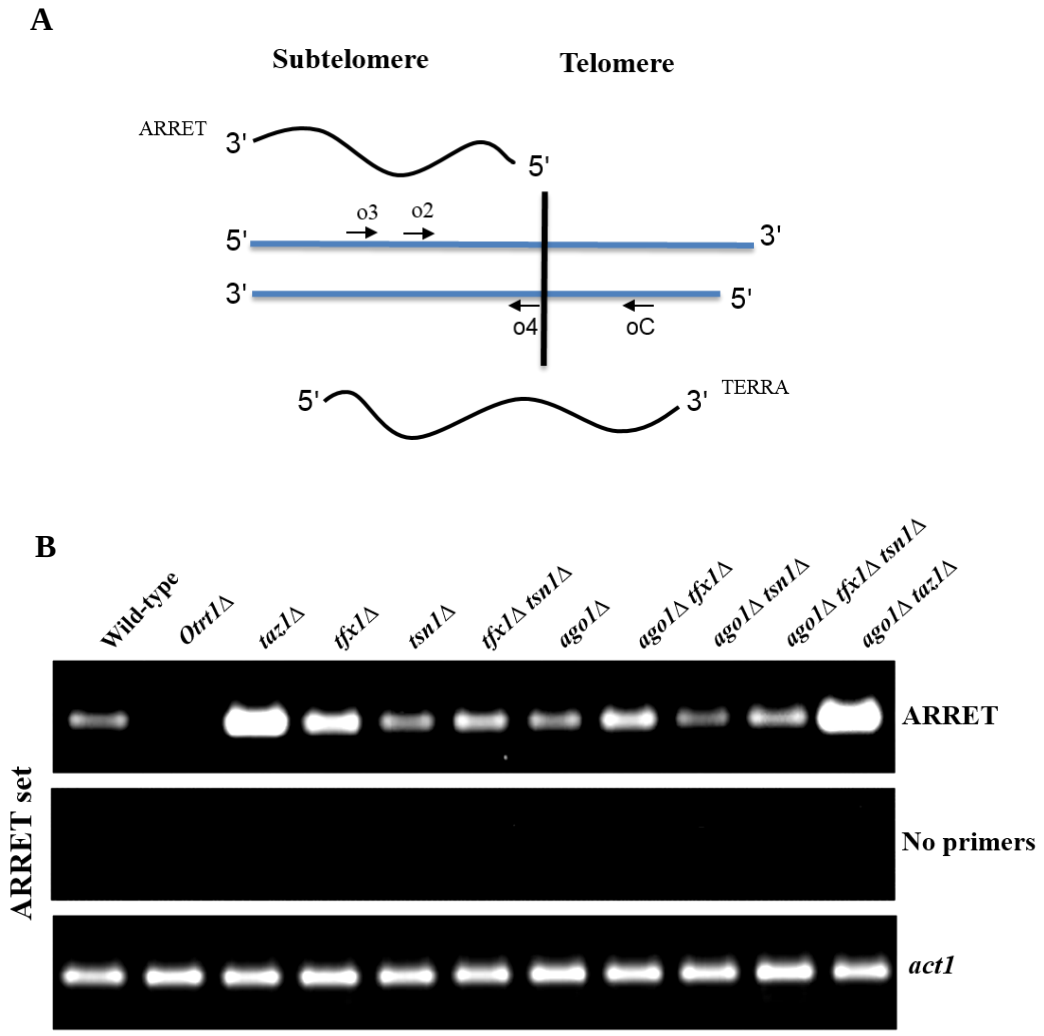

Figure 4.3 Qualitative analysis of ARRETs in a range of *S. pombe* mutant strains.
A. Diagrammatic illustration of *S. pombe* telomeres exhibiting the sub-telomeric and telomeric regions. Transcriptions of ARRETs and TERRAs are shown in their approximate locations. Oligonucleotide positions used in the synthesis of first-strand cDNA, and RT-PCR and qRT-PCR are indicated as arrows. For example, o3 was used to prime cDNA for ARRETs, whereas oC was used to prime cDNA for TERRAs. Moreover, o2/o4 was used for PCR amplification for both ARRETs and TERRAs. **B.** Agarose gel image displaying RT-PCR products utilising primers specific for ARRETs. Here, *act1* gene expression was used as a control to show the quality of RNA in all samples. No primer samples were used as a negative control, and no primers were used in the cDNA synthesis step, showing that there was no endogenous priming. The *Otrt1Δ* strain, which has no telomeres, was used as a negative control to show that no band can be detected in *Otrt1Δ* cells. The *taz1Δ* mutant was used as a positive control, and this has already been shown to exhibit elevation of all telomeric transcripts (Greenwood & Cooper, 2012). The data show that loss of Tfx1, but not Tsn1, results in an elevation of ARRET levels. The mutation of *tsn1* in a *tfx1*Δ background reduces this elevation. The *ago1Δ* mutant exhibited no measurable increase in ARRET levels. However, the mutation of *tfx1*, but not *tsn1*, in the *ago1Δ* background increased the levels of ARRET. These high levels of ARRET transcripts were alleviated following the additional mutation of *tsn1*.

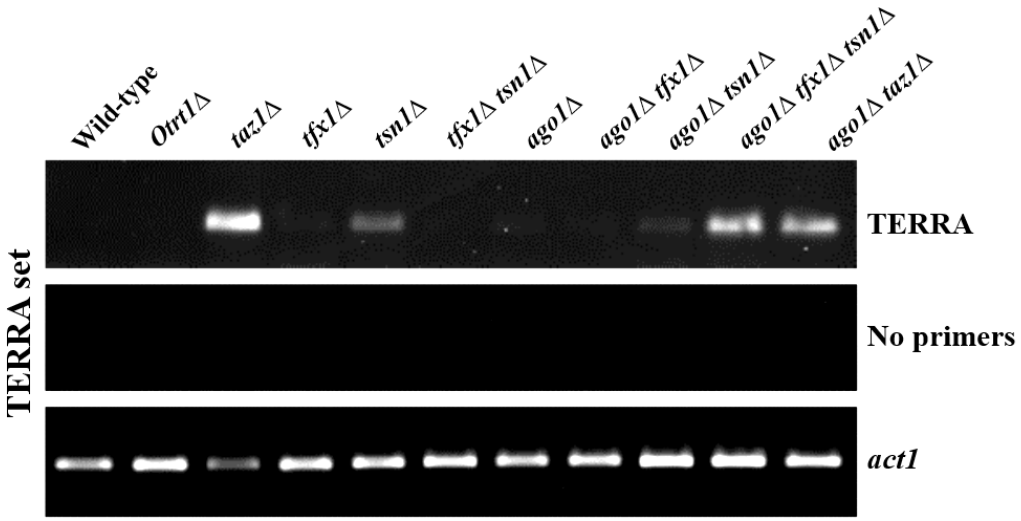

Figure 4.4 Qualitative analysis of TERRAs in a range of *S. pombe* mutant strains.
Agarose gel image displays RT-PCR products utilising the primer specific for TERRAs. The *act1* gene expression was used as a control to show the quality of RNA in all samples. No primer samples were used as a negative control, which resulted in no primers being used in the cDNA synthesis step, showing that there is no endogenous priming. The *Otrt1Δ* strain, which has no telomeres, was used as a negative control to show that no band could be detected in *Otrt1Δ* cells. The *taz1Δ* mutant was used as a positive control, and this has already been shown to exhibit elevation of all telomeric transcripts (Greenwood & Cooper, 2012). The data show that the loss of Tsn1, but not Tfx1, results in an increased accumulation of TERRA levels. This elevated level of TERRAs was reduced to the WT level following additional mutation of *tfx1*. No increase of TERRAs could be detected in the *ago1Δ* single mutant and *ago1Δ tfx1Δ* double mutant. The elevation of TERRA in the *tsn1Δ* mutant background was somewhat alleviated following the mutation of *ago1*. However, TERRA levels were highly elevated in the *ago1Δ tfx1*Δ *tsn1*Δ triple mutant.

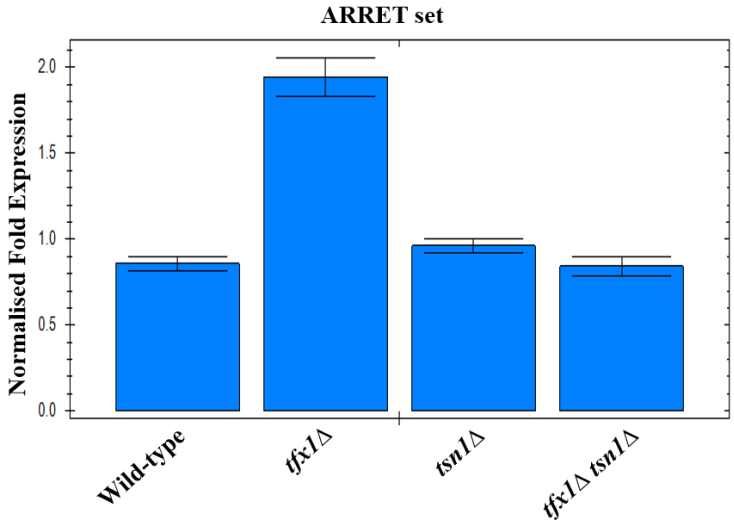

Figure 4.5 Quantitative real time PCR analysis confirming the reciprocal regulation of ARRETs by Tsn1 and Tfx1.

The plot demonstrates that loss of Tfx1 results in an elevation of ARRETs, whereas no measurable increase in the level of ARRET is observed in *tsn1*Δ. Notably, mutation of *tsn1* in a *tfx1*Δ background results in a reduction of ARRET levels to those seen in the WT. Here, *act1* was used to normalise the results, and Bio-RAD CFX Manager was utilised for the data analysis. The error bars show the standard error for triplicate repeats. Pairwise Student's *t*-tests were performed to determine the *p*-values between WT and the indicated mutant stains. All *p*-values were > 0.05 except WT *vs.* *tfx1*Δ, which was < 0.01.

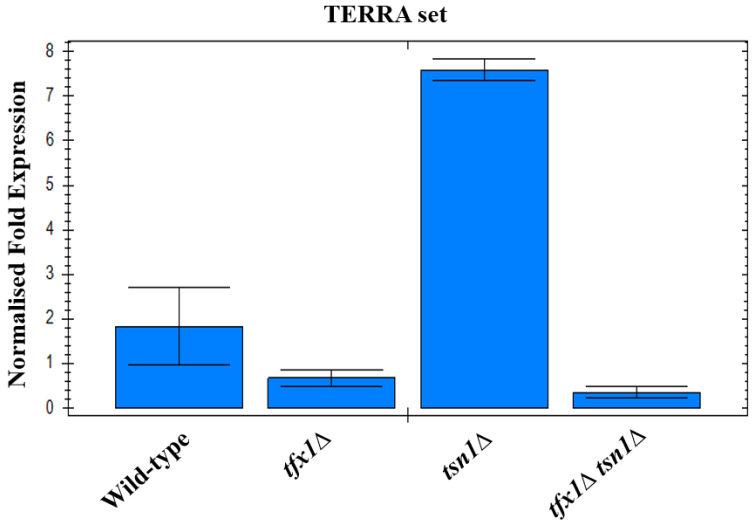

Figure 4.6 Quantitative real time PCR analysis confirming the reciprocal regulation of TERRAs by Tsn1 and Tfx1.
The data show that TERRA levels were highly elevated in *tsn1*Δ, whereas *tfx1*Δ showed statistically indistinguishable levels of TERRA from those observed in the WT. Clearly, mutation of *tfx1* in a *tsn1*Δ background restores TERRA to levels comparable to (or slightly lower than) those of WT. Here, *act1* was used to normalise the results, and Bio-RAD CFX Manager was utilised for the data analysis. The error bars show the standard error for triplicate repeats. Student's *t*-tests were performed to determine *p*-values between WT and the indicated mutant stains. All *p*-values were > 0.05 except WT *vs. tsn1*Δ, which was < 0.01.

4.2.3 DNA damage sensitivity analysis for the *ago1Δ tfx1*Δ *tsn1*Δ triple mutant

A direct role in the DNA damage response has been recently identified for murine TRAX (Wang et al., 2016b), and TERRAs have been implicated in protection of telomeres from the DNA damage response (Azzalin & Lingner, 2015; Cusanelli & Chartrand, 2015; Maicher et al., 2014; Rippe & Luke, 2015; Wang et al., 2015; Schoeftner & Blasco, 2008). In the present study, we found that TERRAs were highly elevated in the *ago1Δ tfx1Δ tsn1Δ* triple mutant, at levels comparable to those recorded in cells lacking the telomere associated protein Taz1 (Figure 4.4). The high elevation of TERRAs in the *ago1Δ tfx1Δ tsn1Δ* triple mutant correlates with the high levels of chromosome instability (as measured by TBZ sensitivity). Here, we set out to use genetics to determine whether the observed phenomenon in the triple mutant is linked to the DNA damage response. To test this, the appropriate *S. pombe* mutant strains were exposed to a wide range of DNA damaging agents, including the DNA replication inhibitor hydroxyurea (HU); phleomycin, which causes DNA double-strand breaks; the DNA-alkylating agent methyl methane sulfonate (MMS); the potent DNA crosslinker mitomycin C (MMC); the DNA enzyme topoisomerase 1 poison camptothecin (CPT); and ultraviolet irradiation (UV).

The *tfx1Δ* and *tsn1Δ* single mutants and *tfx1Δ tsn1Δ* double mutant exhibited no sensitivity to any of the indicated DNA damaging agents relative to the WT strain (Figure 4.7), consistent with the findings of Jaendling et al. (2008). Interestingly, we found that the triple mutant *ago1Δ tfx1Δ tsn1Δ* exhibited an increase in sensitivity in response to HU, phleomycin, MMS, MMC and UV damaging agents relative to *ago1Δ* (and the *ago1Δ tfx1Δ* and *ago1Δ tsn1Δ* double mutants, which were indistinguishable from the *ago1Δ* single mutant; Figures 4.8, 4.9, 4.10, 4.11 and 4.12). However, the *ago1*Δ *tfx1*Δ *tsn1*Δ triple mutant was not sensitive to CPT (Figure 4.13), although we cannot absolutely dismiss the possibility that there might be a mild effect for the triple mutant to CPT, as we only used a concentration of CPT (1.2 μg/ml) that does not affect the WT strain. Therefore, further analysis is required to confirm this result. Collectivelly, these results may indicate that the observed hyper-elevation of TERRAs in the *ago1Δ tfx1Δ tsn1Δ* triple mutant is linked to increased DNA damage sensitivity.

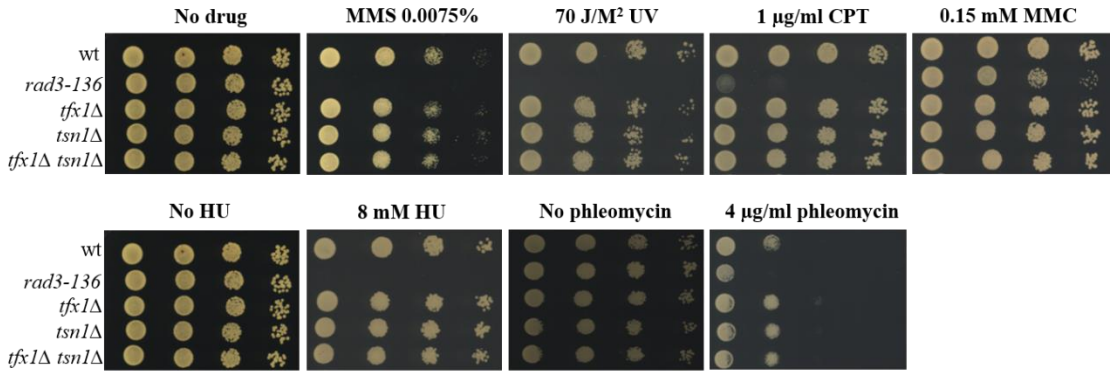

Figure 4.7 DNA damaging agents sensitivity spot assays for the *tfx1*Δ *tsn1*Δ double mutant. Serial dilutions of the indicated *S. pombe* mutants were made and exposed to a wide range of DNA damaging agents, including methyl methane sulfonate (MMS), ultraviolet (UV), camptothecin (CPT), mitomycin C (MMC), hydroxyurea (HU) and phleomycin. The plates were then incubated at 30°C for 3–4 days. Here, *rad3-136* cells (check point defective) were utilised as a positive control for the damaging agents. Neither the single mutants *tfx1Δ* and *tsn1Δ* nor the *tfx1Δ tsn1Δ* double mutant showed any measurable increase in sensitivity relative to the WT strain in response to the indicated damaging agents.

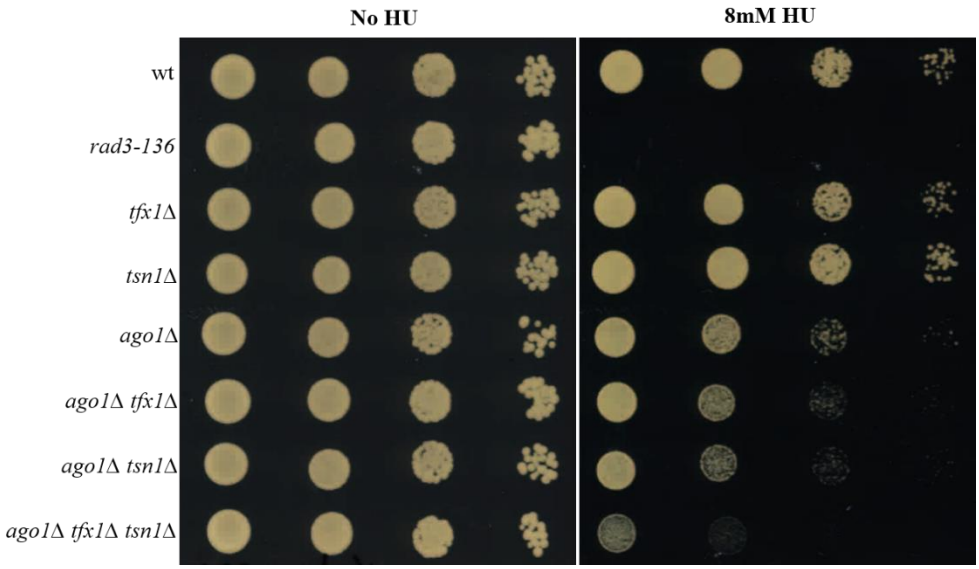

Figure 4.8 The *ago1*Δ *tfx1*Δ *tsn1*Δ triple mutant is hypersensitive to hydroxyurea (HU).
Serial dilutions of the indicated *S. pombe* mutants were generated and exposed to 8 mM HU. The plates were then incubated at 30°C for 4 days. Here, *rad3-136* cells (check point defective) were utilised as a positive control. While the *ago1*Δ single mutant and *ago1*Δ *tfx1*Δ and *ago1*Δ *tsn1*Δ double mutant displayed similar intermediate sensitivities to HU, the *ago1*Δ *tfx1*Δ *tsn1*Δ triple mutant developed an extremely high sensitivity to HU.

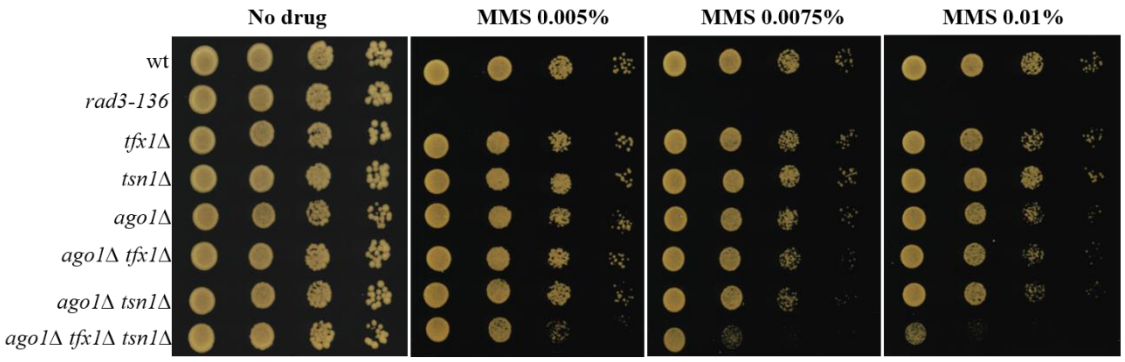

Figure 4.9 The *ago1*Δ *tfx1*Δ *tsn1*Δ triple mutant is hypersensitive to methyl methane sulfonate (MMS).

Serial dilutions of the indicated *S. pombe* mutants were set up and exposed to different concentrations of MMS. The plates were then incubated at 30°C for 4 days. Here, *rad3-136* cells (check point defective) were utilised as a positive control for the damaging agent. The *ago1*Δ single mutant and *ago1*Δ *tfx1*Δ and *ago1*Δ *tsn1*Δ double mutants showed indistinguishable phenotype sensitivities to MMS, whereas the *ago1*Δ *tfx1*Δ *tsn1*Δ triple mutant exhibited a marked hypersensitivity to MMS.

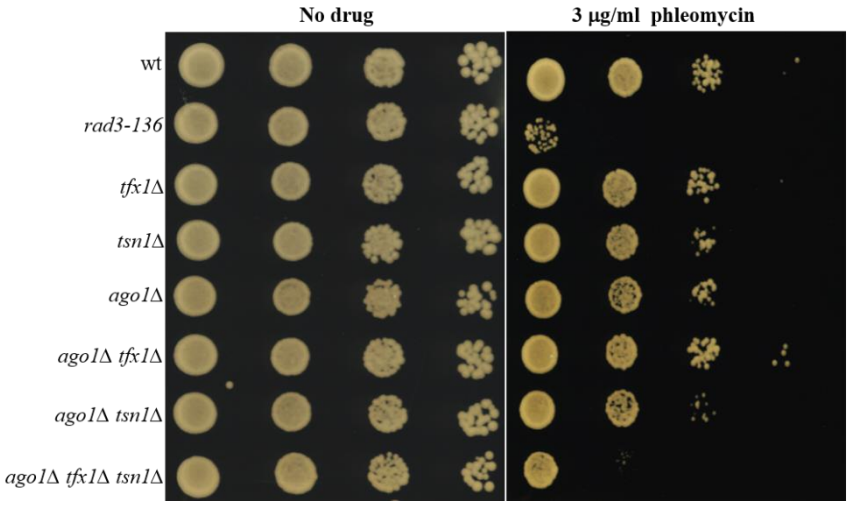

Figure 4.10 The *ago1*Δ *tfx1*Δ *tsn1*Δ triple mutant is hypersensitive to phleomycin.
Serial dilutions of the indicated *S. pombe* mutants were set up and exposed to 3 µg/ml of phleomycin. The plates were then incubated at 30°C for 4 days. Here, *rad3-136* cells (check point defective) were utilised as a positive control for the damaging agent. The data show that the *ago1*Δ *tfx1*Δ *tsn1*Δ triple mutant exhibited a higher sensitivity to phleomycin relative to the *ago1*Δ single mutant and *ago1*Δ *tfx1*Δ and *ago1*Δ *tsn1*Δ double mutants.

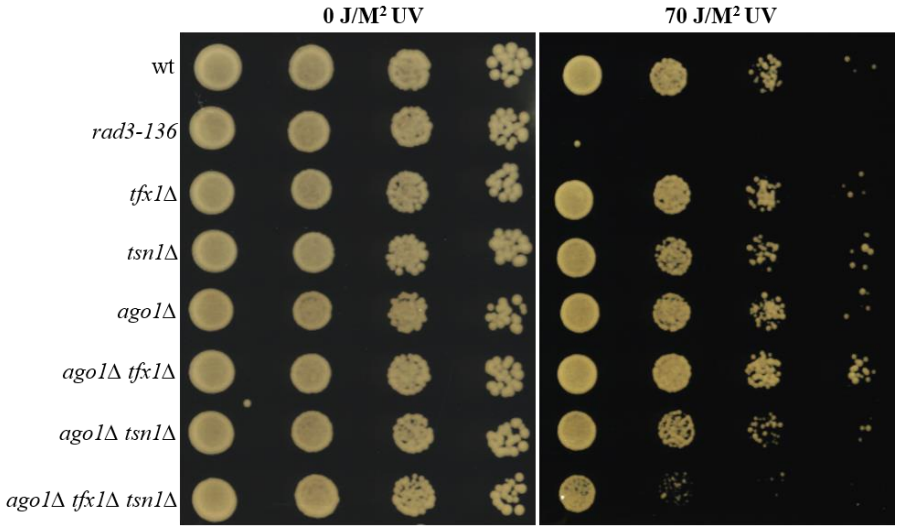

Figure 4.11 The *ago1*Δ *tfx1*Δ *tsn1*Δ triple mutant is hypersensitive to ultraviolet (UV).
Serial dilutions of the indicated *S. pombe* mutants were set up and exposed to 70 J/M^2 UV. The plates were then incubated at 30°C for 4 days. Here, *rad3-136* cells (check point defective) were utilised as a positive control for the damaging agent. The data show that *ago1*Δ *tfx1*Δ *tsn1*Δ triple mutant displayed increased sensitivity to UV, relative to *ago1*Δ single mutant, *ago1*Δ *tfx1*Δ and *ago1*Δ *tsn1*Δ double mutants.

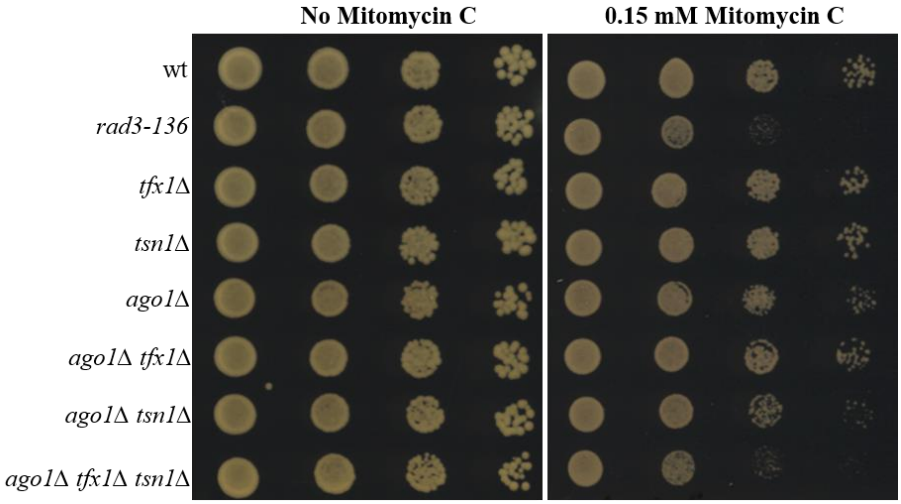

Figure 4.12 The *ago1*Δ *tfx1*Δ *tsn1*Δ triple mutant is sensitive to Mitomycin C (MMC).
Serial dilutions of the indicated *S. pombe* mutants were made and exposed to 0.15 mM MMC. The plates were then incubated at 30°C for 4 days. Here, *rad3-136* cells (check point defective) were utilised as a positive control for the damaging agent. The *ago1*Δ single mutant and *ago1*Δ *tfx1*Δ and *ago1*Δ *tsn1*Δ double mutants showed a similar phenotype sensitivity to MMS, whereas the *ago1*Δ *tfx1*Δ *tsn1*Δ triple mutant exhibited a higher sensitivity, which was comparable to that observed in the *rad3-136* strain.

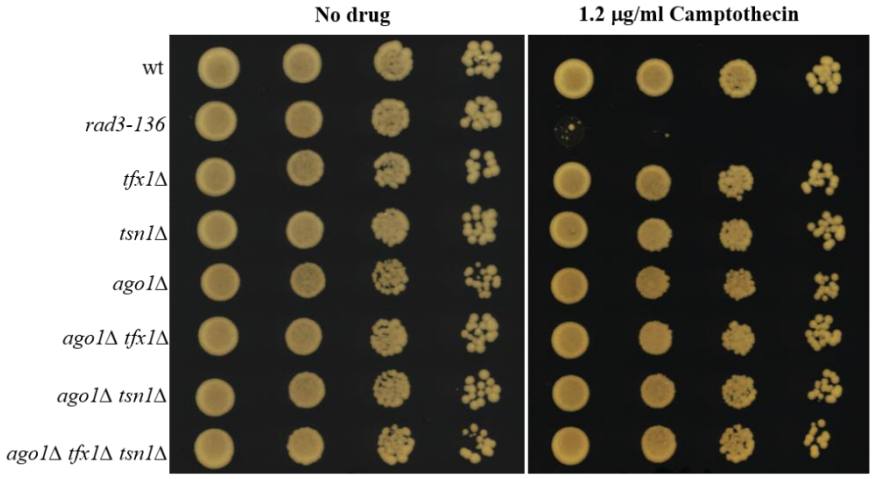

Figure 4.13 The *ago1*Δ *tfx1*Δ *tsn1*Δ triple mutant is not sensitive to camptothecin (CPT).
Serial dilutions of the indicated *S. pombe* mutants were set up and exposed to 1.2 µg/ml CPT. The plates were then incubated at 30°C for 4 days. Here, *rad3-136* cells (check point defective) were utilised as a positive control for the damaging agent. No measurable increase in sensitivity to CPT was observed in any mutants compared with the WT strain, including the *ago1*Δ *tfx1*Δ *tsn1*Δ triple mutant.

4.3 Discussion

4.3.1 The *ago1Δ bqt4Δ* double mutant is hypersensitive to TBZ

In eukaryotic genomes, each chromosome has distinct loci that ensure the proper segregation of chromosomes, including centromeres and telomeres (Steiner & Henikoff, 2015). In *S. pombe*, RNAi machinery is needed for heterochromatin establishment and gene silencing at the centromeres, which are required for the accurate segregation of chromosomes (Volpe et al., 2002; Volpe et al., 2003; Buhler & Gasser, 2009; Lorenzi et al., 2015; Sadeghi et al., 2015). The current study showed that the chromosomal segregation defects of Ago1-deficient cells can be partially suppressed by the *tfx1Δ* mutation, without a restoration of heterochromatin gene silencing at centromeres. In addition, we revealed that the *tlhΔ4* and *taz1Δ* mutants also partially suppress the *ago1Δ* mutant defects, suggesting that disruption of telomeric factors partially rescue *ago1*Δ mutant chromosome-instability defects. Thus, these findings may implicate Tfx1 in restricting segregation in cells via a centromere-independent, telomere-dependent mechanism. Taking these results together, it is speculated that chromosomes fail to segregate normally in the *ago1Δ* mutant, due, in part, to centromeric heterochromatin dysfunction, which is exacerbated by the fact telomeres are tethered to the NE. This hypothesis was tested by mutating the *bqt4* gene, which is defective in the tethering of the telomeres to the NE (Chikashige et al., 2009). The appropriate strains were exposed to TBZ with the aim of addressing whether the de-tethering of telomeres from the NE was required to suppress the *ago1*Δ defective phenotype. However, unexpectedly, it was found that the *ago1Δ bqt4Δ* double mutant showed TBZ greater sensitivity than the *ago1*Δ single mutant (Figure 4.2). These results demonstrated that the observed rescue of chromosomal mis-segregation in the *ago1Δ* mutant may not be due to de-tethering of telomeres from the NE, and they suggested that another telomere- dependent mechanism is at play in rescuing Ago1 defects. However, another function for Bqt4 that is required for proper segregation in the absence of Ago1 cannot be ruled out; this might mask the effect of de-tethering, so we cannot conclude *tfx1Δ* is defective in telomere tethering. Thus, further work is needed to confirm these results. For example, fluorescent localisation analysis can be conducted to determine whether telomeres are released from the NE when *tfx1* is disrupted.

4.3.2 Tfx1 and Tsn1 (C3PO) differentially regulate telomere transcripts

Translin and TRAX have mainly been implicated in the regulation of RNA, rather than DNA regulation, in various biological pathways (Wu et al., 1997; Liu et al., 2009; Jaendling & McFarlane, 2010; Ye et al., 2011; Li et al., 2012; Asada et al., 2014; Asada et al., 2016). *S. pombe* Tsn1 and Tfx1 were proposed to function on telomeric sequences (Jacob et al., 2004; Laufman et al., 2005), although no evidence of this was established prior to the present study. The phenotypic similarities found in this study between *tfx1*Δ and other telomere dysregulation mutations indicated a possible functional role of *S. pombe* Tfx1, and possibly Tsn1, in regulating telomere dynamics. To determine the nature of the function of Tfx1, and if any, of Tsn1 at the telomeres, levels of ARRET and TERRA transcripts were analysed in a range of *S. pombe* mutants. Remarkably, it was found that Tfx1 suppresses sub-telomeric ARRET transcripts in a Tsn1-dependent fashion (Figures 4.3 and 4.5), and in contrast, Tsn1 is required to suppress telomeric TERRA transcripts in a Tfx1-dependent fashion (Figures 4.4 and 4.6). This indicates that there is a reciprocal mechanism to control telomere- and sub-telomere-associated transcripts by Tfx1 and Tsn1. For example, in the absence of Tfx1, Tsn1 is required to stabilise ARRET levels, and Tfx1 is necessary to maintain elevated TERRA levels in the absence of Tsn1. These findings not only identify novel telomere regulatory factors (Tfx1 and Tsn1), but also further evidence that there is a functional distinction between Tsn1 and Tfx1, at least in *S. pombe.*

Earlier, it was shown that in the absence of Tsn1, levels of Tfx1 are greatly reduced (Jaendling et al., 2008). Thus, these current findings demonstrate that the residual Tfx1 in the *tsn1Δ* background is sufficient to regulate the telomere-associated transcripts. This finding is interesting, as it provides additional evidence that the low levels of residual Tfx1 found in the *tsn1Δ* mutant provide biological functions in regulating chromosomal stability. Furthermore, murine TRAX was found to prevent murine Translin from binding to mRNA (Chennathukuzhi et al., 2001), and there may be a similar control regulation by Tfx1 to inhibit Tsn1 from binding to telomeric RNAs. TERRA was recently found to be required for telomerase association and telomere length control in several organisms, including *S. pombe* (Wang et al., 2015; Moravec et al., 2016).

In *S. cerevisiae*, mutation of the *rat1* gene leads to an increased accumulation of TERRAs and telomere shortening because of telomerase dysfunction (Luke et al., 2008). However, the accumulation of TERRAs observed in *tsn1Δ* is not associated with large-scale telomere length changes (Gomez-Escobar, personal communication; see Appendix 2). This indicates that the elevated transcript levels in *tsn1*Δmutant are not due to a measurable change in the lengths of telomeres.

The necessity of Tsn1 and Tfx1 for the proper regulation of telomere-associated transcription is an indication of the fundamental importance of this protein pair. Up to now, no measurable phenotypic change in genome stability has been found when these genes are disrupted, in *S. pombe* at least, suggesting that Tsn1 and Tfx1 may play auxiliary or redundant functions in centrally essential processes.

Supporting the possibility that Tsn1 and Tfx1 play auxiliary or redundant functions, we revealed that the mutations of both *tsn1* and *tfx1* in *ago1Δ* cells exhibited high sensitivity to the TBZ, at levels greater than the sensitivity observed in the *ago1Δ* single mutant – although deletion of both *tfx1* and *tsn1* together caused no measurable alteration in chromosome stability (Figure 3.1). Interestingly, the high levels of genomic instability of cells lacking Ago1 and Tsn1/Tfx1 correlated with the high elevation of telomeric TERRA levels in the triple mutant (Figure 4.4), suggesting a functional redundancy.

Interestingly, we found that mutation of *tfx1*, but not *tsn1*, in an *ago1Δ* background increased the levels of sub-telomere-associated transcripts ARRET. This elevation was slightly decreased when *tsn1* was mutated in the *ago1Δ tfx1Δ* background (Figure 4.3), suggesting that this elevation depends on Tsn1. These results are somewhat consistent with the TBZ sensitivity data (Figure 3.1). Using a quantitative approach, tiled microarrays, we found that the silenced sub-telomeric *tlh* genes were activated in the *ago1*Δ *tfx1*Δ background (Figure 3.7). Importantly, we revealed that mutating all four *tlh* genes partially suppressed the chromosomal segregation defects of *ago1*Δ cells (i.e. measured by TBZ growth assay; Figure 3.12) to levels comparable to those seen in the *ago1Δ tfx1Δ* background (Figure 3.1). Taken together, these results suggest that modulating the transcriptional status in the sub-telomere regions may have been responsible for the observed suppression of Ago1 defects of the *ago1Δ tfx1Δ* double mutant. Our results imply the existence of a counterbalance between centromeres and telomeres to maintain chromosome stability.

Since the dysregulation of ARRET and TERRA transcripts is the only notable defect phenotype recorded up to date for *S. pombe tsn1*Δ and *tfx1*Δ single mutants, *S. pombe* represents a perfect model for studying this important function of these paralogues. Additional work by a co-worker in the McFarlane group demonstrated that this function may be partially conserved in humans, albeit in a telomere-specific fashion (Gomez-Escobar et al., 2016). However, further work is required to determine the precise mechanism by which TSN and TSNAX control the telomere transcript levels (stability *vs.* production), for example, by measuring the H3K9-me levels and RNA Pol II occupancy in sub-telomeric regions. In addition, fluorescence localisation analysis is needed to determine whether Tsn1 and Tfx1 function directly or indirectly on these RNAs (i.e. TERRAs and ARRETs) and the telomeric regions.

It has been recently proposed that TSN and TSNAX could be druggable targets for miRNA function restoration in tumours and emerging Dicer deficiencies (Asada et al., 2014; Asada et al., 2016). However, the finding that Tsn1 and Tfx1 are required for the control of telomere transcription levels should be taken into consideration before targeting these factors as anticancer agents.

4.3.3 The *ago1Δ tfx1Δ tsn1Δ* triple mutant is hypersensitive to DNA damaging agents

TRAX has recently been shown to have a direct role in the DNA damage response (Wang et al., 2016b), and TERRAs have been linked to the DNA damage response at telomeres (Maicher et al., 2014; Azzalin & Lingner, 2015; Cusanelli & Chartrand, 2015; Rippe & Luke, 2015; Wang et al., 2015). The finding that the *ago1Δ tfx1Δ tsn1Δ* triple mutant exhibits significant elevation in the TERRA transcripts, comparable to the elevation seen in *taz1Δ* (Figure 4.4) – which is associated with hyper-levels of genomic instability (Figure 3.1) – led us to ask whether the observed phenomenon in the triple mutant is linked to the DNA damage response. Therefore, the appropriate mutants were exposed to a wide range of DNA damaging agents, including HU, phleomycin, MMS, MMC, UV and CPT. Interestingly, we found that the *ago1*Δ *tfx1*Δ *tsn1*Δ triple mutant exhibited increased sensitivity in response to HU, phleomycin, MMS, MMC and UV damaging agents relative to the *ago1*Δ mutant (and *ago1*Δ *tfx1*Δ and *ago1*Δ *tsn1*Δ double mutants, which showed similar phenotype sensitivities of the *ago1*Δ; Figures 4.8, 4.9, 4.10, 4.11 and 4.12).

Interestingly, the *taz1*Δ mutant also had significantly elevated TERRAs (Greenwood & Cooper, 2012; Figure 4.4), and it exhibited increased sensitivity to several DNA damaging agents, including HU, MMS, and bleomycin (Miller & Cooper, 2003). Taken together, these results suggest that the elevated telomeric TERRA transcripts in the *ago1*Δ *tfx1*Δ *tsn1*Δ triple mutant may be linked to compromised DNA repair. However, further experiments are required to confirm these interesting results and determine their underlying mechanism.

S. pombe TERRA was recently shown to be required for telomere length control (Moravec et al., 2016). However, the hyper-elevation of TERRAs found in the *ago1*Δ *tfx1*Δ *tsn1*Δ triple mutant was not accompanied by a measurable large change in telomere length (see Appendix 2). Thus, there is no current evidence to link this phenomenon to telomeric length alteration.

4.4 Conclusion

1- Tfx1 and Tsn1 are novel telomere regulatory factors.
2- Tsn1 and Tfx1 can function independently of one another.
3- Tfx1 controls sub-telomeric ARRET transcript levels.
4- Tsn1 functions to control telomeric TERRA transcripts.
5- There is a reciprocal control of telomere-associated transcripts by Tsn1 and Tfx1.
6- Modulation of the transcriptional status at the sub-telomere regions may be responsible for driving the *ago1Δ* suppressor phenotype.
7- The hyper-elevation of telomeric TERRAs in the *ago1Δ tfx1Δ tsn1Δ* triple mutant may be linked to increased DNA damage sensitivity.

Chapter 5: Results

Analysis of Tfx1 and Tsn1 functions in a Dcr1-deficient background

5. Analysis of Tfx1 and Tsn1 functions in a Dcr1-deficient background

5.1 Introduction

The correct segregation of chromosomes is essential for ensuring that the genetic information is transferred into new daughter cells with high fidelity (Brouwers et al., 2017; Mutazono et al., 2017). Errors in this process can lead to cancers (Santaguida & Amon, 2015; Potapova & Gorbsky, 2017). The formation and maintenance of heterochromatin are vital for controlling many genomic functions, including gene silencing and chromosome segregation (Lejeune et al., 2010; Li & Zhang, 2012; Tadeo et al., 2013; Cusanelli & Chartrand, 2015; Zocco et al., 2016). In *S. pombe*, the RNAi machinery is necessary for heterochromatin establishment at several genomic loci, such as centromeres and sub-telomeres; however, for maintenance, it is only essential in the centromeres (Kanoh et al., 2005; Buhler & Gasser; 2009; Lorenzi et al., 2015). The loss of the key component genes of the RNAi machinery, including *ago1* and *dcr1*, influences centromeric heterochromatin function, leading to mis-segregation of chromosomes and a high sensitivity to the microtubule inhibitor TBZ (Volpe et al., 2002; Volpe et al., 2003; Buhler & Gasser, 2009; Creamer & Partridge, 2011; Chan & Wong, 2012; Lee et al., 2013; Tadeo et al., 2013; Holoch & Moazed, 2015; Sadeghi et al., 2015; Shimada et al., 2016).

In higher eukaryotes, the TRAX and Translin (C3PO) complex is involved in the removal of the passenger strand during RNAi-facilitated mRNA regulation (Liu et al., 2009; Ye et al., 2011). Analysis of *S. pombe* Tfx1 and Tsn1 functions in an *ago1*Δ mutant background has revealed that mutation of *tfx1*, but not *tsn1*, partially rescues the chromosome segregation defect of *ago1*Δ cells (see Chapter 3). Therefore, we also wanted to determine whether this genetic interaction is true in terms of the other RNAi regulatory genes, such as *dcr1*. However, Dcr1 was recently shown to have an RNAi-independent function, in which Dcr1, but not Ago1, promotes transcription termination at sites of replication stress and DNA damage (Castel et al., 2014; Ren et al., 2015). These findings demonstrate that there is a functional separation between Dcr1 and Ago1 in *S. pombe*. Given the above, the work in this chapter aims to analyse the function of Tsn1 and Tfx1 in a Dcr1-deficient background.

5.2 Results

5.2.1 Mutation of *tfx1* and *tsn1* increases the chromosomal instability of the *dcr1Δ* cells

We set out to explore the relationship between Tfx1 and Tsn1 and the RNAi component Dcr1. (all appropriate strains used in this study were constructed by others in the McFarlane group, but they were verified here using PCR of the appropriate loci prior to use).

5.2.1.1 TBZ sensitivity spot assay

TBZ is a microtubule-disrupting drug, and cells that are defective in full centromere function, such as *dcr1*Δ mutants, display sensitivity to it (Volpe et al., 2002; Volpe et al., 2003; Buhler & Gasser, 2009; Lee et al., 2013; Sadeghi et al., 2015). To determine whether Tfx1 and Tsn1 have a redundant role with the RNAi regulatory gene *dcr1*, appropriate mutants were tested for their response to TBZ (Figure 5.1). As expected, the *dcr1Δ* single mutant showed sensitivity to TBZ relative to the WT strain. Interestingly, we found that the *dcr1*Δ *tfx1*Δ double mutant is more sensitive to TBZ than the *dcr1Δ* single mutant is (Figure 5.1). Remarkably, the *dcr1*Δ *tsn1Δ* double mutants were hypersensitive to TBZ in comparison with the *dcr1*Δ mutant (and the *dcr1*Δ *tfx1*Δ double mutant; we tested two independently constructed *dcr1*Δ *tsn1*Δ double mutant strains; Figure 5.1). Notably, a few colonies were found to supress the high TBZ sensitivity in both the *dcr1Δ tfx1Δ* and *dcr1Δ tsn1Δ* background strains, especially at 33°C (this is discussed in Section 5.3.1; Figure 5.1). Collectively, the results suggest that Tfx1 and Tsn1 are required to maintain chromosome stability in the absence of Dcr1.

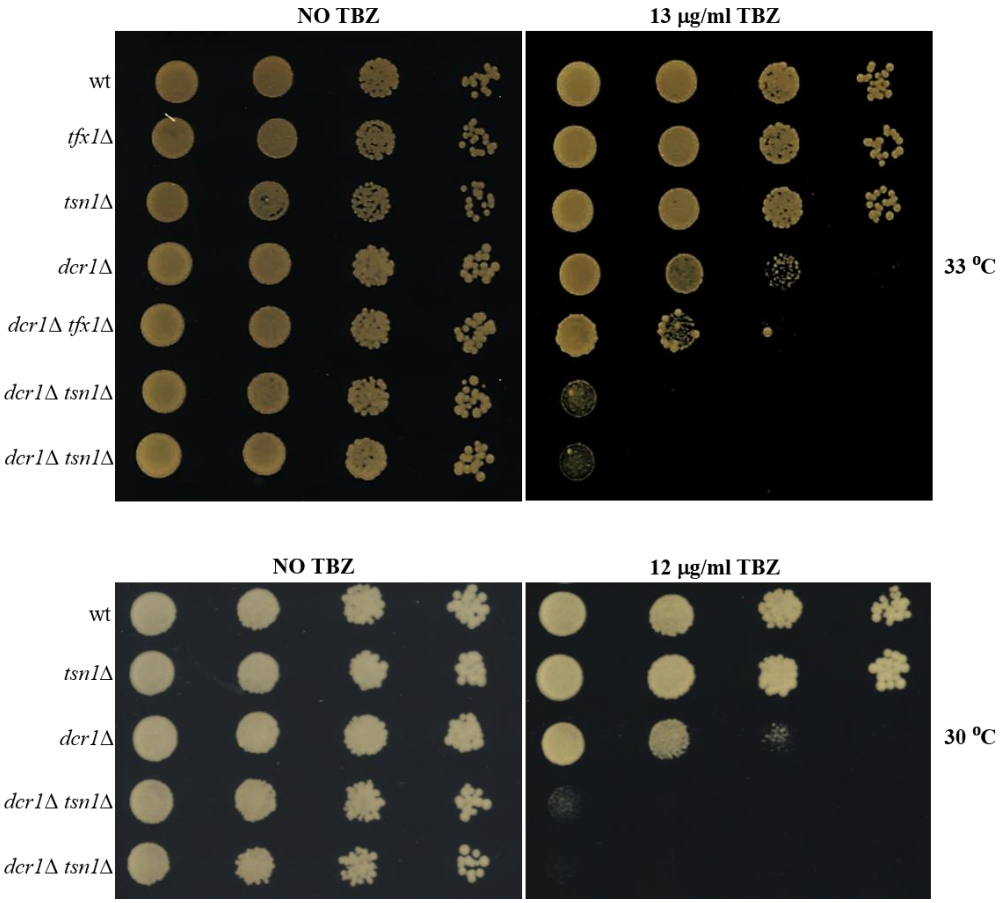

Figure 5.1 Mutation of *tfx1* and *tsn1* increases TBZ sensitivity of the *dcr1Δ* mutant.

Serial dilutions of the indicated *S. pombe* mutants were made and exposed to different concentrations of TBZ. The plates were then incubated at 30°C and 33°C for approximately 3 days. The *dcr1*Δ single mutant displayed increased sensitivity to TBZ in comparison with the WT strain. Mutation of *tfx1* increased the *dcr1Δ* TBZ sensitivity. In addition, both *dcr1*Δ *tsn1*Δ double mutant strains (BP2748 and BP2749) were hypersensitive to TBZ, with a sensitivity greater than that of the *dcr1*Δ single mutant (and *dcr1*Δ *tfx1*Δ double mutant).

5.2.1.2 Microscopic analysis of aberrant mitoses

Sensitivity to TBZ is not a direct measure of chromosome stability. Loss of RNAi component Dcr1 results in a high incidence of unsegregated chromosomes (Volpe et al., 2003; Figure 5.2.A). To further explore the possibility that *tfx1* and *tsn1* mutation increases the chromosomal instability of the *dcr1*Δ mutant, we stained DNA in mitotically dividing cells and monitored for the frequency of anaphase defects. As previously reported, it was found that mutation of *dcr1* displayed high levels of cells with abnormal mitoses (Figure 5.2.B). As observed for the TBZ sensitivity, *dcr1*Δ *tfx1*Δ exhibited more aberrant mitotic events than the *dcr1*Δ single mutant (Figure 5.2.B). In addition, mutation of *tsn1* significantly increased the abnormal mitosis events of the *dcr1Δ* cells (Figure 5.2.B), which is consistent with its TBZ sensitivity phenotype (Figure 5.1; examples of the WT and *dcr1Δ* phenotypes are shown in Figure 5.2.A). These analyses indicate that the chromosome segregation defects caused by the loss of Dcr1 increases following *tfx1* and *tsn1* mutation.

Collectively, the findings suggest that the *tfx1* and *tsn1* mutation increased the chromosomal instability of the *dcr1*Δ cells, with a greater effect seen in the *dcr1Δ tsn1Δ* double mutant. This provides new evidence of the functions of Tfx1 and Tsn1 in maintaining genomic stability.

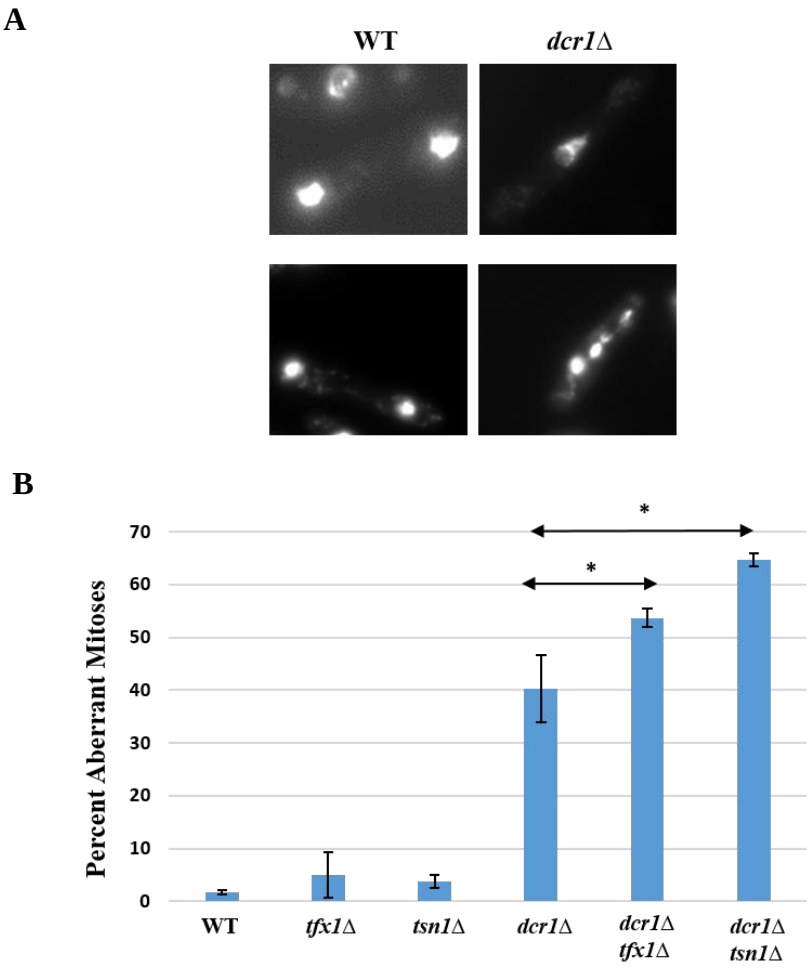

Figure 5.2 Fluorescence microscope analysis of *S. pombe* strains, grown at 30°C and stained with DAPI, showing the percentage of aberrant mitosis.
A. Example phenotypes of WT (left) and *dcr1Δ* (right) cells in the anaphase with DAPI stain under the fluorescence microscope.
B. The plot shows that the *dcr1*Δ single mutants exhibited approximately 40% mitotic (anaphase) defects. However, both the *dcr1Δ tfx1*Δ and *dcr1Δ tsn1*Δ double mutants had significantly increased numbers of aberrant anaphase events due to the loss of Dcr1. * = *p*-value < 0.05; Student's *t*-test; error bars show the standard deviation. The percentage of aberrant mitosis was obtained from the average of three independent experiments by counting at least 100 cells per sample in each experiment.

5.2.2 Investigation of whether Tfx1 and Tsn1 have roles in the DNA damage response in the absence of Dcr1

Distinct from what was observed with the *ago1*Δ background (see Chapter 3), analysis of Tfx1 and Tsn1 functions in the *dcr1*Δ mutant background revealed that *tfx1* and *tsn1* mutation increased the chromosomal instability of the *dcr1*Δ mutant (as measured by TBZ sensitivity, Figure 5.1, and assessed by monitoring endogenous chromosome segregation, Figure 5.2). These results suggest that Tfx1 and Tsn1 are required for maintaining chromosome stability in the absence of Dcr1. Translin and TRAX have been implicated in the DNA repair response (Jaendling & McFarlane, 2010), although direct evidence for this assertion is limited. More recently, however, Wang et al. (2016) found that murine TRAX is associated with the ATM-mediated pathway for DSB repair. Given this, as well as the finding that Dcr1 – but not Ago1 – is required in the DNA damage response (Castel et al., 2014), we set out to determine whether Tfx1 and Tsn1 have any redundant roles in the DNA damage response pathway in the absence of Dcr1 that contribute to genome stability. To address this, the appropriate *S. pombe* mutant strains were tested for their response to an extensive range of DNA-damaging agents; this allowed us to test a variety of DNA damage repair pathways. These damaging agents included hydroxyurea (HU; Figure 5.3), phleomycin (Figure 5.4), ultraviolet (UV) irradiation (Figure 5.5), camptothecin (CPT; Figure 5.6), methyl methane sulfonate (MMS; Figure 5.7) and mitomycin C (MMC; Figure 5.8).

Interestingly, we found that the *dcr1*Δ *tsn1*Δ double mutant, but not *dcr1Δ tfx1Δ*, exhibits increased sensitivity, relative to the *dcr1*Δ mutant, to HU, phleomycin, UV and CPT (mild effect) agents. However, neither the *dcr1*Δ *tfx1*Δ nor *dcr1*Δ *tsn1*Δ double mutant showed any increased sensitivity compared to the *dcr1*Δ single mutant in response to MMS or MMC drugs. Taken together, these analyses indicate that Tsn1, but not Tfx1, is required in the DNA damage recovery response in the absence of Dcr1, revealing a presently unknown function of Tsn1 in the DNA damage response pathway.

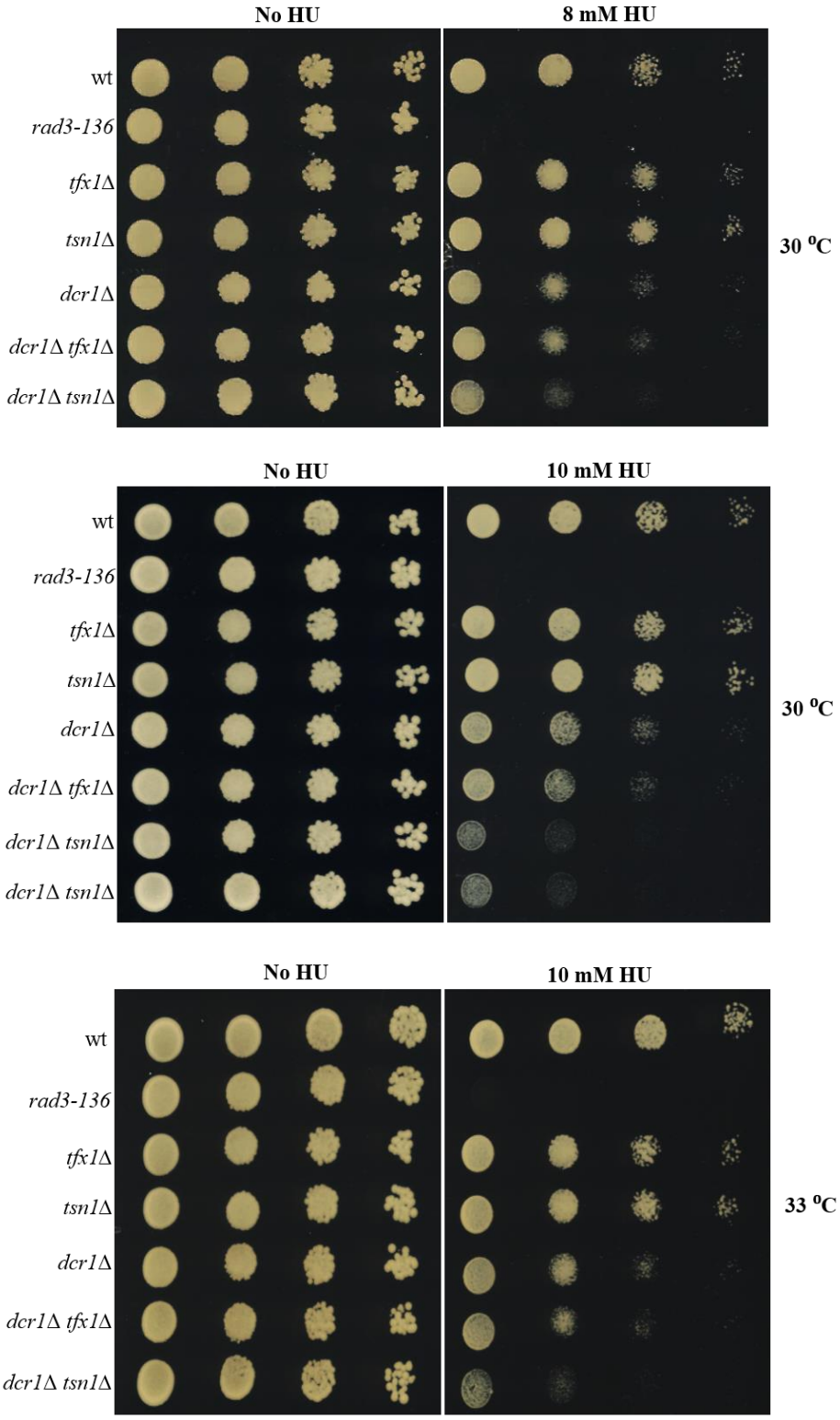

Figure 5.3 Mutation of *tsn1*, but not *tfx1*, increased the *dcr1Δ* hydroxyurea (HU) sensitivity. Serial dilutions of the indicated *S. pombe* mutants were generated and exposed to different concentrations of HU. The plates were then incubated at 30°C and 33°C for 4 days. Here, *rad3-136* cells (checkpoint defective) were used as a positive control. Mutation of *tsn1* in a *dcr1Δ* background increased HU sensitivity (we tested two independently constructed *dcr1*Δ *tsn1*Δ double mutant strains), whereas a *tfx1Δ* mutation did not.

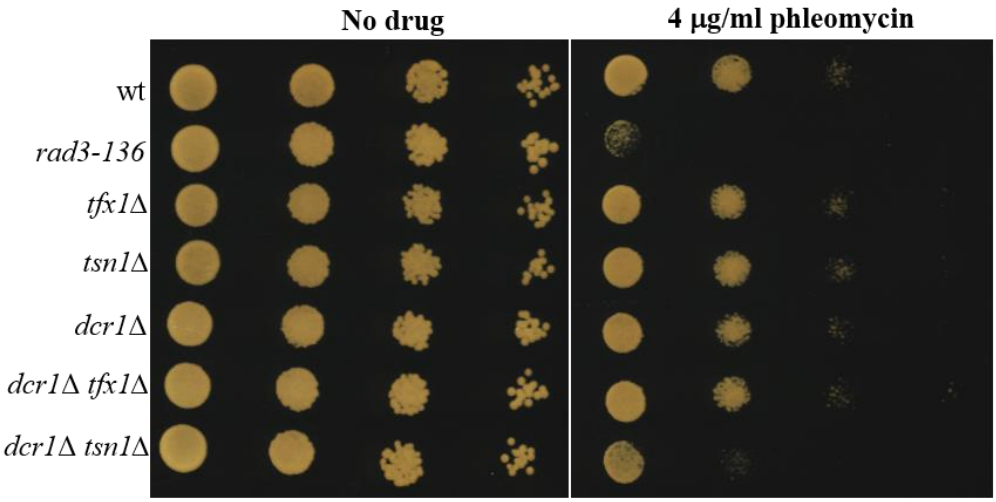

Figure 5.4 Mutation of *tsn1*, but not *tfx1*, increased *dcr1Δ* phleomycin sensitivity.
Serial dilutions of the indicated *S. pombe* mutants were set up and exposed to 4 µg/ml of phleomycin. The plates were then incubated at 30°C for 4 days. Here, *rad3-136* cells (checkpoint defective) were used as a positive control for the drug. The data show that the *dcr1*Δ *tsn1*Δ double mutant, but not *dcr1*Δ *tfx1*Δ, displayed increased sensitivity to phleomycin relative to the *dcr1*Δ mutant.

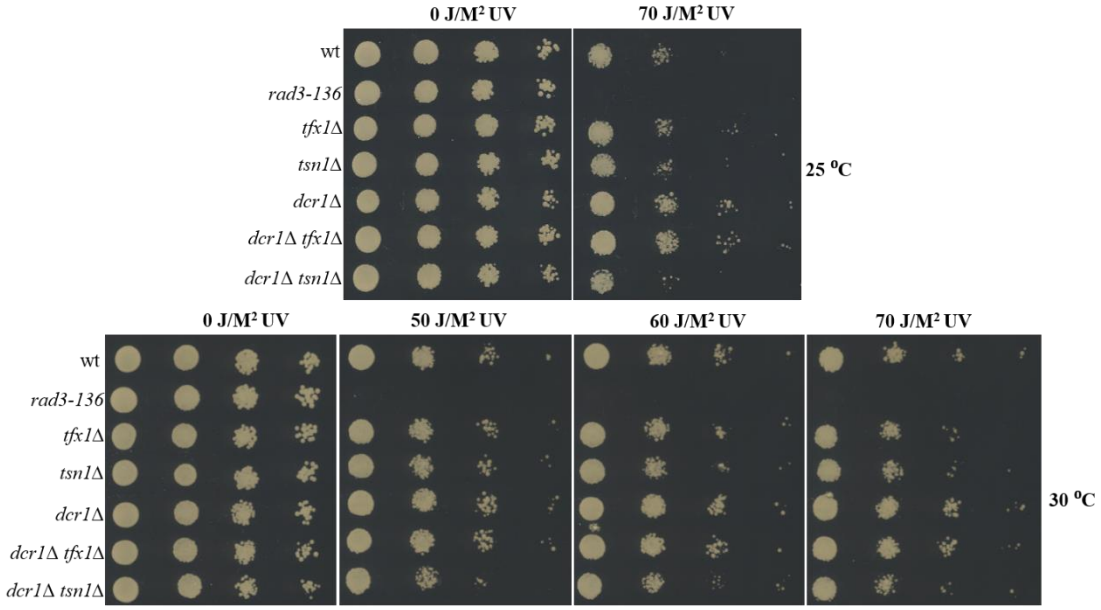

Figure 5.5 The *dcr1*Δ *tsn1*Δ double mutant, but not *dcr1*Δ *tfx1*Δ, is sensitive to ultraviolet (UV).

Serial dilutions of the indicated *S. pombe* mutants were set up and exposed to different doses of UV irradiation. The plates were then incubated at 25°C and 30°C for 4 days. Here, *rad3-136* cells (checkpoint defective) were used as a positive control. The data show that the *dcr1*Δ *tsn1*Δ double mutant, but not *dcrΔ1 tfx1*Δ, exhibited increased sensitivity to UV in comparison with the *dcr1*Δ single mutant.

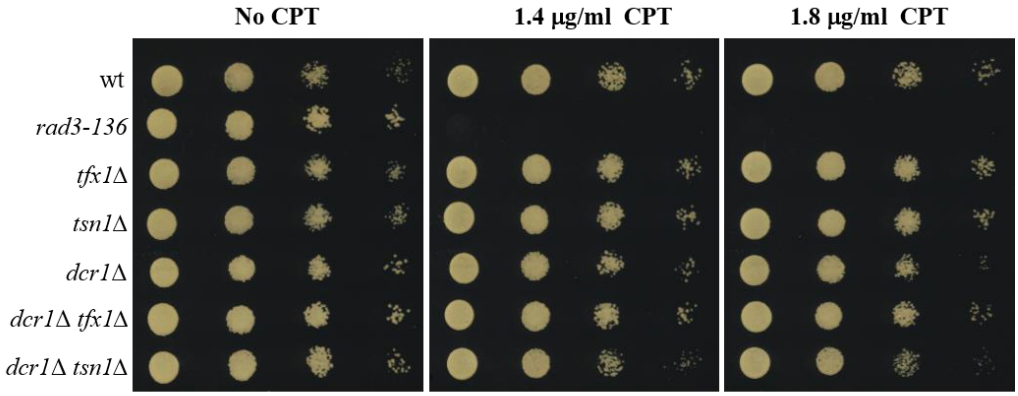

Figure 5.6 Camptothecin (CPT) sensitivity spot assay for a range of *S. pombe* mutants.
Serial dilutions of the indicated *S. pombe* mutants were set up and exposed to different concentrations of CPT. The plates were then incubated at 30°C for 4 days. Here, *rad3-136* cells (checkpoint defective) were used as a positive control for the drug. The data show that the *dcr1Δ tsn1Δ* double mutant, but not *dcr1Δ tfx1Δ*, may have displayed a slight increase in sensitivity to CPT in comparison with the *dcr1Δ* mutant.

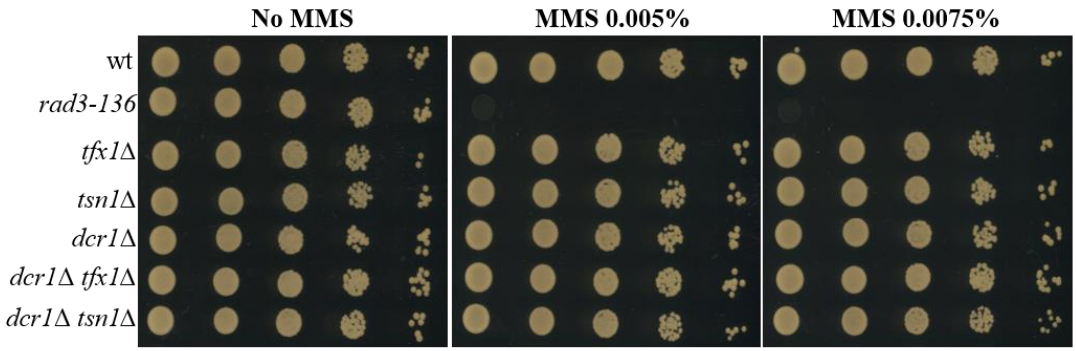

Figure 5.7 Methyl methane sulfonate (MMS) sensitivity spot assay.
Serial dilutions of the indicated *S. pombe* mutants were set up and exposed to different concentrations of MMS. The plates were then incubated at 30°C for 4 days. Here, *rad3-136* cells (checkpoint defective) were utilised as a positive control for the drug. None of the *dcr1Δ tfx1Δ* or *dcr1Δ tsn1Δ* double mutants exhibited increased sensitivity to MMS relative to the *dcr1*Δ strain.

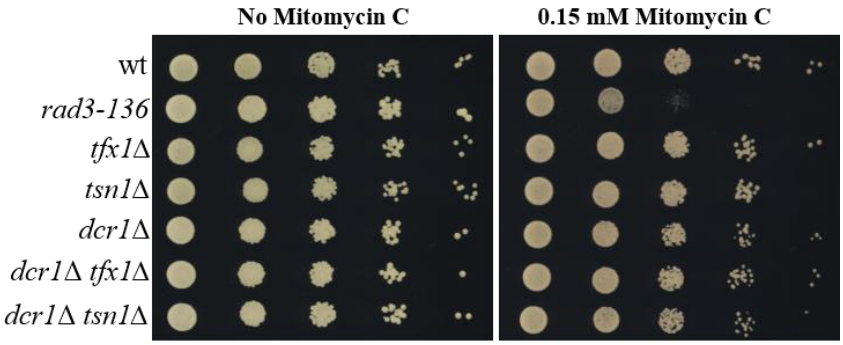

Figure 5.8 Mitomycin C (MMC) sensitivity spot assay.
Serial dilutions of the indicated *S. pombe* mutants were made and exposed to 0.15 mM MMC. The plates were then incubated at 30°C for 4 days. Here, *rad3-136* cells (checkpoint defective) were utilised as a positive control for the drug. Neither the *dcr1Δ tfx1Δ* nor *dcr1Δ tsn1Δ* double mutants displayed a measurable increase of sensitivity to MMC in comparison with the *dcr1*Δ strain.

5.2.3 Levels of telomeric transcriptome in *dcr1*Δ backgrounds

The historical analysis of sub-telomeric heterochromatin regions to determine a role for the RNAi machinery was carried out based on a study of the *dcr1Δ* mutant (Kanoh et al., 2005). To further explore the behaviour of Tsn1 and Tfx1 in the absence of Dcr1, ARRET (sub-telomeric regions; Figure 4.3.A) and TERRA (telomeric regions; Figure 4.3.A) transcript levels were analysed in the *dcr1*Δ single mutant and *dcr1*Δ *tsn1*Δ and *dcr1*Δ *tfx1*Δ double mutants using previously developed RT-PCR/qRT-PCR assays (Greenwood & Cooper, 2012; Lorenzi et al., 2015).

Analysis of the sub-telomeric ARRET transcript levels showed no elevation in levels of ARRET, relative to the WT strain, in the *dcr1*Δ single mutant; indeed, a small decrease was observed but this was statistically insignificant (Figures 5.9 and 5.10). Interestingly, the mutation of *tsn1* in the *dcr1*Δ background resulted in an increased accumulation of ARRET levels (Figures 5.9 and 5.10); this elevation of ARRET transcript levels correlated with increased DNA damage sensitivity in *dcr1Δ tsn1Δ* cells (this is discussed in Section 5.3.3). However, the elevation of ARRET in the *tfx1*Δ was not as pronounced in the *dcr1*Δ *tfx1*Δ double mutant, as measured qualitatively by RT-PCR assay (Figure 5.9) and quantitatively by qRT-PCR assay (Figure 5.10); the functional implications of this result are unclear.

Analysis of TERRAs in *dcr1Δ* backgrounds exhibited no measurable elevation in the transcript levels of TERRA in the *dcr1Δ* single mutant and *dcr1Δ tfx1Δ* double mutant relative to the WT strain (Figure 5.11). Notably, however, the elevated level of TERRAs in the *tsn1Δ* mutant background was somewhat suppressed following the additional mutation of *dcr1*, as measured qualitatively by RT-PCR (Figure 5.11); the functional consequences of this result are not clear at this stage.

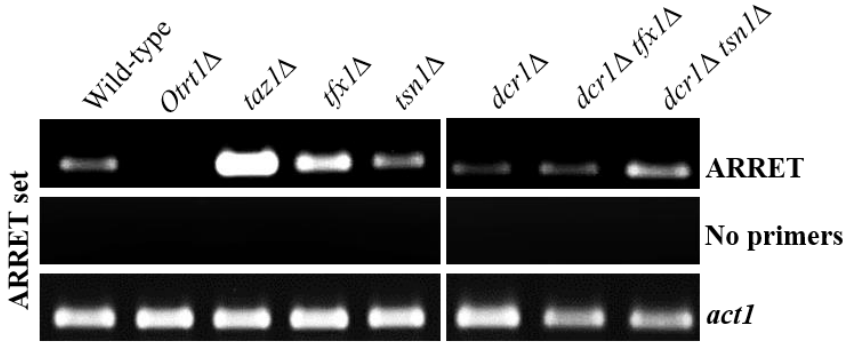

Figure 5.9 Qualitative analysis of sub-telomeric ARRET transcripts in *dcr1*Δ mutant backgrounds.

The agarose gel image displays RT-PCR products utilising the primer specific for ARRETs (Figure 4.3.A). The *act1* gene expression was used as a positive control to show the quality of RNA in all samples. No primer samples were used as a negative control, and no primers were used in the cDNA synthesis step, showing that there was no endogenous priming. The *Otrt1Δ* strain, which has no telomeres, was used as a negative control to show that no band could be detected in the *Otrt1Δ* cells. The *taz1Δ* mutant was used as a positive control, and this has already been shown to exhibit elevation of all telomeric transcripts (Greenwood & Cooper, 2012). No measurable increase of ARRETs could be detected in the *dcr1Δ* and *tsn1*Δ single mutants relative to the WT strain. However, the ARRET levels were stabilised in the *dcr1*Δ *tsn1*Δ double mutant in comparison with the single mutants. In addition, the data showed that the elevation of ARRETs in the *tfx1*Δ strain was somewhat reduced by the loss of *dcr1*.

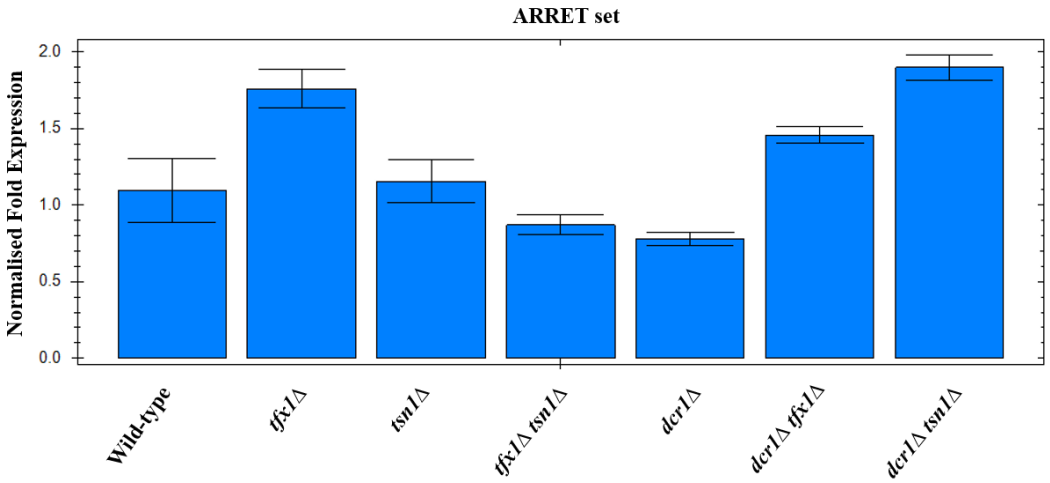

Figure 5.10 Quantitative real-time PCR analysis of ARRETs in *dcr1*Δ mutant backgrounds. The plot demonstrates that the *dcr1*Δ and *tsn1*Δ single mutants showed statistically indistinguishable levels of ARRET from that observed in the WT strain. However, ARRET levels were significantly elevated in the *dcr1Δ tsn1*Δ double mutant compared with the *dcr1*Δ and *tsn1*Δ single mutants. The *dcr1Δ* mutation in a *tfx1*Δ background resulted in a reduction of ARRETs relative to the *tfx1*Δ single mutant. Here, *act1* was used to normalise the results, and Bio-RAD CFX Manager was employed for the data analysis. The error bars are the standard error for triplicate repeats. Pairwise Student's *t*-tests were performed to determine the *p*-values of WT *vs*. *dcr1Δ*, $p = 0.2$; *tfx1Δ vs*. *dcr1Δ tfx1*Δ, $p = 0.09$; *dcr1Δ vs. dcr1Δ tfx1*Δ, $p < 0.01$ and *dcr1Δ vs. dcr1Δ tsn1*Δ, $p < 0.01$.

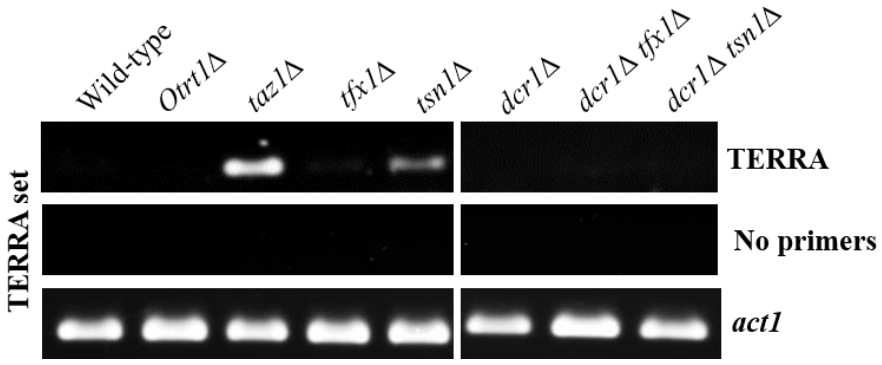

Figure 5.11 Qualitative analysis of telomeric TERRA transcripts in the *dcr1*Δ mutant backgrounds.

The agarose gel image displays the RT-PCR products utilising the primer specific for TERRA (Figure 4.3.A). The *act1* gene expression was used as a positive control to show the quality of RNA in all samples. No primer samples were used as a negative control, which resulted in no primers being used in the cDNA synthesis step, showing that there was no endogenous priming. The *Otrt1Δ* strain, which has no telomeres, was used as a negative control to show that no band could be detected in the *Otrt1Δ* cells. The *taz1Δ* mutant was used as a positive control, and this has already been shown to exhibit elevation of all telomeric transcripts (Greenwood & Cooper, 2012). While TERRA levels were not detectable in the WT strain, no measurable elevation of TERRAs could be detected in either the *dcr1Δ* single mutant or *dcr1Δ tfx1Δ* double mutant. However, the elevation of TERRAs observed in the *tsn1*Δ mutant was clearly somewhat suppressed following additional mutation of *dcr1*.

5.3 Discussion

5.3.1 Loss of Tfx1 and Tsn1 increases the chromosome instability of Dcr1-defective cells

During mitosis and meiosis, establishment of centromeric heterochromatin is essential for the correct segregation of chromosomes (Buhler & Gasser, 2009; Schoeftner & Blasco, 2009; Stimpson & Sullivan, 2010; Zeng et al., 2010; Schmidt & Cech, 2015; Mutazono et al., 2017). In *S. pombe*, heterochromatin formation and maintenance in centromeres depend on the RNAi pathway (Volpe et al., 2002; Volpe et al., 2003; Buhler & Gasser, 2009; Creamer & Partridge, 2011; Chan & Wong, 2012; Lee et al., 2013; Tadeo et al., 2013; Holoch & Moazed, 2015; Sadeghi et al., 2015; Shimada et al., 2016; Mutazono et al., 2017). Cells that are defective in the RNAi system, such as those in the *ago1*Δ and *dcr1*Δ mutants, display a high incidence of aberrant mitoses and high sensitivity to the microtubule toxin TBZ (Volpe et al., 2002; Volpe et al., 2003; Buhler & Gasser, 2009; Lee et al., 2013; Sadeghi et al., 2015). Deletion of the *S. pombe tfx1* was found to partly suppress the chromosomal segregation defect of *ago1Δ* cells (see Chapter 3). Elsewhere, it has been demonstrated that mutation of *taz1* also rescues the defect phenotype of *ago1*Δ cells and other RNAi regulatory genes, including *dcr1*, (Tadeo et al., 2013). Thus, we set out to determine whether mutation of *tfx1*, and if any, of *tsn1* in the Dcr1-defective cells could also result in a similar rescue phenotype. We found, however, that the loss of *tfx1* increases the *dcr1*Δ TBZ sensitivity (Figure 5.1); this differs from the observed rescue phenotype in the *dcr1Δ taz1Δ* cells (Tadeo et al., 2013), suggesting a distinct mechanism is at play. In addition, the *dcr1*Δ *tsn1*Δ double mutant was hypersensitive to TBZ relative to the *dcr1*Δ single mutant; indeed, the TBZ sensitivity was greater than that for the dcr1Δ *tfx1*Δ double mutant (Figure 5.1). Taken together, these results provide further evidence of the need for C3PO functioning in preserving chromosome stability. In addition, the finding that the mutation of *tsn1* in a *dcr1*Δ background is much more sensitive to TBZ than the mutation of *tfx1* suggests a more central function for Tsn1 in the absence of Dcr1 when it comes to maintaining genomic stability.

Following the TBZ sensitivity results, microscopic analysis was used to measure the frequency of nonsegregated chromosomes in anaphase cells in appropriate strains. We found that chromosomal segregation defects caused by the loss of Dcr1 also increased following the mutation of *tfx1* and *tsn1* (Figure 5.2.B), with more significant segregation defects seen in the *dcr1*Δ *tsn1*Δ double mutant. This is consistent with the TBZ sensitivity pattern.

Collectively, our data demonstrated that the chromosomal instability of *dcr1*Δ cells is enhanced following mutation of *tfx1* and *tsn1*. Moreover, they indicated that the observed rescue of Ago1 defects, by the loss of *tfx1* is distinct and may reflect a very different mechanistic defect. Supporting the findings that loss of Tsn1 increases the chromosomal instability defect of *dcr1*Δ cells, co-workers in the McFarlane group also revealed that the mutation of *tsn1,* but not *tfx1*, is found to increase mini-chromosome instability caused by the loss of Dcr1 (Z. Al-shehri, PhD thesis, Bangor University; N. Al-mobadel, PhD thesis, Bangor University). These results further support the suggestion that Tsn1 makes a more significant contribution than Tfx1 does to maintaining chromosome stability in the absence of Dcr1.

Importantly, further analysis found that centromeric heterochromatin transcription is identical for the *dcr1*Δ and *dcr1Δ tsn1Δ* strains (Z. Al-shehri, PhD thesis, Bangor University; R. McFarlane, personal communication). These results indicate that the increases in chromosome mis-segregation and instability defects observed in the *dcr1*Δ *tsn1*Δ double mutant are not due to increased centromeric heterochromatin dysfunction, suggesting that a distinct pathway is compromised by the loss of Tsn1 function; this pathway appears to be independent of RNAi, but related to genome stability regulation.

It is important to note that there are a few colonies in the *dcr1*Δ *tfx1*Δ and *dcr1*Δ *tsn1*Δ mutant backgrounds that suppress the high TBZ sensitivity (Figure 5.1). These suppressor cells were mostly seen at 33°C, suggesting a temperature-suppression phenotype. This could suggest a possible factor activated in these few cells that resulted in the genome instability suppression phenotype. Thus, further analysis, such as a cDNA library screen, is needed to decipher the factor that results in the rescue effect.

5.3.2 Tsn1, but not Tfx1, is required in the DNA damage response in the absence of Dcr1

Translin and TRAX have been implicated in the DNA repair response (Jaendling & McFarlane, 2010; Wang et al., 2016b), and Dcr1, but not other RNAi components, has recently been shown to have a role in the DNA damage response (Castel et al., 2014; Ren et al., 2015). Given these findings, we set out to determine whether the increase in chromosomal instability observed in the *dcr1*Δ *tfx1*Δ and *dcr1*Δ *tsn1*Δ strains is due to defects in the DNA repair pathways. To test this, appropriate mutants were exposed to a wide range of DNA damaging agents, including HU, phleomycin, UV, CPT, MMS and MMC.

Interestingly, we found that the *dcr1*Δ *tsn1*Δ double mutant, but not the *dcr1*Δ *tfx1*Δ double mutant, exhibited increased sensitivity to HU, phleomycin, CPT and UV relative to the *dcr1*Δ mutant. However, neither the *dcr1*Δ *tfx1*Δ nor *dcr1*Δ *tsn1*Δ double mutant showed increased sensitivity in response to MMS and MMC agents in comparison with the *dcr1*Δ mutant, although we cannot absolutely dismiss the possibility that there might be a slight effect for the double mutants to MMS and/or MMC, as we only used concentrations of MMS and MMC that do not affect the WT strain. Thus, further work is required to confirm these results. These interesting results suggest that the increase in chromosomal instability observed in the *dcr1*Δ *tsn1*Δ double mutant is due to the failure to repair DNA damage; moreover, they indicate that Tsn1, but not Tfx1, is required in the DNA damage response in the absence of Dcr1. In addition, the failure of the *tfx1* mutation to have a similar increase of sensitivity to any of the DNA-damaging agents indicates further evidence of the functional separation between Tfx1 and Tsn1 in *S. pombe*, and it suggests that the increase in chromosomal instability observed in the *dcr1*Δ *tfx1*Δ double mutant is not due to a DNA repair defect. Importantly, most of the DNA-damaging reagents used suggest that the hypersensitivity of the *dcr1*Δ *tsn1*Δ double mutant is somehow related to the S phase. Supporting this, the non–S phase–related agent, MMS (a mismatch repair–type mechanism) did not show measurable sensitivity to phenotype differences between the *dcr1*Δ and *dcr1 tsn1*Δ mutants (Figure 5.7). In addition, the finding that the *dcr1*Δ *tsn1*Δ double mutant is hypersensitive to the ribonucleotide reductase (RN) inhibitor HU agent is an indication that this phenomenon may indeed be related to replication. Supporting this, Castel et al. (2014) found that Dcr1 is required to remove RNA Pol II–mediated transcription from sites of collision between transcription and replication, which preserves the genomic stability (Ren et al., 2015). However, in the absence of Dcr1, there are more collisions caused between the DNA replication machinery and RNA Pol II–mediated RNA:DNA hybrids. This results in DNA replication fork collapses and DSB formation, which may lead to chromosomal instability and rearrangements (Figure 1.4; Castel et al., 2014; Brambati et al., 2015). This may explain the *dcr1*Δ mutant sensitivity to HU (Figure 5.3).

To date, Translin has been shown to have a great affinity for controlling RNA species; therefore, it may be the case that Tsn1 plays a role in reducing the stability of RNA:DNA hybrids in the absence of Dcr1, which suppresses recombination and maintains genome stability. Consequently, mutation of *tsn1* in the *dcr1*Δ background may stimulate recombination that results in chromosomal translocations, causing a hypersensitivity to HU (Figure 5.3).

Taking the findings together, we propose that Tsn1 serves to suppress transcription-DNA replication-associated recombination in the absence of Dcr1, which could account for the original proposed role for Translin in driving chromosomal translocations (Aoki et al., 1995). Castel et al. (2014) separated the Dcr1 function in this specific mechanism from the RNAi regulation mechanism; moreover, we found that the *ago1*Δ and *ago1*Δ *tsn1*Δ strains show similar HU sensitivities (Figure 4.8), representing further support for the postulated role of Tsn1 secondary to Dcr1 in the RNA regulation of breakage.

The phleomycin agent is generally known to create DSBs in the cell cycle, and the increased sensitivity of the *dcr1*Δ *tsn1*Δ double mutant compared with the *dcr1*Δ mutant to HU and phleomycin agents (Figures 5.3 and 5.4) suggests that these breaks occurred in the S phase, which is further evidence for the involvement of Tsn1, in the absence of Dcr1, in the repair of DSBs that induce recombination. A similar hypersensitivity phenotype of the *dcr1*Δ *tsn1*Δ double mutant, relative to the *dcr1*Δ mutant, was found using a more specific chromosomal breaking agent, bleomycin (data not shown).

MMC is known to cause interstrand crosslinks. Therefore, in the presence of MMC, the two strands of DNA became crosslinked; consequently, the replication fork is strongly blocked and cannot proceed. Thus, unlike in HU, replication fork collapse and DSBs are not consequently created in the presence of MMC. We found no increased sensitivity to MMC in the *dcr1*Δ *tsn1*Δ double mutant relative to the *dcr1*Δ single mutant, which was indistinguishable from the WT strain (Figure 5.8). The lack of sensitivity to MMC of cells that are defective in *dcr1*Δ and *dcr1*Δ *tsn1*Δ is important because in MMC-mediate cross-link damage, RNA:DNA hybrids are not important, and at present, it seems that *dcr1*Δ and *dcr1*Δ *tsn1*Δ mutant cells can survive as well as the WT cells in the presence of MMC (Figure 5.8). However, Dcr1, and possibly Tsn1, are required to remove RNA:DNA hybrids in the presence of HU-induced replication fork stalling, and the *dcr1*Δ mutant exhibited a sensitivity to HU relative to the WT, which further increased following the mutation of *tsn1* (Figure 5.3). Therefore, the different phenotype responses to DNA damage reagents in these mutants provide further evidence to support the suggestion that the phenomenon observed in the *dcr1*Δ *tsn1*Δ double mutant is related to the transcription replication collision mechanism, and it is also consistent with our proposal that, in the absence of Dcr1, Tsn1 may be involved in removing RNA:DNA hybrids and suppressing recombination.

In the next chapter, the possibility that the hypersensitivities of the *dcr1*Δ *tsn1*Δ double mutant to the chromosomal breaking and DNA replication inhibitor drugs are due to an elevation of recombination will be addressed directly.

5.3.3 Sub-telomeric transcripts are dysregulated in the *dcr1*Δ *tsn1*Δ double mutant

Dcr1 is implicated in sub-telomeric heterochromatin formation, which is necessary for transcription silencing, recombination suppression and the maintenance of telomere integrity (Kanoh et al., 2005; Bisht et al., 2008; Tadeo et al., 2013; Zocco et al., 2016). To further explore the behaviour of Tfx1 and Tsn1 in Dcr1-deficiency cells, RT-PCR/qRT-PCR analysis was used for assessing levels of telomere-associated transcripts in mutants that were defective in the *dcr1Δ* single mutant and *dcr1Δ tfx1Δ* and *dcr1Δ tsn1Δ* double mutants. Remarkably, we found that sub-telomeric ARRET levels were highly elevated in the *dcr1*Δ *tsn1*Δ double mutant relative to the *tsn1*Δ and *dcr1*Δ single mutants, which were statistically indistinguishable from the WT (Figures 5.9 and 5.10). The sub-telomeric *tlh* genes were consistently de-repressed in the *dcr1*Δ *tsn1*Δ cells (R. McFarlane, communication). This dysregulation of the sub-telomeric transcripts *tlh* and ARRET in the *dcr1*Δ *tsn1*Δ double mutant correlates with defects in the DNA damage response pathway observed in cells lacking both *dcr1* and *tsn1* (see Section 5.2.2), possibly pointing to a functional link. Therefore, we cannot dismiss the possibility that the increased *dcr1*Δ *tsn1*Δ sensitivity to damaging agents, relative to *dcr1*Δ, is due to a failure to repair telomeric DNA. One possible approach can be taken to test this: The *dcr1*Δ and *dcr1*Δ *tsn1*Δ mutant strains can be constructed in the *Otrt1*Δ strain background, which has no telomeres, or alternatively in a HAATI strain (Jain et al., 2010), and these constructed strains can be exposed to the DNA damaging agents. For example, if the *dcr1*Δ and *dcr1*Δ *tsn1*Δ strains exhibit similar sensitivities to the DNA-damaging reagents, then this may indicate that the observed phenomenon in the *dcr1*Δ *tsn1*Δ cells is a telomere-specificity effect.

5.4 Conclusion

1. The mutation of *tfx1* or *tsn1* increases the chromosomal instability of the *dcr1*Δ mutant.
2. Tsn1, but not Tfx1, is required in the DNA damage response in the absence of Dcr1.
3. Tsn1 may serve to suppress transcription-DNA replication–associated recombination in the absence of Dcr1.
4. The hypersensitivity of the *dcr1*Δ *tsn1*Δ double mutant to damaging agents may be due to a failure to repair telomeric DNA.

Chapter 6: Results

Tsn1 suppresses recombination in the absence of Dcr1

6. Tsn1 suppresses recombination in the absence of Dcr1

6.1 Introduction

One significant oncogenic element responsible for cancer initiation and progression is genetic alteration, including chromosomal translocations. Translocations take place due to abnormal recombination events between nonhomologous chromosomes (Tucker, 2010; Nambiar & Raghavan, 2011; Zheng, 2013; Harewood & Fraser, 2014; Roukos & Misteli, 2014). Translin was initially implicated in chromosomal translocation formation in human leukaemia cells (Aoki et al., 1995), but it has subsequently been found to be involved in the control of different RNA processing mechanisms (Wu et al., 1997; Liu et al., 2009; Ye et al., 2011; Li et al., 2012; Asada et al., 2014; Gomez-Escobar et al., 2016). However, the link between these mechanisms and cancer-associated chromosomal translocations has not yet been elucidated. Previous analysis of *tsn1*Δ null mutants in *S. pombe* showed no measurable defects in mechanisms involving recombination, such as DNA damage recovery (Jaendling et al., 2008). Prior to the current study, however, it had not yet been tested whether Translin has a redundant role in the recombination and DNA repair processes, which could account for its proposed function in oncogenic translocation formation (Jaendling & Mcfarlane, 2010). In the present study, it was found that Tsn1 is required in the DNA damage response in the absence of Dcr1 (see Chapter 5). Given the role of Dcr1 in removing RNA Pol II-mediated RNA:DNA hybrids from replication-pausing sites, such as rDNA and tRNA genes – where collisions occur between the replication fork and transcription in the absence of Dcr1 (Castel et al., 2014; Molla-Herman et al., 2015; Ren et al., 2015; Loya & Reines, 2016; Gadaleta & Noguchi, 2017) – and because RNA:DNA hybrids at these sites are highly recombinogenic (Castel et al., 2014; Loya & Reines, 2016; Aguilera & Gómez-González, 2017), we speculated that the increased sensitivity of the *dcr1Δ tsn1Δ* double mutant to the replication-stressing agent (e.g., HU) and chromosomal breaking agent (e.g., phleomycin), relative to the *dcr1*Δ single mutant, was due to increased formation of recombination stimulating lesions in the *dcr1Δ tsn1Δ* cells, suggested a role for Tsn1 in suppressing the transcription–DNA replication–associated recombination in the absence of Dcr1. Therefore, the work in this chapter aims to explore this possibility by measuring the recombination frequency at a tRNA gene (tDNA) in a *dcr1Δ* single mutant and a *dcr1Δ tsn1Δ* double mutant.

6.1.1 An overview of the genetic assay used in this study

tRNA genes, which are the template for RNA Pol III transcribed tRNAs, accumulate RNA Pol II in *dcr1Δ* cells compared to wild-type (Castel et al., 2014). This suggests that antisense transcription by RNA Pol II is taking place at tRNA genes (Castel et al., 2014). The McFarlane team previously established a plasmid-by-chromosome recombination system to monitor recombination frequency at tRNA genes inserted into the *ade6* locus (Pryce et al., 2009; Figure 6.1). This system was previously utilised to show that *S. pombe* tRNA genes inserted in *ade6*$^{+}$ slowed DNA replication fork progression, demonstrating that tRNA genes provide strong replication fork barrier (RFB) activity (Pryce et al., 2009). In brief, a single tRNA gene, *tRNA*^{GLU}, was introduced independently in both orientations into the *Bst*XI site in the *S. pombe* genomic *ade6* locus, thereby rendering the strains auxotrophic for adenine (Figure 6.1.A). In addition, the pSRS5 plasmid was created, which carries a distinct *ade6* mutant allele, *ade6-ΔG1483*. This allele has a point mutation distal to the position into which *tRNA*^{GLU} was introduced (Figure 6.1.B). Recombination between the *S. pombe* chromosome-borne *ade6::tRNA*^{GLU} allele and plasmid-borne *ade6-ΔG1483* allele can result in an adenine prototroph (Ade^{+}), which can be used to genetically measure the frequency of recombination events.

Based on the work of Castel et al. (2014), we hypothesised that RNA Pol II–mediated RNA:DNA hybrids would be generated at the *ade6::tRNA*^{GLU} locus ; it is known this tRNA gene insert generates a RFB, although it is unknown whether RNA Pol II/III transcription occurs at this tRNA gene. Therefore, we set up this system to ask whether recombination increases at a tDNA site when *drc1* and *tsn1* are mutated. To explore this, appropriate mutant strains, containing *ade6::tRNA*^{GLU}, were constructed (see Section 6.2.1; Figures 6.2, 6.3 and 6.4). Following this, these constructed strains were transformed with the pSRS5 plasmid (see Section 2.5.2), and they were then subjected to fluctuation tests to quantify the recombination frequencies (see Section 6.2.3; Figures 6.8, 6.9).

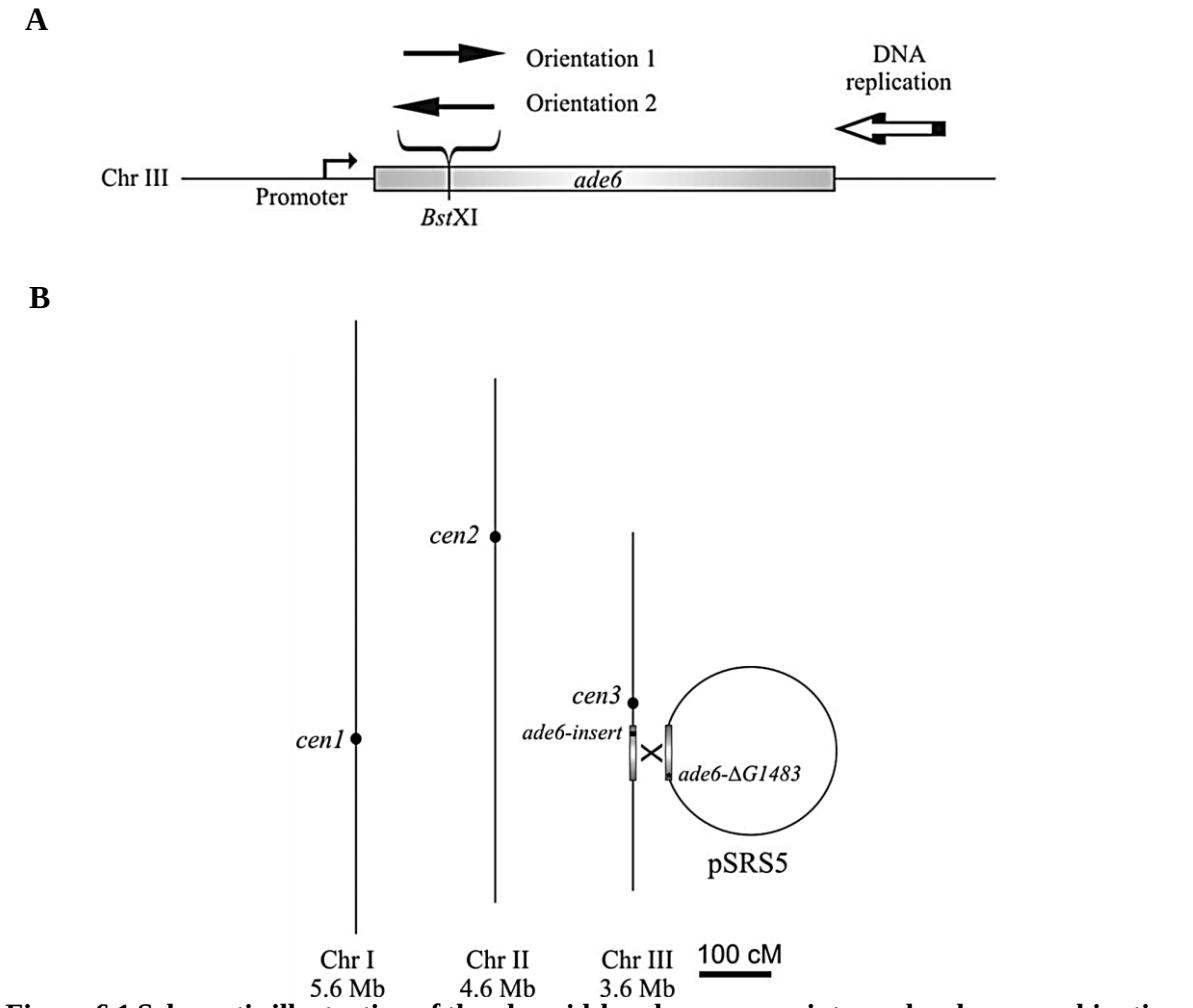

Figure 6.1 Schematic illustration of the plasmid-by-chromosome intermolecular recombination system used to measure a recombination frequency at *ade6::tRNA^{GLU}*.

A. *tRNA^{GLU}* was inserted independently in both orientations 1 and 2 (black arrows above the *Bst*XI site) into the *ade6* ORF (open rectangle) at the *Bst*XI site. The expression of *ade6* is from left to right; the angular arrow shows the promoter. The predominant direction of DNA replication is indicated by the large open arrow. In orientation 1, a head-to-head collision between the RNA Pol III and DNA replication is expected. In contrast, orientation 2 would be predicted to generate head-to-tail collisions between the Pol III and replication machinery. Conversely, orientation 1 would generate a head-to-tail collision between the replication fork and RNA Pol II, and orientation 2 would generate a head-to-head collision between the replication fork and RNA Pol II. **B.** The three chromosomes of *S. pombe* are indicated by the vertical lines. The *ade6* locus is found on the smallest chromosome, Chr III, where the inserted *tRNA^{GLU}* (depicted in A) is located. The large open circle represents the pSRS5 plasmid, which carries a second *ade6* allele (*ade6-ΔG1483*) with a point mutation at the 3′ end of *ade6*, distal to the position where *tRNA^{GLU}* was inserted. The mutations in the chromosomal and plasmid alleles will be recombined to produce a prototroph (Ade$^+$). The prototroph production frequency can be used to quantify the recombination frequency (adapted from Pryce et al., 2009).

6.2 Results

6.2.1 Constructing appropriate mutant strains

As previously indicated, all the *S. pombe* strains were generated by replacement with antibiotic-resistant cassettes using PCR-based gene-targeting methods (Bähler et al., 1998; see Section 2.3). The *tsn1* and *dcr1* genes were deleted from the parent *ade6::tRNA*^{GLU} strains (BP1478 and BP1508) to generate the single mutants *tsn1*Δ in orientation 1 (BP3335), *tsn1*Δ in orientation 2 (BP3336), *dcr1*Δ in orientation 1 (BP3313) and *dcr1*Δ in orientation 2 (BP3343; Figures 6.2, 6.3 and 6.4). To generate the double mutant in orientation 1 (BP3314), *tsn1* was deleted from the newly constructed single mutant *dcr1*Δ background (BP3313; Figure 6.2), and to generate the double mutant in orientation 2 (BP3362), *dcr1* was deleted from the newly constructed single mutant *tsn1*Δ background (BP3336; Figure 6.3).

Plasmids containing the required antibiotic-resistant cassettes were isolated from *E. coli* (see Table 2.3). Here, *kanMX6* and *natMX6* were the replacement cassettes used to delete *tsn1* and *dcr1*. For example, *kanMX6* was utilised for the *tsn1*Δ mutants (BP3335, BP3336 and BP3314) and *dcr1*Δ mutant (BP3343), and *natMX6* was used for the *dcr1*Δ mutants (BP3313 and BP3362). The replacement cassettes were amplified using PCR with primers designed with 80 bp homologous sequences directly flanking the *tsn1* and *dcr1* ORFs upstream and downstream; they also contained a 20 bp homologous sequence to the antibiotic-resistant markers on the *kanMX6* and *natMX6* genes of the plasmids (Figure 3.8). The purified PCR product was then chemically transformed into the appropriate *S. pombe* strains (see Section 2.5.1). To confirm the correct gene deletions, the *tsn1*Δ and *dcr1*Δ candidates were screened via PCR (Figures 6.2, 6.3 and 6.4) using three sets of primers, as previously shown in Figure 3.9.

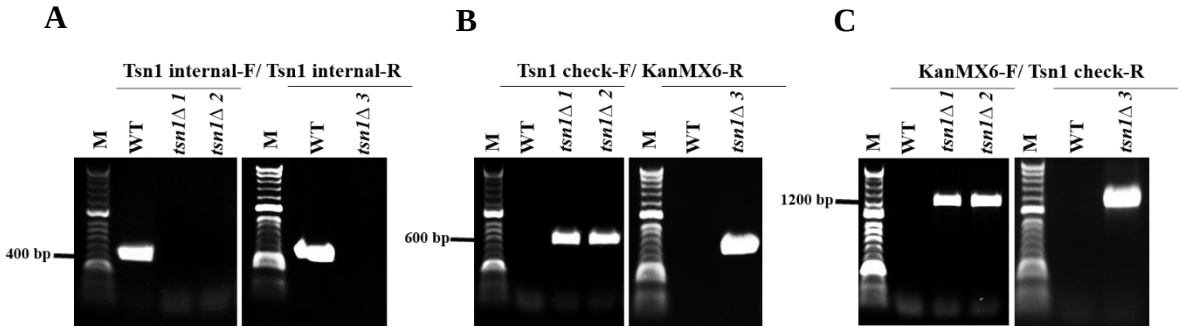

Figure 6.2 PCR screening of successful *tsn1Δ* candidates.

A. Agarose gel image displays PCR products for the WT strain and *tsn1*Δ 1, 2 and 3 (BP3335 *tsn1*Δ in ori 1, BP3336 *tsn1*Δ in ori 2 and BP3314 *dcr1Δ tsn1*Δ in ori 1, respectively) using the Tsn1-int-F and Tsn1-int-R primers. The expected PCR product sizes of the *tsn1* gene was 475 bp. The gel image shows no PCR products in the successful *tsn1*Δ candidate strains. **B.** PCR products for the WT and *tsn1*Δ candidate strains using Tsn1 check-F and KanMX6-R primers. Band sizes of approximately 619 bp were seen in the *tsn1*Δ strains, but not in the *tsn1*$^{+}$ strains (WT). **C.** KanMX6-F and Tsn1 check-R primers were utilised to amplify the WT and *tsn1*Δ candidate strains. A product size of approximately 1200 bp was present in the *tsn1*Δ strains, but not in the *tsn1*$^{+}$ strains (WT). M = markers and ori = orientation.

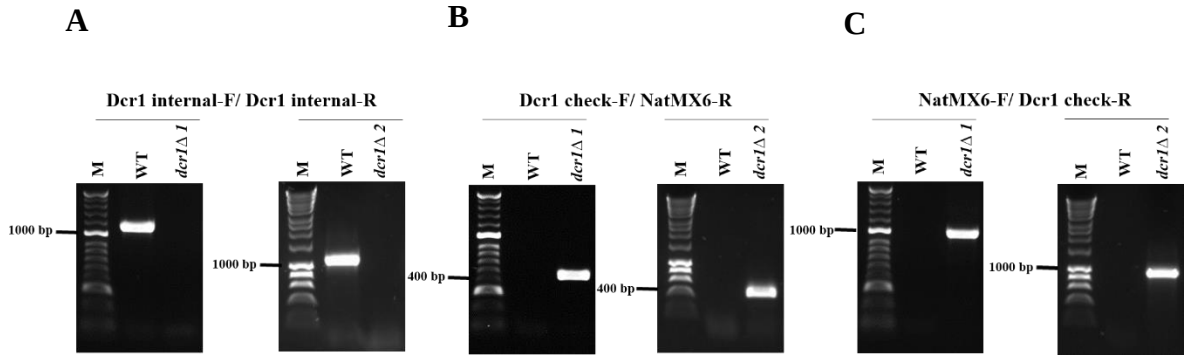

Figure 6.3 PCR screening of successful *dcr1Δ* candidates.

A. Agarose gel image displays PCR products for the WT strain, and *dcr1*Δ 1 and 2 (BP3313 *dcr1*Δ in ori 1 and BP3362 *tsn1Δ dcr1*Δ in ori 2, respectively) using Dcr1-int-F and Dcr1-int-R primers. The expected PCR product sizes of the *dcr1* gene was 1139 bp. The gel image shows no PCR products in the successful *dcr1*Δ candidate strains. **B.** PCR products for the WT and *dcr1*Δ candidate strains using the Dcr1 check-F and NatMX6-R primers. Band sizes of approximately 487 bp were seen in the *dcr1*Δ strains, but not in the *dcr1*$^{+}$ strains (WT). **C.** NatMX6-F and Dcr1 check-R primers were utilised to amplify the WT and *dcr1*Δ candidate strains. A product size of approximately 969 bp was present in the *dcr1*Δ strains, but not in the *dcr1*$^{+}$ strains (WT). M = markers and ori = orientation.

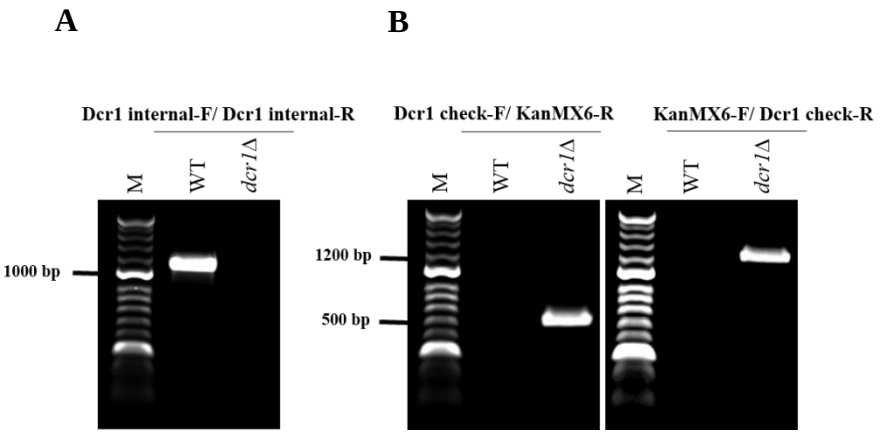

Figure 6.4 PCR screening of successful *dcr1Δ* candidates.

A. Agarose gel image displays PCR products for the WT strain and *dcr1*Δ strains (BP3343 *dcr1*Δ in ori 2) using the Dcr1-int-F and Dcr1-int-R primers. The expected PCR product size of the *dcr1* gene was approximately 1139 bp. The gel image shows no PCR products in the successful *dcr1*Δ candidate strain. **B.** PCR products for the WT and *dcr1*Δ candidate strains using Dcr1 check-F and KanMX6-R primers. A band size of approximately 550 bp was seen in the *dcr1*Δ strain, but not in the *dcr1*$^{+}$ strain (WT). KanX6-F and Dcr1 check-R primers were utilised to amplify the WT and *dcr1*Δ candidate strains. A product size of approximately 1298 bp was present in the *dcr1*Δ strain, but not in the *dcr1*$^{+}$ strain (WT). M = markers and ori = orientation.

6.2.2 TBZ and DNA damaging agent sensitivity tests for the newly constructed strains

The data in Chapter 5 showed that the *dcr1*Δ *tsn1*Δ double mutant displayed increased sensitivity, relative to the *dcr1*Δ mutant, in response to the microtubule destabilizing drug TBZ, as well as HU and phleomycin DNA damaging drugs. Here, we set out to further confirm this by repeating these experiments with the newly constructed strains (i.e. appropriate mutants were generated in both orientations of the *ade6::tRNA*^{GLU} strains). Consistent with the data in Chapter 5, the *dcr1Δ tsn1Δ* double mutants exhibited more sensitivity, relative to the *dcr1Δ* mutants, to TBZ (Figure 6.5), as well as the DNA damaging agents, HU and phleomycin (Figures 6.6 and 6.7). Taken together, these results further confirm that Tsn1 is required in the DNA damage recovery response in the absence of Dcr1, and they support the proposed role of Tsn1 in suppressing recombination in the absence of Dcr1, which will be addressed directly in the next section.

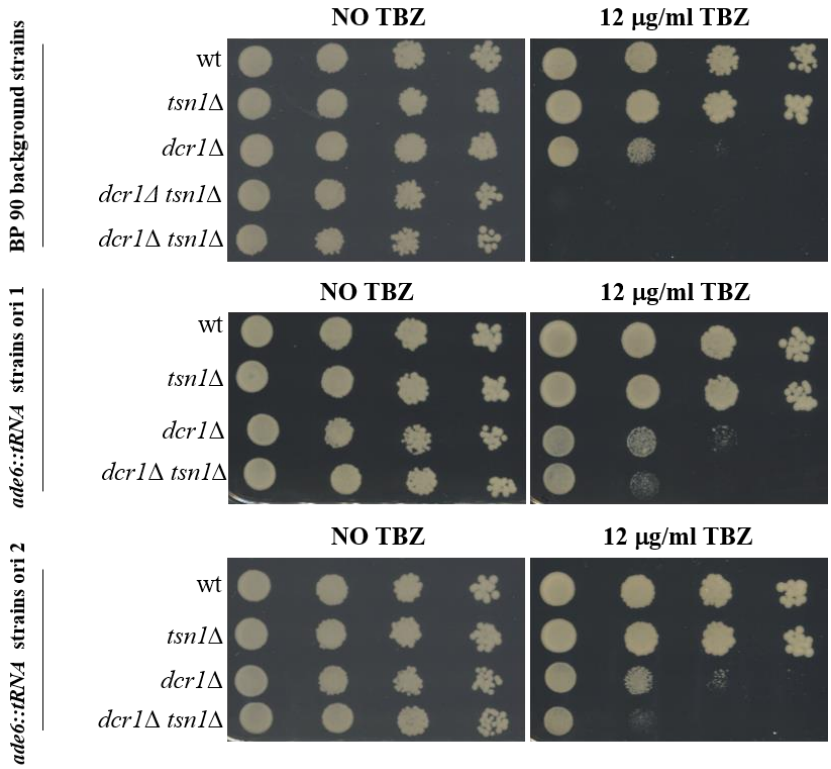

Figure 6.5 TBZ sensitivity spot test confirming the increased sensitivity of the *dcr1Δ tsn1Δ* cells.

Serial dilutions of the indicated *S. pombe* mutants were set up and exposed to different concentrations of TBZ. The plates were then incubated at 30°C for approximately 3 days. The *dcr1*Δ *tsn1*Δ double mutants (BP2748, BP2749, BP3314 and BP3362) exhibited increased sensitivity to TBZ relative to the *dcr1Δ* mutants.

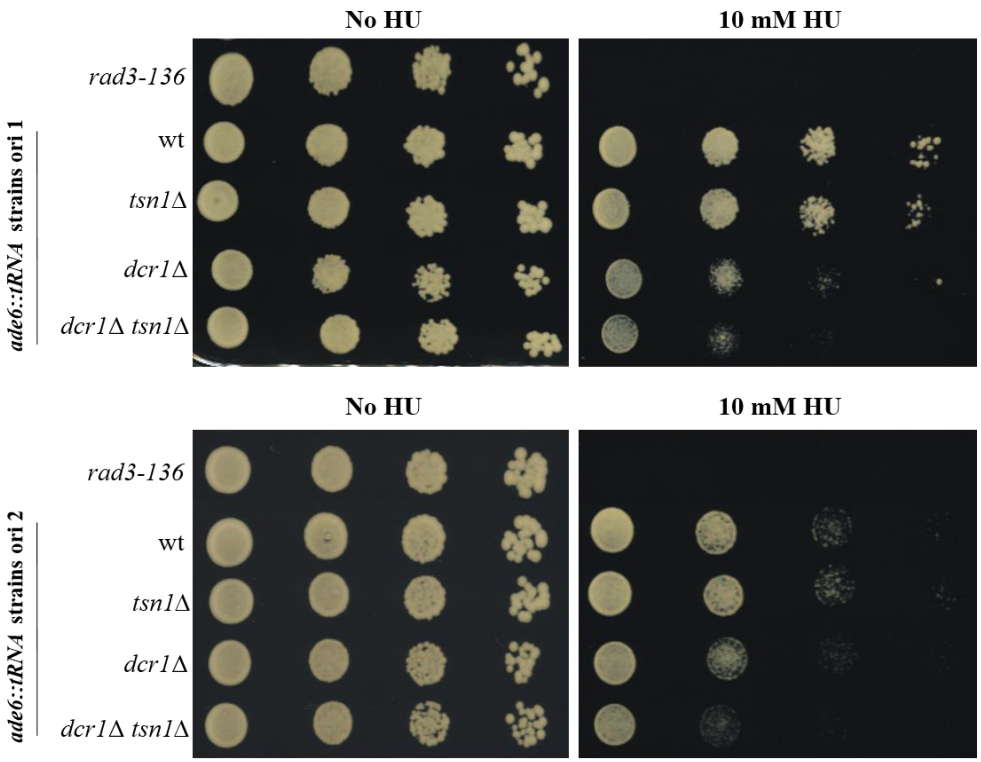

Figure 6.6 HU sensitivity spot assay confirming the increased sensitivity of the *dcr1Δ tsn1Δ* cells.

Serial dilutions of the indicated *S. pombe* mutants were made and exposed to 10 mM HU. The plates were then incubated at 30°C for approximately 4 days. Here, *rad3-136* cells (checkpoint defective) were used as a positive control for the damaging agent. The *dcr1*Δ *tsn1*Δ double mutants (BP3314 and BP3362) showed increased sensitivity to HU in comparison with the *dcr1*Δ single mutants.

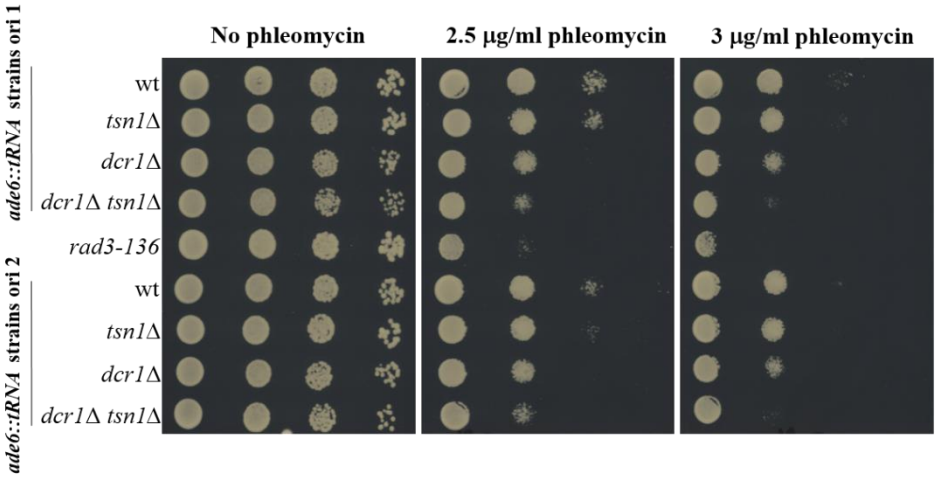

Figure 6.7 Phleomycin sensitivity spot assay confirming the hypersensitivity of the *dcr1Δ tsn1Δ* double mutant.

Serial dilutions of the indicated *S. pombe* mutants were made and exposed to different concentrations of the phleomycin agent. The plates were then incubated at 30°C for approximately 4 days. Here, *rad3-136* cells (checkpoint defective) were used as a positive control for the damaging agent. The *dcr1*Δ *tsn1*Δ double mutants (BP3314 and BP3362) displayed increased sensitivity to phleomycin compared with the *dcr1*Δ single mutants.

6.2.3 Analysis of recombination frequencies for the *tsn1*Δ, *dcr1*Δ and *dcr1*Δ *tsn1*Δ mutants at tRNA genes

To test whether the increased sensitivity of the *dcr1Δ tsn1Δ* double mutant to the DNA damaging agents is related to elevated recombination at a known RFB, the *tsn1*Δ, *dcr1*Δ and *dcr1*Δ *tsn1*Δ in both tRNA gene orientations were assessed for plasmid-by-chromosome recombination frequency. Fluctuation analysis was performed on these mutant strains alongside the WT strains using the pSRS5 plasmid to measure the recombination frequency (adenine prototrophs per 10^6 viable cells; see Section 2.14).

In orientation 1 of the *ade6::tRNA*^{GLU} strains, the fluctuation test showed no statistically significant increase in the recombination frequency in the *tsn1*Δ and *dcr1*Δ single mutants or the *dcr1*Δ *tsn1*Δ double mutant compared with the WT strain (Figure 6.8). *swi1*Δ strains, which exhibit elevated recombination in this assay (Pryce et al., 2009) were used as a positive control. These results indicate that recombinogenic lesions are not stimulated in the *dcr1*Δ mutants for orientation 1. In orientation 2, loss of *tsn1* displayed no statistically meaningful increase of recombination frequency compared with the WT strain. However, we found that the *dcr1*Δ mutation exhibited an approximately two-fold increase in recombination frequency compared with the WT, suggesting an orientation-specific effect (Figure 6.9). Interestingly, this elevated level of recombination was further increased following the additional mutation of *tsn1* in the *dcr1*Δ background (Figure 6.9), and the increase between *dcr1*Δ and *dcr1*Δ *tsn1*Δ is statistically significant. Comparing the WT to the *dcr1*Δ *tsn1*Δ gives a statistically significant increase of almost 4-fold. These results demonstrate that the hypersensitivity to damaging agents observed in the *dcr1*Δ *tsn1*Δ double mutant, relative to the *dcr1Δ* mutant, is linked to orientation-dependent increased recombination at a known RFB.

A

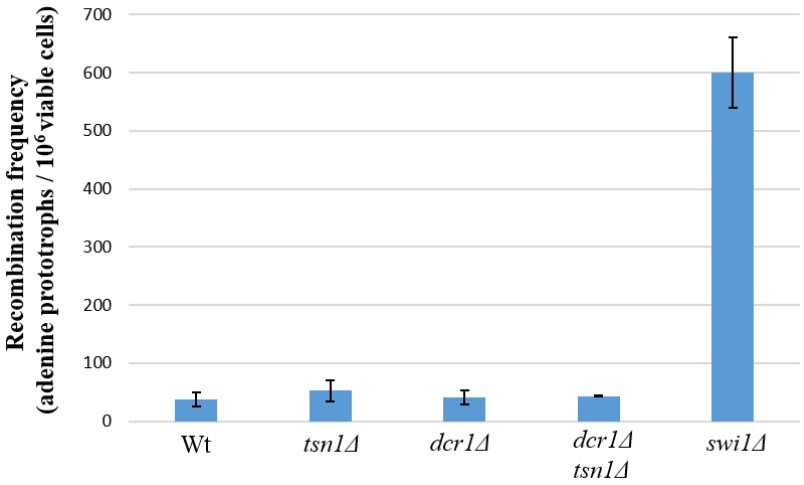

B

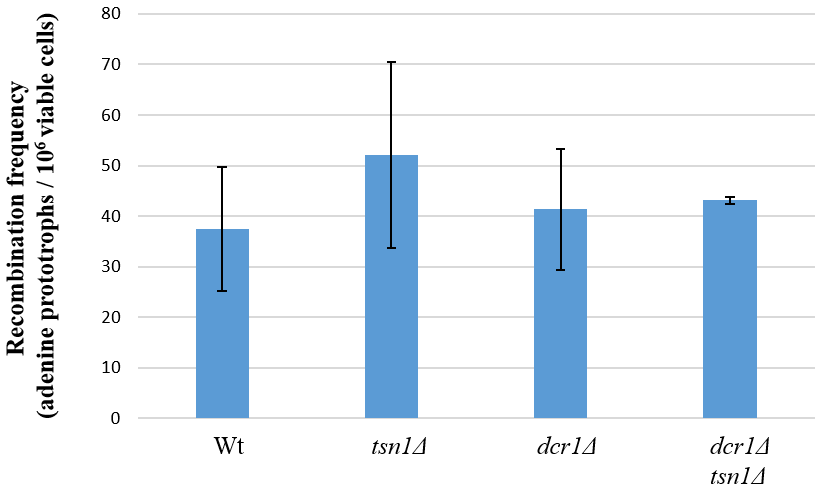

Figure 6.8 Plasmid-by-chromosome intermolecular recombination assay for the *ade6::tRNA^{GLU}* –orientation 1 strains.

A. The plot displays the mean values of at least four independent median values obtained from the fluctuation test for plasmid-by-chromosome intermolecular recombination frequencies for the indicated *S. pombe* mutants. The data showed that the recombination frequency of *tsn1*Δ, *dcr1*Δ and *dcr1*Δ *tsn1*Δ mutants exhibited no statistically significant change from that obtained for the WT strain. Here, the *swi1*Δ mutant (BP1685) was used as a positive control, and this has already been shown to exhibit elevation of recombination at *ade6::tRNA^{GLU}* (Pryce et al., 2009). **B.** Same data with the *swi1*Δ values removed. The error bars show the standard deviation. Pairwise Student's t-tests were performed to determine the p-values between the WT and indicated mutant strains. All p-values were > 0.05 except WT vs. *swi1*Δ, which was < 0.01.

A

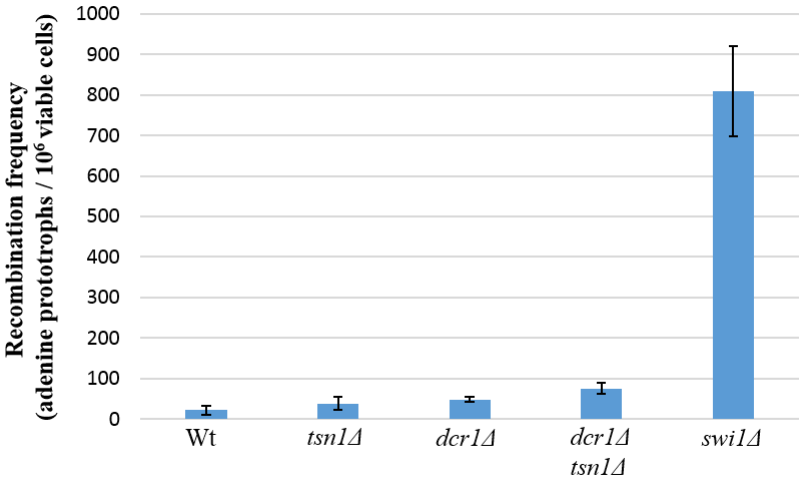

B

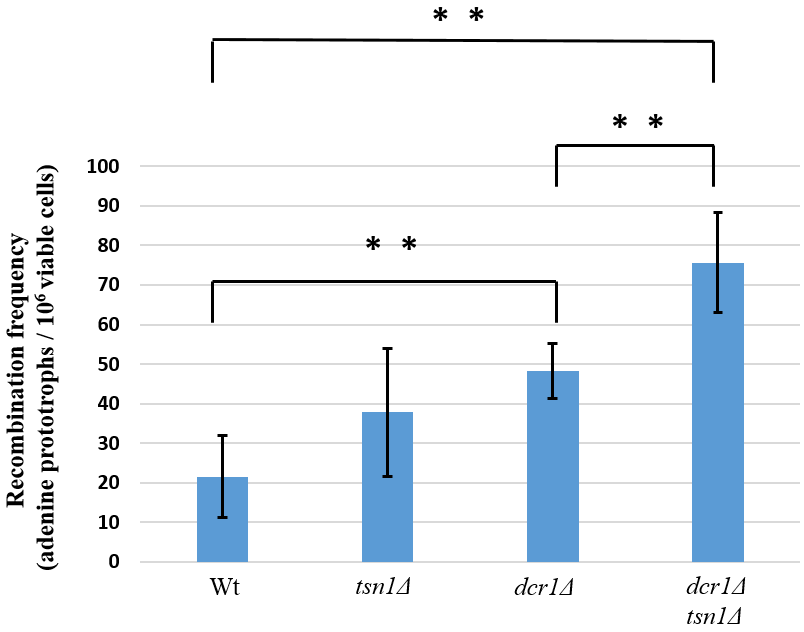

Figure 6.9 Plasmid-by-chromosome intermolecular recombination assay for the *ade6::tRNA^{GLU}* –orientation 2 strains.

A. The plot displays the mean values of at least four independent median values obtained from fluctuation test for plasmid-by-chromosome intermolecular recombination frequencies for the indicated *S. pombe* mutants. The data showed that the *tsn1*Δ mutant had a recombination frequency that was statistically indistinguishable from that of the WT strain. However, mutation of *dcr1*Δ resulted in an approximately two-fold increase in the recombination frequency in comparison with the WT strain. In addition, the recombination frequency of the *dcr1Δ tsn1*Δ double mutant was significantly elevated compared with the *dcr1*Δ mutant (and the WT strain). Here, the *swi1*Δ mutant (BP1687) was used as a positive control, and this has already been shown to exhibit elevation of recombination at *ade6::tRNA^{GLU}* (Pryce et al., 2009). **B.** Same data with the *swi1*Δ values removed. The error bars are the standard deviation. Pairwise Student's t-tests were performed to determine the p-values of WT vs. *tsn1Δ*, $p > 0.05$; WT vs. *dcr1Δ*, $p < 0.01$; *dcr1Δ* vs. *dcr1Δ tsn1*Δ, $p < 0.01$; and WT vs. *dcr1Δ tsn1*Δ, $p < 0.01$.

6.3 Discussion

6.3.1 The newly constructed *dcr1*Δ *tsn1*Δ double mutants are hypersensitive to TBZ, HU and phleomycin

In Chapter 5, we showed that the mutation of *tsn1* in a *dcr1Δ* background increased TBZ sensitivity. Moreover, the sensitivity of the *dcr1Δ* mutant to the HU and phleomycin damaging agents is increased by a *tsn1*Δ mutation, but not a *tfx1*Δ mutation. Given these results, we set out to repeat these experiments with newly constructed strains containing two independently isolated *tsn1*Δ single mutants (BP3335 and BP3336), *dcr1*Δ single mutants (BP3313 and BP3343) and *dcr1*Δ *tsn1*Δ double mutants (BP3314 and BP3362; Figures 6.2, 6.3 and 6.4). Consistently, all the *dcr1Δ tsn1Δ* double mutant strains displayed increased sensitivity, relative to the *dcr1Δ* mutant strains, to TBZ, as well as the DNA damaging agents HU and phleomycin (Figures 6.5, 6.6 and 6.7). The fact that the four independent knockout *dcr1Δ tsn1Δ* strains (i.e. BP2748, BP2749, BP3314 and BP3362) behaved in a similar fashion validate this finding. However, while the *dcr1*Δ *tsn1*Δ double mutants (BP2748 and BP2749) constructed in the BP90 strain background appear to exhibit a slightly higher level of sensitivity than that for the *dcr1*Δ *tsn1*Δ double mutants (BP3314 and BP3362) constructed in the *ade6::tRNA*^{GLU} background to some of the indicated agents, this suggests that the strain background may have a minor influence on this phenomenon. Collectively, these findings further support the suggestion that the phenomenon observed in the *dcr1Δ tsn1Δ* double mutant may be due to an increase of replication–associated recombination initiating lesions, e.g., replication fork blockage.

6.3.2 The *dcr1*Δ *tsn1*Δ double mutant elevates recombination

The accumulation of RNA:DNA hybrids is a central internal cause of DNA damage; these hybrids block the progression of the replication fork, causing the fork to collapse and inducing genomic instability (Aguilera & Garcia-Muse, 2012; Bermejo et al., 2012; Lin & Pasero, 2012; Castel et al., 2014; Felipe-Abrio et al., 2015; Brambati et al., 2015; Santos-Pereira & Aguilera, 2015; Ohle et al., 2016; Aguilera & Gómez-González, 2017).

Moreover, the RNA:DNA hybrids that stabilise at the sites of collision between the replication and transcription machineries can be highly recombinogenic; if they are not removed, they may cause translocations (Lin & Pasero, 2012; Wahba et al., 2013; Castel et al., 2014; Brambati et al., 2015). As indicated, Dcr1 was recently found to remove RNA:DNA hybrids from sites of collision, such as rDNA and tRNA genes, which resolves the transcription-replication collisions and maintains genomic stability (Castel et al., 2014; Ren et al., 2015). However, in the absence of Dcr1, it was found that there is accumulation of these hybrids at these transcription sites (Castel et al., 2014), which may explain the sensitivity of the *dcr1Δ* single mutant to the DNA replication–pausing HU agent and chromosome–breaking phleomycin. Interestingly, it was found that the sensitivity of the *dcr1Δ* mutant to these agents greatly increased following the additional mutation of *tsn1*. Given the original proposed role for Translin in generating chromosomal translocations (Aoki et al., 1995), and the great affinity known for this protein in targeting RNA molecules (Jaendling & Mcfarlane, 2010; Gomez-Escobar et al., 2016), we speculated that Tsn1 may be required in the absence of Dcr1 to reduce the stability of RNA:DNA hybrids, limiting the induction of recombinogenic lesions that preserve genomic stability. If this hypothesis is correct, then the mutation of *tsn1* in the *dcr1Δ* background will result in a further increase of RNA:DNA hybrid levels, accompanied with an elevation of recombination frequency, that could result in translocations. Interestingly, a parallel biochemical analysis, DNA:RNA immunoprecipitation (DRIP), by a co-worker in our group showed that the level of RNA:DNA hybrids in the *dcr1*Δ *tsn1*Δ double mutant is higher than that of the *dcr1*Δ single mutant; this was found at certain transcribed loci, including in rDNA and natural tRNA genes (Gomez-Escobar, personal communication; data not shown). These results indicate that Tsn1 can partly substitute for Dcr1 function in reducing RNA:DNA hybrid levels.

To explore whether the increased level of RNA:DNA hybrids observed in the double mutant correlates with an increase in recombination frequency, the *tsn1Δ*, *dcr1Δ* and *dcr1Δ tsn1Δ* mutants were constructed in distinct strains that had the $tRNA^{GLU}$ inserted individually in both orientations in the genomic *ade6* locus, as described in Section 6.2.1. Using this recombination assay system, fluctuation analyses were conducted on the indicated strains alongside the WT strains. In both orientations of the $tRNA^{GLU}$ strains, the recombination frequency of the *tsn1Δ* single mutants was found to be statistically indistinguishable from the frequency of recombination events seen in the WT strain (Figures 6.8 and 6.9), which is consistent with the previous work of Jaendling et al. (2008).

However, we do observe elevated RNA:DNA hybrids in this background (Gomez-Escobar, personal communication), suggesting RNA:DNA hybrids alone do not increase recombination when Dcr1 is present. In orientation 1, where RNA Pol III – which mediates the transcription of tRNA genes – is expected to collide head-to-head with replication machinery (Pryce et al., 2009; Figure 6.1), mutation of *dcr1* showed no statistically meaningful increase in recombination frequency compared to the WT strain (Figure 6.8). In this orientation, we hypothesised that RNA Pol II could mediate the transcription of the other strand, which is in the same direction as the replication fork (i.e. a co-directional collision between RNA Pol II and the replication fork). If this is the case, this suggests that a head-to-tail collision between the replication fork and RNA Pol II (i.e. RNA:DNA hybrids) does not generate substrates for recombination. However, in the opposite orientation (orientation 2), where a head-to-head collision is predicted to occur between replication fork and RNA Pol II, the loss of Dcr1 resulted in a roughly two-fold elevation in recombination frequency compared with the WT strain (Figure 6.9). Interestingly, in orientation 2, the mutation of *tsn1* in the *dcr1*Δ background resulted in a further increase in the frequency of recombination events (Figure 6.9). In contrast, in orientation 1, we saw no measurable increase of recombination frequency in the *dcr1Δ tsn1Δ* double mutant compared with the *dcr1Δ* mutant, which had a level of recombination frequency that was statistically indistinguishable from that of the WT strain (Figure 6.8). These data showed an orientation-dependent increase of recombination occurring at *ade6::tRNA*^{GLU} in the *dcr1*Δ mutant, which is further exacerbated in the *dcr1Δ tsn1Δ* mutant (Figure 6.9).

The results are somewhat consistent with the work of Castel et al. (2014), who reported that the antisense transcription by RNA Pol II takes place at some tRNA genes. However, unfortunately, we do not know if it is actually RNA Pol II transcription (i.e. RNA:DNA hybrids) causing the barrier to DNA replication that stimulates recombination of the *dcr1Δ* mutants at this specific site, *ade6::tRNA*^{GLU}, or if RNA Pol II/III transcription even occurs at this tRNA gene. It may be that RNA Pol III binding alone causes the barrier, or even just the DNA sequence (with no RNA polymerases bound or any type of transcription). Therefore, at this stage, we cannot conclude that a transcription causes the barrier that induces recombination in the Dcr1-deficient strains, and thus, additional experiments – for example, assess RNA Pol II occupancy by CHIP at *ade6::tRNA*^{GLU} – are required to determine whether RNA Pol II binds at this locus.

Nevertheless, our results showed that the *dcr1*Δ *tsn1*Δ double mutant exhibited a greater recombination frequency than the *dcr1*Δ mutant did, indicating that the hypersensitivity of the *dcr1Δ tsn1Δ* cells to the DNA damaging agents could be due to an increase of recombination initiating lesions in the *S. pombe* genome, or a failure to process lesions correctly. However, this should be investigated further in a physical analysis of RFB activity (i.e. 2D gel electrophoresis analysis for Dcr1-deficient strains containing $tRNA^{GLU}$ elements), which would address whether the elevation of the recombination level in the *dcr1Δ tsn1Δ* double mutant, relative to the *dcr1Δ* single mutant, is concomitant with an increase in RFB intensity. Moreover, further DRIP analysis is needed at this specific locus, *ade6::*$tRNA^{GLU}$, to investigate whether the elevation of recombination frequency in the double mutant is associated with an increase of RNA:DNA hybrids.

Taken together, the observations from our experiments suggest a role for Tsn1 secondary to Dcr1 in reducing the stability of the RNA:DNA hybrids, which results in suppressing transcription–DNA replication–associated recombination in the absence of Dcr1. Thus, it maintains chromosomal stability, although it cannot fully compensate for the loss of Dcr1, since the single mutant of *dcr1Δ* displays some sensitivity to the damaging agents and exhibits an increased recombination level. Importantly, these observations may provide a credible explanation for why Translin was associated with translocations in cancer and other genetic diseases. In addition, these findings may indicate that the phenomenon observed in the *dcr1Δ tsn1Δ* double mutant occurs generally throughout the genome and is unlikely to be restricted to telomeres.

6.4 Conclusion

1. The hypersensitivity of the *dcr1*Δ *tsn1*Δ cells to DNA damaging agents is linked to increase in recombination stimulating lesions.
2. Tsn1 is required to suppress recombination in the absence of Dcr1.
3. The increased recombination observed in Dcr1-deficient strains at tDNA is an orientation-specific effect, suggesting it is linked to RNA polymerase (II or III) activity.

Chapter 7: Final Discussion

7. Final Discussion

7.1 Introduction

The human protein Translin was first found associated with the break point junctions of chromosomal translocations in lymphoid malignancies in humans (Aoki et al., 1995). Since it was first identified, it has been shown to be associated with a range of chromosomal rearrangements in different human diseases (Kanoe et al., 1999; Hosaka et al., 2000; Chalk et al., 1997; Abeysinghe et al., 2003; Wei et al., 2003; Visser et al., 2005; Gajecka et al., 2006a; Gajecka et al., 2006b; Jaendling & Mcfarlane, 2010). Translin can form an octameric ring (Kasai et al., 1997), and such structures are often linked to DNA repair and recombination (Jaendling et al., 2008; Fukuda et al., 2008; Ishida et al., 2002; Jaendling & Mcfarlane, 2010; VanLoock et al., 2001), suggesting a possible involvement of Translin in chromosome dynamics and the DNA repair processes. Subsequently, numerous studies have implicated Translin in DNA damage responses (Kasai et al., 1997; Hasegawa & Isobe, 1999; Fukuda et al., 2008; Jaendling & Mcfarlane, 2010), although direct evidence for this is limited. Translin and its partner TRAX are highly conserved sets of proteins from humans to *S. pombe*, indicating that they probably play a fundamentally important biological role in the cell (Martienssen et al., 2005; Laufman et al., 2005; Jaendling & Mcfarlane, 2010). However, the single mutations of *S. pombe, tsn1* and *tfx1,* show no obvious phenotypic alteration (Laufman et al., 2005; Jaendling et al., 2008), suggesting that they could function in redundant or secondary pathways (Jaendling & Mcfarlane, 2010). The Translin-TRAX complex has been shown to bind nucleic acids, with a preference for RNA, and it has RNase activity (Eliahoo et al., 2010; 2015; Jaendling & McFarlane, 2010; Li et al., 2011; Parizotto et al., 2013; Wang et al., 2004; Martienssen et al., 2005; Laufman et al., 2005; Jaendling & Mcfarlane, 2010). It has been demonstrated that there is a close functional relationship between the two proteins, for example, Translin is required to maintain the stability of TRAX levels (Jaendling et al., 2008; Claussen et al., 2006; Yang et al., 2004; Jaendling & Mcfarlane, 2010; Chennathukuzhi et al., 2003). Moreover, from their nucleic acid sequence binding preferences, it has been proposed that Translin and TRAX might play a role at telomeres (Jacob et al., 2004; Laufman et al., 2005; Jaendling & McFarlane, 2010), although no direct evidence has been provided to support this prior to the current study.

Studies in distinct organisms have shown that there is great diversity in the function of TRAX and Translin, including their mRNA dynamics in neurons and spermatogenesis, genome stability, DNA damage response, cell growth regulation, tRNA maturation, and most recently, in the oncogenic degradation of pre-miRNAs (Aoki et al., 1995; Wu et al., 1997; Jaendling et al., 2008; Li et al., 2012; Jaendling & McFarlane, 2010; Wang et al., 2016b; Asada et al., 2014). Importantly, in humans and *Drosophila*, Translin and TRAX have been shown to make up the C3PO complex, which enhances the cleavage of the passenger strand from siRNA involved in Argonaute (Ago1)-mediated heterochromatin formation and gene silencing (Liu et al., 2009; Ye et al., 2011; Holoch & Moazed, 2015; Tian et al., 2011). Currently, the chromosomal instability observed in Ago1-deficient cells is believed to be caused solely by centromere heterochromatin disruption leading to compromised centromere function (Volpe et al., 2003; Holoch & Moazed, 2015). However, the work reported here challenges this proposal by demonstrating that the chromosomal instability of *ago1*Δ cells can be partially suppressed by a *tfx1*Δ mutation without restoring the pericentromeric heterochromatin gene silencing. Extending the analysis of Tsn1 and Tfx1 function has identified important new insights into distinct functions for these factors in controlling the telomere and sub-telomere-associated transcript levels, a role that seems to be conserved in human cells. Further, this work has revealed differential roles for these conserved proteins in the DNA damage response in the absence of the RNAi regulator Dcr1. These observations not only provide a clear functional distinction between Tsn1 and Tfx1 in *S. pombe*, but also reveal a counter balance between centromeres and telomeres in preserving chromosomal stability. Additionally, our data provide several lines of evidence to show that the residual Tfx1 found in a *tsn1Δ* background could play a functional role. These fundamental observations are discussed in more detail below.

7.2 Tsn1-Tfx1 (C3PO) function in regulating telomere transcription

Translin and TRAX are implicated in different biological functions that seem to require the regulation of RNA molecules rather than DNA. Here, we add to their known functional roles by showing that Tsn1 and Tfx1 function in regulating telomeric RNAs. Tfx1 functions to control sub-telomeric ARRET transcript levels in a Tsn1-dependent fashion, and, in a reciprocal control mechanism, Tsn1 serves to suppress telomeric TERRA transcript levels in a Tfx1-dependent fashion. These findings reveal important and novel telomere-associated regulatory factors (Tsn1 and Tfx1), and identify a novel mechanism for telomeric transcriptome regulation (Figure 7.1). Interestingly, further analysis by a co-worker in the McFarlane group found that some human TERRAs are regulated by Tsn1/TSNAX in humans, demonstrating a degree of conservation of this function at some telomeres in humans (Gomez-Escobar et al., 2016). However, a recent work aimed at identifying the proteins that interact with telomere DNA and TERRA did not show TSN or TSNAX (Luo et al., 2015), suggesting an indirect regulation of telomere-associated transcripts by these proteins in humans. Future work could focus on investigating whether mutation of *tsn1* (*TSN*) or *tfx1* (*TSNAX*) alters the levels of methylated histone H3 lysine 9 (H3K9-me) and/or pol II occupancy in sub-telomeric regions, thus addressing how Translin and TRAX contribute to sub-telomeric gene silencing. Importantly, the current study found that the centromeric transcript levels of both *tsn1*Δ and *tfx1*Δ single mutants were indistinguishable from the WT strain, demonstrating that Tsn1 and Tfx1 function in regulating telomeric, but not centromeric, transcript levels.

The finding that Translin and TRAX are required for controlling telomere-associated transcripts indicates the importance of these conserved proteins, and yet their disruption is tolerated, in fission yeast at least, suggesting that these factors may have a redundant crucial function in essential processes. This is supported by the fact that cells lacking the RNAi regulator Ago1 and Tsn1/Tfx1 exhibit a phenotype consistent with high levels of genome instability (as measured by the TBZ sensitivity assay) and highly elevated levels of telomeric TERRA.

These findings suggest that Tsn1-Tfx1 together provide a redundant joint function to maintain genome stability in the absence of Ago1, pointing to a direct link between the C3PO complex and chromosome stability regulation. The fact that dysregulation of the TERRA transcript is the only measurable defect phenotype recorded to date for *S. pombe tsn1*Δ single mutant indicates that alteration of the levels of telomeric TERRA alone in *S. pombe* has limited or no influence on cell proliferation. However, the hyper-elevation of TERRAs observed in the *ago1*Δ *tsn1*Δ *tfx1*Δ triple mutant is correlated with increased DNA damage sensitivity. This phenomenon has also been seen for the *taz1*Δ mutant, which also has elevated TERRA levels, (Miller & Cooper, 2003; Greenwood & Cooper, 2012; Figure 4.4), suggesting that the significant elevation of TERRA levels may result in compromised DNA repair. From these analyses we propose that telomere functional fidelity may be preserved via an interplay between the C3PO (Tsn1/Tfx1) complex and Ago1. However, further analysis is required to confirm these results and determine their underlying mechanism.

To date, Translin has been shown to be necessary for maintaining the TRAX level, and several studies demonstrate that loss of Translin results in a total loss of the TRAX level (Yang et al., 2004; Jaendling et al., 2008; Park et al., 2017). However, we now challenge this long-standing belief by finding that Tfx1 is required to maintain the elevated levels of TERRA in the absence of Tsn1 (Figure 7.1), demonstrating that the very low Tfx1 levels found in the *tsn1*Δ background are sufficient to provide the function for the regulation of telomere-associated transcript level. Additionally, the fact that the *ago1*Δ *tfx1*Δ *tsn1*Δ triple mutant has a hyper TBZ sensitive phenotype relative to the *ago1*Δ *tsn1*Δ phenotype (which is indistinguishable from that of the *ago1*Δ mutant) indicates that the residual Tfx1 in the *tsn1*Δ background is sufficient to suppress TBZ hypersensitivity. So, our data demonstrate that the very low level of residual Tfx1 existing in a *tsn1*Δ mutant remains adequate to fulfil a biological role in genome stability maintenance.

Translin (TSN) and TRAX (TSNAX) have recently been found to play an oncogenic role, and have been proposed as potential chemotherapeutic targets (Asada et al., 2014, Asada et al., 2016). Therefore, an understanding of their normal functions is of fundamental importance before targeting these factors as anticancer agents. The finding that Translin and TRAX function to control the telomeres, which are vital in cancer progression, adds new insight to our understanding of these important proteins.

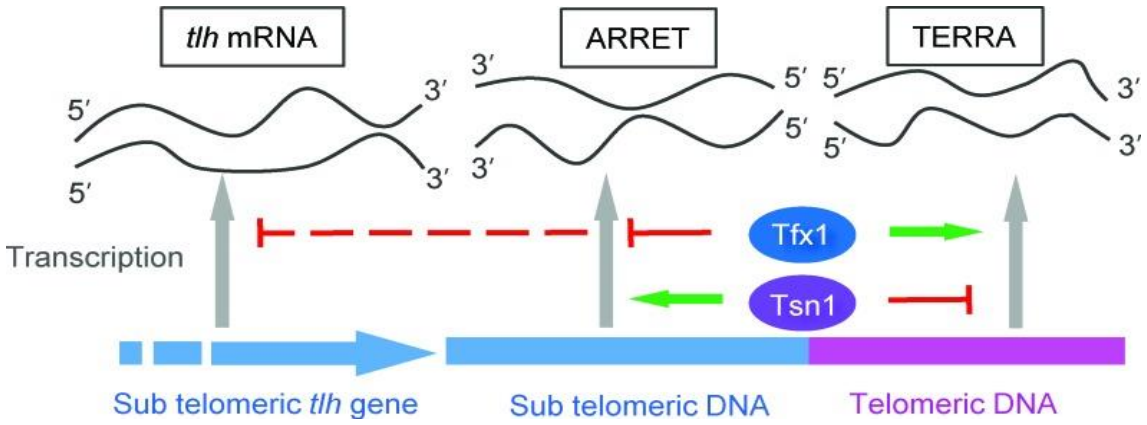

Figure 7.1 Schematic model of the reciprocal control mechanism of telomere and sub-telomere-associated transcripts by Tsn1 and Tfx1.
Tfx1 negatively controls sub-telomeric *tlh* and ARRET transcript levels (upper red full/broken lines), but positively maintains (upper green arrow) elevated levels of telomeric TERRAs observed in the *tsn1Δ* background. The inverse is true for Tsn1, it negatively suppresses TERRAs (lower red line), but positively preserves (lower green arrow) elevated levels of sub-telomeric ARRET (but not the sub-telomeric *tlh* transcript levels, suggesting a possible transcript/positional specificity to this regulation) observed in the *tfx1Δ* background (adapted from Gomez-Escobar et al., 2016).

7.3 Tfx1 function enforces a restriction on chromosome segregation

This study revealed a novel aspect of chromosome/centromere biology, which challenges the current belief that the chromosome instability of Ago1-deficient cells is imposed solely by a dysfunction of the centromeres caused by a defect in the centromeric heterochromatin (Volpe et al., 2003; Holoch & Moazed, 2015). It was found that mutation of *tfx1*, but not of *tsn1*, partially suppress the chromosome instability phenotype of the *ago1*Δ cells, a phenomenon that has also been demonstrated for *taz1*Δ mutants (Tadeo et al., 2013; Figure 3.15). It was shown that suppression caused by loss of Taz1 is due to a restoration of heterochromatin gene silencing at the centromere and a model proposed that loss of Taz1 function results in a re-distribution of heterochromatin factors from the sub-telomeres to the centromeric heterochromatin regions to compensate for the defective state caused by the loss of Ago1 (Tadeo et al., 2013; Figure 3.17). However, in the case of the *ago1*Δ *tfx1*Δ strain, we found that mutation of *tfx1* in an *ago1Δ* background resulted in no diminishment in the activation of centromeric heterochromatin transcription caused by loss of Ago1, indicating that loss of Tfx1 does not restore centromeric heterochromatin function. Therefore, the heterochromatin redistribution model is unlikely to be operating in this case, suggesting that a distinct centromere-independent suppression mechanism is in play. From this, we demonstrated that chromosomal instability due to loss of Ago1 was not solely due to disruption of the centromeric heterochromatin. Further, we found that the chromosome instability phenotype caused by the loss of the other RNAi regulator, Dcr1, was enhanced following the additional mutation of *tfx1* (and *tsn1*), which differs from the reported rescue of the Dcr1 defect by the *taz1*Δ mutation (Tadeo et al., 2013), further indicating Tsn1 and Tfx1 function in an as yet unidentified role to control genome stability. Moreover, these findings not only reveal that Tfx1 and Tsn1 are necessary for maintaining chromosome stability in the absence of Dcr1, but they also demonstrate that there is a functional distinction between Ago1 and Dcr1 in *S. pombe*, which supports the work of Castel et al. (2014) in which they separated the Dcr1 function in the DNA damage recovery response from the RNAi regulation mechanism (i.e. Ago1; see below). Remarkably, we revealed that the mutation of the four sub-telomeric *tlh* genes also caused suppression of the *ago1Δ* chromosomal instability.

This demonstrates that the compromised telomeres suppressed the chromosome instability defects of the *ago1*Δ mutant, and points to a possible relationship between the centromeres and telomeres that maintains chromosome stability. Importantly, the lack of heterochromatin gene silencing restoration at centromeres in the *ago1*Δ *tfx1*Δ cells indicates that cells can cope with a defective centromeric heterochromatin (i.e. in an *ago1*Δ mutant) when some features of the normal chromosome biology—which are facilitated by Tfx1—are disrupted. This indicates that Tfx1 imposes a segregational restriction mechanism on cells, obviously via a centromere-independent, telomere-dependent function, which we hypothesise may be related to chromosomal architecture within the nucleus.

7.4 Tsn1 is required to suppress recombination in the absence of Dcr1

The initial discovery that Translin binds to the breakpoint junctions of chromosomal translocations in human cancers led to the proposal that Translin is implicated in the initiation and regulation of recombination (Jaendling & Mcfarlane, 2010; Parizotto et al., 2013), although its direct mechanistic role in this process has not yet been demonstrated. However, previous analyses of the *S. pombe* Tsn1 and Tfx1 demonstrate that they do not play a primary role in recombination and its related processes such as DNA damage recovery (Jaendling et al., 2008). Recent work in different organisms has implicated the two pairing proteins in the control of RNA metabolism, including the RNAi pathway (Liu et al., 2009; Ye et al., 2011). However, what links Translin and TRAX to cancer-associated chromosomal translocations and how this relates to RNA metabolism has not yet been elucidated. In more recent times, the *S. pombe* RNAi regulator Dcr1 was shown to have an RNAi-independent role in the RNA regulation of breakage in which it removes RNA Pol II-mediated highly recombinogenic RNA:DNA hybrids from distinct sites of collision between transcription and replication, such as rDNA and tRNA genes, which maintains genomic stability (Castel et al., 2014; Ren et al., 2015). Following this, we revealed that the sensitivity of the *dcr1Δ* mutant to the DNA double-strand breaks and the replication inhibitor agents is greatly increased following the additional mutation of *tsn1*.

This remarkable finding implicates Tsn1 in DNA damage recovery response in the absence of Dcr1, linking Translin function to the chromosome maintenance mechanism, which is the first link of this important conserved protein to a cancer causing mechanism. Based on the original proposed role of Translin in mediating chromosomal rearrangement breakpoints (Aoki et al., 1995; Gajecka et al., 2006), and the stronger affinity of *S. pombe* Tsn1 for RNA than DNA (Jaendling & Mcfarlane, 2010), we proposed that Tsn1 may play a secondary role to Dcr1 in reducing the stability of RNA:DNA hybrids throughout the genome, which suppress transcription-DNA replication-associated recombination in the absence of Dcr1, rescuing chromosomal stability. However, further analysis of the Tsn1 function in the absence of Dcr1 revealed that the sub-telomere-associated transcripts *tlh* and ARRET are de-repressed in the *dcr1Δ tsn1Δ* double mutant. Thus, the fact that the defects in DNA damage recovery response in *dcr1Δ tsn1Δ* cells correlate with dysregulation of sub-telomeric transcription led us to think that the observed phenomenon in the double mutant might be a telomere-specific effect (i.e. a failure to repair telomeric DNA). However, this possibility was questioned by the later finding within our group that the *dcr1Δ tsn1Δ* double mutant exhibits an increase in RNA:DNA hybrids relative to the *dcr1Δ* single mutant at distinct genomic loci including in the rDNA and natural tRNA genes. Interestingly, these hybrids are also elevated in the *tsn1Δ* single mutant at these transcribed loci (Gomez-Escobar, personal communication), demonstrating that Tsn1 plays a novel role in regulating RNA:DNA hybrid levels. Future work could confirm this observation by performing whole genome RNA:DNA immunoprecipitation (DRIP)-seq analysis, which would also indicate whether the Tsn1 function in removing RNA:DNA hybrids is extended to other genomic loci. Remarkably, the elevated level of RNA:DNA hybrids found in the *dcr1Δ tsn1Δ* double mutant is accompanied with a statistically significant increase in recombination relative to the *dcr1Δ* single mutant (which exhibited a roughly two-fold increase in the level of recombination frequency compared with the WT). This was observed at a known RFB, *ade6::tRNA*^{GLU} locus. Interestingly, the elevated recombination seen in Dcr1-deficient strains at this tRNA gene was an orientation-specific effect, suggesting it is related to the activity of RNA Pol II or III. However, *tsn1Δ* single mutant showed no statistically significant increase of recombination frequency in comparison to the WT (Jaendling et al., 2008; Figures 6.8 and 6.9), suggesting that RNA:DNA hybrids alone are not sufficient to generate substrates for recombination in the presence of Dcr1.

Our findings suggested that the hypersensitivity of *dcr1Δ tsn1Δ* cells to the DNA damaging drugs is linked to the increased formation of recombination stimulating lesions in the *S. pombe* genome, or it may be due to a failure to repair lesions accurately, possibily leading to translocations. This proposes a novel mechanistic role for Tsn1 in suppressing replication-associated recombination in the absence of Dcr1. This remarkable new finding may address the outstanding question of over two decades of why Translin is linked to chromosomal translocation formation in human cancers. Consequently, no doubt, it will result in significant follow-up studies in human cells to investigate whether Translin (TSN), similarly to *S. pombe*, is involved in the initiation or regulation of recombination in Dicer-deficient cells.

7.5 Distinct functions for Tsn1 and Tfx1

To date, almost all studies that have identified a function for Translin and TRAX have indicated a close functional relationship between these conserved proteins. Here, we show that in *S. pombe* Tsn1 and Tfx1 can function independently of each other, demonstrating that these factors do not function only as a heteromeric complex. First, the elevation of sub-telomeric transcripts *tlh* and ARRET occurred only upon loss of Tfx1 not of Tsn1. In contrast, loss of Tsn1, but not Tfx1, resulted in increased transcript levels of the telomere-associated TERRA (Figure 7.1). Similarly, in the *ago1Δ* backgrounds, the *tlh* and ARRET transcript levels were only up-regulated when *tfx1* was mutated, but not *tsn1*, from which it is proposed that the dysregulation of transcription in the sub-telomeric regions may be responsible for the partial rescue of chromosome instability caused by loss of Ago1. Further, the fact that loss of Tsn1 could not supress the chromosome instability caused by loss of Ago1 to the high levels observed for *tfx1Δ,* together with the finding that Tsn1, but not Tfx1, is required in DNA damage recovery response in the absence of Dcr1 provide additional evidence that the functions of Tsn1 and Tfx1 can be separated in *S. pombe*.

7.6 Closing remarks

Over the past two decades, since the initial discovery of Translin, Translin and TRAX have been implicated in a number of distinct biological processes, including RNA interference control. In this study, we used a model experimental system (fission yeast) to report two major findings that offer new insight into the functions of these important proteins. First, Tsn1 and Tfx1 play differential roles in controlling transcript levels from the telomeres and sub-telomeres. Second, Tsn1, but not Tfx1, is required in the DNA damage recovery response in the absence of Dcr1. Evidence has been presented to propose a new fundamental role for Tsn1 in suppressing replication-associated recombination in the absence of Dcr1, which could account for its original proposed role in generating chromosomal translocations in human cancers. In addition, this study identified a novel fundamental aspect of chromosome/centromere biology. The study showed that the chromosomal instability of *ago1*Δ cells is not solely due to the disruption of centromeric heterochromatin formation and may be linked to telomere dynamics. Given the fact that Translin and TRAX functions are linked to a diverse range of important biological activities, as well as being oncogenic drug targets, these findings provide new insight into the complexity of basic biological function and drug targeting of these highly conserved factors. Further studies will now be required to further elucidate the molecular mechanisms of the novel pathways revealed here.

8. References

Abeysinghe, S.S., Chuzhanova, N., Krawczak, M., Ball, E.V. & Cooper, D.N. 2003. Translocation and gross deletion breakpoints in human inherited disease and cancer I: nucleotide composition and recombination-associated motifs. *Human Mutation.* 22 (3). pp. 229-244.

Admire, A., Shanks, L., Danzl, N., Wang, M., Weier, U., Stevens, W., Hunt, E. & Weinert, T. 2006. Cycles of chromosome instability are associated with a fragile site and are increased by defects in DNA replication and checkpoint controls in yeast. *Genes & Development.* 20 (2). pp. 159-173.

Aguilera, A. & Gaillard, H. 2014. Transcription and recombination: when RNA meets DNA. *Cold Spring Harbor Perspectives in Biology.* 6 (8). pp. 10.1101/cshperspect.a016543.

Aguilera, A. & Garcia-Muse, T. 2012. R loops: from transcription byproducts to threats to genome stability. *Molecular Cell.* 46 (2). pp. 115-124.

Aguilera, A. & García-Muse, T. 2013. Causes of genome instability. *Annual Review of Genetics.* 47 pp. 1-32.

Aguilera, A. & Gomez-Gonzalez, B. 2008. Genome instability: a mechanistic view of its causes and consequences. *Nature Reviews.Genetics.* 9 (3). pp. 204-217.

Aguilera, A. & Gómez-González, B. 2017. DNA-RNA hybrids: the risks of DNA breakage during transcription. *Nature Structural & Molecular Biology.* 24 (5). pp. 439-443.

Allshire, R.C., Javerzat, J., Redhead, N.J. & Cranston, G. 1994. Position effect variegation at fission yeast centromeres. *Cell.* 76 (1). pp. 157-169.

Almobadel, N. (2013), PhD thesis, the functional characterisation of leukaemia- associated protein TRAX, Bangor University.

Alper, B.J., Lowe, B.R. & Partridge, J.F. 2012. Centromeric heterochromatin assembly in fission yeast—balancing transcription, RNA interference and chromatin modification. *Chromosome Research.* 20 (5). pp. 521-534.

Alshehri, Z. (2013), PhD thesis, the functional characterisation of leukaemia-associated protein TRAX, Bangor University.

Amon, J.D. & Koshland, D. 2016. RNase H enables efficient repair of R-loop induced DNA damage. *eLife.* 5 pp. 10.7554/eLife.20533.

Anderson, G.R. 2001. Genomic instability in cancer. *Current Science.* pp. 501-507.

Aoki, K., Inazawa, J., Takahashi, T., Nakahara, K. & Kasai, M. 1997. Genomic structure and chromosomal localization of the gene encoding translin, a recombination hotspot binding protein. *Genomics.* 43 (2). pp. 237-241.

Aoki, K., Ishida, R. & Kasai, M. 1997. Isolation and characterization of a cDNA encoding a Translin-like protein, TRAX. *FEBS Letters.* 401 (2-3). pp. 109-112.

Aoki, K., Suzuki, K., Sugano, T., Tasaka, T., Nakahara, K., Kuge, O., Omori, A. & Kasai, M. 1995. A novel gene, Translin, encodes a recombination hotspot binding protein associated with chromosomal translocations. *Nature Genetics.* 10 (2). pp. 167-174.

Aquino, G., Marra, L., Cantile, M., De Chiara, A., Liguori, G., Curcio, M.P., Sabatino, R., Pannone, G., Pinto, A., Botti, G. & Franco, R. 2013. MYC chromosomal aberration in differential diagnosis between Burkitt and other aggressive lymphomas. *Infectious Agents and Cancer.* 8 (1). pp. 37.

Aronica, L., Kasparek, T., Ruchman, D., Marquez, Y., Cipak, L., Cipakova, I., Anrather, D., Mikolaskova, B., Radtke, M., Sarkar, S., Pai, C.C., Blaikley, E., Walker, C., Shen, K.F., Schroeder, R., Barta, A., Forsburg, S.L. & Humphrey, T.C. 2016. The spliceosome-associated protein Nrl1 suppresses homologous recombination-dependent R-loop formation in fission yeast. *Nucleic Acids Research.* 44 (4). pp. 1703-1717.

Asada, K., Canestrari, E. & Paroo, Z. 2016. A druggable target for rescuing microRNA defects. *Bioorganic &Medicinal Chemistry Letters.* 26 (20). pp. 4942-4946.

Asada, K., Canestrari, E., Fu, X., Li, Z., Makowski, E., Wu, Y.C., Mito, J.K., Kirsch, D.G., Baraban, J. & Paroo, Z. 2014. Rescuing dicer defects via inhibition of an anti-dicing nuclease. *Cell Reports.* 9 (4). pp. 1471-1481.

Audergon, P.N., Catania, S., Kagansky, A., Tong, P., Shukla, M., Pidoux, A.L. & Allshire, R.C. 2015. Epigenetics. Restricted epigenetic inheritance of H3K9 methylation. *Science.* 348 (6230). pp. 132-135.

Aves, S.J. 2009. DNA replication initiation. *Methods in Molecular Biology.* 521 pp. 3-17.

Azzalin, C.M. & Lingner, J. 2015. Telomere functions grounding on TERRA firma. *Trends in Cell biology.* 25 (1). pp. 29-36.

Azzalin, C.M., Reichenbach, P., Khoriauli, L., Giulotto, E. & Lingner, J. 2007. Telomeric repeat containing RNA and RNA surveillance factors at mammalian chromosome ends. *Science.* 318 (5851). pp. 798-801.

Bah, A., Wischnewski, H., Shchepachev, V. & Azzalin, C.M. 2012. The telomeric transcriptome of *Schizosaccharomyces pombe*. Nucleic Acids Research. 40 (7). pp. 2995-3005.

Bakhshi, A., Jensen, J.P., Goldman, P., Wright, J.J., McBride, O.W., Epstein, A.L. & Korsmeyer, S.J. 1985. Cloning the chromosomal breakpoint of t (14; 18) human lymphomas: clustering around JH on chromosome 14 and near a transcriptional unit on 18. *Cell.* 41 (3). pp. 899-906.

Ballestar, E. 2011. An introduction to epigenetics. In: *Epigenetic Contributions in Autoimmune Disease.* Springer: pp. 1-11.

Bartkova, J., Horejsí, Z., Koed, K. & Dramer, A. 2005. DNA damage response as a candidate anti-cancer barrier in early human tumorigenesis. *Nature.* 434 (7035). pp. 864.

Batte, A., Brocas, C., Bordelet, H., Hocher, A., Ruault, M., Adjiri, A., Taddei, A. & Dubrana, K. 2017. Recombination at subtelomeres is regulated by physical distance, double-strand break resection and chromatin status. *The EMBO journal,* 36(17), pp.2609-2625.

Bauer, A.J. & Martin, K.A. 2017. Coordinating regulation of gene expression in cardiovascular disease: Interactions between chromatin modifiers and transcription factors. Frontiers in cardiovascular medicine. 4 pp. 19.

Bayne, E.H., White, S.A., Kagansky, A., Bijos, D.A., Sanchez-Pulido, L., Hoe, K.L., Kim, D.U., Park, H.O., Ponting, C.P., Rappsilber, J. & Allshire, R.C. 2010. Stc1: a critical link between RNAi and chromatin modification required for heterochromatin integrity. Cell. 140 (5). pp. 666-677.

Bermejo, R., Lai, M.S. & Foiani, M. 2012. Preventing replication stress to maintain genome stability: resolving conflicts between replication and transcription. *Molecular cell.* 45 (6). pp. 710-718.

Berti, M. & Vindigni, A. 2016. Replication stress: getting back on track. *Nature structural & Molecular Biology.* 23 (2). pp. 103-109.

Biessmann, H. & Mason, J.M. 1997. Telomere maintenance without telomerase. *Chromosoma.* 106 (2). pp. 63-69.

Bisht, K.K., Arora, S., Ahmed, S. and Singh, J., 2008. Role of heterochromatin in suppressing subtelomeric recombination in fission yeast. *Yeast*, *25*(8), pp.537-548.

Boboila, C., Alt, F.W. & Schwer, B. 2012. 1 Classical and alternative end-joining pathways for repair of lymphocyte-specific and general DNA double-strand breaks. *Advances in Immunology.* 116 pp. 1.

Brambati, A., Colosio, A., Zardoni, L., Galanti, L. & Liberi, G. 2015. Replication and transcription on a collision course: eukaryotic regulation mechanisms and implications for DNA stability. *Frontiers in Genetics.* 6 pp. 166.

Branzei, D. & Foiani, M. 2007. Interplay of replication checkpoints and repair proteins at stalled replication forks. *DNA repair.* 6 (7). pp. 994-1003.

Brouwers, N., Mallol Martinez, N. & Vernos, I. 2017. Role of Kif15 and its novel mitotic partner KBP in K-fiber dynamics and chromosome alignment. PloS one. 12 (4). pp. e0174819.

Brugmans, L., Kanaar, R. & Essers, J. 2007. Analysis of DNA double-strand break repair pathways in mice. *Mutation Research/Fundamental and Molecular Mechanisms of Mutagenesis.* 614 (1). pp. 95-108.

Buhler, M. & Gasser, S.M. 2009. Silent chromatin at the middle and ends: lessons from yeasts. *EMBO Journal.* 28 (15). pp. 2149-2161.

Burgers, P.M.J. & Kunkel, T.A. 2017. Eukaryotic DNA replication fork. *Annual Review of Biochemistry.* 86 pp. 417-438.

Carmichael, J.B., Provost, P., Ekwall, K. & Hobman, T.C. 2004. ago1 and dcr1, two core components of the RNA interference pathway, functionally diverge from rdp1 in regulating cell cycle events in *Schizosaccharomyces pombe*. *Molecular biology of the cell.* 15 (3). pp. 1425-1435.

Castel, S.E. & Martienssen, R.A. 2013. RNA interference in the nucleus: roles for small RNAs in transcription, epigenetics and beyond. *Nature Reviews Genetics.* 14 (2). pp. 100-112.

Castel, S.E., Ren, J., Bhattacharjee, S., Chang, A.Y., Sanchez, M., Valbuena, A., Antequera, F. & Martienssen, R.A. 2014. Dicer promotes transcription termination at sites of replication stress to maintain genome stability. *Cell.* 159 (3). pp. 572-583.

Chalk, J.G., Barr, F.G. & Mitchell, C.D. 1997. Translin recognition site sequences flank chromosome translocation breakpoints in alveolar rhabdomyosarcoma cell lines. *Oncogene*. 15 (10). pp. 1199-1205.

Chan, F.L. & Wong, L.H. 2012. Transcription in the maintenance of centromere chromatin identity. *Nucleic Acids Research.* 40 (22). pp. 11178-11188.

Chang, E.Y. & Stirling, P.C. 2017. Replication fork protection factors controlling R-loop bypass and suppression. *Genes.* 8 (1). pp. 10.3390/genes8010033.

Chang, H.H.Y., Pannunzio, N.R., Adachi, N. & Lieber, M.R. 2017. Non-homologous DNA end joining and alternative pathways to double-strand break repair. *Nature reviews.Molecular Cell Biology,* 18(8), p.495.

Chang, Y., Wang, P., Li, W.H., Chen, L., Chang, C., Sung, P., Yang, M., Cheng, L., Lai, Y. & Cheng, Y. 2013. Balanced and unbalanced reciprocal translocation: an overview of a 30-year experience in a single tertiary medical center in Taiwan. *Journal of the Chinese Medical Association.* 76 (3). pp. 153-157.

Chatterjee, S. 2017. Telomeres in health and disease. *Journal of Oral and Maxillofacial Pathology :* (1). pp. 87-91.

Chennathukuzhi, V., Stein, J.M., Abel, T., Donlon, S., Yang, S., Miller, J.P., Allman, D.M., Simmons, R.A. & Hecht, N.B. 2003. Mice deficient for testis-brain RNA-binding protein exhibit a coordinate loss of TRAX, reduced fertility, altered gene expression in the brain, and behavioral changes. *Molecular and Cellular Biology.* 23 (18). pp. 6419-6434.

Chennathukuzhi, V.M., Kurihara, Y., Bray, J.D. & Hecht, N.B. 2001. Trax (translin-associated factor X), a primarily cytoplasmic protein, inhibits the binding of TB-RBP (translin) to RNA. *Journal of Biological Chemistry.* 276 (16). pp. 13256-13263.

Chiaruttini, C., Vicario, A., Li, Z., Baj, G., Braiuca, P., Wu, Y., Lee, F.S., Gardossi, L., Baraban, J.M. & Tongiorgi, E. 2009. Dendritic trafficking of BDNF mRNA is mediated by translin and blocked by the G196A (Val66Met) mutation. *Proceedings of the National Academy of Sciences of the United States of America.* 106 (38). pp. 16481-16486.

Chikashige, Y., Yamane, M., Okamasa, K., Tsutsumi, C., Kojidani, T., Sato, M., Haraguchi, T. & Hiraoka, Y. 2009. Membrane proteins Bqt3 and -4 anchor telomeres to the nuclear envelope to ensure chromosomal bouquet formation. *Journal of Cell Biology.* 187 (3). pp. 413-427.

Chilkova, O., Stenlund, P., Isoz, I., Stith, C.M., Grabowski, P., Lundstrom, E.B., Burgers, P.M. & Johansson, E. 2007. The eukaryotic leading and lagging strand DNA polymerases are loaded onto primer-ends via separate mechanisms but have comparable processivity in the presence of PCNA. Nucleic Acids Research. 35 (19). pp. 6588-6597.

Choi, J.D. & Lee, J. 2013. Interplay between Epigenetics and Genetics in Cancer. *Genomics & informatics.* 11 (4). pp. 164-173.

Clark, D.P. & Pazdernik, N.J. 2012. *Molecular Biology.* Elsevier: .

Claussen, M., Koch, R., Jin, Z.Y. & Suter, B. 2006. Functional characterization of *Drosophila* Translin and Trax. *Genetics.* 174 (3). pp. 1337-1347.

Cooper, J.P., Nimmo, E.R., Allshire, R.C. and Cech, T.R., 1997. Regulation of telomere length and function by a Myb-domain protein in fission yeast. *Nature*, *385*(6618), p.744-747.

Creamer, K.M. & Partridge, J.F. 2011. RITS-connecting transcription, RNA interference, and heterochromatin assembly in fission yeast. *RNA.* 2 (5). pp. 632-646.

Cusanelli, E. & Chartrand, P. 2015. Telomeric repeat-containing RNA TERRA: a noncoding RNA connecting telomere biology to genome integrity. *Frontiers in Genetics.* 6 pp. 143.

Daley, J.M., Palmbos, P.L., Wu, D. & Wilson, T.E. 2005. Nonhomologous end joining in yeast. *Annu.Rev.Genet.* 39 pp. 431-451.

Davis, A.J. & Chen, D.J. 2013. DNA double strand break repair via non-homologous end-joining. *Translational Cancer Research.* 2 (3). pp. 130-143.

Duch, A., de Nadal, E. & Posas, F. 2013. Dealing with transcriptional outbursts during S phase to protect genomic integrity. *Journal of Molecular Biology.* 425 (23). pp. 4745-4755.

Dudin, O., Merlini, L., Bendezú, F.O., Groux, R., Vincenzetti, V. and Martin, S.G., 2017. A systematic screen for morphological abnormalities during fission yeast sexual reproduction identifies a mechanism of actin aster formation for cell fusion. *PLoS Genetics*, *13*(4), p.e1006721.

Duzdevich, D., Warner, M.D., Ticau, S., Ivica, N.A., Bell, S.P. & Greene, E.C. 2015. The dynamics of eukaryotic replication initiation: origin specificity, licensing, and firing at the single-molecule level. *Molecular Cell.* 58 (3). pp. 483-494.

Egan, E.D., Braun, C.R., Gygi, S.P. and Moazed, D., 2014. Post-transcriptional regulation of meiotic genes by a nuclear RNA silencing complex. *RNA*, *20*(6), pp.867-881.

Ekwall, K., Cranston, G. & Allshire, R.C. 1999. Fission yeast mutants that alleviate transcriptional silencing in centromeric flanking repeats and disrupt chromosome segregation. *Genetics.* 153 (3). pp. 1153-1169.

Eliahoo, E., Litovco, P., Ben Yosef, R., Bendalak, K., Ziv, T. & Manor, H. 2014. Identification of proteins that form specific complexes with the highly conserved protein Translin in< i> Schizosaccharomyces pombe. *Biochimica et Biophysica Acta (BBA)-Proteins and Proteomics.* 1844 (4). pp. 767-777.

Erdemir, T., Bilican, B., Cagatay, T., Goding, C.R. & Yavuzer, U. 2002a. Saccharomyces cerevisiae C1D is implicated in both non-homologous DNA end joining and homologous recombination. *Molecular Microbiology.* 46 (4). pp. 947-957.

Erdemir, T., Bilican, B., Oncel, D., Goding, C.R. & Yavuzer, U. 2002b. DNA damage-dependent interaction of the nuclear matrix protein C1D with Translin-associated factor X (TRAX). *Journal of Cell Science.* 115 (Pt 1). pp. 207-216.

Espejel, S., Franco, S., Rodriguez-Perales, S., Bouffler, S.D., Cigudosa, J.C. & Blasco, M.A. 2002. Mammalian Ku86 mediates chromosomal fusions and apoptosis caused by critically short telomeres. *EMBO Journal.* 21 (9). pp. 2207-2219.

Essani, K., Glieder, A. & Geier, M. 2015. Combinatorial pathway assembly in yeast.

Evrin, C., Clarke, P., Zech, J., Lurz, R., Sun, J., Uhle, S., Li, H., Stillman, B. & Speck, C. 2009. A double-hexameric MCM2-7 complex is loaded onto origin DNA during licensing of eukaryotic DNA replication. *Proceedings of the National Academy of Sciences of the United States of America.* 106 (48). pp. 20240-20245.

Faggioli, F., Vijg, J. & Montagna, C. 2011. Chromosomal aneuploidy in the aging brain. *Mechanisms of Ageing and Development.* 132 (8-9). pp. 429-436.

Felipe-Abrio, I., Lafuente-Barquero, J., Garcia-Rubio, M.L. & Aguilera, A. 2015. RNA polymerase II contributes to preventing transcription-mediated replication fork stalls. *The EMBO Journal.* 34 (2). pp. 236-250.

Fennell, A., Fernández-Álvarez, A., Tomita, K. and Cooper, J.P., 2015. Telomeres and centromeres have interchangeable roles in promoting meiotic spindle formation. *J Cell Biol*, *208*(4), pp.415-428.

Feretzaki, M. & Lingner, J. 2017. A practical qPCR approach to detect TERRA, the elusive telomeric repeat-containing RNA. *Methods.* 114 pp. 39-45.

Ferguson, D.O. & Alt, F.W. 2001. DNA double strand break repair and chromosomal translocation: lessons from animal models. *Oncogene.* 20 (40). pp. 5572-5579.

Ferguson, L.R., Chen, H., Collins, A.R., Connell, M., Damia, G., Dasgupta, S., Malhotra, M., Meeker, A.K., Amedei, A., Amin, A., Ashraf, S.S., Aquilano, K., Azmi, A.S., Bhakta, D.,

Bilsland, A., Boosani, C.S., Chen, S., Ciriolo, M.R., Fujii, H., Guha, G., Halicka, D., Helferich, W.G., Keith, W.N., Mohammed, S.I., Niccolai, E., Yang, X., Honoki, K., Parslow, V.R., Prakash, S., Rezazadeh, S., Shackelford, R.E., Sidransky, D., Tran, P.T., Yang, E.S. & Maxwell, C.A. 2015. Genomic instability in human cancer: Molecular insights and opportunities for therapeutic attack and prevention through diet and nutrition. *Seminars in Cancer Biology.* 35 Suppl pp. S5-24.

Fiorenza, A. & Barco, A. 2016. Role of Dicer and the miRNA system in neuronal plasticity and brain function. *Neurobiology of Learning and Memory.* 135 pp. 3-12.

Foulkes, W.D., Priest, J.R. & Duchaine, T.F. 2014. DICER1: mutations, microRNAs and mechanisms. *Nature Reviews.Cancer.* 14 (10). pp. 662-672.

Fragkos, M. & Naim, V. 2017. Rescue from replication stress during mitosis. *Cell Cycle.* 16 (7). pp. 613-633.

Fu, X., Shah, A. & Baraban, J.M. 2016. Rapid reversal of translational silencing: Emerging role of microRNA degradation pathways in neuronal plasticity. *Neurobiology of Learning and Memory.* 133 pp. 225-232.

Fukuda, Y., Ishida, R., Aoki, K., Nakahara, K., Takashi, T., Mochida, K., Suzuki, O., Matsuda, J. & Kasai, M. 2008. Contribution of Translin to hematopoietic regeneration after sublethal ionizing irradiation. *Biological & Pharmaceutical Bulletin.* 31 (2). pp. 207-211.

Gadaleta, M.C. & Noguchi, E. 2017. Regulation of DNA replication through natural impediments in the eukaryotic genome. *Genes.* 8 (3). pp. 10.3390/genes8030098.

Gaillard, H. & Aguilera, A. 2016. Transcription as a threat to genome integrity. *Annual Review of Biochemistry.* 85 pp. 291-317.

Gajecka, M., Glotzbach, C.D. & Shaffer, L.G. 2006a. Characterization of a complex rearrangement with interstitial deletions and inversion on human chromosome 1. *Chromosome Research.* 14 (3). pp. 277-282.

Gajecka, M., Pavlicek, A., Glotzbach, C.D., Ballif, B.C., Jarmuz, M., Jurka, J. & Shaffer, L.G. 2006b. Identification of sequence motifs at the breakpoint junctions in three t (1; 9)(p36. 3; q34) and delineation of mechanisms involved in generating balanced translocations. *Human Genetics.* 120 (4). pp. 519-526.

Gan, Q., Yoshida, T., McDonald, O.G. & Owens, G.K. 2007. Concise review: epigenetic mechanisms contribute to pluripotency and cell lineage determination of embryonic stem cells. *Stem Cells.* 25 (1). pp. 2-9.

Garcia-Muse, T. & Aguilera, A. 2016. Transcription-replication conflicts: how they occur and how they are resolved. *Nature Reviews.Molecular Cell Biology.* 17 (9). pp. 553-563.

Gates, R.A. & Fink, R.M. 2008. *Oncology nursing secrets.* Elsevier Health Sciences.

Gelot, C., Magdalou, I. & Lopez, B.S. 2015. Replication stress in mammalian cells and its consequences for mitosis. *Genes.* 6 (2). pp. 267-298.

Gomez-Escobar, N., Almobadel, N., Alzahrani, O., Feichtinger, J., Planells-Palop, V., Alshehri, Z., Thallinger, G.G., Wakeman, J.A. and McFarlane, R.J., 2016. Translin and Trax differentially regulate telomere-associated transcript homeostasis. *Oncotarget*, *7*(23), p.33809.

Gordon, D.J., Resio, B. & Pellman, D. 2012. Causes and consequences of aneuploidy in cancer. *Nature Reviews. Genetics.* 13 (3). pp. 189.

Goto, D.B. & Nakayama, J. 2012. RNA and epigenetic silencing: Insight from fission yeast. *Development, Growth & Differentiation.* 54 (1). pp. 129-141.

Grabarz, A., Barascu, A., Guirouilh-Barbat, J. & Lopez, B.S. 2012. Initiation of DNA double strand break repair: signaling and single-stranded resection dictate the choice between homologous recombination, non-homologous end-joining and alternative end-joining. *American Journal of Cancer Research.* 2 (3). pp. 249-268.

Greenwood, J. & Cooper, J.P. 2012a. Non-coding telomeric and subtelomeric transcripts are differentially regulated by telomeric and heterochromatin assembly factors in fission yeast. *Nucleic Acids Research.* 40 (7). pp. 2956-2963.

Gupta, G.D. & Kumar, V. 2012. Identification of nucleic acid binding sites on translin-associated factor X (TRAX) protein. *PloS One.* 7 (3). pp. e33035.

Gupta, G.D., Makde, R.D., Rao, B.J. & Kumar, V. 2008. Crystal structures of Drosophila mutant translin and characterization of translin variants reveal the structural plasticity of translin proteins. *FEBS Journal.* 275 (16). pp. 4235-4249.

Gurtner, A., Falcone, E., Garibaldi, F. & Piaggio, G. 2016. Dysregulation of microRNA biogenesis in cancer: the impact of mutant p53 on Drosha complex activity. *Journal of Experimental & Clinical Cancer Research.* 35 (1). pp. 45.

Hammond, C.M., Stromme, C.B., Huang, H., Patel, D.J. & Groth, A. 2017. Histone chaperone networks shaping chromatin function. *Nature Reviews. Molecular Cell Biology.* 18 (3). pp. 141-158.

Han, J., Gu, W. & Hecht, N.B. 1995. Testis-brain RNA-binding protein, a testicular translational regulatory RNA-binding protein, is present in the brain and binds to the 3′ untranslated regions of transported brain mRNAs. *Biology of Reproduction.* 53 (3). pp. 707-717.

Han, J.R., Yiu, G.K. & Hecht, N.B. 1995. Testis/brain RNA-binding protein attaches translationally repressed and transported mRNAs to microtubules. *Proceedings of the National Academy of Sciences of the United States of America.* 92 (21). pp. 9550-9554.

Hansen, K.R., Ibarra, P.T. & Thon, G. 2006. Evolutionary-conserved telomere-linked helicase genes of fission yeast are repressed by silencing factors, RNAi components and the telomere-binding protein Taz1. *Nucleic Acids Research.* 34 (1). pp. 78-88.

Harewood, L. & Fraser, P. 2014. The impact of chromosomal rearrangements on regulation of gene expression. *Human Molecular Genetics.* 23 (R1). pp. R76-82.

Harland, J.L., Chang, Y.T., Moser, B.A. & Nakamura, T.M. 2014. Tpz1-Ccq1 and Tpz1-Poz1 interactions within fission yeast shelterin modulate Ccq1 Thr93 phosphorylation and telomerase recruitment. *PLoS Genetics.* 10 (10). pp. e1004708.

Harrison, C.J. & Foroni, L. 2002. Cytogenetics and molecular genetics of acute lymphoblastic leukemia. *Reviews in Clinical and Experimental Hematology.* 6 (2). pp. 91-113.

Hasegawa, T. & Isobe, K. 1999. Evidence for the interaction between Translin and GADD34 in mammalian cells. *Biochimica et Biophysica Acta (BBA)-General Subjects.* 1428 (2). pp. 161-168.

Hasegawa, T., Xiao, H., Hamajima, F. & Isobe, K. 2000. Interaction between DNA-damage protein GADD34 and a new member of the Hsp40 family of heat shock proteins that is induced by a DNA-damaging reagent. *Biochemical Journal.* 352 Pt 3 pp. 795-800.

Hastings, P.J., Lupski, J.R., Rosenberg, S.M. & Ira, G. 2009. Mechanisms of change in gene copy number. *Nature Reviews.Genetics.* 10 (8). pp. 551-564.

Hasty, P. & Montagna, C. 2014. Chromosomal Rearrangements in Cancer: Detection and potential causal mechanisms. *Molecular & cellular oncology.* 1 (1). pp. e29904.

Hata, A. & Kashima, R. 2016. Dysregulation of microRNA biogenesis machinery in cancer. *Critical Reviews in Biochemistry and Molecular Biology.* 51 (3). pp. 121-134.

Hegarty, S.V., Sullivan, A.M. & O'Keeffe, G.W. 2016. The Epigenome as a therapeutic target for Parkinson's disease. *Neural regeneration research.* 11 (11). pp. 1735-1738.

Heyer, W., Ehmsen, K.T. & Liu, J. 2010. Regulation of homologous recombination in eukaryotes. *Annual Review of Genetics.* 44 pp. 113-139.

Hiriart, E., Vavasseur, A., Touat-Todeschini, L., Yamashita, A., Gilquin, B., Lambert, E., Perot, J., Shichino, Y., Nazaret, N., Boyault, C., Lachuer, J., Perazza, D., Yamamoto, M. & Verdel, A. 2012. Mmi1 RNA surveillance machinery directs RNAi complex RITS to specific meiotic genes in fission yeast. *EMBO Journal.* 31 (10). pp. 2296-2308.

Hockemeyer, D. & Collins, K. 2015. Control of telomerase action at human telomeres. *Nature Structural & Molecular Biology.* 22 (11). pp. 848-852.

Hogenbirk, M.A., Heideman, M.R., de Rink, I., Velds, A., Kerkhoven, R.M., Wessels, L.F. & Jacobs, H. 2016. Defining chromosomal translocation risks in cancer. *Proceedings of the National Academy of Sciences of the United States of America.* 113 (26). pp. E3649-56.

Holoch, D. & Moazed, D. 2015. RNA-mediated epigenetic regulation of gene expression. *Nature Reviews Genetics.* 16 (2). pp. 71-84.

Hosaka, T., Kanoe, H., Nakayama, T., Murakami, H., Yamamoto, H., Nakamata, T., Tsuboyama, T., Oka, M., Kasai, M. & Sasaki, M.S. 2000. Translin binds to the sequences adjacent to the breakpoints of the TLS and CHOP genes in liposarcomas with translocation t (12; 16). *Oncogene.* 19 (50). pp. 5821.

Hsu, M. & Lue, N.F. 2017. Analysis of Yeast Telomerase by Primer Extension Assays. *Methods in molecular biology (Clifton, N.J.).* 1587 pp. 83-93..

Hu, W., Jiang, Z.D., Suo, F., Zheng, J.X., He, W.Z. and Du, L.L., 2017. A large gene family in fission yeast encodes spore killers that subvert Mendel's law. *eLife*, *6*.

Ishida, R., Okado, H., Sato, H., Shionoiri, C., Aoki, K. & Kasai, M. 2002. A role for the octameric ring protein, Translin, in mitotic cell division. *FEBS letters.* 525 (1-3). pp. 105-110.

Jacob, E., Pucshansky, L., Zeruya, E., Baran, N. & Manor, H. 2004. The human protein translin specifically binds single-stranded microsatellite repeats, d (GT) n, and G-strand telomeric repeats, d (TTAGGG) n: a study of the binding parameters. *Journal of Molecular Biology.* 344 (4). pp. 939-950.

Jaendling, A. & Mcfarlane, R. 2010. Biological roles of translin and translin-associated factor-X: RNA metabolism comes to the fore. *Biochem.J.* 429 pp. 225-234.

Jaendling, A., Ramayah, S., Pryce, D.W. & McFarlane, R.J. 2008. Functional characterisation of the Schizosaccharomyces pombe homologue of the leukaemia-associated translocation breakpoint binding protein translin and its binding partner, TRAX. *Biochimica et biophysica acta.* 1783 (2). pp. 203-213.

Jain, D. & Cooper, J.P. 2010. Telomeric strategies: means to an end. *Annual Review of Genetics.* 44 pp. 243-269.

Jain, D., Hebden, A.K., Nakamura, T.M., Miller, K.M. and Cooper, J.P., 2010. HAATI survivors replace canonical telomeres with blocks of generic heterochromatin. *Nature*, *467*(7312), p.223.

Jones, R.M. & Petermann, E. 2012. Replication fork dynamics and the DNA damage response. *The Biochemical journal.* 443 (1). pp. 13-26.

Kalantari, R., Chiang, C.M. & Corey, D.R. 2016. Regulation of mammalian transcription and splicing by Nuclear RNAi. *Nucleic acids research.* 44 (2). pp. 524-537.

Kang, S., Kang, M.S., Ryu, E. & Myung, K. 2017. Eukaryotic DNA replication: Orchestrated action of multi-subunit protein complexes. *Mutation research.*

Kanoe, H., Nakayama, T., Hosaka, T., Murakami, H., Yamamoto, H., Nakashima, Y., Tsuboyama, T., Nakamura, T., Ron, D., Sasaki, M.S. & Toguchida, J. 1999. Characteristics of genomic breakpoints in TLS-CHOP translocations in liposarcomas suggest the involvement of Translin and topoisomerase II in the process of translocation. *Oncogene.* 18 (3). pp. 721-729.

Kanoh, J., Sadaie, M., Urano, T. & Ishikawa, F. 2005. Telomere binding protein Taz1 establishes Swi6 heterochromatin independently of RNAi at telomeres. *Current biology :* 15 (20). pp. 1808-1819.

Kasai, M., Aoki, K., Matsuo, Y., Minowada, J., Maziarz, R.T. & Strominger, J.L. 1994. Recombination hotspot associated factors specifically recognize novel target sequences at the

site of interchromosomal rearrangements in T-ALL patients with t (8; 14)(q24; q11) and t (1; 14)(p32; q11). *International Immunology.* 6 (7). pp. 1017-1025.

Kasai, M., Matsuzaki, T., Katayanagi, K., Omori, A., Maziarz, R.T., Strominger, J.L., Aoki, K. & Suzuki, K. 1997. The translin ring specifically recognizes DNA ends at recombination hot spots in the human genome. *Journal of BiologicalChemistry.* 272 (17). pp. 11402-11407.

Kasparek, T.R. & Humphrey, T.C. 2011. DNA double-strand break repair pathways, chromosomal rearrangements and cancer. *Seminars in Cell & Developmental Biology.* 22 (8). pp. 886-897.

Katto, J. & Mahlknecht, U. 2011. Epigenetic regulation of cellular adhesion in cancer. *Carcinogenesis.* 32 (10). pp. 1414-1418.

Kawamata, T. & Tomari, Y. 2010. Making RISC. *Trends in Biochemical Sciences.* 35 (7). pp. 368-376.

Khalil, H., Tummala, H. & Zhelev, N. 2012. ATM in focus: A damage sensor and cancer target. *Biodiscovery.* 5.

Koyama, M., Nagakura, W., Tanaka, H., Kujirai, T., Chikashige, Y., Haraguchi, T., Hiraoka, Y. & Kurumizaka, H. 2017. In vitro reconstitution and biochemical analyses of the *Schizosaccharomyces pombe* nucleosome. *Biochemical and Biophysical Research communications.* 482 (4). pp. 896-901.

Krejci, L., Altmannova, V., Spirek, M. & Zhao, X. 2012. Homologous recombination and its regulation. *Nucleic Acids Research.* 40 (13). pp. 5795-5818.

Kumar, M.S., Pester, R.E., Chen, C.Y., Lane, K., Chin, C., Lu, J., Kirsch, D.G., Golub, T.R. & Jacks, T. 2009. Dicer1 functions as a haploinsufficient tumor suppressor. *Genes & Development.* 23 (23). pp. 2700-2704.

Kupiec, M. 2014. Biology of telomeres: lessons from budding yeast. *FEMS Microbiology Reviews.* 38 (2). pp. 144-171.

Kusevic, D., Kudithipudi, S., Iglesias, N., Moazed, D. & Jeltsch, A. 2017. Clr4 specificity and catalytic activity beyond H3K9 methylation. *Biochimie.* 135 pp. 83-88.

Labbé, C., Lorenzo-Betancor, O. & Ross, O.A. 2016. Epigenetic regulation in Parkinson's disease. *Acta Neuropathologica.* 132 (4). pp. 515-530.

Labib, K. & Hodgson, B. 2007. Replication fork barriers: pausing for a break or stalling for time? *EMBO Reports.* 8 (4). pp. 346-353.

Laufman, O., Ben Yosef, R., Adir, N. & Manor, H. 2005. Cloning and characterization of the Schizosaccharomyces pombe homologs of the human protein Translin and the Translin-associated protein TRAX. *Nucleic Acids Research.* 33 (13). pp. 4128-4139.

Lee, S.Y., Rozenzhak, S. & Russell, P. 2013. gammaH2A-binding protein Brc1 affects centromere function in fission yeast. *Molecular and Cellular Biology.* 33 (7). pp. 1410-1416.

Lejeune, E., Bayne, E.H. & Allshire, R.C. 2010. On the connection between RNAi and heterochromatin at centromeres. *Cold Spring Harbor symposia on quantitative Biology.* 75 pp. 275-283.

Lei, M. 2005. The MCM complex: its role in DNA replication and implications for cancer therapy. Current Cancer Drug Targets. 5 (5). pp. 365-380.

Leman, A.R. & Noguchi, E. 2013. The replication fork: understanding the eukaryotic replication machinery and the challenges to genome duplication. *Genes.* 4 (1). pp. 1-32.

Lengauer, C., Kinzler, K.W. & Vogelstein, B. 1998. Genetic instabilities in human cancers. *Nature.* 396 (6712). pp. 643.

Li, J. & Xu, X. 2016. DNA double-strand break repair: a tale of pathway choices. *Acta Biochimica Et Biophysica Sinica.* 48 (7). pp. 641-646.

Li, L., Gu, W., Liang, C., Liu, Q., Mello, C.C. & Liu, Y. 2012. The translin–TRAX complex (C3PO) is a ribonuclease in tRNA processing. *Nature Structural & Molecular Biology.* 19 (8). pp. 824-830.

Li, Q. & Zhang, Z. 2012. Linking DNA replication to heterochromatin silencing and epigenetic inheritance. *Acta Biochimica Et Biophysica Sinica.* 44 (1). pp. 3-13.

Li, T., Mary, H., Grosjean, M., Fouchard, J., Cabello, S., Reyes, C., Tournier, S. & Gachet, Y. 2017. MAARS: A novel high content acquisition software for the analysis of mitotic defects in fission yeast. *Molecular Biology Of the Cell.*

Li, X. & Heyer, W. 2008. Homologous recombination in DNA repair and DNA damage tolerance. *Cell Research.* 18 (1). pp. 99-113.

Li, Z., Wu, Y. & Baraban, J.M. 2008. The Translin/Trax RNA binding complex: clues to function in the nervous system. *Biochimica Et Biophysica Acta.* 1779 (8). pp. 479-485.

Lieber, M.R. 2010. The mechanism of double-strand DNA break repair by the nonhomologous DNA end-joining pathway. *Annual Review of Biochemistry.* 79 pp. 181-211.

Lieber, M.R., Yu, K. & Raghavan, S.C. 2006. Roles of nonhomologous DNA end joining, V(D)J recombination, and class switch recombination in chromosomal translocations. *DNA Repair.* 5 (9-10). pp. 1234-1245.

Lin, Y.L. & Pasero, P. 2012. Interference between DNA replication and transcription as a cause of genomic instability. *Current Genomics.* 13 (1). pp. 65-73.

Liu, Y., Ye, X., Jiang, F., Liang, C., Chen, D., Peng, J., Kinch, L.N., Grishin, N.V. & Liu, Q. 2009. C3PO, an endoribonuclease that promotes RNAi by facilitating RISC activation. *Science.* 325 (5941). pp. 750-753.

Llorente, B., Smith, C.E. & Symington, L.S. 2008. Break-induced replication: what is it and what is it for? *Cell cycle.* 7 (7). pp. 859-864.

Lluis, M., Hoe, W., Schleit, J. & Robertus, J. 2010. Analysis of nucleic acid binding by a recombinant translin–trax complex. *Biochemical and Biophysical Research Communications.* 396 (3). pp. 709-713.

Lombard, D.B., Chua, K.F., Mostoslavsky, R., Franco, S., Gostissa, M. & Alt, F.W. 2005. DNA repair, genome stability, and aging. *Cell.* 120 (4). pp. 497-512.

Lord, C.J. & Ashworth, A. 2012. The DNA damage response and cancer therapy. *Nature.* 481 (7381). pp. 287.

Lord, C.J. & Ashworth, A. 2016. BRCAness revisited. *Nature Reviews.Cancer.* 16 (2). pp. 110-120.

Lorenzi, L.E., Bah, A., Wischnewski, H., Shchepachev, V., Soneson, C., Santagostino, M. & Azzalin, C.M. 2015. Fission yeast Cactin restricts telomere transcription and elongation by controlling Rap1 levels. *EMBO Journal.* 34 (1). pp. 115-129.

Loya, T.J. and Reines, D., 2016. Recent advances in understanding transcription termination by RNA polymerase II. F1000Research, 5.

Luger, K., Dechassa, M.L. & Tremethick, D.J. 2012. New insights into nucleosome and chromatin structure: an ordered state or a disordered affair? *Nature reviews Molecular Cell Biology.* 13 (7). pp. 436-447.

Lujan, S.A., Williams, J.S. & Kunkel, T.A. 2016. DNA Polymerases Divide the Labor of Genome Replication. *Trends in Cell Biology.* 26 (9). pp. 640-654.

Luo, Z., Dai, Z., Xie, X., Feng, X., Liu, D., Songyang, Z. & Xiong, Y. 2015. TeloPIN: a database of telomeric proteins interaction network in mammalian cells. *Database : Journal of Biological Databases and Curation.* 2015 pp. 10.1093/database/bav018. Print 2015.

Maeshima, K., Imai, R., Tamura, S. & Nozaki, T. 2014. Chromatin as dynamic 10-nm fibers. *Chromosoma.* 123 (3). pp. 225-237.

Maestroni, L., Matmati, S. & Coulon, S. 2017. Solving the Telomere Replication Problem. *Genes.* 8 (2). pp. 10.3390/genes8020055.

Maicher, A., Lockhart, A. & Luke, B. 2014. Breaking new ground: digging into TERRA function. *Biochimica Et Biophysica Acta.* 1839 (5). pp. 387-394.

Malkova, A. & Ira, G. 2013. Break-induced replication: functions and molecular mechanism. *Current opinion in genetics & development.* 23 (3). pp. 271-279. Malone, C.D. & Hannon, G.J. 2009. Small RNAs as guardians of the genome. *Cell.* 136 (4). pp. 656-668.

Mandell, J.G., Goodrich, K.J., Bahler, J. & Cech, T.R. 2005. Expression of a RecQ helicase homolog affects progression through crisis in fission yeast lacking telomerase. *Journal of Biological Chemistry.* 280 (7). pp. 5249-5257.

Manning, B.J. & Yusufzai, T. 2017. The ATP-dependent chromatin remodeling enzymes CHD6, CHD7, and CHD8 exhibit distinct nucleosome binding and remodeling Activities. *Journal of Biological Chemistry.*

Manolis, K.G., Nimmo, E.R., Hartsuiker, E., Carr, A.M., Jeggo, P.A. & Allshire, R.C. 2001. Novel functional requirements for non-homologous DNA end joining in *Schizosaccharomyces pombe*. *EMBO Journal.* 20 (1-2). pp. 210-221.

Martienssen, R.A., Zaratiegui, M. & Goto, D.B. 2005. RNA interference and heterochromatin in the fission yeast *Schizosaccharomyces pombe*. *TRENDS in Genetics.* 21 (8). pp. 450-456.

McEachern, M.J. & Haber, J.E. 2006. Break-induced replication and recombinational telomere elongation in yeast. *Annual Review of Biochemistry.* 75 pp. 111-135.

McFarlane, R.J., Al-Zeer, K. & Dalgaard, J.Z. 2011. Eukaryote DNA replication and recombination: an intimate association. In: *DNA Replication-Current Advances.* InTech: .

McGranahan, N., Burrell, R.A., Endesfelder, D., Novelli, M.R. & Swanton, C. 2012. Cancer chromosomal instability: therapeutic and diagnostic challenges. *EMBO Reports.* 13 (6). pp. 528-538.

Meaburn, K.J., Misteli, T. & Soutoglou, E. 2007. Spatial genome organization in the formation of chromosomal translocations. *Seminars in Cancer Biology.* Elsevier: pp. 80.

Mehta, A. & Haber, J.E. 2014. Sources of DNA double-strand breaks and models of recombinational DNA repair. *Cold Spring Harbor Perspectives in Biology.* 6 (9). pp. a016428.

Mei, F., Kehui, X. & Wenming, X. 2016. Research advances of Dicer in regulating reproductive function. *Yi chuan = Hereditas.* 38 (7). pp. 612-622.

Meng, Z. & Lu, M. 2017. RNA interference-induced innate immunity, Off-Target effect, or immune Adjuvant? *Frontiers in Immunology.* 8, p.331.

Miller, K.M. and Cooper, J.P., 2003. The telomere protein Taz1 is required to prevent and repair genomic DNA breaks. *Molecular Cell*, *11*(2), pp.303-313.

Mirkin, E.V. & Mirkin, S.M. 2007. Replication fork stalling at natural impediments. *Microbiology and Molecular Biology reviews : MMBR.* 71 (1). pp. 13-35.

Mizuguchi, T., Barrowman, J. and Grewal, S.I., 2015. Chromosome domain architecture and dynamic organization of the fission yeast genome. *FEBS Letters*, *589*(20PartA), pp.2975-2986.

Mladenov, E. & Iliakis, G. 2011. Induction and repair of DNA double strand breaks: the increasing spectrum of non-homologous end joining pathways. *Mutation Research.* 711 (1-2). pp. 61-72.

Moazed, D. 2009. Small RNAs in transcriptional gene silencing and genome defence. *Nature.* 457 (7228). pp. 413-420.

Molla-Herman, A., Vallés, A.M., Ganem-Elbaz, C., Antoniewski, C. and Huynh, J.R., 2015. tRNA processing defects induce replication stress and Chk2-dependent disruption of piRNA transcription. *EMBO Journal*, *34*(24), pp.3009-3027.

Moravec, M., Wischnewski, H., Bah, A., Hu, Y., Liu, N., Lafranchi, L., King, M.C. and Azzalin, C.M., 2016. TERRA promotes telomerase-mediated telomere elongation in *Schizosaccharomyces pombe*. *EMBO Reports*, *17*(7), pp.999-1012.

Moreno-Moreno, O., Torras-Llort, M. & Azorin, F. 2017. Variations on a nucleosome theme: The structural basis of centromere function. *BioEssays : News and Reviews in Molecular, Cellular and Developmental Biology.* 39 (4). pp. 10.1002/bies.201600241. Epub 2017 Feb 21.

Mutazono, M., Morita, M., Tsukahara, C., Chinen, M., Nishioka, S., Yumikake, T., Dohke, K., Sakamoto, M., Ideue, T., Nakayama, J.I., Ishii, K. & Tani, T. 2017. The intron in centromeric noncoding RNA facilitates RNAi-mediated formation of heterochromatin. *PLoS Genetics.* 13 (2). pp. e1006606

Nambiar, M. & Raghavan, S.C. 2011. How does DNA break during chromosomal translocations? *Nucleic Acids Research.* 39 (14). pp. 5813-5825.

Nambiar, M., Choudhary, B., Rao, C.R. & Raghavan, S.C. 2008. Amplification of chromosomal translocation junctions from paraffin-embedded tissues of follicular lymphoma patients. *Biomedical Materials.* 3 (3). pp. 034103.

Nikolov, I. & Taddei, A. 2016. Linking replication stress with heterochromatin formation. *Chromosoma.* 125 (3). pp. 523-533.

Novo, C.L. Londoño-Vallejo, J.A. 2013. Telomeres and the nucleus. *Seminars in Cancer Biology.* Elsevier: pp. 116.

Nuckolls, N.L., Núñez, M.A.B., Eickbush, M.T., Young, J.M., Lange, J.J., Yu, J.S., Smith, G.R., Jaspersen, S.L., Malik, H.S. and Zanders, S.E., 2017. wtf genes are prolific dual poison-antidote meiotic drivers. *eLife*, *6*.

Nurse, P. 2002. Cyclin dependent kinases and cell cycle control. *Biosci Rep.* 22 (56). pp. 487-499.

Oestergaard, V.H. & Lisby, M. 2017. Transcription-replication conflicts at chromosomal fragile sites-consequences in M phase and beyond. *Chromosoma.* 126 (2). pp. 213-222.

Ohle, C., Tesorero, R., Schermann, G., Dobrev, N., Sinning, I. & Fischer, T. 2016. Transient RNA-DNA Hybrids Are Required for Efficient Double-Strand Break Repair. *Cell.* 167 (4). pp. 1001-1013.e7.

Ohno, Y., Ogiyama, Y., Kubota, Y., Kubo, T. & Ishii, K. 2016. Acentric chromosome ends are prone to fusion with functional chromosome ends through a homology-directed rearrangement. *Nucleic Acids Research.* 44 (1). pp. 232-244.

Ordog, T., Syed, S., Hayashi, Y. & Asuzu, D.T. 2012. Epigenetics and chromatin dynamics: a review and a paradigm for functional disorders. *Neurogastroenterology & Motility.* 24 (12). pp. 1054-1068.

Pan, L., Hildebrand, K., Stutz, C., Thoma, N. & Baumann, P. 2015. Minishelterins separate telomere length regulation and end protection in fission yeast. *Genes & Development.* 29 (11). pp. 1164-1174.

Parizotto, E.A., Lowe, E.D. & Parker, J.S. 2013. Structural basis for duplex RNA recognition and cleavage by Archaeoglobus fulgidus C3PO. *Nature Structural & Molecular Biology.* 20 (3). pp. 380-386.

Parker, M.W., Botchan, M.R. & Berger, J.M. 2017. Mechanisms and regulation of DNA replication initiation in eukaryotes. *Critical Reviews in Biochemistry and Molecular Biology.* 52 (2). pp. 107-144.

Patterson, A.D., Hollander, M.C., Miller, G.F. & Fornace, A.J.,Jr 2006. Gadd34 requirement for normal hemoglobin synthesis. *Molecular and cellular biology.* 26 (5). pp. 1644-1653.

Pellegrini, L. & Costa, A. 2016. New insights into the mechanism of DNA duplication by the eukaryotic replisome. *Trends in Biochemical Sciences.* 41 (10). pp. 859-871.

Peng, G. & Lin, S.Y. 2011. Exploiting the homologous recombination DNA repair network for targeted cancer therapy. *World Journal of Clinical Oncology.* 2 (2). pp. 73-79.

Petermann, E., Orta, M.L., Issaeva, N., Schultz, N. & Helleday, T. 2010. Hydroxyurea-stalled replication forks become progressively inactivated and require two different RAD51-mediated pathways for restart and repair. *Molecular Cell.* 37 (4). pp. 492-502.

Plosky, B.S. 2016. The Good and Bad of RNA:DNA Hybrids in Double-Strand Break Repair. *Molecular Cell.* 64 (4). pp. 643-644.

Pryce, D.W., Ramayah, S., Jaendling, A. & McFarlane, R.J. 2009. Recombination at DNA replication fork barriers is not universal and is differentially regulated by Swi1. *Proceedings of the National Academy of Sciences of the United States of America.* 106 (12). pp. 4770-4775.

Pushpavalli, S.N., Bag, I., Pal-Bhadra, M. & Bhadra, U. 2012. Drosophila Argonaute-1 is critical for transcriptional cosuppression and heterochromatin formation. *Chromosome Research.* 20 (3). pp. 333-351.

Raghavan, S.C. & Lieber, M.R. 2006. DNA structures at chromosomal translocation sites. *Bioessays.* 28 (5). pp. 480-494.

Remus, D. & Diffley, J.F. 2009. Eukaryotic DNA replication control: lock and load, then fire. *Current Opinion in Cell Biology.* 21 (6). pp. 771-777.

Ren, J., Castel, S.E. & Martienssen, R.A. 2015. Dicer in action at replication-transcription collisions. *Molecular & Cellular Oncology.* 2 (3). pp. e991224.

Reyes-Turcu, F.E. & Grewal, S.I. 2012. Different means, same end-heterochromatin formation by RNAi and RNAi-independent RNA processing factors in fission yeast. *Current Opinion in Genetics & Development.* 22 (2). pp. 156-163.

Rippe, K. & Luke, B. 2015. TERRA and the state of the telomere. *Nature Structural & Molecular Biology.* 22 (11). pp. 853-858.

Roukos, V. & Misteli, T. 2014. The biogenesis of chromosome translocations. *Nature Cell Biology.* 16 (4). pp. 293-300.

Roumelioti, F.M., Sotiriou, S.K., Katsini, V., Chiourea, M., Halazonetis, T.D. & Gagos, S. 2016. Alternative lengthening of human telomeres is a conservative DNA replication process with features of break-induced replication. *EMBO Reports.* 17 (12). pp. 1731-1737.

Sadaie M, Iida T, Urano T, Nakayama J 2004. A chromodomain protein, Chp1, is required for the establishment of heterochromatin in fission yeast. EMBO J 23: 3825–3835

Sadeghi, L., Prasad, P., Ekwall, K., Cohen, A. & Svensson, J.P. 2015. The Paf1 complex factors Leo1 and Paf1 promote local histone turnover to modulate chromatin states in fission yeast. *EMBO Reports.* 16 (12). pp. 1673-1687.

Sahu, S., Philip, F. & Scarlata, S. 2014. Hydrolysis rates of different small interfering RNAs (siRNAs) by the RNA silencing promoter complex, C3PO, determines their regulation by phospholipase Cbeta. *The Journal of Biological Chemistry.* 289 (8). pp. 5134-5144.

Sakofsky, C.J. & Malkova, A. 2017. Break induced replication in eukaryotes: mechanisms, functions, and consequences. *Critical Reviews in Biochemistry and Molecular biology.* 52 (4). pp. 395-413.

Sakofsky, C.J., Ayyar, S. & Malkova, A. 2012. Break-induced replication and genome stability. *Biomolecules.* 2 (4). pp. 483-504.

Santaguida, S. & Amon, A. 2015. Short-and long-term effects of chromosome mis-segregation and aneuploidy. *Nature Reviews Molecular Cell Biology.* 16 (8). pp. 473-485.

Santos-Pereira, J.M. & Aguilera, A. 2015. R loops: new modulators of genome dynamics and function. *Nature Reviews.Genetics.* 16 (10). pp. 583-597.

Sarek, G., Marzec, P., Margalef, P. & Boulton, S.J. 2015. Molecular basis of telomere dysfunction in human genetic diseases. *Nature Structural & Molecular Biology.* 22 (11). pp. 867-874.

Schmidt, J.C. & Cech, T.R. 2015. Human telomerase: biogenesis, trafficking, recruitment, and activation. *Genes & Development.* 29 (11). pp. 1095-1105.

Schoeftner, S. & Blasco, M.A. 2008. Developmentally regulated transcription of mammalian telomeres by DNA-dependent RNA polymerase II. *Nature Cell Biology.* 10 (2). pp. 228-236.

Schoeftner, S. & Blasco, M.A. 2009. A 'higher order' of telomere regulation: telomere heterochromatin and telomeric RNAs. *EMBO Journal.* 28 (16). pp. 2323-2336.

Schwartz, M., Zlotorynski, E., Goldberg, M., Ozeri, E., Rahat, A., le Sage, C., Chen, B.P., Chen, D.J., Agami, R. & Kerem, B. 2005. Homologous recombination and nonhomologous end-joining repair pathways regulate fragile site stability. *Genes & Development.* 19 (22). pp. 2715-2726.

Shen, H., Xu, W. & Lan, F. 2017. Histone lysine demethylases in mammalian embryonic development. *Experimental & Molecular Medicine.* 49 (4). pp. e325.

Shiroiwa, Y., Hayashi, T., Fujita, Y., Villar-Briones, A., Ikai, N., Takeda, K., Ebe, M. & Yanagida, M. 2011. Mis17 is a regulatory module of the Mis6-Mal2-Sim4 centromere complex that is required for the recruitment of CenH3/CENP-A in fission yeast. *PloS One.* 6 (3). pp. e17761.

So, A., Le Guen, T., Lopez, B.S. and Guirouilh-Barbat, J., 2017. Genomic rearrangements induced by unscheduled DNA double strand breaks in somatic mammalian cells. *The FEBS journal*, *284*(15), pp.2324-2344.Song, M.S. & Rossi, J.J. 2017. Molecular mechanisms of Dicer: endonuclease and enzymatic activity. *The Biochemical Journal.* 474 (10). pp. 1603-1618.

Srivatsan, A., Tehranchi, A., MacAlpine, D.M. & Wang, J.D. 2010. Co-orientation of replication and transcription preserves genome integrity. *PLoS Genetics.* 6 (1). pp. e1000810.

Stein, J.M., Bergman, W., Fang, Y., Davison, L., Brensinger, C., Robinson, M.B., Hecht, N.B. & Abel, T. 2006. Behavioral and neurochemical alterations in mice lacking the RNA-binding protein translin. *The Journal of neuroscience : the official Journal of the Society for Neuroscience.* 26 (8). pp. 2184-2196.

Steiner, F.A. & Henikoff, S. 2015. Diversity in the organization of centromeric chromatin. *Current Opinion in Genetics & Development.* 31 pp. 28-35.

Stillman, B. 2008. DNA polymerases at the replication fork in eukaryotes. *Molecular Cell.* 30 (3). pp. 259-260.

Stimpson, K.M. & Sullivan, B.A. 2010. Epigenomics of centromere assembly and function. *Current Opinion in Cell Biology.* 22 (6). pp. 772-780.

Stunnenberg, R., Kulasegaran-Shylini, R., Keller, C., Kirschmann, M.A., Gelman, L. & Buhler, M. 2015. H3K9 methylation extends across natural boundaries of heterochromatin in the absence of an HP1 protein. *EMBO Journal.* 34 (22). pp. 2789-2803.

Sugiura, I., Sasaki, C., Hasegawa, T., Kohno, T., Sugio, S., Moriyama, H., Kasai, M. & Matsuzaki, T. 2004. Structure of human translin at 2.2 Å resolution. *Acta Crystallographica Section D: Biological Crystallography.* 60 (4). pp. 674-679.

Sugiyama, T., Kantake, N., Wu, Y. & Kowalczykowski, S.C. 2006. Rad52-mediated DNA annealing after Rad51-mediated DNA strand exchange promotes second ssDNA capture. *EMBO Journal.* 25 (23). pp. 5539-5548.

Suseendranathan, K., Sengupta, K., Rikhy, R., D'Souza, J.S., Kokkanti, M., Kulkarni, M.G., Kamdar, R., Changede, R., Sinha, R. & Subramanian, L. 2007. Expression pattern of Drosophila translin and behavioral analyses of the mutant. *European Journal of Cell Biology.* 86 (3). pp. 173-186.

Suwaki, N., Klare, K. & Tarsounas, M. 2011. RAD51 paralogs: roles in DNA damage signalling, recombinational repair and tumorigenesis. *Seminars in Cell & Developmental Biology.* 22 (8). pp. 898-905.

Svobodova, E., Kubikova, J. & Svoboda, P. 2016. Production of small RNAs by mammalian Dicer. *Pflugers Archiv : European Journal of Physiology.* 468 (6). pp. 1089-1102.

Swahari, V., Nakamura, A. and Deshmukh, M., 2016. The paradox of dicer in cancer. *Molecular & Cellular Oncology*, *3*(3), p.e1155006.

Swarts, D.C., Makarova, K., Wang, Y., Nakanishi, K., Ketting, R.F., Koonin, E.V., Patel, D.J. & van der Oost, J. 2014. The evolutionary journey of Argonaute proteins. *Nature Structural & Molecular Biology.* 21 (9). pp. 743-753.

Symington, L.S. & Gautier, J. 2011. Double-strand break end resection and repair pathway choice. *Annual Review of Genetics.* 45 pp. 247-271.

Tabarestani, S. & Movafagh, A. 2016. New Developments in Chronic Myeloid Leukemia: Implications for Therapy. *Iranian Journal of Cancer Prevention.* 9 (1). pp. e3961-3961. eCollection 2016 Feb.

Tadeo, X., Wang, J., Kallgren, S.P., Liu, J., Reddy, B.D., Qiao, F. & Jia, S. 2013. Elimination of shelterin components bypasses RNAi for pericentric heterochromatin assembly. *Genes & Development.* 27 (22). pp. 2489-2499.

Takagi, M. 2017. DNA damage response and hematological malignancy. *International Journal of Hematology.*

Takahashi K, Chen ES, Yanagida M (2000) Requirement of Mis6 centromere 730 connector for localizing a CENP-A-like protein in fission yeast. Science 288:731 2215-2219.

Talens, F., Jalving, M., Gietema, J.A. & Van Vugt, M.A. 2017. Therapeutic targeting and patient selection for cancers with homologous recombination defects. *Expert Opinion on Drug Discovery.* 12 (6). pp. 565-581.

Tang, L., Nogales, E. & Ciferri, C. 2010. Structure and function of SWI/SNF chromatin remodeling complexes and mechanistic implications for transcription. *Progress in Biophysics and Molecular Biology.* 102 (2-3). pp. 122-128.

Tashiro, S., Asano, T., Kanoh, J. & Ishikawa, F. 2013. Transcription-induced chromatin association of RNA surveillance factors mediates facultative heterochromatin formation in fission yeast. *Genes to cells : Devoted to Molecular & Cellular Mechanisms.* 18 (4). pp. 327-339.

Thakur, J., Talbert, P.B. & Henikoff, S. 2015. Inner Kinetochore Protein Interactions with Regional Centromeres of Fission Yeast. *Genetics.* 201 (2). pp. 543-561.

Tian, H., Gao, Z., Li, H., Zhang, B., Wang, G., Zhang, Q., Pei, D. & Zheng, J. 2015. DNA damage response--a double-edged sword in cancer prevention and cancer therapy. *Cancer Letters.* 358 (1). pp. 8-16.

Tian, Y., Simanshu, D.K., Ascano, M., Diaz-Avalos, R., Park, A.Y., Juranek, S.A., Rice, W.J., Yin, Q., Robinson, C.V. & Tuschl, T. 2011. Multimeric assembly and biochemical characterization of the Trax–translin endonuclease complex. *Nature Structural & Molecular Biology.* 18 (6). pp. 658-664.

Tubbs, A. & Nussenzweig, A. 2017. Endogenous DNA damage as a source of genomic instability in cancer. *Cell.* 168 (4). pp. 644-656.

Tucker, J.D. 2010. Chromosome translocations and assessing human exposure to adverse environmental agents. *Environmental and Molecular Mutagenesis.* 51 (8-9). pp. 815-824.

Uckelmann, M. and Sixma, T.K., 2017. Histone ubiquitination in the DNA damage response. *DNA repair*, *56*, pp.92-101.

Vancevska, A., Douglass, K.M., Pfeiffer, V., Manley, S. & Lingner, J. 2017. The telomeric DNA damage response occurs in the absence of chromatin decompaction. *Genes & Development.*

VanLoock, M.S., Yu, X., Kasai, M. & Egelman, E.H. 2001. Electron microscopic studies of the translin octameric ring. *Journal of Structural Biology.* 135 (1). pp. 58-66.

Visser, R., Shimokawa, O., Harada, N., Kinoshita, A., Ohta, T., Niikawa, N. & Matsumoto, N. 2005. Identification of a 3.0-kb major recombination hotspot in patients with Sotos syndrome who carry a common 1.9-Mb microdeletion. *The American Journal of Human Genetics.* 76 (1). pp. 52-67.

Voglova, K., Bezakova, J. & Herichova, I. 2016. Progress in micro RNA focused research in endocrinology. *Endocrine regulations.* 50 (2). pp. 83-105. Volpe, T. & Martienssen, R.A. 2011. RNA interference and heterochromatin assembly. *Cold Spring Harbor Perspectives in Biology.* 3 (9). pp. a003731.

Volpe, T. & Martienssen, R.A. 2011. RNA interference and heterochromatin assembly. *Cold Spring HarborPerspectives in Biology.* 3 (9). pp. a003731.

Volpe, T., Schramke, V., Hamilton, G.L., White, S.A., Teng, G., Martienssen, R.A. & Allshire, R.C. 2003. RNA interference is required for normal centromere function in fission yeast. *Chromosome research : an International Journal on the Molecular, Supramolecular and Evolutionary Aspects of Chromosome Biology.* 11 (2). pp. 137-146.

Volpe, T.A., Kidner, C., Hall, I.M., Teng, G., Grewal, S.I. and Martienssen, R.A., 2002. Regulation of heterochromatic silencing and histone H3 lysine-9 methylation by RNAi. *Science*, *297*(5588), pp.1833-1837.

Wahba, L., Gore, S.K. & Koshland, D. 2013. The homologous recombination machinery modulates the formation of RNA-DNA hybrids and associated chromosome instability. *eLife.* 2 pp. e00505.

Wang, C., Zhao, L. & Lu, S. 2015. Role of TERRA in the regulation of telomere length. *International Journal of Biological Sciences.* 11 (3). pp. 316-323.

Wang, J., Boja, E.S., Oubrahim, H. & Chock, P.B. 2004. Testis brain ribonucleic acid-binding protein/translin possesses both single-stranded and double-stranded ribonuclease activities. *Biochemistry.* 43 (42). pp. 13424-13431.

Wang, J., Cohen, A.L., Letian, A., Tadeo, X., Moresco, J.J., Liu, J., Yates, J.R.,3rd, Qiao, F. & Jia, S. 2016a. The proper connection between shelterin components is required for telomeric heterochromatin assembly. *Genes & Development.* 30 (7). pp. 827-839.

Wang, J.Y., Chen, S.Y., Sun, C.N., Chien, T. & Chern, Y. 2016b. A central role of TRAX in the ATM-mediated DNA repair. *Oncogene.* 35 (13). pp. 1657-1670.

Weberpals, J.I., Koti, M. & Squire, J.A. 2011. Targeting genetic and epigenetic alterations in the treatment of serous ovarian cancer. *Cancer Genetics.* 204 (10). pp. 525-535.

Wei, Y., Sun, M., Nilsson, G., Dwight, T., Xie, Y., Wang, J., Hou, Y., Larsson, O., Larsson, C. & Zhu, X. 2003. Characteristic sequence motifs located at the genomic breakpoints of the translocation t (X; 18) in synovial sarcomas. *Oncogene.* 22 (14). pp. 2215.

Westhorpe, F.G. & Straight, A.F. 2014. The centromere: epigenetic control of chromosome segregation during mitosis. *Cold Spring Harbor Perspectives in Biology.* 7 (1). pp. a015818.

Wood, V., Gwilliam, R., Rajandream, M., Lyne, M., Lyne, R., Stewart, A., Sgouros, J., Peat, N., Hayles, J. & Baker, S. 2002. The genome sequence of *Schizosaccharomyces pombe*. *Nature.* 415 (6874). pp. 871-880.

Woolcock, K.J. & Buhler, M. 2013. Nuclear organisation and RNAi in fission yeast. *Current Opinion in Cell Biology.* 25 (3). pp. 372-377.

Woolcock, K.J., Gaidatzis, D., Punga, T. & Buhler, M. 2011. Dicer associates with chromatin to repress genome activity in Schizosaccharomyces pombe. *Nature Structural & Molecular Biology.* 18 (1). pp. 94-99.

Wu, X.Q., Gu, W., Meng, X. & Hecht, N.B. 1997. The RNA-binding protein, TB-RBP, is the mouse homologue of translin, a recombination protein associated with chromosomal

translocations. *Proceedings of the National Academy of Sciences of the United States of America.* 94 (11). pp. 5640-5645.

Yang, K., Guo, R. & Xu, D. 2016. Non-homologous end joining: advances and frontiers. *Acta Biochimica Et Biophysica Sinica.* 48 (7). pp. 632-640.

Yang, S. & Hecht, N.B. 2004. Translin associated protein X is essential for cellular proliferation. *FEBS Letters.* 576 (1-2). pp. 221-225.

Yang, S., Cho, Y.S., Chennathukuzhi, V.M., Underkoffler, L.A., Loomes, K. & Hecht, N.B. 2004. Translin-associated factor X is post-transcriptionally regulated by its partner protein TB-RBP, and both are essential for normal cell proliferation. *The Journal of Biological Chemistry.* 279 (13). pp. 12605-12614.

Yang, W. & Ernst, P. 2017. Distinct functions of histone H3, lysine 4 methyltransferases in normal and malignant hematopoiesis. *Current Opinion in Hematology.*

Yao, Y. & Dai, W. 2014. Genomic Instability and Cancer. *Journal of Carcinogenesis & Mutagenesis.* 5 pp. 1000165.

Ye, X., Huang, N., Liu, Y., Paroo, Z., Huerta, C., Li, P., Chen, S., Liu, Q. & Zhang, H. 2011. Structure of C3PO and mechanism of human RISC activation. *Nature Structural & Molecular Biology.* 18 (6). pp. 650-657.

Yu, Z., & Hecht, N. B. (2008). The DNA/RNA-binding protein, translin, bindsmicroRNA122a and increases its in vivo stability. *Journal of Andrology*, *29*(5), 572.

Zaboikin, M., Zaboikina, T., Freter, C. & Srinivasakumar, N. 2017. Non-Homologous End Joining and Homology Directed DNA Repair Frequency of Double-Stranded Breaks Introduced by Genome Editing Reagents. *PloS One.* 12 (1). pp. e0169931.

Zaratiegui, M., Castel, S.E., Irvine, D.V., Kloc, A., Ren, J., Li, F., de Castro, E., Marin, L., Chang, A.Y., Goto, D., Cande, W.Z., Antequera, F., Arcangioli, B. & Martienssen, R.A. 2011. RNAi promotes heterochromatic silencing through replication-coupled release of RNA Pol II. *Nature.* 479 (7371). pp. 135-138.

Zeng, W., Ball, A.R.,Jr & Yokomori, K. 2010. HP1: heterochromatin binding proteins working the genome. *Epigenetics.* 5 (4). pp. 287-292.

Zhang, B., Pan, X., Cobb, G.P. & Anderson, T.A. 2007. microRNAs as oncogenes and tumor suppressors. *Developmental Biology.* 302 (1). pp. 1-12.

Zhang, J., Liu, H., Yao, Q., Yu, X., Chen, Y., Cui, R., Wu, B., Zheng, L., Zuo, J., Huang, Z. and Ma, J., 2016. Structural basis for single-stranded RNA recognition and cleavage by C3PO. *Nucleic Acids Research*, *44*(19), pp.9494-9504.

Zhang, T., Cooper, S. & Brockdorff, N. 2015. The interplay of histone modifications - writers that read. *EMBO Reports.* 16 (11). pp. 1467-1481.

Zhang, Y., Gostissa, M., Hildebrand, D. G., Becker, M. S., Boboila, C., Chiarle, R., & Alt, F. W. (2010). The role of mechanistic factors in promoting chromosomal translocations found in lymphoid and other cancers. Advances in Immunology, 106, 93-133.

Zhao, X., Wei, C., Li, J., Xing, P., Li, J., Zheng, S. & Chen, X. 2017. Cell cycle-dependent control of homologous recombination. *Acta Biochimica Et Biophysica Sinica.* pp. 1-14.

Zheng, J. 2013. Oncogenic chromosomal translocations and human cancer (Review). *Oncology Reports.* 30 (5). pp. 2011-2019.

Zocco, M., Marasovic, M., Pisacane, P., Bilokapic, S. & Halic, M. 2016. The Chp1 chromodomain binds the H3K9me tail and the nucleosome core to assemble heterochromatin. *Cell Discovery.* 2 pp. 16004.

9. Appendecies

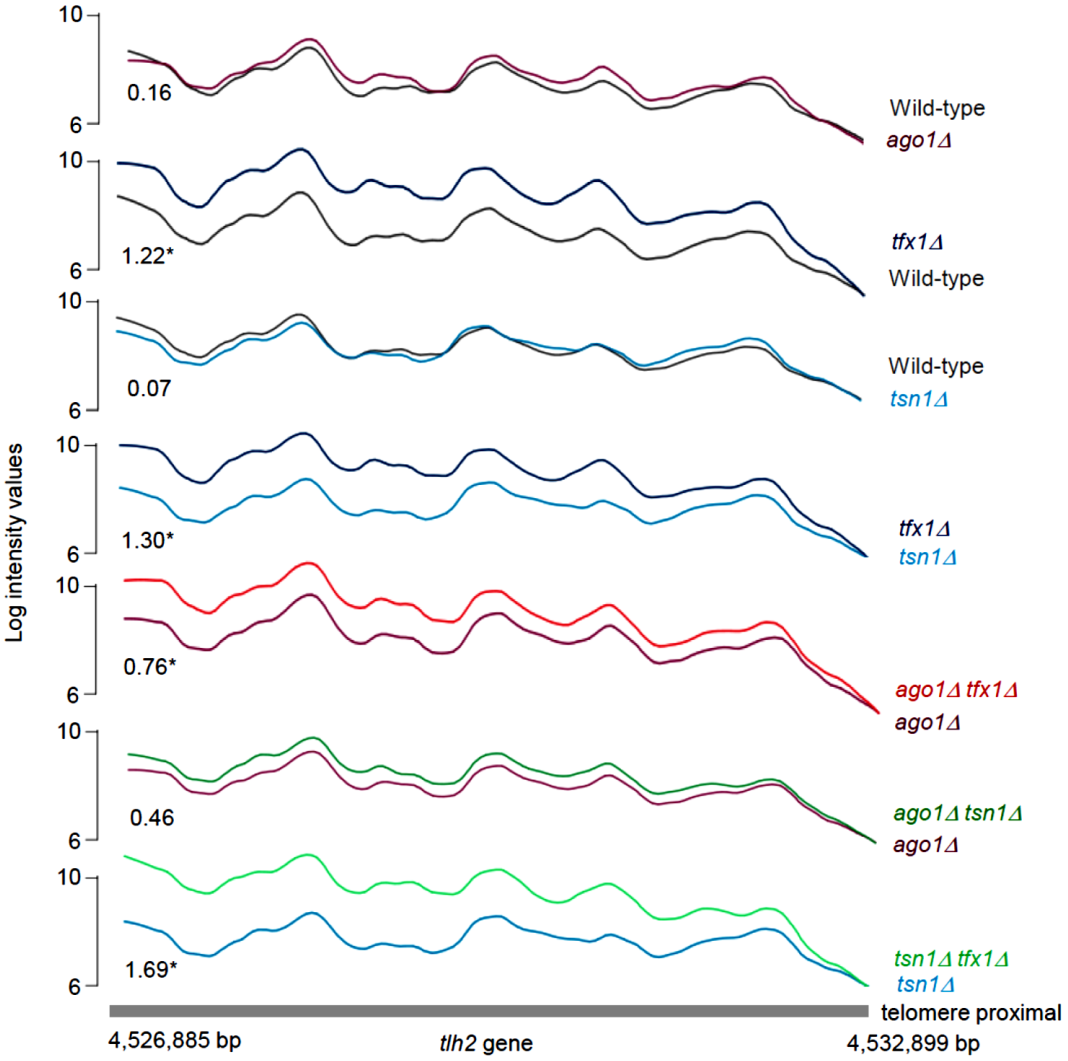

Appendix 1 The sub-telomeric *tlh2* transcript is elevated in the *ago1Δ tfx1Δ* double mutant.

Analysis of tiled whole genome expression data comparing *ago1Δ* with *ago1Δ tfx1Δ* showed that the sub-telomeric *tlh2* gene transcript is activated. The *tlh2* gene is also upregulated in the *tfx1Δ* single mutants. Similar activation of *tlh2* is not seen in the *tsn1Δ* mutant. The plots show the transcriptional activity for the *tlh2* open reading frame. Seven pairwise plots of transcriptional signals are shown for various strains. The log 2-fold change (lg2FC) for each plot is given as a numerical value within the plot (* = P<0.05).

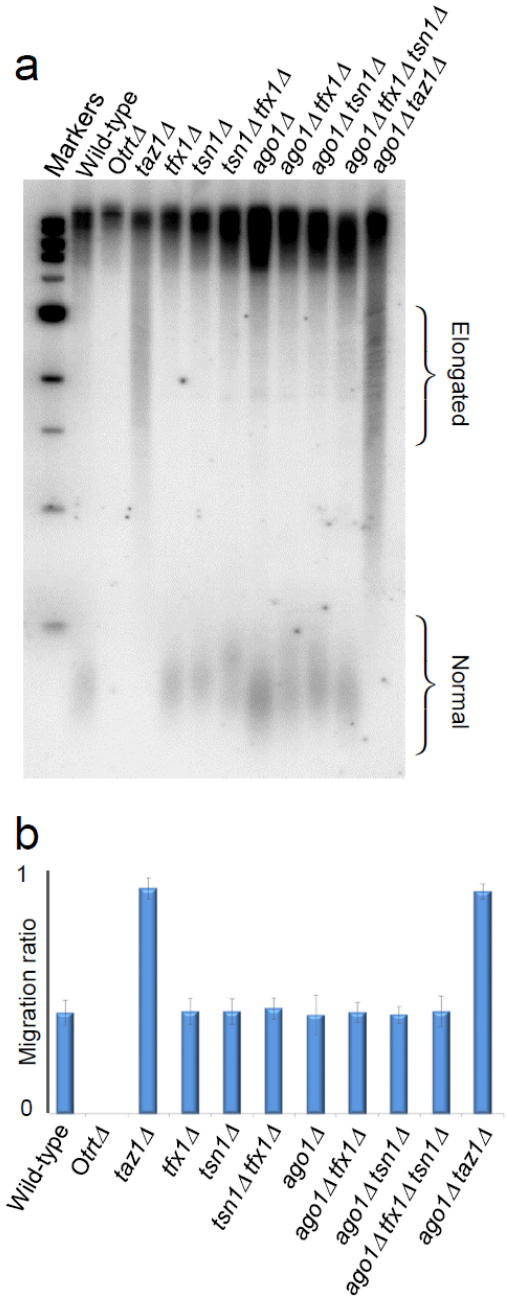

Appendix 2 Mutation of *tfx1* or *tsn1* does not alter telomere length.

a. Example of a southern blot of digested genomic DNA probed with a telomere-specific probe demonstrating that mutation of *tfx1* or *tsn1* does not display any measurable length change compared to the WT strain. The *Otrt1Δ* strain, which has no telomeres, was used as a negative control. The *taz1Δ* mutant was used as a positive control, and this has already been shown to exhibit a greatly elongated telomere.

b. Quantification of telomere length in various strains confirms that there is no change in the mean length of telomeres following loss of *tfx1* or *tsn1* in any strains tested as compared to the WT strain. Error bars show standard deviation.